The Effect of Small Cations on the Delayed Rectifier and the Resting Potassium Conductance of Frog Sartorius Muscle

by

Louise Ann Gay, B.Sc.

Thesis submitted for the degree of Doctor of Philosophy

Department of Physiology, University of Leicester

1979

ProQuest LLC
789 East Eisenhower Parkway
P.O. Box 1346
Ann Arbor, MI 48106-1346

CONTENTS

Chapter 1. General Introduction

It is a widely held view that the influx of Na^+ and the efflux of K^+ which are associated with the rising and falling phases of the action potential in most nerve and muscle fibres occur by way of aqueous channels in the cell membrane (Hille, 1970, 1975a; Armstrong, 1975a,b,c). Moreover, each channel is believed to contain voltage-sensitive molecules which gate the channel (that is, determine whether the channel is open or shut) and a special region, called the selectivity filter (Hille, 1975a), which is able to distinguish between several ionic species and, particularly, between Na^+ and K^+ ions.

Other experiments in nerve suggest that the inner end of the K channel is wider than the outer region which includes the selectivity filter (for reviews see Armstrong, 1975a,b; French & Adelman, 1976), and that K^+ ions move through this channel in single-file (Hodgkin & Keynes, 1955). However, these conclusions have yet to be supported by experiments in muscle. Indeed, a number of experiments which will be described in this chapter support the notion that K channels in muscle differ from those in nerve.

Thus the experiments performed here and described in the first part of this thesis (chapters 3 and 4) were designed to investigate the properties of the K channel in skeletal muscle. Two aspects were chosen, both of which have already been studied in detail in nerve. The first deals with the effects of pH on the K channel, and the second with the properties of the selectivity filter. The conclusion drawn from these experiments is that there are differences in the structure of K channels in nerve and muscle, but that these differences are largely quantitative.

In contrast to the permeability mechanisms which underlie the action potential, comparatively little is known about the K permeability mechanism known as the anomalous or in-going rectifier (Adrian, 1969). Inward rectification was first reported by Katz (1949), who showed that the input resistance of frog skeletal muscle fibres bathed in an isotonic K_2SO_4 solution was much larger when the membrane was depolarized by a constant current than when the membrane was hyperpolarized. This rectification is in the opposite direction to that predicted from the constant field equation (Goldman, 1943; Hodgkin & Katz, 1949) for a membrane in which K permeability is assumed to be independent of the membrane potential. Accordingly, Hodgkin & Horowicz (1959) showed that the resting K permeability in muscle was a function of the driving force on K^+, varying from 0.05 x 10^{-6} cm/s when there was a large outward driving force to 8 x 10^{-6} cm/s when the driving force was large and inward.

Inward rectification has also been reported in starfish egg cells (Hagiwara & Takahashi, 1974), cardiac Purkinje fibres (Noble, 1965, 1975; Noble & Tsien, 1968), and in certain nerve cells (Kandel & Tauc, 1966; Nelson & Frank, 1967), but does not occur in myelinated nerves of the frog or in squid axons under normal conditions.

The present work on inward rectification began in 1976. At that time Horowicz, Gage & Eisenberg (1968) and Adrian (1969) had developed models for inward rectification in which K^+ was transported across the membrane in association with a lipid-soluble carrier molecule, while Armstrong (1975a) had produced a pore model in which the permeability of the membrane to K^+ depended

on the presence or absence of a blocking particle associated with the pore. Each of these models, which are discussed in chapter 8, fails to reproduce at least one aspect of inward rectification in muscle. However, the present study, and those published recently by Hille & Schwarz (1978) and Standen & Stanfield (1978d), supports the hypothesis that K^+ ions cross the resting membrane by way of a pore.

To avoid confusion, this pore will be referred to as the resting K channel or the inward rectifier channel. The channel associated with the extra efflux of K^+ in stimulated muscle will be referred to as the delayed K channel or the delayed rectifier channel because the current which passes through this channel turns on after a delay when the membrane is depolarized.

The nerve axon can be treated as a cylinder. However, the electrophysiological properties of muscle are likely to be more complex owing to the presence of a network of membranes known as the sarcotubular system (Andersson-Cedergren, 1959; Page, 1965; Peachey, 1965). It is appropriate, therefore, to mention some aspects of the morphology of skeletal muscle in the frog before considering the ionic currents in this preparation.

The sarcotubular system comprises the sarcoplasmic reticulum, a system of longitudinal tubes whose function is the storage, release and re-uptake of the calcium which, when liberated into the sarcoplasm, produces contraction (Ebashi & Endo, 1968), and the transverse tubular system (T-system) whose role is to transmit electrical signals from the surface membrane deep into the interior of the fibre such that the contraction of axial myofibrils can be more nearly synchronised with those close to the surface (Huxley & Taylor, 1958; for recent reviews see Costantin, 1975; Endo, 1977).

The T-tubules are formed as invaginations of the surface membrane at several points on the circumference of the fibre at the Z-line in frog muscle (Huxley & Taylor, 1958). Electronmicrographs suggest that the tubules branch in such a way as to form an extensive lattice (Peachey, 1965) concentrated largely in the plane of the Z-line (Peachey & Schild, 1968). Moreover, studies with extracellular markers such as ferritin (Huxley, 1964; Peachey & Schild, 1968), horseradish peroxidase (Eisenberg & Eisenberg, 1968) and certain fluorescent dyes (Endo, 1966) have demonstrated that the lumen of the T-system is in direct continuity with the external solution.

About 80% of the tubular membrane is in close apposition to the terminal cisternae of the sarcoplasmic reticulum, forming structures known as triads (Franzini-Armstrong, 1970). The exact nature of the relationship between the tubular membrane and the membrane of the sarcoplasmic reticulum at the triad is unknown, though Schneider & Chandler (1973) have pointed to a possible similarity in the density of charged groups which give rise to the activator currents in muscle, which are believed to play an essential role in excitation-contraction coupling, and which are restricted to the membrane phase, and the number of electron dense projections (or feet) which extend at intervals between the tubular membrane and the terminal cisternae (Franzini-Armstrong, 1970). In their model of excitation-contraction coupling (Chandler, Rakowski & Schneider, 1976b), the mobilization of these charges when the fibre is depolarized results in the opening of Ca channels in the membranes of the terminal cisternae at the base of the feet. In view of the specialized nature of the triads, it is possible that the ionic conductances associated with the T-

tubules are concentrated in that part of the tubular membrane which is outside the triads (Gage & Eisenberg, 1969a).

The influence of the T-tubules on the electrical properties of muscle have been studied using a technique known as glycerolation (Fujino, Yamaguchi & Suzuki, 1961; Howell & Jenden, 1967; Gage & Eisenberg, 1967; Eisenberg & Eisenberg, 1968; Howell, 1969), whereby muscle fibres equilibrated in Ringer made hypertonic by glycerol are returned to a glycerol-free solution in order to disconnect the transverse tubules from the surface membrane. When detubulation is about 98% complete (Eisenberg & Eisenberg, 1968) the specific membrane capacitance is reduced by about two-thirds (Gage & Eisenberg, 1969a). This technique also demonstrates that a large part of the resting K conductance is in the membrane of the tubules, and because of this the tubular membrane provides an alternative pathway for K^+ to leave and enter the cell in the resting state other than across the surface membrane.

In the present context, the T-system is also of interest because a number of studies suggest that there may be transient changes in the composition of the external solution within the tubular lumen. In 1949, Katz showed that when an inward current was injected into skeletal muscle fibres, the membrane potential increased rapidly at first, but thereafter increased more slowly, taking several hundred milliseconds to reach a steady-state. Adrian & Freygang (1962a,b) have investigated this slow change in potential and concluded that it is due to a depletion of K^+ within an extracellular space presumed to be the lumen of the tubules. In their model, depletion occurred because the transport number for K^+ across the tubular wall exceeded that across a membrane at the mouth of the tubules. More recent experiments (which are

discussed in chapters 6 & 7) suggest that under certain conditions depletion can account for only part of the slow increase in resistance (Almers, 1972a,b). However, it appears that the depletion hypothesis (Adrian & Freygang, 1962a) is essentially correct, though the idea that there is a membrane at the mouth of the T-tubules is untenable in view of the experiments with extracellular markers.

The depletion hypothesis is also supported by the earlier experiments of Hodgkin & Horowicz (1960a). These authors showed that when the external K^+ concentration was raised in an almost step-wise fashion, the rate at which the fibres depolarized was about three times greater than the rate at which they repolarized, when, after a few seconds, external K^+ was returned to its initial level. They explained this by assuming that the removal of K^+ from a local region outside the fibre (the tubular lumen) was delayed.

The experiments of Hodgkin & Horowicz (1960a) also produce the following important results. First, since single dissected muscle fibres were used, the results cannot be explained by diffusion delays in the space between fibres. That depletion originates from the T-system is also supported by experiments that show that the slow increase in resistance reported by Katz (1949) and Adrian & Freygang (1962a) is removed by detubulation (Gage & Eisenberg, 1969b). Secondly, since the estimated volume of the T-system obtained by Hodgkin & Horowicz is similar to those reported by Peachey (1965) and Mobley & Eisenberg (1975) from electronmicrographs, it appears that the sarcoplasmic reticulum contributes little or nothing to the size of the depleted space. Finally, these experiments support the idea that part of

the resting K conductance is in the walls of the T-system.

The present interest in tubular K^+ depletion arises from the fact that, according to Almers (1972a), the time dependence of the inward current in resting muscle fibres bathed in a high K_2SO_4 solution containing no Na^+ is due not to depletion, but to a fall in the permeability of the membrane to K^+, while Standen & Stanfield (1978c) report that this permeability change, which can be shown to occur in certain conditions, is abolished in Na-free Ringer. In chapter 6, a method is described which allows one to distinguish between these two alternatives, and it is concluded that depletion does occur in an isotonic K_2SO_4 solution such as that used by Katz (1949). (See Baumgarten & Isenberg, 1977, for a recent report of K depletion and accumulation in the extracellular space of Purkinje fibres).

In addition to the Na conductance, the inwardly rectifying K conductance and the delayed K conductance, there are four more membrane conductances which have been recorded in frog skeletal muscle fibres, and which deserve mention here even though they have not been studied in the course of this work.

The first to be considered is the slow K conductance described by Adrian, Chandler & Hodgkin (1970b) and Stanfield (1970a). Like the delayed K conductance (Adrian et al., 1970a), this turns on along a sigmoidal time course when the membrane is depolarized beyond about -50 mV, but it reaches a maximum value which is only about one tenth that of the delayed conductance. Moreover, it turns on so slowly that it is not activated to any great extent during a normal action potential. Adrian et al. (1970b) have suggested, however, that it is responsible for the late depolarizing afterpotential which follows a train of impulses in frog skeletal

muscle fibres. Since the latter is abolished by glycerolation (Gage & Eisenberg, 1969b), the slow increase in K permeability may originate from the T-system. However, the properties of the slow K conductance have not been studied in glycerolated muscle fibres to see if this conductance increase is also abolished.

Recently, Beaty & Stefani (1976a) have reported calcium-dependent electrical activity in frog muscle fibres bathed in a solution containing tetraethylammonium to reduce the delayed current. This electrical activity follows the action potential, and in chloride-free solution comprises a slow depolarization as well as a slow transient response during which the membrane potential may reach + 23 mV. Beaty & Stefani attribute these responses to an influx of Ca^{2+}, which, they suggest, might play a role in excitation-contraction coupling.

Voltage clamp experiments also indicate that there is a voltage-dependent influx of Ca^{2+} in depolarized muscle (Beaty & Stefani, 1976b; Stanfield, 1977; Potreau & Raymond, 1978; see also Raymond & Potreau, 1977). This is located largely in the T-system, (Potreau & Raymond, 1978) and turns on at a potential close to the mechanical threshold (Stanfield, 1977; Potreau & Raymond, 1978).

The most interesting question concerning the Ca influx is whether or not it plays an essential role in tension development following a single action potential under normal conditions. Using the data of Bianchi & Shanes (1959), Potreau & Raymond (1978) have argued that the influx of Ca^{2+} during an action potential is about 20 times too small to activate the contractile proteins in frog skeletal muscle fibres, though a Ca influx may

play a role in contraction if depolarization is prolonged. This is supported by experiments which show that the Ca current turns on too slowly to be activated to any great extent during a single action potential (Stanfield, 1977). Other experiments which suggest that a Ca influx is not essential is that twitches persist when the external Ca^{2+} concentration is reduced to 10^{-9}M (Armstrong, Bezanilla & Horowicz, 1972) and that D600, which abolishes the Ca^{2+} dependent responses (Beaty & Stefani, 1976a), facilitates rather than depresses tension development (Dörrscheidt-Käfer, 1977).

Takeda (1977) has reported a Na^{+} dependent inward current in depolarized muscle fibres immersed in a solution containing the Ca^{2+} chelating agent EDTA. This Na current is blocked by picrotoxin and appears to originate from the T-system since it is not found in glycerolated fibres. However, this current is not blocked by tetrodotoxin (10^{-6}g/ml) at concentrations which are sufficient to block the Na current responsible for the rising phase of the spike in most nerve and muscle fibres (for reviews see Kao, 1966; Narahashi, 1974). Takeda used the frog Rana catesbiana for his experiments.

In a different species (Rana esculenta), Caillé, Ildefonse & Rougier (1975, 1978) and Mandrino (1977) have separated the Na current into two components, both of which are blocked by tetrodotoxin. The faster of these components is in the surface membrane and the slower component appears to reside in the tubular membrane. It is difficult, however, to be certain that the slower Na current is not due to regenerative activity in other uncontrolled parts of the muscle fibre. On the other hand, the presence of a tetrodotoxin-sensitive Na channel in the T-system is

supported by the tritiated TTX binding studies of Jaimovich et al. (1976) and indirectly by studies which suggest that a tubular action potential is necessary in order to obtain a normal twitch (Adrian, Costantin & Peachey, 1969; Bezanilla, Caputo, Gonzales-Serratos & Venosa, 1972; Bastian & Nakajima, 1972, 1974).

Finally, it is well established that the anion conductance in frog muscle is due to chloride. The chloride conductance contributes about 68% of the total membrane conductance at the resting potential in muscle fibres immersed in a normal KCl Ringer (Hodgkin & Horowicz, 1959; Hutter & Noble, 1960; Hutter & Warner, 1967a; Eisenberg & Gage, 1969) and less than this when the fibres are hyperpolarized (Hodgkin & Horowicz, 1959; Hutter & Warner, 1972), or placed in a hypertonic Ringer (Sperelakis & Schneider , 1968). Since glycerolation has little or no effect on the chloride conductance (Eisenberg & Gage, 1969), and since a sudden step-wise change in the external chloride concentration produces a rapid change in the membrane potential which follows a similar time course whether the chloride concentration is raised or lowered (Hodgkin & Horowicz, 1960a), it is unlikely that the chloride conductance is located to any great extent in the tubular membrane.

The role of Na^+ and K^+ in the action potential was first described in detail by Hodgkin & Katz (1949) for the squid axon, and by Nastuk & Hodgkin (1950) for skeletal muscle of the frog. However, since much of our present understanding of the way in which these ions give rise to the spike is a result of the experiments of Hodgkin & Huxley (1952a,b,c,d; see also Hodgkin, Huxley & Katz, 1952), who recorded the membrane currents of squid axons under conditions in which the membrane potential was controlled in a step-wise manner (the voltage-clamp technique), it is appropriate to discuss these experiments here.

These authors found that when the membrane was depolarized, say, to 0 mV, the membrane current had four components. First, the beginning and end of the voltage step produced a transient capacity current. Second, there was an ionic leakage current which was independent of time and proportional to the applied voltage. The third component was the Na current, which was inward at 0 mV. This reached a maximum after about one millisecond, then inactivated completely. Finally, they showed that the K current was outward at 0 mV, that it developed more slowly than the Na current, and that it did not inactivate. More recent studies show that the K current does inactivate slowly in the squid (Erhenstein & Gilbert, 1966), but that this inactivation is not complete.

Hodgkin & Huxley (1952d) developed a mathematical model which described the time and voltage-dependence of the ionic currents and from which they were able to reconstruct the action potential with a reasonably high degree of accuracy (see also Hodgkin, 1964). In this model the sodium and the potassium conductances (g_{Na} and g_K, respectively) are given by

$$g_{Na} = \bar{g}_{Na}\, m^3\, h \qquad (1.1)$$

and

$$g_K = \bar{g}_K\, n^4 \qquad (1.2)$$

where m, n, and h are parameters which depend on the membrane potential and on time, and where $\bar{g}_{Na}$ and $\bar{g}_K$ are the maximum possible sodium and potassium conductances. A more detailed account of the model for the K conductance is given in chapter 3. Here, it is sufficient to say that the model assumes that the conductance of each Na channel is controlled by an activation gating mechanism (m^3) which opens when the membrane is depolarized, and an inactivation gate (h) that closes under these conditions. Each delayed K channel is also controlled by an activation gating mechanism

(n^4) that opens in response to depolarization. In muscle, there must also be at least one inactivation gate for the K channel since the delayed current inactivates completely during a maintained depolarization (Adrian, Chandler & Hodgkin, 1970a). It is clear that the Hodgkin-Huxley model does not account for all of the properties of ionic currents recorded in a variety of preparations (for a review see Goldman, 1976). However, its value lies in the fact that since the parameters m, n, and h are well defined, the ionic currents can be compared unambiguously in a number of experimental situations.

Although it is more than 25 years since Hodgkin & Huxley published their model of the ionic currents in the squid axon, comparatively little is known about the structure of the voltage-sensitive molecules presumed to gate the channels except that proteins are probably involved. This conclusion is based on the finding that the proteolytic enzyme, pronase, removes Na inactivation in the squid when added to the internal perfusate (Armstrong, Bezanilla & Rojas, 1973), and zinc slows the kinetics of K activation in the squid axon (Begenisich& Lynch, 1974) and skeletal muscle fibres (Stanfield, 1975). In muscle, the kinetics are altered in such a way as to suggest that zinc is able to bind to one or more of the gating particles (n) associated with each K channel (Stanfield, 1975); a result which is also consistent with the view (Hodgkin & Huxley, 1952d) that the movement of gating particles within the membrane are independent of one another. Zinc also reduces the maximum K conductance in muscle, though this effect may be due to zinc binding at some external site and thereby blocking the channel rather than an effect on channel gating (Stanfield, 1975).

The contemporary interest in the structure of ionic channels has developed largely as a result of the experiments of Armstrong and his co-workers, who studied the properties of the delayed rectifier in nerve in the presence of tetraethylammonium ions (TEA) and its derivatives. In the next few pages, I shall attempt to show how these and other pharmacological studies have contributed to the description of the delayed K channel which was given at the beginning of this chapter.

Quaternary ammonium ions are permanently charged, monovalent cations. The charge is located on the nitrogen atom,which,in the case of TEA, also forms the central atom to which four ethyl chains are connected. In most of the other quaternary compounds tested by Armstrong the length of one of the hydrocarbon chains was increased to contain from three to twelve carbon atoms; this increases the hydrophobic property of the molecule.

In 1965, Armstrong & Binstock showed that in squid axons bathed in a 440 mM-K solution, and injected with TEA, the outward current associated with the delayed K channels was very nearly abolished whilst the inward current was largely unaffected. In axons injected with a lower concentration of TEA, Armstrong (1966) was able to study the kinetics of the blockade. Instead of increasing with time, the outward currents declined to a steady level, and inward currents, which normally decline monotonically as K channels close at the end of the depolarizing step, reached a peak and then declined more slowly than in the absence of TEA. From these studies it was deduced that internal TEA blocks K currents when these are outward, though the blockade takes longer to develop when the TEA concentration is reduced. When the K current is inward, TEA is displaced from its blocking site within the channel

and pushed back into the axoplasm. The slow decline in inward currents in TEA-treated axons was noted as evidence suggesting that the channel must be cleared of TEA before the activation gate can close (Armstrong, 1966).

In general, as the length of one of the hydrocarbon chains is increased the blockade becomes stronger (Armstrong, 1969, 1971, 1975a,b). Thus the nonyltriethylammonium ion, in which one of the ethyl chains of TEA is replaced by the straight chain C_9H_{19}, is more potent than pentyltriethylammonium, which is more potent than TEA when each is applied internally. The explanation suggested by Armstrong is that the hydrocarbon chain interacts with the lipid component of the membrane while the charged part of the molecule occludes the channel.

Hucho (1977) has shown that the binding site of the photoaffinity label 4-azido-2-nitrobenzyltriethylammonium fluoroborate in homogenised crayfish axons is likely to be a phospholipid or small proteolipid. The main evidence that the label binds to a K channel component is that nonyltriethylammonium is able to displace the photolabel from its binding site before covalent binding occurs, and that the photolabel blocks delayed currents in frog sciatic nerve, though with a lower affinity than TEA (Hucho, Bergman, Dubois, Rojas & Kiefer, 1976).

The kinetic model developed by Armstrong to account for the action of internal quaternary ammonium ions on the K channel assumes that only one such ion blocks each K channel. Moreover, it is assumed that only open channels are blocked; this is based on the observation that in axons injected with quaternary ammonium ions, the delayed current during a large depolarization increases normally at first, reaches a peak and then declines. In axons

injected with nonyltriethylammonium, this drug-induced inactivation can be complete.

Recovery from the blockade has also been studied in nonyltriethylammonium-injected axons. Recovery is accelerated by increasing the external potassium concentration or by holding the membrane at a more negative potential (Armstrong, 1971, 1975a,b); in both cases the inward K current is increased. However, since large hyperpolarizing pulses applied after block has occurred delay the late phase of recovery, the presence of nonyltriethylammonium within the channel may interfere with the ability of the activation gate to close, as suggested from the experiments with TEA (Armstrong, 1966), or the gate may close trapping the blocking ion (Armstrong, 1971, 1975a,b).

From these studies, Armstrong has concluded that the activation gate is at, or close to, the inner end of the K channel and that this end of the channel is sufficiently large to accommodate a hydrated K ion or TEA, both of which have a radius of about 8Å. Long chain derivatives of TEA are also accommodated since the long hydrocarbon chain can penetrate the hydrophobic part of the membrane. The outer part of the channel, which represents the selectivity filter, is narrower since it excludes TEA and its derivatives. K^+, however, can pass through the selectivity filter once it has shed most of its water of hydration.

In general, quaternary ammonium ions are without effect when applied externally to squid axons (Armstrong & Binstock, 1965; Armstrong, 1969); this indicates that these cations do not penetrate the membrane to any great extent and that the blocking site is only accessible from the axoplasm.

In a comparable series of experiments, Armstrong & Hille (1972) showed that the effects of TEA, pentyltriethylammonium ion and

nonyltriethylammonium ion applied internally to the frog node of Ranvier were strikingly similar to those reported for squid axons. Hence it is generally assumed that the receptor for internal quaternary ammonium ions is similar in both preparations.

Fink & Wettwer (1978) have investigated the effects of iontophoretic injection of TEA into frog skeletal muscle fibres, and report a concentration-dependent depression of the delayed current when this is outward or inward. Whilst the results are not described in detail, it was shown that when sufficient TEA is injected to reduce the outward current by 76% of the control, the current increases monotonically and without the initial delay observed in squid axons (Armstrong, 1966) or myelinated nerve fibres (Hille & Armstrong, 1972) containing TEA. This suggests that the blockade of delayed K channels in muscle by internal TEA is independent of channel gating. On the other hand, such a result is also to be expected if the activation gating mechanism is between the TEA receptor and the sarcoplasm, but the kinetics of channel gating are slow compared to the rate of formation and dissociation of the TEA-receptor complex (Armstrong & Hille, 1972).

In contrast to the squid axon, external quaternary ammonium ions block the delayed K currents in frog muscle (Kao & Stanfield, 1970; Stanfield, 1970a; Fink & Wettwer, 1978; see also Hagiwara & Watanabe, 1955), in frog node (Hille, 1967; Vierhaus & Ulbricht, 1971; Armstrong & Hille, 1972) and in Xenopus node (Koppenhöfer, 1967). Since this blockade is more or less independent of the membrane potential (Hille, 1967; Stanfield, 1970a), it is

likely that the receptor is on the outer surface of the membrane and is separate from the receptor reached by internal quaternary ammonium ions (Koppenhöfer & Vogel, 1969; Armstrong & Hille, 1972). In frog muscle (Stanfield, 1970a) and in Xenopus node (Koppenhöfer, 1967) external TEA also slows the rate of K activation, though in frog node (Hille, 1967; Armstrong & Hille, 1972) no effect on the kinetics of K activation is seen. The significance of this is at present unknown.

Amines, and in particular the aminopyridines and strychnine, have also been used for the study of K channel mechanisms. An important feature of these molecules is that they exist in both cationic and neutral forms. The neutral form is lipid soluble, which might account for the fact that in nerve the aminopyridines block the delayed rectifier in the same way whether they are added to the internal or external solution. It also accounts for the fact that external application of strychnine has the same effect as internal application of methylstrychnine, which, since it is a quaternary ammonium ion, is unlikely to cross the membrane (Shapiro, 1977a,b).

Interest in the aminopyridines as K channel blockers began when Pelhate and Pichon (1974) reported that 4-aminopyridine (4-AP) blocked the delayed rectifier of cockroach axons about 400 times as effectively as TEA, but was without effect on the Na current. This specific action of aminopyridines has been confirmed in studies on squid axons (Meves & Pichon, 1977; Yeh, Oxford, Wu & Narahashi, 1976a; Kirsch & Narahashi, 1978), myelinated nerve fibres (Ulbricht & Wagner, 1976), Myxicola giant axons (Schauf, Colton, Colton & Davis, 1976), and frog skeletal muscle (Gillespie & Hutter, 1975). However in Myxicola axons (Schauf, Colton, Colton & Davis, 1976) 2-, 3- and 4-AP are not as potent as TEA.

In the present context, the most interesting finding is that the action of 4-AP on skeletal muscle differs in some respects from its action on nerve. In nerve (Meves & Pichon, 1977; Yeh et al., 1976a,b; Ulbricht & Wagner, 1976),4-AP in concentrations of about 1 mM or less reduces inward and outward delayed currents. The blockade is also time- and voltage-dependent: in the steady-state the blockade decreases as the membrane potential is made more positive. This is in contrast to the blockade produced by intracellular quaternary ammonium ions which increases under those conditions (Hille, 1975a). In addition, the rate of recovery from block during a depolarizing step is considerably faster than the rate of restoration at the holding potential in a variety of conditions. This voltage- and time-dependence has three consequences. First, 4-AP slows the onset of the K current during depolarization under voltage clamp conditions. Secondly, repetitive depolarization accelerates the rate of rise of the K current during the second and subsequent pulses in a manner which depends on the preparation, the pulse interval and duration, and the concentration of 4-AP. Thirdly, since the rate of recovery during a depolarizing step is slow compared to the rate of K channel gating in the presence of 4-AP, it is difficult to test the idea of Yeh et al. (1976b) that the release of 4-AP from its binding site occurs predominantly from K channels in which the activation gate is open.

This last point is of considerable interest since it relates to the mechanism of action of the aminopyridines,which is at present unknown. The blockade of Na currents in myelinated nerve by amine anaesthetics is similar in that it is voltage-, time- and frequency-dependent (Courtney, 1975; Hille, 1977a,b). Hille's (1977b) model for the action of these anaesthetics is that

they bind to a site within the channel between the selectivity filter and the activation gate. Access to the site by the cationic form of the drug is achieved from the axoplasm, and only through the mouth of the channel when the gate is open. The drug in its neutral form can by-pass the gating mechanism by diffusing through the lipid portion of the membrane to the site.

Aminopyridines may also act in the neutral form, the aminopyridine-receptor complex being stabilized when the activation gate is shut. On the other hand, since recovery from the blockade does not saturate at potentials at which the K channels are normally fully activated (Meves & Pichon, 1977; Yeh et al., 1976b; Ulbricht & Wagner, 1976), a more direct effect of potential on the degree of blockade is to be expected (Meves & Pichon, 1977). If 4-AP reaches a site within the channel in its cationic form, then from the voltage-dependence of the blockade it is probable that 4-AP enters the channel from the external solution.

In muscle, external 4-AP also blocks the delayed current in a manner which is enhanced by a hyperpolarizing prepulse (Gillespie, 1977). However, the delayed current is not depressed by 4-AP if the prepulse is itself preceded by a depolarization which is assumed to close the inactivation gate for the duration of the hyperpolarizing prepulse. From this, Gillespie (1977) has concluded that 4-AP^+ is attracted into the channel by the hyperpolarizing prepulse only when the inactivation gate is open. Thus the inactivation gate is between the 4-AP binding site and the external solution.

Alkaline solutions slow the repolarization phase of the action potential in frog muscle fibres stimulated frequently in

the presence of 4-AP; this effect is ascribed to the action of sarcoplasmic 4-AP$^+$ (Gillespie, 1977; see also Gillespie & Hutter, 1975). In these conditions, the delayed currents resemble those recorded in nerve with intracellular nonyltriethylammonium ions (Armstrong, 1971; Armstrong & Hille, 1972): that is, the current increases normally at the start of the depolarizing step, but after a delay becomes inactivated by the drug. However, this result, which has been confirmed by iontophoretic injection of 4-AP into muscle (Fink & Wettwer, 1978), is consistent with the view that the activation gate is close to the inner end of the channel (Gillespie, 1977) only if it is assumed that internal 4-AP reaches its binding site in the channel via a hydrophilic pathway.

The tertiary amine, strychnine, also blocks delayed currents in nerve in a manner which resembles the block by strongly hydrophobic quaternary ammonium ions (Shapiro, 1977a), to which it is closely related. The most interesting feature of this blockade is that it is a much steeper function of the membrane potential than that shown by internal TEA (Hille, 1975a). This leads to the result that the larger molecule (strychnine) is able to penetrate further into the K channel from the axoplasm than TEA (Shapiro, 1977a). A possible explanation for this is that strychnine is able to move through part of the membrane field with its hydrophobic end in the lipid and its charged part in the channel. In this way the effective dimensions of the molecule would be reduced.

One advantage of using the alkali metal ions (Li^+, Na^+, K^+, Rb^+ and Cs^+) as probes of K channels is that their physical and chemical properties are generally better characterised than those of large organic molecules. The first observation that the alkali

metals interfered with the movement of K^+ in delayed channels was made by Baker, Hodgkin & Shaw (1962) who found that axons perfused internally with Cs_2SO_4 instead of K_2SO_4 developed long-duration action potentials before they became inexcitable due to depolarization of the resting membrane. That this was due to a decrease in the efflux of K^+ during the action potential was confirmed by Sjodin (1966) working with intact axons injected with Cs^+, and by Chandler & Meves (1965) and Adelman & Senft (1966) who used voltage-clamped axons in which part of the internal K^+ was replaced by Cs^+. Other internal alkali cations also reduce the delayed K current, the order of decreasing effectiveness being Cs > Rb > Na (Chandler & Meves, 1965; see also Bezanilla & Armstrong, 1972; French & Adelman, 1976).

A number of other experiments concerning the actions of Cs^+ on delayed K channels can be summarized by saying that internal Cs^+ reduces the delayed current in nerve when this is outward, while external Cs^+ blocks inward but not outward K currents (Adelman, 1968; Adelman & Senft, 1968; Bezanilla & Armstrong, 1972). Similar results have been obtained by Dubois & Bergman (1975, 1977) using frog myelinated nerves. While recent experiments confirm that internal Na^+ reduces outward K currents in squid axons (Bezanilla & Armstrong, 1972; French & Wells, 1977) and in frog node of Ranvier (Bergman, 1970), external Na^+, like external TEA, is without effect on delayed K channels in the squid (Bezanilla & Armstrong, 1972).

In nerve, the effectiveness of internal Li^+ (Bezanilla & Armstrong, 1972), Na^+ (Bergman, 1970; Bezanilla & Armstrong, 1972) and Cs^+ (Adelman & Senft, 1966; Dubois & Bergman, 1975, 1977; Bezanilla & Armstrong, 1972) as K channel blockers increases as

the membrane potential is made more positive. The effect of Cs^+, the largest of the alkali cations considered (ionic radius = 1.69Å), has been used to support the view that the inner mouth of the delayed channel is wider than the outer part of the channel (Bezanilla & Armstrong, 1972; Armstrong, 1975a,b) such that Cs^+ can only enter the inner part. In agreement with this, Pickard et al. (1964), Sjodin (1966) and Hille (1973) have demonstrated that Cs^+ does not pass through delayed channels in nerve to any great extent. On this basis, however, the outer part of the channel must also be enlarged since there is evidence that Cs^+ is able to penetrate a considerable distance into the channel from the outside in these preparations (Bergman, 1975, 1977; Adelman & French, 1977). The effect of Cs^+ on inwardly rectifying K conductances is discussed in chapter 5.

Another interesting property of ionic channels is their ability to distinguish between different ions, and particularly, the alkali metals. Chapter 4 deals with the selectivity of the delayed K channel in muscle and compares the results with previous studies in nerve. The aim here is to outline some of the possible mechanisms which underlie selectivity in excitable cells. Reference is made to experiments with Na and K channels.

In 1965, Chandler & Meves showed that axons perfused internally with a high K solution and bathed in a K-free Ringer in which choline replaced Na^+, developed early outward K currents at potentials at which the early current in intact axons would have been inward, and carried by Na^+. Moreover, the time course of the early K permeability change was similar to that normally shown by Na^+. From the reversal potential of the early current in the presence of different alkali cations, the authors deduced that

the selectivity sequence for the Na channel was $P_{Li} \approx P_{Na} > P_K > P_{Rb} > P_{Cs}$. The selectivity sequences for the Na channels in myelinated nerve fibres (Hille, 1972) and frog muscle (Campbell, 1976) are similar.

In almost all biological and non-biological systems, a large number of which are discussed by Diamond & Wright (1969), only eleven selectivity sequences comprising the five alkali cations given above are expressed, although more than a hundred different permutations of order exist. Eisenman (1962, 1963) has investigated the mechanism of selectivity shown by cation-selective glasses, and suggested that selectivity in membranes is achieved in a similar way (Eisenman, 1963, 1965; see also Diamond & Wright, 1969; Jack, Noble & Tsien, 1975). These glasses possess fixed negative charges which bind the cations: preferential binding is shown towards the cation, which, in moving from its hydrated state in solution to its dehydrated state as part of the ion-site complex gives rise to the most negative change in free energy. Sites with a high field strength, such as those with a high density of fixed negative charges, or those able to approach close to the cations, show a preference for small cations. Thus the sequence shown by these sites is Li > Na > K > Rb > Cs (sequence XI). At the other extreme, sites with a low field strength (low density of negative charges, or a remote site) tend to bind large cations, producing the sequence Cs > Rb > K > Na > Li. The sequences shown by Na channels in nerve (Chandler & Meves, 1965; Hille, 1972; Campbell, 1976) are those expected for a site with a relatively high field strength.

In ion selective glasses, the permeability ratio P_A/P_B for cations A^+ and B^+ depends not only on the relative occupancy of

the sites by A^+ and B^+ under equilibrium conditions (which depends on the field strength of the site and the size of the cation), but also on the relative mobilities of the cations in the glass (U_A/U_B). This is analogous to the situation in biological membranes where the binding term is usually replaced by a constant which reflects the relative partitioning of A^+ and B^+ between the solution and the membrane.

Mullins (1975) has argued against the notion that equilibrium binding is a suitable mechanism for selectivity in ionic channels on the grounds that the ion which is the tightest bound would have the lowest mobility in the channel. Although this may be true in some cases, Eisenman (1965) cites the example of a K selective glass which binds 34 K^+ ions for every Na^+ ion; U_K/U_{Na} is 0.3, thus although P_K/P_{Na} is only about 10.2 (that is, 34 x 0.3), the selectivity sequence is unchanged from that predicted from equilibrium binding.

From their theoretical treatments of selectivity in aqueous pores, Armstrong (1975b; see also Amstrong, 1975a; Armstrong & Bezanilla, 1972) and Hille (1975a,c) have concluded that equilibrium binding may play a role in determining selectivity but that it is not the only mechanism. They consider ionic channels to be systems of energy wells and peaks such that the progress of an ion in each channel is described by Eyring rate theory (Woodbury, 1971). A permeant ion is able to negotiate these peaks but an impermeant ion will be unable to cross either the outer energy peak, or an internal peak. In the latter case, the impermeant ion would interfere with the movement of permeant ions in the pore in a potential-dependent manner. In this treatment, selectivity is found to be a function of the heights of the energy peaks and independent of the depth of the wells. The

depth of energy wells, on the other hand, determines the mobility of cations in the pore. Thus the properties of the binding site(s) associated with peaks will influence selectivity since for a pair of cations the peak height will be lower for the preferentially bound cation.

Pore size provides an explanation for the exclusion of large ions which is not based on the assumption that the postulated binding site has a low field strength. Clearly, an ion whose dehydrated radius is larger than that of the channel at its narrowest point will be impermeant. By setting the minimum pore diameter to 3.0-3.3Å, Hille (1973, 1975a) has accounted for the fact that all cations which have diameters in the range 2.66- 3.0Å (that is, K^+, Tl^+, Rb^+, and NH_4^+) are permeant in the delayed K channels of frog myelinated nerve fibres (Hille, 1973) and squid axons (Bezanilla & Armstrong, 1972; Armstrong, 1975a,b; Landowne, 1975; Binstock & Lecar, 1969), whereas those inorganic and organic cations which would only fit into a pore with a diameter of at least 3.3Å to 8Å (for example, Cs^+, 3.38Å and TEA^+, 8Å) are excluded.

By comparison, the minimum pore diameter of Na channels is larger, being 3.1Å x 5.1Å in the frog node (Hille, 1971, 1972, 1975a,c) and in frog muscle fibres (Campbell, 1976).

One of the most interesting findings concerning the permeability of organic cations in the Na channel is that hydroxylammonium, which has the structure H_3N^+-OH, and dimensions of about 4.5Å x 3.8Å x 3.8Å, is almost as permeant as Na^+, whereas methylammonium (H_3N^+-CH_3), which is of a similar size to hydroxylammonium, is not measurably permeant (Hille, 1971). The explanation for this is that hydroxylammonium is able to form hydrogen bonds with the pore wall: hydrogen bond formation reduces the

effective diameter of the cation so that it is not excluded on grounds of size, and it also reduces the magnitude of the energy barrier presented by the selectivity filter since the cation is essentially solvated within the pore. Hydrogen bond formation also accounts for the fact that another four organic molecules are permeant in Na channels whereas their methyl ($-CH_3$) derivatives are not (Hille, 1971, 1975a).

The hydrogen bond consists of a hydrogen atom bridging two electronegative atoms. In biological systems, the electronegative atoms are usually oxygen or nitrogen, thus Hille (1971) postulates that the selectivity filter of the Na channel consists of a ring of 6 oxygen atoms which allow the passage of Na^+ hydrated by up to three water molecules. At least one of these oxygens is believed to belong to a carboxylic acid group (see below).

The model of the selectivity filter developed by Hille (1973) for the K channel of nerve consists of a ring of five oxygens (one less than for the Na channel) which are arranged to form an opening of 3.0Å, through which K^+ passes in association with up to two water molecules. Ammonium, which, with a diameter of about 3.0Å, is the largest of the permeant cations, is assumed to form hydrogen bonds with up to two oxygen atoms. Since ammonium is assumed to form an electrostatic bond with a third oxygen belonging to a carboxyl group, two of the oxygen atoms in the model can be replaced by other atoms.

One reason for assuming that the channels are lined by oxygens rather than nitrogen atoms is that a number of lipid soluble carrier molecules, such as valinomycin and nonactin, form complexes with single alkali cations, which they are then able to

transport across the membrane. In valinomycin and nonactin, the transported cation is held in a ring of six and eight oxygen atoms, respectively (Ohnisi & Urry, 1970; Urry, 1971; Kilbourn et al., 1967). However, both these carriers transport K^+ in preference to Na^+.

More direct evidence concerning the nature of the groups which play a role in selectivity in Na and delayed K channels comes from titration experiments. Some of these are discussed in chapter 3. Here, it is sufficient to say that in a number of preparations the maximum Na and delayed K conductances are reduced at low pH in a manner which suggests that this is due to the titration of a carboxylic acid group which is part of the way across the membrane (see, for example, Woodhull, 1973; Hille, 1973). In the case of Na channels, this view is also supported by experiments which show that the specific binding of tritiated tetrodotoxin (TTX) and saxitoxin (STX) to Na channels in unmyelinated nerve fibres (Henderson & Wang, 1972; Henderson, Ritchie & Strichartz, 1973, 1974) and the reduction in the maximum Na conductance in myelinated nerve fibres by tetrodotoxin (Ulbricht & Wagner, 1975a,b) are reduced at low pH. The apparent acid dissociation constant (pK_a) for the proton and toxin binding site is about 5.5 for TTX and 5.9 for STX (Henderson et al., 1974). In intact nerve (Ulbricht & Wagner, 1975a) the pK_a for this site is voltage-dependent, supporting the notion that the carboxylic acid group is inside the channel. It is interesting to note, however, that the reduction in the maximum Na conductance by TTX in the same preparation is independent of the holding potential (Ulbricht & Wagner, 1975a).

The model developed by Mullins (1959, 1975) to account for selectivity in ionic channels assumes that during permeation an ion is totally dehydrated, or retains one or two hydration shells depending on the diameter of the orifice formed by the groups lining the channel. Na and K channels are regarded as moderately selective, and since the dimensions of the alkali metals with one hydration shell are more nearly equal than those of the dehydrated ions, Mullins postulates that the alkali metals move through both channels with one hydration shell, except for the inner portion of the K channel in nerve which accommodates two hydration shells. A further assumption is that the diameter of the ion with one shell of hydration must be close to that of the orifice for the cation to be permeant, so that in this model both small and large cations can be excluded from the pore on grounds of size. Moreover, the diameter of the outer portion of the K channel must be less than that of the Na channel if K channels are to be more permeable to K^+ than to Na^+, and Na channels more permeable to Na^+ than K^+.

An important argument against Mullins' model is that it makes no provision for the influence on selectivity of electrostatic interactions between the charge on the ion and charges associated with the channel, whereas the experiments described above argue strongly in favour of the view that fixed anions play a role in determining the permeability of ionic channels.

Throughout this chapter it has been assumed that K^+ moves across the membrane by way of aqueous pores. It is appropriate, therefore, to conclude this chapter by reviewing the evidence which supports this hypothesis, particularly in the case of the delayed K conductance. Some of the evidence has been considered in papers by Armstrong (1975a,b,c).

The first line of evidence relates to calculations by Parsegian (1969) of the energy requirements for four types of ion movement across a lipid layer with a thickness comparable to that of a cell membrane. The results show, as one might expect, that there is a considerable energy barrier to the movement of single ions. The permeation of covalently bonded ion pairs requires less energy, but, as Parsegian has pointed out, the electrolytes involved in biological systems are unlikely to form such bonds. Moreover, the movement of covalently bonded atoms would not be expected to be detected as a current.

The energy required is significantly reduced if the ion crosses the membrane by way of an aqueous pore, or as part of a lipid-soluble carrier-ion complex. Further, for the examples considered by Parsegian (1969) (that is, an ion with a diameter of 4Å, and a pore or carrier with a diameter of 10Å), the energy required for movement through the pore is some 2.5 to 4 times less than that associated with the carrier mechanism.

This result alone is insufficient evidence for the assumption that ions move by way of pores since the energy required for the formation and maintenance of pores and carriers is not taken into account (Parsegian, 1969). However, Armstrong (1975a) has argued that the temperature dependence for the movement of Na^+ and K^+ across the membrane of the squid axon is much lower than that expected from Parsegian's data for the carrier mechanism, but is comparable to that expected for a pore.

Secondly, the mode of action of several K channel blocking ions and, in particular, the nonyltriethylammonium ion (Armstrong, 1971) can be explained in terms of a pore model, but it is difficult to interpret the action of these agents in terms of a carrier model (Armstrong, 1975a). This point is

discussed in more detail in chapter 8 in relation to the resting K conductance.

Thirdly, Ussing (1949) has shown that if the movement of an ion, X, across the membrane is unaffected by the presence of other permeating ions, the influx (M^X_{inf}) and efflux (M^X_{eff}) of X will be related by the following expression

$$\frac{M^X_{eff}}{M^X_{inf}} = \left[\frac{[X]_i}{[X]_o}\right]^N e^{zNFV_1/RT} \qquad (1.3)$$

where $[X]_i$ and $[X]_o$ are the internal and external concentrations of X, z is its valence, V_1 is the membrane potential, F/RT is a thermodynamic constant, and where N is 1. In 1955, Hodgkin & Keynes found that eqn. (1.3) described the ratio of unidirectional K fluxes in Sepia axons, provided N was about 2.5. From this, they suggested that K^+ ions move through a pore in the membrane and in single-file, the pore containing two or three K^+ ions at any one time. Single-file behaviour has also been reported for the delayed K conductance in the squid axon (Landowne, 1975; Begenisich & De Weer, 1977) and the resting K conductance in skeletal muscle (Horowicz, Gage & Eisenberg, 1968).

An alternative explanation for these findings is that K^+ ions are transported across the membrane by a carrier molecule which moves only when empty or when occupied by more than one K^+ ion (Hodgkin & Keynes, 1955; Horowicz et al., 1968). Hodgkin & Keynes (1955) have argued against such a model on the grounds that a carrier which transports two K^+ ions is also likely to transport one.

Eventually it may be possible to distinguish between carrier and pore models for the K channel with a technique similar to that

used by Neher, Sakmann & Steinbach (1978). Using a micropipette whose tip was placed on the outer surface of the membrane, these authors have recorded the current flowing through a single channel in a region of muscle membrane which contains extrajunctional acetylcholine receptors. An important conclusion from this work is that acetylcholine-sensitive channels have a constant conductance when open. On the other hand, the conductance associated with the movement of a single carrier of the type suggested by Horowicz et al. (1968) would be expected to have two values since in that model both the occupied and the empty carrier are charged. At any rate, the evidence, though inconclusive, favours the view that K^+ ions move across the membrane by way of channels.

Chapter 2. Solutions and Methods

The preparation

Single or paired sartorius muscles from English frogs, Rana temporaria, were used in all experiments. This preparation is highly suited for electrophysiological work: since the fibres are large and are usually arranged in parallel extending the whole length of the muscle, individual fibres can often be traced for more than 2 mm without further dissection. In addition, in cleaned preparations, the point at which fibres insert onto the pelvic tendon can usually be measured to within 5 or 10 μm; such accuracy is important if consistent values for the membrane current are to be obtained with the three-electrode voltage clamp method (see page 42). There are also no slow fibres in the frog sartorius, as Kuffler & Vaughan Williams showed in 1953. This means that all the fibres belong to the fast or twitch group.

Removal of the sartorius is a standard dissection so only a brief account is given here. The skin was removed from the legs of a frog whose brain and spinal cord had been destroyed. The pelvic girdle was then divided at, or close to, the midline so that at least one sartorius muscle remained intact. The distal tendon of this muscle was ligatured with cotton thread, then cut. The sartorius, together with its pelvic tendon and a piece of pelvic bone, was dissected free of underlying tissue and pinned out deep surface uppermost in a perspex dissecting dish containing isotonic chloride Ringer. With the aid of a binocular microscope, cut fibres from adjacent muscles were removed and the preparation cleaned of excess connective tissue.

The cleaned preparation was allowed to equilibrate for at least 30 mins in a volume of fresh chloride Ringer which exceeded 100 ml. The composition of this solution is given on page 34. In most experiments a further period of equilibration was necessary in either a chloride-free sulphate solution, a hypertonic solution, or in both of these. The composition of these solutions is given in the Solutions and Methods section of individual chapters.

After passing through this series of solutions, the preparation was transferred to the recording chamber and pinned out deep surface uppermost in a volume of Ringer (about 10 mls) sufficient to cover the surface fibres by 1-2 mm. In isotonic solutions, the muscle was stretched to about 130% of its resting length in order to reduce the ability of the fibres to contract, and to assist in penetration. In stretched preparations the effective membrane surface area per unit length may be reduced by as much as 10 - 14% (Dulhunty & Franzini-Armstrong, 1975). The temperature of solutions was controlled by enclosing the chamber in a jacket circulated with a water-ethylene glycol mixture. A glass cover-slip which formed a large part of the floor of the otherwise perspex chamber ensured good heat exchange. The temperature was monitored by a thermistor set into the side of the chamber close to the muscle.

In most experiments the chamber was not perfused since perfusion reduced the efficiency of temperature control and increased the probability that impalements would be lost before the experiment was completed. To change the solution, the chamber was emptied and refilled at least three times with the

new solution. A minimum of 10 mins was allowed for equilibration of the extracellular space, after which the solution was again renewed. In those experiments in which perfusion was used, the temperature of the Ringer was controlled before it entered the chamber.

Solutions

All solutions were made up in distilled water using Analar grade reagents wherever possible. Notable exceptions were Cs_2SO_4, Rb_2SO_4, Li_2SO_4 and Tl_2SO_4 (Laboratory Reagent, Hopkin & Williams). More refined salts of caesium and rubidium were used in later experiments (Suprapur, Merck) but these gave the same results as Laboratory Grade Reagents. Ringer solutions were refrigerated during storage; those containing sucrose were used for not more than 1 week. Tl_2SO_4 precipitated within 24 hours when prepared as a stock solution; similarly a precipitate appeared in Ringer solutions containing Tl_2SO_4 when stored overnight. However, in the course of an experiment a precipitate was not observed when solid Tl_2SO_4 was added to the Ringer immediately before use, so this procedure was always followed.

Chloride Ringer. This was prepared from 1 M stock solutions of chloride salts. Chloride Ringer was used for dissection and usually had the same composition as that given by Adrian (1956): 115 mM-NaCl; 2.5 mM-KCl; 1.8 mM-$CaCl_2$; 2.15 mM-Na_2HPO_4; 0.85 mM-NaH_2PO_4; pH 7.2. This Ringer was modified to contain the same buffer as the experimental solution in which the records were obtained. In chapter 7, phosphate was replaced by 1 mM HEPES (N-2-hydroxyethylpiperazine-N'-2-ethanesulphonic acid), and the pH adjusted to 7.2 with NaOH. The composition of

chloride Ringer containing tris-maleate plus acetylglycine as buffer is given in the Solutions & Methods section to chapter 3.

Sulphate Ringer. These solutions were prepared from 0.5 M stock solutions of Na_2SO_4 and K_2SO_4, and a 10 mM stock solution of $CaSO_4$. The composition of the different Ringer solutions used is based on Table 1 of Hodgkin & Horowicz (1959), and is described in the Solutions & Methods section of individual chapters.

Hypertonic solutions. In order to study the properties of the sodium conductance or the delayed potassium conductance it is necessary to depolarize the voltage-clamped membrane to potentials positive to the mechanical threshold. Since in isotonic solutions the resulting movement is often sufficient to dislodge the electrodes, in such experiments the ability of the muscle to contract was greatly reduced by the addition of 350 mM sucrose to the Ringer. This increased the tonicity of the solution about 2.5 times (Adrian, Chandler & Hodgkin, 1970a; Stanfield, 1970a, 1975). Although the twitch is reduced or abolished in hypertonic solutions, the electrical properties are largely unaffected (Howarth, 1958; Hodgkin & Horowicz, 1957). Since muscles survived less well in hypertonic solutions than in isotonic Ringer, most of these experiments were performed in the cold.

Tetrodotoxin (TTX: Sankyo) This was present in some experiments selectively to block sodium channels. The stock solution (10^{-4} g/ml) was prepared by adding 1 mg TTX to 10 ml distilled water and was kept at about $4^{\circ}C$. 0.1 ml of stock solution was added to the Ringer in the recording chamber to give a working concentration of 10^{-6} g/ml.

Microelectrodes

Glass microelectrodes (Ling & Gerard, 1949) were used for

recording the membrane potential of muscle fibres and for injecting current into the cells. Electrodes were pulled from lengths of low-sodium, capillary glass tubing (Pyrex-Corning; outside diameter 1.2 mm) and were filled with electrolyte solution by boiling for about 2 mins under vacuum. Filled electrodes were stored tip downwards in the filling solution at about 4°C.

Microelectrodes used for recording were normally filled with 3M-KCl solution (Nastuk & Hodgkin, 1950). Selected electrodes had resistances between 7 MΩ and 25 MΩ and tip potentials less negative than -5 mV; such electrodes would have a tip diameter of about 0.5 μm (Nastuk & Hodgkin, 1950), which is small compared to the diameter of muscle fibres (about 40 - 120 μm). Electrodes were normally prepared within 24 hours of use and those with the appropriate tip characteristics on the morning of the experiment were selected. Longer periods of storage tended to yield electrodes with large tip potentials.

Microelectrodes for use in current injection were filled with 2 M-K_3 citrate since the resistance of citrate electrodes does not change during the passage of current as much as the resistance of KCl-filled electrodes. Selected electrodes had resistances between 4 MΩ and 10 MΩ and tip potentials less negative than -5 mV. Electrodes stored for at least 24 hours were preferred since storage tended to reduce their resistance and improve their current passing ability. Erosion of the tip by citrate solution is probably responsible for these changes.

KCl-filled microelectrodes are unsuitable for use in solutions containing thallous ions (Mullins & Moore, 1960). From the

solubility product of TlCl (Sillén & Martell, 1964), it is estimated that this salt will precipitate in the presence of 3M-KCl when the Tl^+ concentration exceeds 10^{-4}M. Such precipitation blocks the electrodes, as reported by Mullins & Moore (1960) and observed in the present study. Since resting potentials recorded by citrate electrodes in thallous-free Ringer were comparable with those recorded with KCl electrodes (see chapter 7), citrate electrodes were used for recording the membrane potential in thallous solutions.

Recording apparatus

The general arrangement for recording potential changes between a microelectrode and a reference electrode is shown in Fig. 2.1A. Microelectrode holders were prepared from plastic syringe cases. The shaft of the electrode was inserted through a small hole (about 1.25 mm) drilled in the sealed end of the case, and was supported by a column of cured silicone rubber compound. The electrolyte in the microelectrode formed a liquid junction with a chloride Ringer solution contained in the upper part of the electrode holder, and into which dipped a chlorided silver wire. The wire was secured by a rubber bung, and connected to the input lead of a voltage follower.

Error in the measurement of cellular potentials can arise when there is a potential at the Ringer - Ag/AgCl wire junction. This potential was offset by including a similar junction in series with the reference (bath) electrode (Fig. 2.1A). Here the chlorided silver wire dipped into a well of chloride Ringer which was in electrical continuity with the solution in the muscle bath via a glass bridge containing 1% agar in Cl Ringer.

Fig. 2.1. A. Diagram to show the main features of the recording apparatus. The membrane potential (V_1) recorded by the microelectrode is fed to the input of a voltage follower (comprising amplifier A1) via a chloride Ringer - Ag/AgCl wire junction. The electrolyte in the microelectrode is 3 M-KCl or 2 M-K_3 citrate. Bath potential is recorded by a low resistance electrode consisting of a 1% agar in chloride Ringer bridge. This signal is also fed to the input of a voltage follower (comprising amplifier A0) via a chloride Ringer - Ag/Agcl wire junction. The output from the calibrator (cal.) is used to back-off the membrane potential once the microelectrode is in the fibre. a and b are test points for use in the measurement of microelectrode resistance. Also shown is the arrangement used to differentiate the membrane potential (dV_1/dt).

B. The two-microelectrode constant-current method. The fibre is impaled by two microelectrodes, one to record the membrane potential V_1 (see Fig. 2.1A) and the other to inject current. The total electrode current (I_o) is determined by the command signal (S) and by an offset current control. I_o is controlled electronically by the feedback amplifier (FB) and measured by an operational amplifier (741) with a resistor (1 MΩ) in the feedback loop. The amplifier has FET inputs.

A

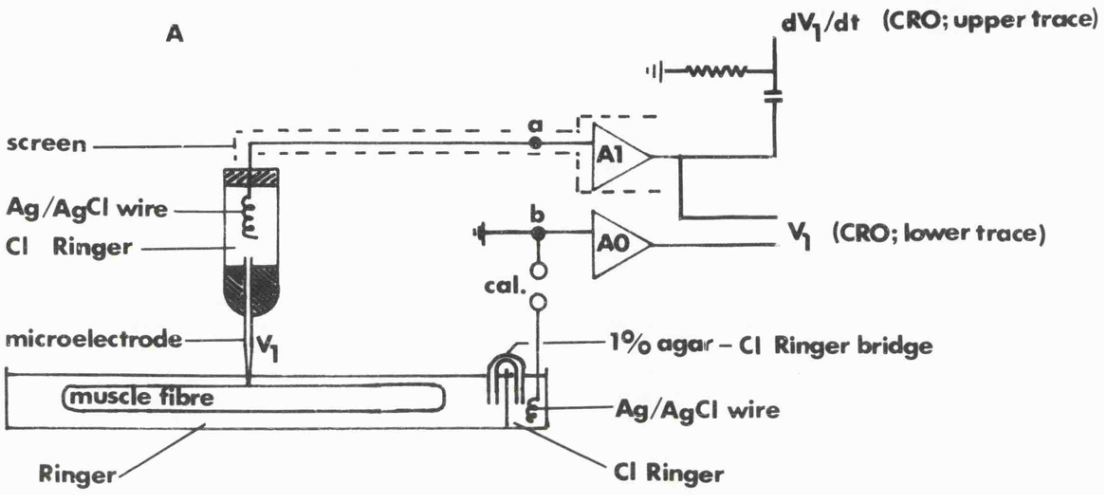
dV_1/dt (CRO; upper trace)
screen
a
A1
Ag/AgCl wire
Cl Ringer
b
A0
V_1 (CRO; lower trace)
cal.
microelectrode
V_1
1% agar – Cl Ringer bridge
muscle fibre
Ag/AgCl wire
Ringer
Cl Ringer

B

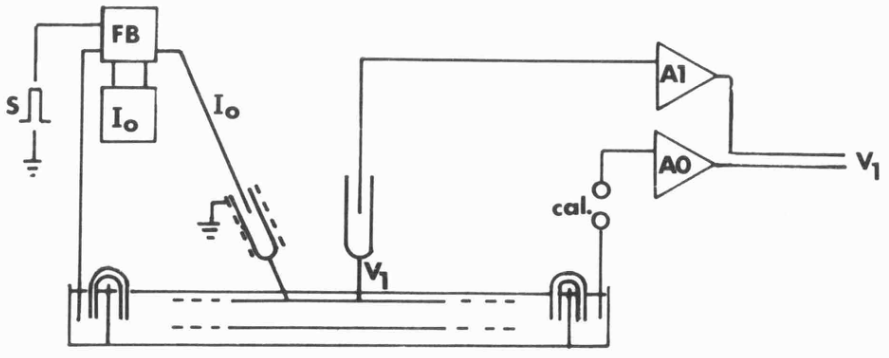
FB
S
I_o
I_o
A1
A0
V_1
cal.
V_1

The junction potential measured with the reference electrode at earth, and with the Ringer in the holder in contact with the Ringer in the bath was usually less than 1mV.

The potential, V_1, recorded by the microelectrode in Fig. 2.1A was fed to the input stage of a voltage follower employing amplifier A1 (Philbrick 1009; input impedance 10^{11} ohms). This was set to have a gain of 10. In order to reduce stray capacity, the voltage follower and its input lead were surrounded by a metal screen which was driven by the inverting input of A1. In addition, A1 was mounted on the micromanipulator close to the microelectrode. A resistor and capacitor feed back from the output to the non-inverting input of A1 and provide a fine and coarse adjustment to compensate for slowing of the signal.

The reference (bath) electrode was connected via a calibrator (cal.) to the input of a second amplifier, A0, (Philbrick 1009) which was the same as A1. A0 was housed in an earthed box. The gain of A0 was set to match the gain of A1. This adjustment was performed routinely: a 100 mV signal from the calibrator was connected directly to the inputs of A1 and A0. The gain of A0 was then altered until the output of the two amplifiers differed by less than 0.1 mV. The rejection of common mode signals was therefore better than 0.1%.

The calibrator was built to a design similar to that described by Adrian (1956). It employed a Weston cell as an internal reference source, and had an output of $\pm$ 210 mV in 100, 10 and 1 mV steps.

With the output from the calibrator at zero, the signal applied to the lower vertical amplifier of the oscilloscope in

Fig. 2.1A is $A(V_1 - V_0)$, where A is the gain of A1 and A0, and V_0 is the potential recorded by the agar-Ringer bridge. So that the present symbols are the same as those used by Adrian et al. (1970a), $A(V_1 - V_0)$ is shortened to V_1.

In most cases a Tektronix 502A dual beam oscilloscope was used. The output from one vertical amplifier of the oscilloscope was connected to an audio-amplifier so that changes in the displayed signal could be monitored while still observing the preparation. The displayed signal was also photographed on stationary 35 mm film; the negatives were enlarged and projected onto a sheet of graph paper from which the measurements were made.

Microelectrode resistance

With the tip of the microelectrode in the Ringer (Fig. 2.1A), a 100 mV signal from the calibrator applied between the bath electrode and earth produced a 100 mV deflection on the oscilloscope. If a resistance equal to that of the microelectrode is then connected between the input to A1 and each (between a and b in Fig. 2.1A), the deflection will be reduced to 50 mV. In practice, a 10 megohm resistor was placed in parallel with the microelectrode, and the resistance of the latter calculated from the observed deflection using Ohm's law.

Microelectrode tip potential

With electrical continuity between the Ringer in the electrode holder and that in the bath, the balance between A1 and A0 was adjusted to compensate for small junction potentials. When the microelectrode is included in the circuit, any deflection of the oscilloscope trace should then be due to the tip potential.

The tip of one or two electrodes from each batch was broken on the floor of the bath to confirm that the deflection disappeared.

Resting membrane potentials

When the output from the calibrator is zero, the membrane potential is equal to the potential recorded by a microelectrode inside the muscle fibre minus that recorded by the bath electrode (Fig. 2.1A). The change in potential which occurred during penetration of the fibre was monitored by a sudden fall in pitch or an audio-signal. The oscilloscope trace, deflected during penetration, was returned to its initial position using the calibrator; this enabled rapid measurement of the membrane potential accurate to at least 0.5 mV. Only surface fibres were penetrated, and results from fibres in which the resting potential fell immediately after penetration were discarded.

Action potentials

Action potentials were recorded by an intracellular microelectrode close to the pelvic end of the muscle. Fibres were stimulated intracellularly by a rectangular current pulse of about 5 ms duration. This was applied through a citrate electrode which was inserted at least 1 mm from the recording electrode. Using this method, only one fibre was stimulated at a time so that in a muscle stretched to 130% of its resting length to reduce movement it was possible to record several action potentials from the same fibre. However, only the results from the first action potential were used.

Action potentials were differentiated electrically in order to obtain the maximum rate of rise and fall. The differentiating circuit consisted of a resistor and capacitor and is illustrated

in the upper right hand side of Fig. 2.1A. The time constant (RC) of the circuit was calibrated with a ramp generator. Circuits with a time constant of 17 μs and 100 μs were used.

Constant current experiments using two microelectrodes

This technique was used to obtain action potentials (chapter 3) and other regenerative changes in the membrane potential (chapter 5). The method is illustrated in Fig. 2.1B: it is similar to that used by Hodgkin & Rushton (1946) and Fatt & Katz (1951) except that here the electrode current is controlled electronically.

The muscle fibre was impaled by two microelectrodes; one to record the membrane potential (V_1), the other to inject current (I_o). The recording electrode was inserted first and the resting potential offset by the calibrator, as described above. Insertion of the current electrode was assisted by passing rectangular pulses of current through the electrode. I_o was measured with a 741 operational amplifier with FET inputs and with a 1MΩ resistor shunted by 100 pF in the feedback loop. The input to the feedback amplifier (FB; 741 operational amplifier), which controlled I_o, was connected to the muscle bath via a 1% agar in Cl-Ringer bridge, and an Ag/AgCl wire. Rectangular command pulses (S) were provided by a pulse generator with a 5V output which was fed through decade potentiometers. To reduce the current artifact, as well as the risk of oscillation in the feedback loop, the current electrode was screened by a length of steel tubing to within 2-3 mm of the tip. The screen was connected to earth.

Details of individual experiments are given in the appropriate chapters.

Voltage clamp experiments using two microelectrodes

This method, described by Weidmann (1955) and Takeuchi & Takeuchi (1959), was used to control the membrane potential at a point close to the midpoint of the fibre (chapter 5), and is illustrated in Fig. 2.2A.

Recording and current electrodes were inserted under constant current conditions (see above). The feedback amplifier (FB) was then switched to keep V_1 at the value determined by the command signal (S) and the calibrator (cal.); this was possible through feedback control of the electrode current (I_o). The calibrator was used to hold fibres at the resting membrane potential while the command signal was used to produce stepwise depolarizations and hyperpolarizations.

I_o was measured as the voltage drop across a 100 kΩ resistor shunted by 1500 pF. This gave the recording circuit a time constant of 0.15 ms which was negligible compared to the time at which measurements were made.

Since the membrane is clamped at a point, the applied voltage step spreads electrotonically towards both ends of the fibre. The membrane current density was calculated from the relationship between the membrane potential and I_o using Cole's theorem (Cole & Curtis, 1941).

Voltage clamp experiments using three microelectrodes

This method, devised by Adrian, Chandler & Hodgkin (1966, 1968, 1970a), was used extensively in the course of this work since it allows the membrane current density to be measured directly from the voltage drop along a length of fibre in the terminal region, where changes in the membrane potential with distance during current injection are small (Jack, Noble & Tsien, 1975).

Figure 2.2. A. The two-microelectrode voltage clamp method. The fibre is impaled by two microelectrodes at, or near the mid-point. One records the membrane potential (V_1) and the other injects current (I_o). The membrane potential in the vicinity of the recording electrode is determined by the command signal (S) and the output from the calibrator (cal.), and is maintained by electronic feedback control of the electrode current. I_o is measured as the IR drop across a 100 kΩ resistor shunted by 1500 pF.

B. The three-microelectrode voltage clamp method. The fibre is impaled by two microelectrodes to record the membrane potentials V_1 and V_2 at distances ℓ and 2ℓ, respectively, from the end of the fibre. A third electrode inserted at $2\ell + \ell'$ from the end of the fibre is used to inject current. The method used to control the membrane potential at ℓ and to measure I_o is the same as that described for the two-electrode clamp (see above). The membrane current density (I_m) is related to $V_2 - V_1$ by the approximate expression,

$$I_m = \frac{(V_2 - V_1)a}{3\ell^2 R_i}$$

where a is the fibre radius and R_i is the internal resistivity.

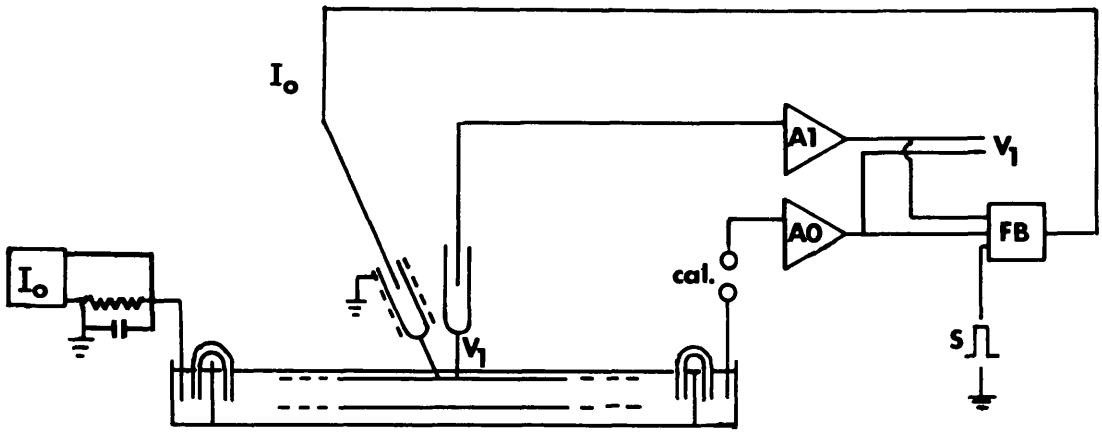

B

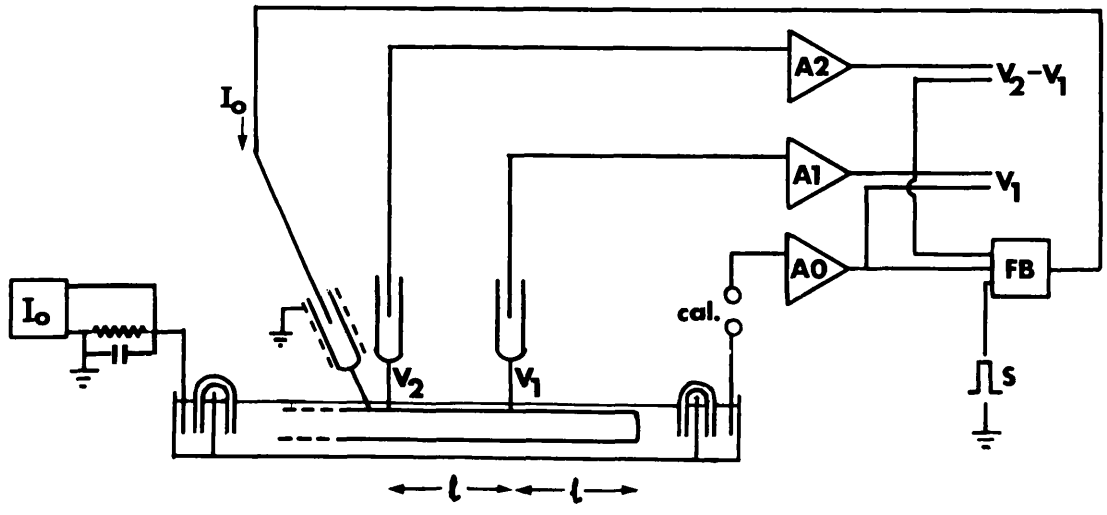

Two microelectrodes were used to record the membrane potentials V_1 and V_2 at distances ℓ and 2ℓ, respectively, from the pelvic end of the fibre as shown in Fig. 2.2B. A third electrode was inserted at distance $2\ell + \ell'$ from the end of the fibre, and was used to inject current. The electrode at ℓ was inserted first and the resting potential backed off with the calibrator. A constant current pulse aided penetration of the fibre by the current electrode and the second recording electrode.

V_2 was fed to the input of amplifier A2 (Philbrick 1009), which was surrounded by a driven screen, and was provided with negative capacity compensation. Inphase signals applied to A1 and A2 were rejected to better than 0.1% by setting the gain of A2. In other respects the apparatus was identical to that for use with two microelectrodes.

Assuming that the fibre is cylindrical, Adrian et al. (1970a) show that the membrane current density (I_m) is related to the potential difference $V_2 - V_1$ by an approximate expression:

$$I_m = \frac{(V_2 - V_1)\, a}{3\ell^2 R_i} \qquad (2.1)$$

where a is the fibre radius, and R_i is the internal resistivity. They show that eqn. (2.1) is accurate to within 5% provided $(V_2 - V_1) / V_1$ is less than 6, or ℓ is less than 2λ. This condition, which was maintained in all experiments, cannot be applied to the regenerative phase of the sodium current: in such cases the error may be greater (Adrian et al., 1970a). Since doubling the inter-electrode distance (ℓ) produces a four-fold increase in $V_2 - V_1$, ℓ was selected according to the magnitude of I_m: ℓ was 110, 125 or 132 μm for large currents (chapters 3 & 4) and 330, 440 or 495 μm for small currents (chapters 5, 6

& 7). ℓ' was usually 50 μm.

As optical measurements of fibre diameter are unreliable, the diameter was assumed to be 80 μm for fibres in isotonic Ringer and for fibres in Ringer made hypertonic by the addition of 350 mM sucrose (Adrian et al., 1970a; Stanfield, 1970a; Almers, 1972a). In hypertonic Ringer, the mean diameter tends to be slightly less than the diameter of fibres in isotonic Ringer (Adrian et al., 1970a; Hodgkin & Nakajima, 1972); however, in the present study a direct comparison between the membrane currents in solutions of different tonicity was not made. R_i was calculated from the values of Hodgkin & Nakajima (1972) assuming a Q_{10} of 1.37 for the effect of temperature. In isotonic solutions, R_i was 180 ohm.cm at 17-18.5°C and 270 ohm.cm at 3-5°C; in hypertonic solutions R_i was 370 ohm.cm at 3-5°C. In view of the assumptions required to calculate I_m, the membrane current is often given in terms of $V_2 - V_1$ and is therefore expressed in millivolts.

Cable properties and fibre radius

The space constant (λ) and fibre radius (a) were determined in the course of some experiments in which fibres were impaled by three microelectrodes (see previous section). A constant current pulse was used to hyperpolarize the fibre at ℓ by about 10 mV, and the steady-state values of I_o, V_1 and $V_2 - V_1$ were recorded. λ was calculated from eqn. (9) of Adrian et al. (1970a):

$$\lambda = \ell \sqrt{\frac{3\,(V_1)}{2\,(V_2 - V_1)}} \qquad (2.2)$$

and the result used to calculate the fibre radius (a) from

$$a^2 = \frac{R_i\, I_o \lambda}{\pi V_1} \cdot \frac{\cosh\,(\ell/\lambda)}{\left[\cosh \frac{2\ell + \ell'}{\lambda}\right]\left[1 + \tanh \frac{2\ell + \ell'}{\lambda}\right]} \qquad (2.3)$$

The internal resistivity (R_i) was assumed. R_i is independent of the fibre diameter (Nakajima & Hodgkin, 1970; Hodgkin & Nakajima, 1972).

Statistics

Standard statistical procedures were used to analyse the results from a group of fibres. In most cases the results are presented as the mean ± the standard error of the mean (mean ± S.E.M) with the number of observations (n) given in parentheses. The mean results for two samples are compared by a Student's t-test; a significant difference between the means is accepted when the probability (P) that they are the same is less than 0.05.

Chapter 3. The effects of pH on the delayed K conductance in frog skeletal muscle fibres.

INTRODUCTION

A number of observations on the pH-sensitivity of nerve can be summarised by saying that pH has two major effects on the early sodium and the delayed potassium currents. First, a reduction in pH shifts the voltage-dependence of the parameters which describe Na activation (Hille, 1968; Drouin & The, 1969; Stillman, Gilbert & Lipicky, 1971; Woodhull, 1973; Drouin & Neumcke, 1974; Schauf & Davis, 1976), Na inactivation (Hille, 1968), and K activation (Drouin & The, 1969; Mozhayeva & Naumov, 1970, 1972a; Hille, 1968; Shrager, 1974; Schauf & Davis, 1976) to more positive values of the membrane potential. This effect is similar to that seen in squid axons (Frankenhaeuser & Hodgkin, 1957; Gilbert & Erhenstein, 1969), in frog skeletal muscle (Costantin, 1968; Campbell & Hille, 1976) and in other tissues (Blaustein & Goldman, 1968; Mozhayeva & Naumov, 1972c; Hille, Woodhull & Shapiro, 1975; Schauf, 1975) when the external Ca^{2+} concentration is raised. It is widely agreed that such shifts are produced by changes in the electrical potential at the surface of the membrane, and that this surface potential is set up by ionized groups which form part of the membrane structure.

Secondly, as mentioned in chapter 1 (page 27), in acidic Ringer the maximum Na and K conductances are reversibly depressed in a manner which suggests that protons are able to titrate some negative charge essential for the movement of ions across the membrane (Hille, 1968, 1973, 1975c; Drouin & The, 1969; Drouin & Neumcke, 1974; Schauf & Davis, 1976).

The experiments described in this chapter were designed to examine the effects of pH on the electrical activity of skeletal muscles. The first experiments extend some of the observations of Brooks & Hutter (1963) on the pH-dependence of the action potential. However, the major part of this work involved the study of membrane currents under voltage-clamp conditions. The results are used to obtain a minimum value for the density of fixed surface charges associated with the delayed K channel.

During the course of these experiments, papers on the pH-sensitivity of the Na conductance (Campbell & Hille, 1976) and the K conductance (Gillespie & Hutter, 1975) in skeletal muscle have appeared. In general, my results confirm these findings and extend those of Gillespie & Hutter.

SOLUTIONS & METHODS

The isotonic chloride Ringer used in the present experiments contained 2.5 mM-KCl, 1.8 mM-CaCl, 117.5 mM-NaCl + NaOH, and was buffered with a mixture of 4 mM Tris (hydroxymethyl) aminomethane, 4 mM maleic acid and 4 mM acetylglycine. The amount of NaOH required to be added to bring the solution to the desired pH (between 4.2 and 9.2) was determined from a titration curve. In order to keep the Na^+ concentration constant, the Cl^- concentration was allowed to vary between 118.5 mM at pH 4.2 and 110.4 mM at pH 9.2. The pH of each solution was checked against one of five standard buffers within 7 hours of use and at the temperature of the experiment, and was readjusted to the correct pH (to within 0.05 of a pH unit), with either NaOH or HCl. The amount of Na^+ (or Cl^-) added at this stage never exceeded 1 mmole/l.

In order to reduce the ability of the muscle fibres to contract, the Ringer was made hypertonic by the addition of 350 mM sucrose for experiments in which the voltage-clamp was used.

Ringer solutions were stored at about 4°C for not more than 3 days (24 hours if the solutions contained sucrose). During storage the pH did not change by more than 0.1 of a pH unit.

The membrane potential was controlled using the three-electrode method of Adrian et al. (1970a; see chapter 2). Initially, an inter-electrode distance of 132 μm was used, but in later experiments this was reduced to 110 μm to facilitate clamp control. All fibres were held at a membrane potential of -100 mV and hyperpolarized and depolarized from this level. In addition, each fibre was clamped at the holding potential for at least 3 mins following impalement to reprime the conductances before measurements were made.

All experiments were performed in the cold (3-5°C, unless otherwise stated) since this increased the time during which useful records could be obtained. Cooling the preparation also slows the membrane currents and this makes it easier to control the membrane potential.

RESULTS

Effect of pH on the resting membrane potential

The mean resting potential of fibres immersed in isotonic chloride Ringer is given in Table 3.1. In the control solution (pH 7.2) the mean resting potential was -88.9 ± 1.3 mV (fourteen fibres). Raising or lowering the pH produced a small depolarization; this was significant at pH 5.2 ($P < 0.05$) but only marginally significant at pH 9.2 ($P \approx 0.05$). Hutter & Warner (1967a) have also reported a small depolarization in acidic conditions while in

TABLE 3.1

Resting and action potentials from muscle fibres in isotonic chloride Ringer at about 4°C

pH	RP‡ (mV)	Overshoot (mV)	$\bar{V}_{rise}$ (V/s)	$\bar{V}_{fall}$ (V/s)	No. of Observations
9.2	-83.8 ± 2.1	48.0 ± 1.2	139.4 ± 4.4	59.8 ± 1.0‡‡	11
8.2	-87.7 ± 1.0	43.7 ± 1.3	127.1 ± 3.3	55.7 ± 1.7	13
7.2	-88.9 ± 1.3	41.2 ± 2.3	120.5 ± 4.6	45.3 ± 1.6	14
6.2	-86.6 ± 2.5	37.9 ± 1.5	100.1 ± 3.3	34.0 ± 1.0	13
5.2	-81.8 ± 2.6	29.0 ± 1.5	46.9 ± 2.2	15.6 ± 1.4	12
4.6	-84.3 ± 2.1	18.7 ± 3.9	25.4 ± 4.5	7.9 ± 1.7	9

‡ Resting potential (= RP) ‡‡ Mean ± S.E. of mean

alkaline conditions the fibres were hyperpolarized. On the other hand, Dörrscheidt-Käfer (1976) has reported depolarizations at pH 4.65 and 10.5 which are larger than the average depolarization seen here in very acidic or alkaline conditions.

Effect of pH on the action potential

Fig. 3.1 shows typical action potentials from eight fibres, either in the control Ringer (pH 7.2) or in a similar solution but at high or low pH. The fibres were stimulated by means of a rectangular current pulse superimposed on an inward current which raised the membrane potential to -100 mV for several seconds prior to stimulation. The current was delivered by a microelectrode inserted at least 1 mm from the recording electrode (see page 40).

The action potentials at the top of Fig. 3.1 were recorded from the same muscle, and show that a reduction in pH from 7.2 (Fig. 3.1a) to 5.2 (Fig. 3.1c) slows both depolarization and repolarization phases of the spike. At pH 9.2 (Fig. 3.1b) the duration of the spike is reduced, and this is associated with an increase in the rate at which depolarization and repolarization occur. Similar results have been reported by Brooks & Hutter (1963).

Effects of pH on the overshoot were more variable, though in most fibres the overshoot was increased in alkaline solutions and reduced when the pH was less than 7.2. This is supported by the finding that in three muscles, the mean overshoot at pH 9.2 is marginally greater than that in the control solution (Table 3.1; $P < 0.05, > 0.02$) while the mean overshoot in the control solution is significantly greater than the value at pH 5.2 (Table 3.1; $P < 0.001$).

The pH-dependent changes in the properties of the spike outlined above were reversible. This can be seen by comparing the

Fig. 3.1 Records of action potentials (V_1) and their derivatives (dV_1/dt) from muscle fibres immersed in normal, acidic and alkaline solutions. Action potentials were recorded with an intracellular microelectrode after the fibres had been hyperpolarized to -100 mV. The fibres were stimulated intracellularly by a brief current pulse delivered by a microelectrode inserted at least 1 mm from the recording electrode, and which was also used to hyperpolarize the fibres. Isotonic chloride Ringer, 3.5-4.5°C.

a-d, records from four fibres in the same muscle. a, pH 7.2; b, pH 9.2; c, pH 5.2; d, pH 7.2. The differentiating circuit has a time constant of 17 μs.

e-h, records from four fibres in a second muscle. e, f & g, pH 4.9; h, pH 7.2. The differentiating circuit has a time constant of 100 μs in e & f.

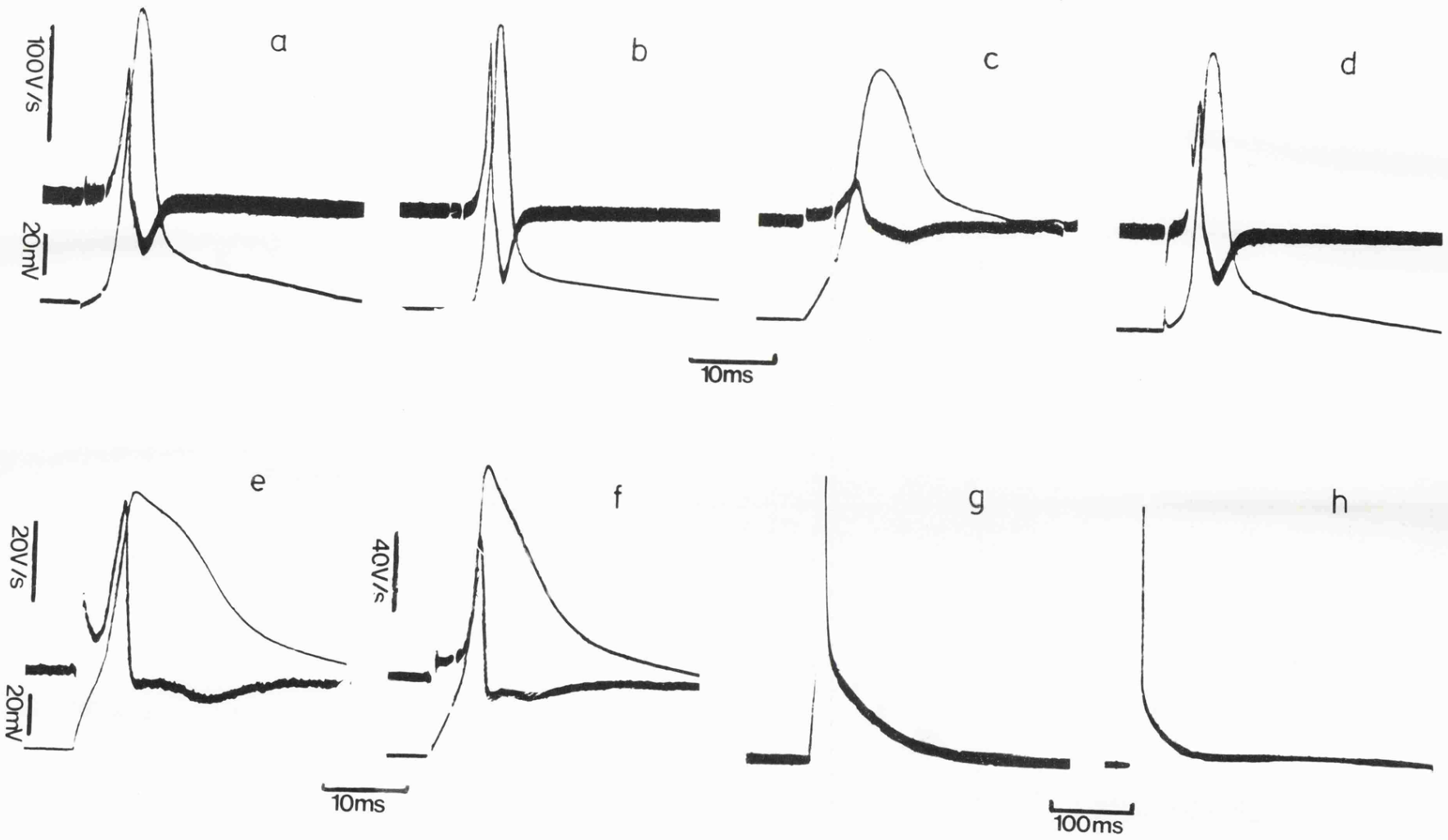
a
b
c
d
100V/s
20mV
10ms
e
f
g
h
20V/s
20mV
40V/s
10ms
100ms

spikes in Fig. 3.1a and 3.1d, which were obtained at pH 7.2 at the beginning and end of the experiment, respectively. In more acidic solutions (pH 4.6 and 4.2), pH-induced changes in the spike appeared to be reversible provided the period of exposure was short.

Records from a muscle exposed to pH 4.9 (Fig. 3.1e,f) and pH 7.2 (Fig. 3.1h) show that in strongly acidic conditions there is a notch on the falling phase of the action potential shortly after the crest. This was also seen in a few fibres at pH 5.2, although it was less pronounced. The notch was not apparent at pH 6.2 or in more alkaline solutions.

There are two reasons for postulating that this notch is produced by regenerative changes in the membrane conductance within the T-system, which are delayed relative to those in the surface membrane. First, Adrian & Peachey (1973) have demonstrated that such conductance changes can account for a hump which is often seen in fibres immersed in chloride-free Ringer at about pH 7.2 (Hutter & Noble, 1960). Although this hump occurs at the start of the after-depolarization when the pH is about 7.2 (Persson, 1963), the present observation that in fibres at pH 4.9 (Fig. 3.1e & f) the hump (or notch) occurs earlier than this in relation to repolarization is consistent with the fact that a reduction in pH increases the duration of the spike. A related point is that while there is little or no evidence of a hump in the present records at pH 7.2 (presumably because a large part of the resting conductance is carried by chloride ions (Hutter & Padsha, 1959; Hodgkin & Horowicz, 1959; Hutter & Noble, 1960; Hutter & Warner, 1967a), at pH 4.9, where the chloride conductance is very much reduced (Hutter & Warner, 1967a,b), the hump is pronounced.

The second reason is that a notch similar to that seen here at low pH also occurs soon after the crest of action potentials from

fibres in which repolarization is slowed by 0.1 mM zinc (Stanfield, 1973). The notch in zinc-treated fibres seems to originate from the T-tubules since it is abolished in fibres detubulated by glycerol prior to zinc treatment (Stanfield, 1973).

The action potentials in Fig. 3.1g (pH 4.9) and Fig. 3.1h (pH 7.2) were recorded with a slow time base to show that acidic solutions prolong the after-depolarization, as described previously by Brooks & Hutter (1963).

Table 3.1 also summarizes the effects of pH on the maximum rates of rise ($\bar{V}_{rise}$) and fall ($\bar{V}_{fall}$) of the action potential. To a first approximation, these parameters are proportional to the height of the positive and negative phases, respectively, of the first derivative of the action potential with respect to time (dV_1/dt). Derivatives were obtained electrically as described in chapter 2 and photographed together with the action potentials in Fig. 3.1,a-f. It can be seen that in action potentials displaying a notch (Fig. 3.1, e & f), the derivative is triphasic. In such cases $\bar{V}_{fall}$ was obtained from the final phase.

As expected, $\bar{V}_{rise}$ and $\bar{V}_{fall}$ are reduced in acidic conditions and increased in alkaline conditions relative to the mean control value (Table 3.1). From pH 7.2 to 5.2, both parameters are reduced by more than 50%. On the other hand, an increase in pH from 7.2 to 9.2 increases $\bar{V}_{rise}$ and $\bar{V}_{fall}$ by only 15.7% and 32.0%, respectively.

The mean value for $\bar{V}_{rise}$ found here at pH 7.2 is somewhat lower than that reported by Nastuk and Hodgkin (1950; $\bar{V}_{rise}$ = 170 V/s in normal frog chloride Ringer at 6.6 and 7.2°C). This will be due, at least in part, to the fact that here a lower temperature is employed (3-5°C). However, the present value for $\bar{V}_{fall}$ is similar to that of 45 V/s reported by Nastuk & Hodgkin (1950) at 7.2°C.

Since the rates of rise and fall of the action potential reflect the rate at which the membrane capacity is charged and discharged by the current crossing the membrane (Hodgkin & Katz, 1949), and since changes in the external pH have no effect on the reversal potential of the Na current in myelinated nerve (Drouin & The, 1969; Drouin & Neumcke, 1974; Woodhull, 1973) or frog skeletal muscle (Campbell & Hille, 1976), the reduced rate of rise and reduced overshoot seen here in acidic solutions are most probably due to a fall in the permeability of the membrane to Na^+. In alkaline conditions the Na permeability appears to be increased during the spike. Changes in the delayed K permeability are more difficult to determine since the rate of repolarization is dependent on the size of the overshoot (Hodgkin & Katz, 1949). However, it is likely that the K permeability is reduced in acidic conditions since in some fibres at pH 4.9 (see for example Fig. 3.1, f & g) repolarization is slow despite the fact that the overshoot is similar to that found at pH 7.2 (Fig. 3.1,h).

Membrane currents at pH 7.2 and pH 5.2 in the absence of tetrodotoxin

Fig. 3.2 shows voltage clamp records from two fibres depolarized to between -70 mV and -2mV, or between -70 mV and 0 mV, in hypertonic chloride Ringer at pH 7.2 (A) and pH 5.2 (B). Records of the membrane potential (V_1) are shown at the top of the figure and membrane currents (V_2-V_1) are below. The number at the end of each current trace is the membrane potential in mV. Since the delayed K current in muscle is inactivated by maintained depolarization (Nakajima, Iwasaki & Obata, 1962; Stanfield, 1970a; Adrian et al., 1970a; Argibay & Hutter, 1973), the records at potentials positive to the threshold of the delayed current were spaced at intervals of 1-2 min. In this way it took about 30 mins to obtain a family of records.

Fig. 3.2 Membrane currents obtained from two fibres in hypertonic chloride Ringer at pH 7.2 and pH 5.2. Tracings of records of the membrane potential (V_1, mV) and membrane current (V_2-V_1, mV) are shown. The membrane is depolarized to the potential given in mV at the end of each current record .

A. pH 7.2. Fibre resting potential, -90 mV; holding potential, - 100 mV; inter-electrode distance (ℓ), 132 μm; temp. 4.0°C.

B. pH 5.2. Fibre resting potential, -73 mV; holding potential, -100 mV; inter-electrode distance (ℓ), 132 μm; temp. 2.9°C.

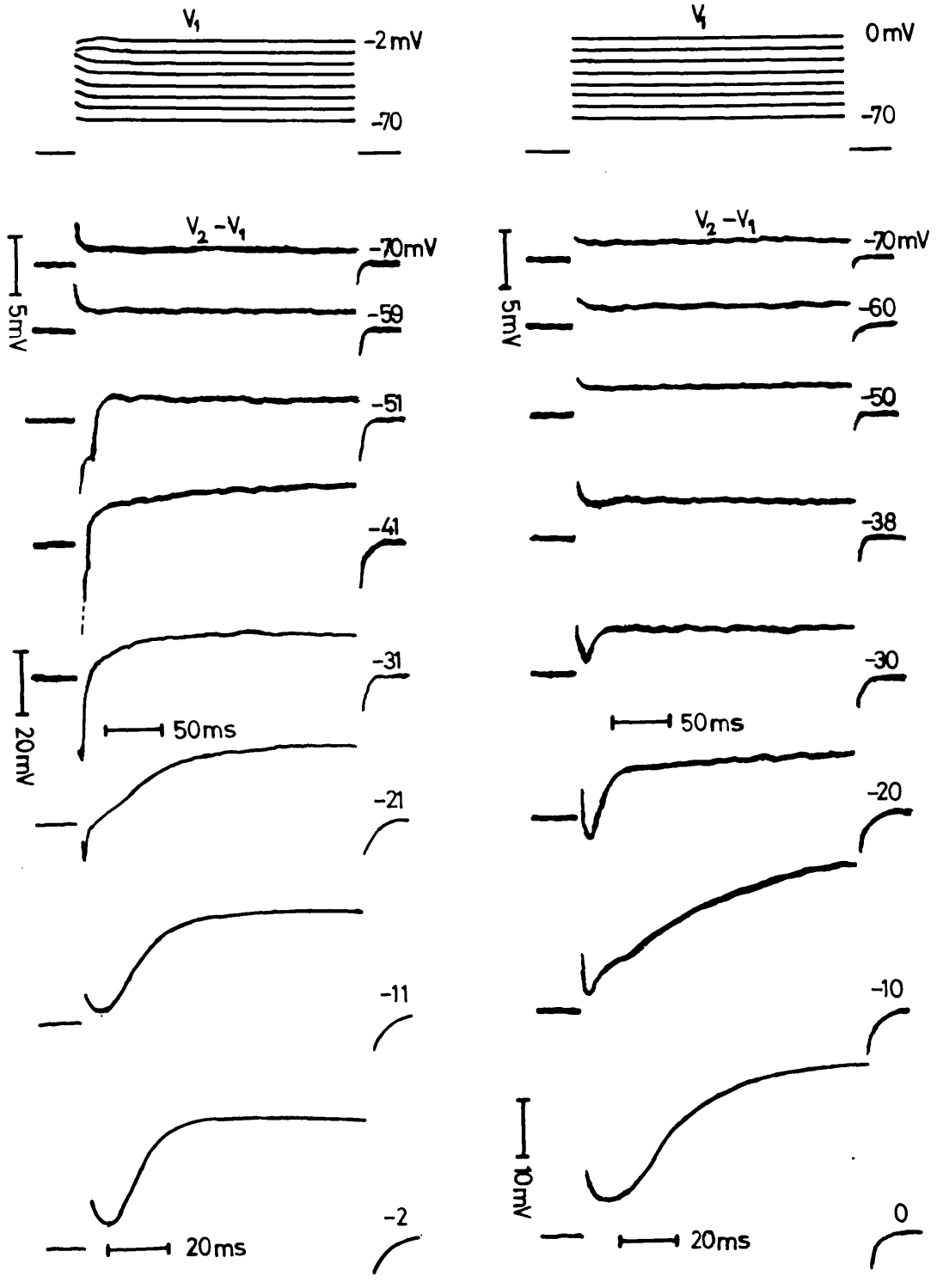
A. pH 7.2
B. pH 5.2
V1
-2 mV
-70
0 mV
V2 -V1
-70 mV
-59
-60
-51
-50
-41
-38
-31
-30
-21
-20
-11
-10
-2
0
5mV
20mV
10mV
50ms
20ms

For small depolarizations in Fig. 3.2A & B, the membrane currents are independent of time after the first 10 ms during which outward capacity currents are flowing. To a first approximation, this initial transient current is a linear function of the membrane potential. The steady-state current is the leakage current.

When the fibres are depolarized to -51 mV at pH 7.2 (Fig. 3.2A) or to -38 mV at pH 5.2 (Fig. 3.2B), a transient inward current is superimposed on the outward leakage current. This inward current is flowing through Na channels since it is absent in solutions which contain tetrodotoxin (Fig. 3.4 a,b,c). For the effect of tetrodotoxin on skeletal muscle fibres see Narahashi et al. (1960) Koketsu & Nishi (1966), Adrian et al. (1970a), Ildefonse & Rougier (1972), Hille & Campbell (1976), and Mandrino (1977). The inward current in Fig. 3.2 also resembles the sodium current in nerve in that it reaches a maximum earlier in the clamp step the more positive the membrane potential.

The double inward currents seen at -51 mV and at -41 mV in the control Ringer (Fig. 3.2A) are probably artifacts due to the fact that the membrane potential is not well controlled at the beginning of the clamp step. During the passage of these currents the membrane potential is positive to the command potential. On the other hand, at pH 5.2 (Fig. 3.2B), there is no evidence to suggest that clamp control is poor. Good control of the membrane potential may be possible in acidic solutions since, as Fig. 3.2 shows, the inward current at pH 5.2 is smaller, and turns on and off more slowly than the inward current in the control Ringer at a similar membrane potential. Adrian et al. (1970a) have also reported an all-or-none component of the inward current between -60 mV and -40 mV using the three-electrode clamp in solutions at pH 7.2. Outside that range

of membrane potentials they found that smooth records of the inward current could be obtained, as is the case in Fig. 3.2A.

There is also a delayed outward component of membrane current in Fig. 3.2 which is carried by K^+ ions. This is not abolished by tetrodotoxin, but in the presence of this drug (Fig. 3.4a,b,c), or at membrane potentials close to the reversal potential for the Na current in the absence of tetrodotoxin (Fig. 3.2A, at -2 mV and 3.2B, at 0 mV), the outward currents are seen to rise along a sigmoid curve in much the same way as in nerve.

Fig. 3.3A,B shows current-voltage relations for the two fibres in Fig. 3.2A,B, plotted when the Na current in each record is at a maximum (open circles) and when the delayed current has reached a steady-state (filled circles). At membrane potentials close to zero, the Na current is buried in the capacity current so the currents are plotted at the time at which the last visible Na current (before the current reversed) was at its peak. The reversal potential of the Na current, which was obtained by extrapolation of the leakage current, is -14 mV in Fig. 3.3A and -5 mV in Fig. 3.3B. In all other fibres examined at pH 7.2 and pH 5.2, the Na current also reversed at a potential which was small and negative. The reversal potential of the Na current found here in hypertonic Ringer is also considerably more negative than the mean membrane potential at the peak of the action potential in isotonic Ringer at pH 7.2 and 5.2 (+ 41.2 mV at pH 7.2 and + 29.0 mV at pH 5.2; see Table 3.1). However, this is to be expected since one effect of the hypertonic solution is to increase the internal Na^+ and K^+ concentrations by up to 2.4 times their values in isotonic Ringer (Adrian et al., 1970a). In addition, the measured reversal potential will be negative to the true reversal potential because no correction has been made for

Fig. 3.3 A,B. Current-voltage relations for the Na current and the delayed K current obtained from two fibres in hypertonic chloride Ringer at pH 7.2 and pH 5.2. Abscissae, membrane potential (V_1, mV); ordinates, membrane current (V_2-V_1, mV). The relationships are plotted at the peak of the inward current (o) and when the current has reached a steady-state (•). Tetrodotoxin not added.

A. pH 7.2. This fibre is the same as in Fig. 3.2A.

B. pH 5.2. This fibre is the same as in Fig. 3.2B.

C,D. Effect of pH on the threshold of the delayed K current (C), and on the parameter $V_{\frac{1}{2}n}$ (D). Mean values for the threshold and $V_{\frac{1}{2}n}$ are given relative to the mean values at pH 7.2. Vertical bars are ± S.E.M. Mean values for $V_{\frac{1}{2}n}$ and for the threshold are taken from Table 3.2. Hypertonic chloride Ringer, 3-5°C; tetrodotoxin, 1 u g/ml.

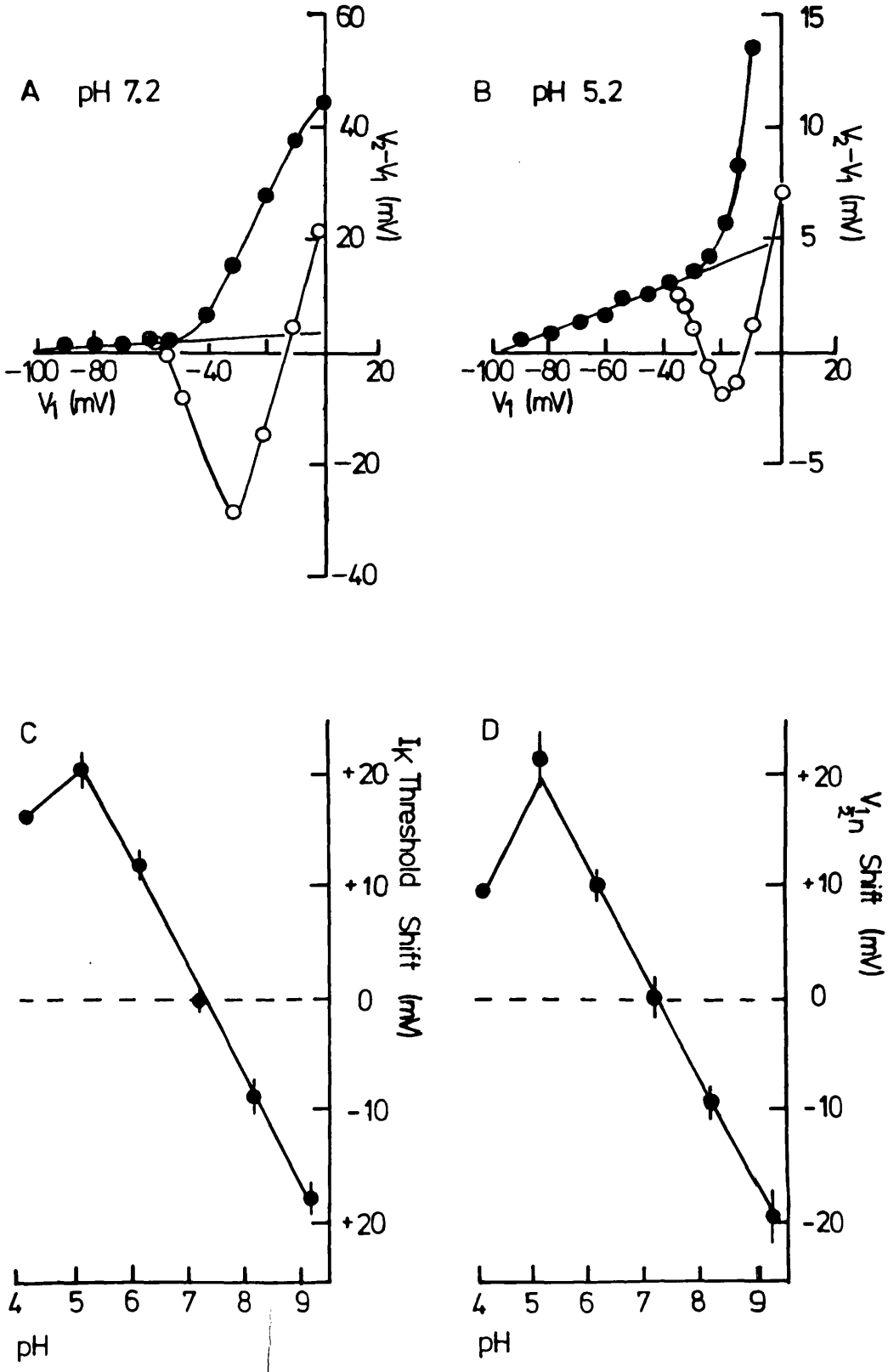
A pH 7.2
60
40
20
-20
-40
-100 -80
-40
20
V1 (mV)
V2-V1 (mV)
B pH 5.2
15
10
5
-5
-100 -80 -60 -40
20
V1 (mV)
V2-V1 (mV)
C
+20
+10
0
-10
+20
IK Threshold Shift (mV)
4 5 6 7 8 9
pH
D
+20
+10
0
-10
-20
V1/2n Shift (mV)
4 5 6 7 8 9
pH

capacity currents flowing at the peak of the Na current. Deficiencies in the clamp may also produce a value for the reversal potential which is too negative.

Effect of acidic solutions on the threshold of the Na and K currents

Fig. 3.3A & B show that an important effect of a reduction in pH is to shift the thresholds of the Na and K currents to more positive membrane potentials. The threshold of the Na current was taken as the most negative membrane potential at which an inward transient current was seen when the membrane was depolarized in 2 mV steps. This was -61.0 ± 2.7 mV (four fibres) at pH 7.2 and -38.0 ± 1.7 mV (three fibres) at pH 5.2. The threshold of the K current in the same fibres was measured from steady-state current-voltage relations, and taken arbitrarily as the membrane potential at which the current increased by 10%. Mean values were -52.3 ± 1.3 mV (four fibres) at pH 7.2 and -29.0 ± 1.0 mV (three fibres) at pH 5.2. Thus the thresholds for the Na and K currents in the absence of tetrodotoxin are shifted by 23 mV and 23.3 mV, respectively, between pH 7.2 and 5.2.

Effects of pH on the properties of the delayed K conductance in hypertonic chloride Ringer containing tetrodotoxin

Fig. 3.4 shows voltage-clamp records and steady-state current-voltage relations from three fibres in the presence of tetrodotoxin. At pH 7.2 the mean threshold for the delayed current was -51.8 ± 0.8 mV (twenty-two fibres), which is not significantly different from the mean value reported in the previous section in the absence of tetrodotoxin ($P \gtrsim 0.3$). Similarly, Kao & Stanfield (1968) have found that tetrodotoxin has no effect on the threshold for the delayed current in muscle using a two-electrode voltage-clamp method. Nor has it any effect on delayed rectification in *Myxicola* axons when the external pH is changed (Schauf & Davis, 1976).

Fig. 3.4 Effect of pH on the delayed K conductance of fibres immersed in a hypertonic chloride Ringer containing tetrodotoxin.

a,b & c, tracings of records of the membrane potential (V_1) and membrane current (V_2-V_1).

Fibre (a) is depolarized to -39 mV and 0 mV. Resting potential, - 77 mV; holding potential, - 100 mV; inter-electrode distance (ℓ), 110 µm; temp. 3.5°C; pH 5.2.

Fibre (b) is depolarized to - 40 mV and - 5 mV. Resting potential, -89 mV; holding potential, - 100 mV; inter-electrode distance (ℓ), 110 µm; temp. 3.0°C; pH 7.2.

Fibre (c) is depolarized to - 40 mV and 0 mV. Resting potential, - 78 mV; holding potential - 100 mV; inter-electrode distance (ℓ), 110 µm; temp. 3.8°C; pH 9.2.

d,e & f, steady-state current-voltage relations. Abscissae, membrane potential (V_1, mV); ordinates, membrane current (V_2-V_1, mV). Filled symbols, run 1; open symbols, run 2. The current-voltage relations in d, e & f are from fibres a, b & c, respectively.

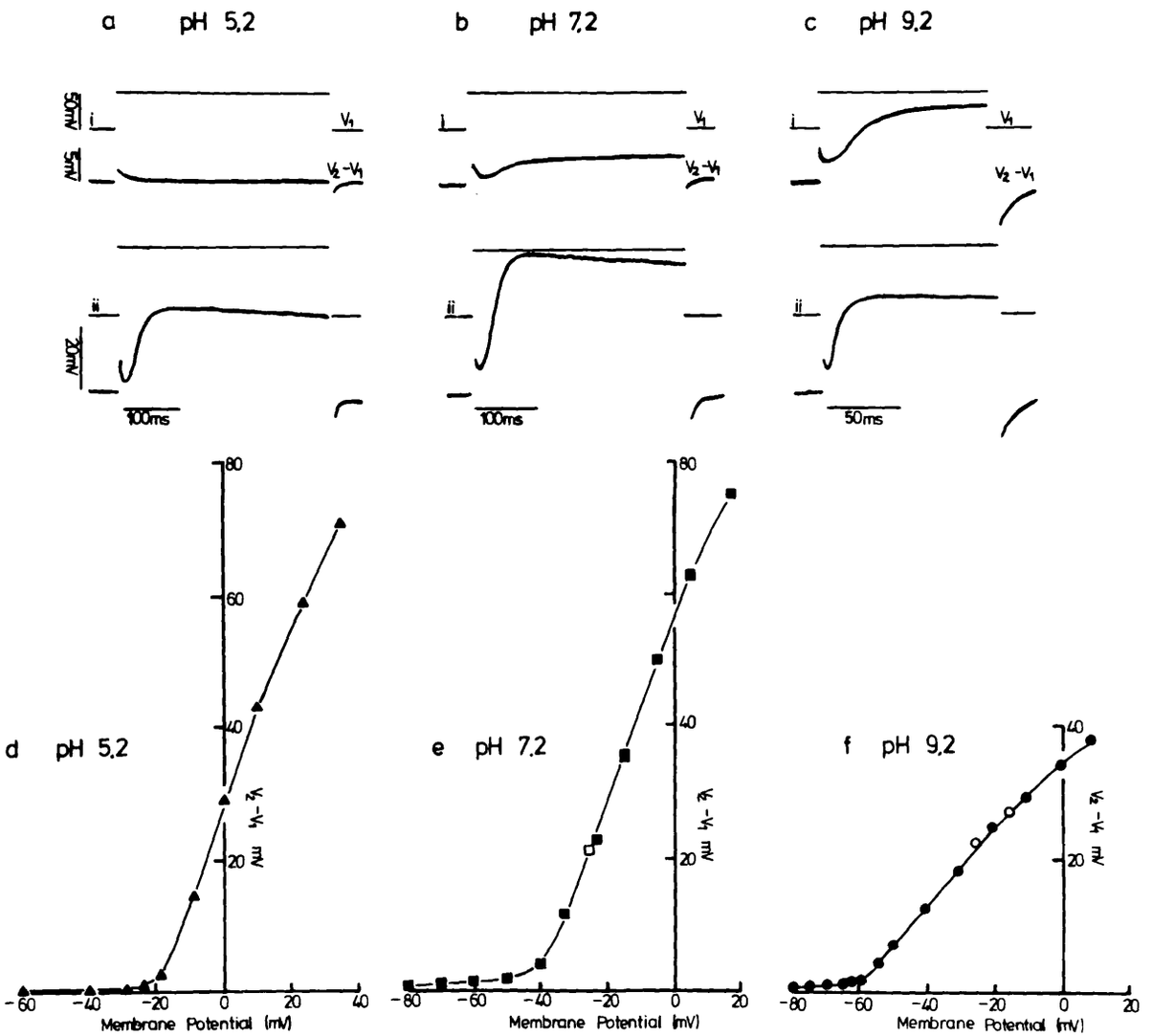
a pH 5.2
b pH 7.2
c pH 9.2
50mV
5mV
20mV
i
ii
V1
V2 -V1
100ms
100ms
50ms
d pH 5.2
e pH 7.2
f pH 9.2
V2 -V1 mV
Membrane Potential (mV)
80
60
40
20
-60
-40
-20
0
20
40
-80

In Fig. 3.4c, the currents at pH 9.2 turn on along a sigmoidal time course in much the same way as currents at pH 7.2 and pH 5.2 (Fig. 3.4a & b). In almost all cases the currents reach a brief plateau (the steady-state current) and then decline slowly. Under the present conditions, the decline would be expected to proceed with a time constant of 1.5 - 3.0 s at + 10 mV (Adrian et al., 1970a) This is too slow to have very much effect on the time course of activation. In a few fibres the delayed currents rose sigmoidally at first, but thereafter increased gradually for the duration of depolarization. Those results have not been analysed further. Adrian et al. (1970a) have also reported a considerable variation in the size of outward currents in hypertonic Ringer, and in the rate at which they develop.

Analysis of the delayed K currents in terms of the model developed by Hodgkin and Huxley

The model used by Hodgkin and Huxley (1952d) to describe membrane currents in the squid axon was discussed briefly in chapter 1. With a few quantitative changes, the model can also be applied to ionic currents in skeletal muscle (Adrian et al., 1970a; Stanfield, 1970a, 1975; Ildefonse & Roy, 1972; Campbell & Hille, 1976; Almers, 1976). Here, the model is only applied to the delayed current since records of the Na current tend to be unreliable for much of the voltage range in which m_∞, the steady-state parameter which describes activation of the Na conductance, is changing.

Two assumptions are used to describe delayed K currents in squid axons and in muscle. The first is that the relationship between the K conductance (g_K) and the maximum K conductance ($\bar{g}_K$) is

$$g_K = \bar{g}_K n^4 \qquad (3.1)$$

(Hodgkin & Huxley, 1952d; Adrian et al., 1970a; Stanfield, 1970a; Almers, 1976), where n^4 is the fraction of K channels open to the passage of current. The second assumption is that n is determined by a first order rate equation,

$$dn/dt = \alpha_n(1-n) - \beta_n n \qquad (3.2)$$

in which α_n and β_n are rate constants which depend on the membrane potential but not on time. A physical basis for eqns. (3.1 & 3.2) is that each K channel is gated by four independent gating particles, all of which must be in the open position for the channel to be open. α_n and β_n determine the rate at which the particles move from the closed to the open position, and from the open to the closed position, respectively.

The solution to eqn. (3.2) is

$$n = n_\infty - (n_\infty - n_o) \exp -(\alpha_n + \beta_n)t \qquad (3.3)$$

when n_o is the value of n before a step-like change in membrane potential, and n_∞ is the value of n when the delayed current has reached a steady-state during the step (Hodgkin & Huxley, 1952d). In muscle at pH 7.2, n_o is zero at the holding potential of -100 mV (Adrian et al., 1970a), so eqn. (3.3) can be simplified to

$$n = n_\infty [1-\exp -(\alpha_n + \beta_n)t] \qquad (3.4)$$

If $g_{K\infty}$ is the delayed K conductance in the steady-state, it follows from eqn . (3.1), that

$$n_\infty = (g_{K\infty}/\bar{g}_K)^{\frac{1}{4}} \qquad (3.5)$$

where

$$n_\infty = \alpha_n/(\alpha_n + \beta_n) \qquad (3.6)$$

Since the instantaneous current-voltage relationship determined from two-step experiments for the delayed current is roughly linear at pH 7.2 (Adrian et al., 1970a) and at pH 5.2 and 9.2 (Fig. 3.6B), the expression which relates the delayed current (I_K) to the conductance

is

$$I_K = g_K (V_1 - V_{R,K}) \qquad (3.7)$$

(Hodgkin & Huxley, 1952,b,d), where $V_{R,K}$ is the reversal potential of the delayed current. $V_{R,K}$ was measured in several fibres as described on page 62. In all other fibres (except one at pH 4.2) a value of -75 mV was assumed since this is close to the mean values found here (Table 3.2) and in previous studies (Adrian et al., 1970a; Stanfield, 1975). At pH 4.2 the assumed value was -65 mV, which is close to the mean at pH 5.2 (Table 3.2).

Fig. 3.5A shows the relationship between $g_{K\infty}/\bar{g}_K$ and the membrane potential for the three fibres illustrated in Fig. 3.4. The experimental points were determined from the steady-state current-voltage relations (Fig. 3.4d-f) using eqn. (3.7) after subtraction of leakage currents extrapolated from the currents recorded during small depolarizations.

Fig. 3.5B shows n_∞ relations for the same fibres calculated from the experimental points using eqn.(3.5). As expected from the current-voltage relations (Fig. 3.4d-f), the relationship between $g_{K\infty}/\bar{g}_K$ and the membrane potential is shifted to the right when the pH is reduced from 7.2 (■) to 5.2 (▲), and to the left when the pH is raised to 9.2 (●).

The theoretical curves in Fig. 3.5 were obtained by assuming that in the steady-state, the proportion of gating particles in the open position (n_∞) is related to the proportion in the closed position ($1-n_\infty$) by the Boltzmann distribution (Keynes & Rojas, 1974; Stanfield, 1975)

$$(1-n_\infty)/n_\infty = \exp\left[-(V_1 - V_{\frac{1}{2}n})\, z'F/RT\right] \qquad (3.8)$$

where z' is the effective valence of the postulated gating particles and $V_{\frac{1}{2}n}$ is the membrane potential at which n_∞ is 0.5. Since

Fig. 3.5 Effect of pH on the delayed K conductance and on n_∞

A, effect of pH on the delayed K conductance. Abscissa, membrane potential (mV); ordinate, $g_{K\infty}/\bar{g}_K$. $g_{K\infty}$ was calculated from the current-voltage relations shown in Fig. 3.4, after subtraction of the leakage currents. The fibre diameter was assumed to be 80 μm, and the internal resistivity 370Ω.cm. The continuous lines were drawn to eqns. (3.5) and (3.9) of the text. TTX was 1 μg/ml.

B, effect of pH on n_∞. Abscissa, membrane potential (mV); ordinate, n_∞. n_∞ is given by $(g_{K\infty}/\bar{g}_K)^{\frac{1}{4}}$. Theoretical curves were drawn to eqn. (3.9) of the text using values for $V_{\frac{1}{2}n}$ and RT/z'F which are given below. Horizontal bars at $n_\infty = 0.5$ indicate the range of values for $V_{\frac{1}{2}n}$ in seven fibres at pH 9.2 (left), nine fibres at pH 7.2 (middle) and nine fibres at pH 5.2 (right). Arrows indicate the mean value of $V_{\frac{1}{2}n}$ at each pH. TTX was 1 μg/ml.

In A & B the symbols are as follows:

Circles, pH 9.2. Same fibre as Fig. 3.4c,f; $\bar{g}_K$, 11.86 mmho.cm^{-2}; $V_{R,K}$, -79 mV; $V_{\frac{1}{2}n}$, -65 mV; RT/z'F, 10 mV; o, run 2; ●, run 1.

Squares, pH 7.2. Same fibre as Fig. 3.4 b,e. $\bar{g}_K$, 22.0 mmho.cm^{-2}; $V_{R,K}$, -79 mV; $V_{\frac{1}{2}n}$, -41 mV; RT/z'F, 11 mV; ■ run 1; □ run 2.

Triangles, pH 5.2. Same fibre as Fig. 3.4a,d. $\bar{g}_K$, 22.40 mmho.cm^{-2}; $V_{R,K}$, -59 mV; $V_{\frac{1}{2}n}$, -21 mV; RT/z'F, 10 mV.

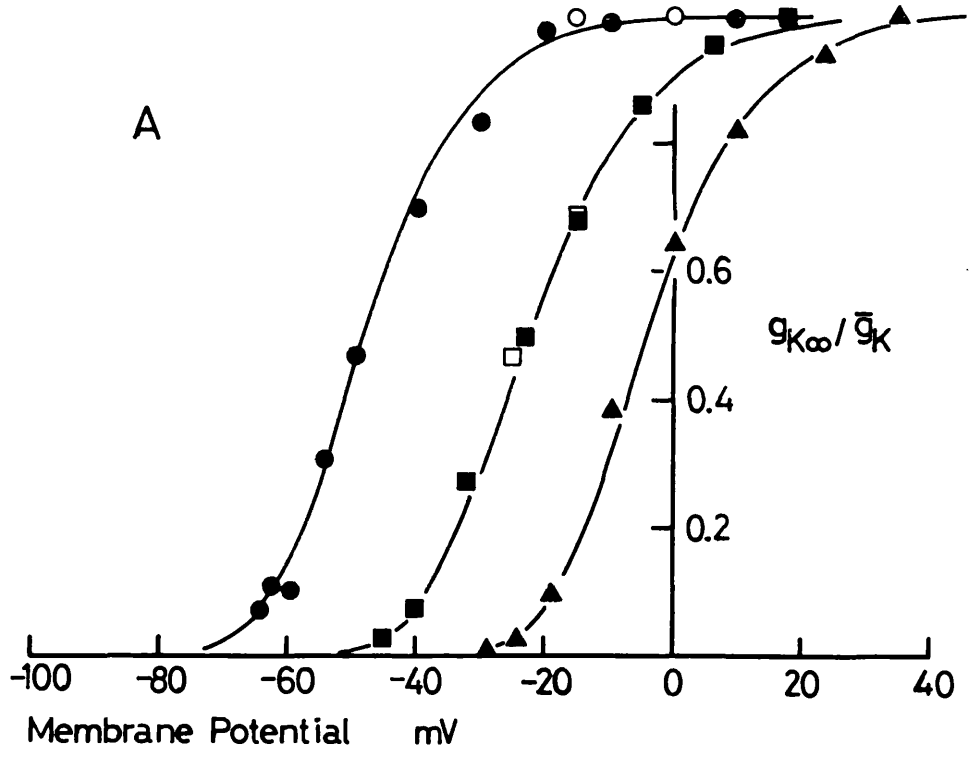
A
0.6
0.4
0.2
$g_{K\infty}/\bar{g}_K$
-100
-80
-60
-40
-20
0
20
40
Membrane Potential mV

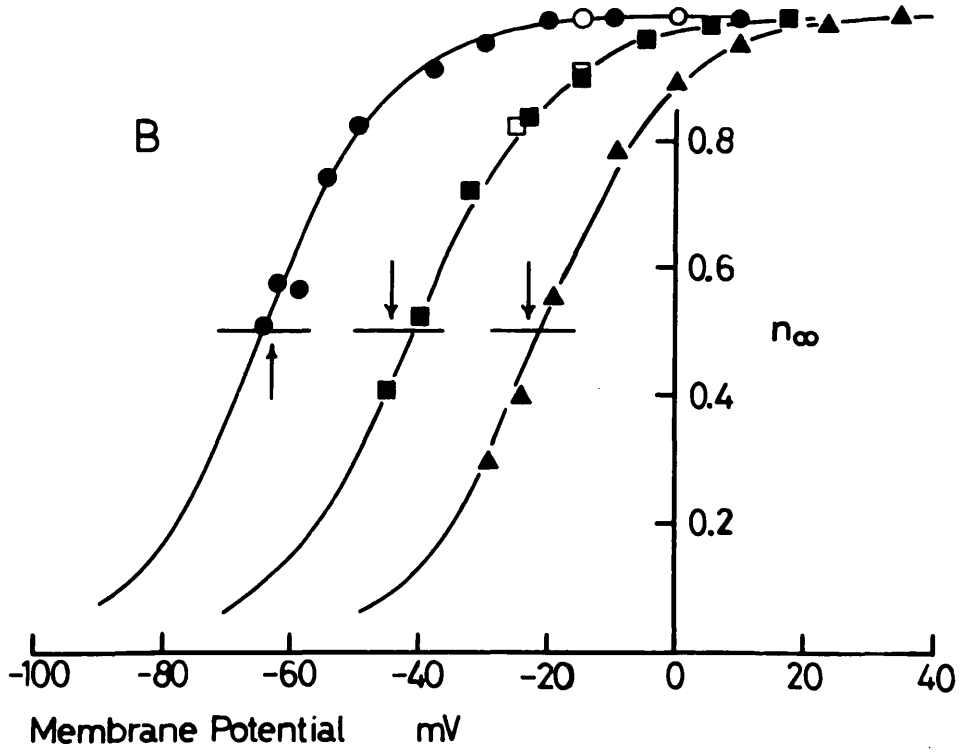
B
0.8
0.6
0.4
0.2
n_∞
-100
-80
-60
-40
-20
0
20
40
Membrane Potential mV

$1-n_\infty + n_\infty = 1$, eqn. (3.8) can be solved for n_∞ to give

$$n_\infty = \frac{1}{1 + \exp\left[-(V_1 - V_{\frac{1}{2}n})\ z'F/RT\right]} \qquad (3.9)$$

which is similar to the expression used by Schneider & Chandler (1973), Chandler, Rakowski & Schneider (1976a), and Adrian & Almers (1976) to describe the potential-dependent charge movement in skeletal muscle.

$z'F/RT$ defines the shape of the n_∞ relation, and $V_{\frac{1}{2}n}$ its position along the voltage axis. The theoretical curves in Fig. 3.5, which are a good fit to the experimental points, are drawn with $RT/z'F$ = 10 mV at pH 5.2 and pH 9.2, and 11 mV at pH 7.2. Values for $V_{\frac{1}{2}n}$ are -65 mV at pH 9.2, -41 mV at pH 7.2, and -21 mV at pH 5.2.

Table 3.2 shows that changes in pH between 4.2 and 9.2 have little or no effect on $RT/z'F$. Since the mean value of $RT/z'F$ is 9.11 mV, and since RT/F is 23.87 mV at 4°C, the effective valence of each gating particle is 2.62. One possibility is that four particles each with a valence of 2.62 must move through the whole of the electrical gradient across the membrane in order for each K channel to be open. Alternatively, the particles may move through only part of the electrical gradient if the valence is greater than 2.62. There is no evidence in these experiments that protons titrate the gating particles. A similar value for z' of 2.65 has been reported by Stanfield (1975) in the presence and absence of 0.1 mM zinc at pH 7.2.

The mean value for $V_{\frac{1}{2}n}$ at pH 7.2 is -44.4 mV (Table 3.2) compared with -44 mV in phosphate-buffered Ringer (Adrian et al., 1970a; their Fig. 19) and -49 mV in a solution buffered with tris (Stanfield, 1975). In Fig. 3.3C & D, the mean values for $V_{\frac{1}{2}n}$ and for the threshold of the delayed current are plotted as a function of

TABLE 3.2

Effect of pH on some properties of the delayed K conductance in hypertonic chloride Ringer; 1 µg/ml tetrodotoxin, about 4°C

pH	RP* (mV)	Threshold (mV)	$V_{R,K}$ (mV)	$V_{\frac{1}{2}n}$ (mV)	RT/zF (mV)	$\bar{g}_K$ ‡‡ (mmho.cm^{-2})
9.2	-79.2 ± 2.0(7)	-69.3 ± 1.4(8)	-74.1 ± 2.7(7)	-63.7 ± 2.0(7)	9.64 ± 0.36(7)	18.0 ± 1.8(7)‡
8.2	-81.4 ± 3.0(8)	-58.6 ± 1.9(13)	-72.6 ± 1.5(5)	-53.6 ± 1.1(8)	8.69 ± 0.31(8)	15.9 ± 2.3(8)
7.2	-82.0 ± 1.9(9)	-51.8 ± 0.8(22)	-77.0 ± 2.7(7)	-44.4 ± 1.7(9)	9.11 ± 0.35(9)	16.7 ± 1.6(8)
6.2	-75.6 ± 1.4(7)	-39.7 ± 1.1(7)	-75.8 ± 3.6(4)	-34.6 ± 0.7(7)	8.57 ± 0.20(7)	18.9 ± 2.7(7)
5.2	-75.3 ± 2.8(7)	-31.3 ± 1.6(12)	-66.2 ± 1.7(6)	-23.0 ± 2.1(9)	9.78 ± 0.32(9)	15.1 ± 1.6(9)
4.2	-76.5 (2)	-35.0 (2)	-65‡	-32.0 (1)	9.0 (1)	6.0 (1)

‡ Mean ± S.E. of mean, no. of observations in parentheses. ‡ Assumed value.

‡‡Calculated assuming a fibre diameter of 80 µm and an internal resistivity of 370 Ω cm.

* Resting potential (= RP)

external pH. In both cases the plots are roughly linear between pH 9.2 and pH 5.2; in this range the threshold and the n_∞ relation are shifted +9.6 mV and +10.0 mV, respectively, for a 10-fold increase in the H^+ concentration. Between pH 5.2 and pH 4.2 both parameters are shifted in opposite direction .

Mean values for the maximum K conductance in hypertonic chloride Ringer from 3.3-4.8°C are given in Table 3.2. It can be seen that between pH 9.2 and 5.2 there is no systematic change in $\bar{g}_K$. At pH 4.2, though in one fibre only, $\bar{g}_K$ is reduced to 35.9% of the mean value at pH 7.2. This is consistent with Gillespie & Hutter's (1975) report of a small reduction in $\bar{g}_K$ from pH 7.2 to 5.0.

The mean value of $\bar{g}_K$ found here at pH 7.2 is also similar to the mean value reported by Stanfield, (1975; 17.8 mmho.cm^{-2}), and is within the range of values reported by Adrian et al. (1970a; 8.5-20 mmho.cm^{-2}).

Effect of pH on the reversal potential of the delayed K currents

The reversal potential of the delayed current ($V_{R,K}$) was measured using a two-step procedure described by Adrian et al. (1970a) and is shown in Fig. 3.6. A more detailed account is given in chapter 4 where the reversal potential is measured in solutions containing 40 mM-K_2SO_4 and in solutions containing other cations. Fig. 3.6A shows five superimposed records of the membrane potential and membrane current from a fibre at pH 9.2. The first step depolarized the membrane to +10 mV to activate a large part of the delayed conductance. During this step the current is beyond the top of the oscilloscope screen. During the second step, which repolarized the membrane to between -60 mV and -100 mV, there is a tail of current which declines as the K channels close. After

Fig. 3.6 Effect of pH on the reversal potential of the delayed current.

A, tracings of records of membrane potential (V_1) and membrane current (V_2-V_1) during a two-step experiment to determine $V_{R,K}$. The first step depolarizes the membrane from the holding potential to + 10 mV. During the second step the membrane is repolarized to the potentials given in the figure. Fibre resting potential, - 78 mV; holding potential, - 100 mV; inter-electrode distance, 110 μm; temp. 3.8°C; pH 9.2; same fibre as Fig. 3.4c,f, and Fig. 3.5 (circles).

B, instantaneous current-voltage relations for three fibres at pH 5.2, ▲; pH 7.2, ■; and pH 9.2, ●. The points were obtained from two-step experiments like that illustrated in Fig. 3.6A. Abscissa, membrane potential (V_1) during step 2; ordinate, instantaneous current. The instantaneous current is the membrane current at the start of step 2, corrected for leak and capacity currents. Lines through the points were fitted by eye and give $V_{R,K}$ = -79 mV at pH 9.2, - 79 mV at pH 7.2, and - 59 mV at pH 5.2. Same fibres as shown in Figs. 3.4 and 3.5.

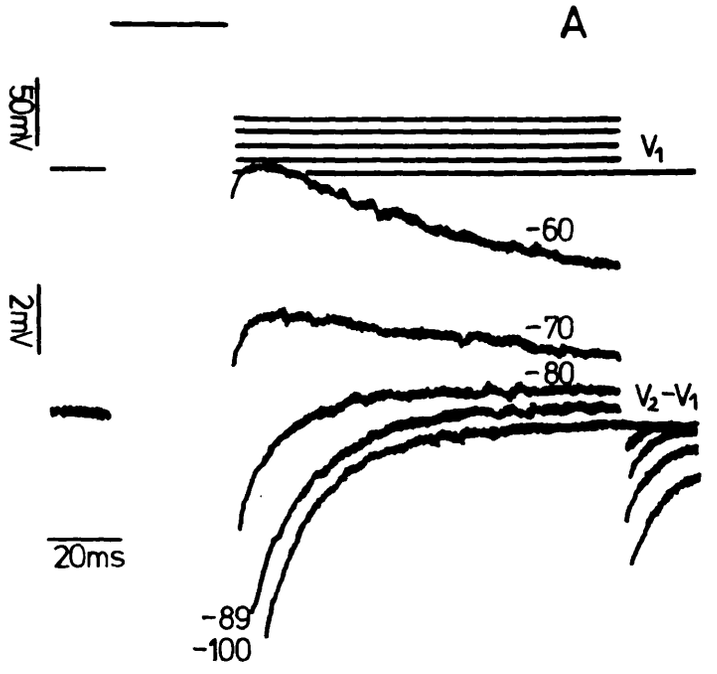
A
50mV
2mV
20ms
V1
-60
-70
-80
V2-V1
-89
-100

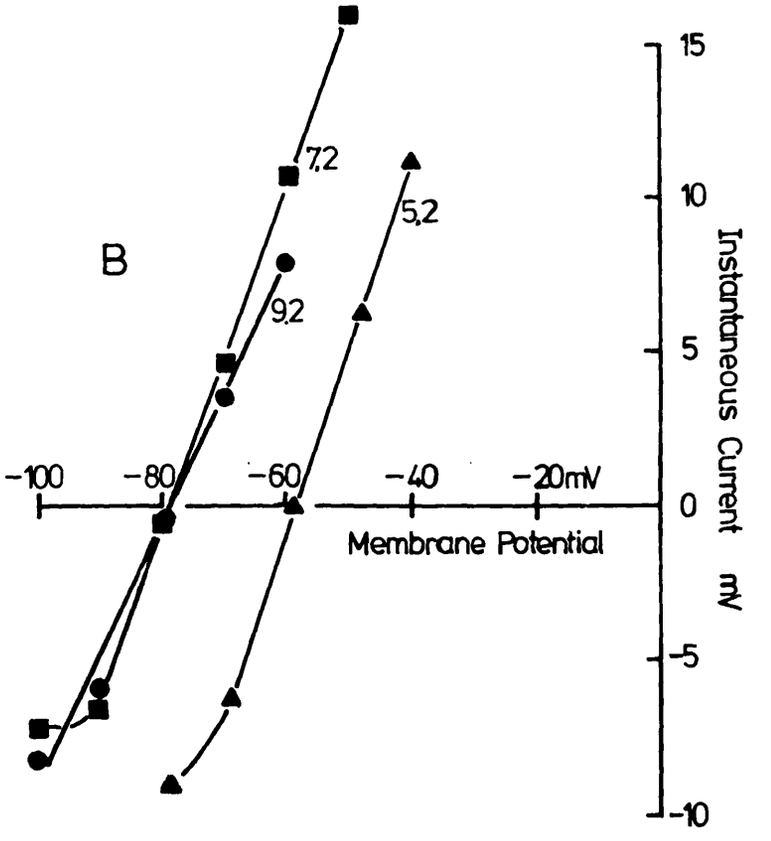
B
7.2
5.2
9.2
-100
-80
-60
-40
-20mV
Membrane Potential
15
10
5
0
-5
-10
Instantaneous Current mV

subtraction of the leakage and capacity currents scaled linearly from currents during small depolarizations, the time course of each tail current was plotted on semilogarithmic paper and extrapolated back to the start of the second step to obtain the instantaneous current.

Instantaneous current-voltage relations plotted for the three fibres shown in Figs. 3.4 & 3.5 are seen in Fig. 3.6B to be linear except at large negative potentials, where the tail currents decline rapidly and are thus difficult to measure. The reversal potential is the membrane potential at which the instantaneous current is zero. The mean value was -77.0 $\pm$ 2.7 mV in seven fibres at pH 7.2. Similar values have been reported by Adrian et al.(1970a) in phosphate-buffered Ringer at pH 7.2 and at 1-4°C (-84.6 mV), and by Stanfield (1975) in tris-buffered Ringer at pH 7.2 and at 4°C (-76.9 mV).

Alkaline solutions in the pH range studied have little or no effect on the reversal potential, as shown in Table 3.2. On the other hand, the mean reversal potential at pH 5.2 is significantly less negative than the mean value at pH 7.2 ($P < 0.01$).

A kinetic analysis of the delayed K currents at pH 7.2 and pH 5.2

If the only effect of a reduction in external pH is to increase the electrical gradient across the membrane, then a shift in the n_∞ relation to more positive membrane potentials will be associated with an equal shift in the relationship between the membrane potential and τ_n, the rate constant which describes activation of the delayed currents. Underlying these shifts at a given membrane potential is a reduction in α_n and an increase in β_n.

In the giant axons of the crayfish (Shrager, 1974) and Myxicola (Schauf & Davis, 1976), the shift in the potential-dependence of τ_n

exceeds that of n_∞ as the external pH is lowered. Shrager (1974) has found that this is due, at least in part, to the fact that from pH 7.5 to pH 5.8, α_n is reduced 3.5-fold whereas there is little or no change in β_n. He suggests that at low pH protons titrate some membrane component, possibly a histidine imidazole residue, and in doing so reduce the ease with which gating particles move from the closed to the open position, and in the reverse direction. A second point considered by Shrager, but one which did not account for his results, is that at low pH the delayed currents might be shifted along the time axis in much the same way that a hyperpolarizing prepulse delays the rise in K currents in nerve during depolarization (Cole & Moore, 1960; Goldman & Schauf, 1973; Shrager, 1974).

An examination of the kinetics of K activation in muscle at normal and low pH was prompted by the observation that during large depolarizations at pH 5.2 (Fig. 3.2B at -10 mV) there is a partial temporal separation of inward and delayed currents similar to that reported by Shrager (1974).

The points in Fig. 3.7A,B were obtained from photographic records of K currents during depolarizations to -23 mV and -5 mV at pH 7.2 (Fig. 3.7A), and during depolarizations to -9.5 mV and +24 mV in a different fibre at pH 5.2 (Fig. 3.7B). Each current is plotted as a fraction of its steady-state value after subtraction of leakage and capacity currents.

It follows from eqns. (3.1, 3.4, 3.5, & 3.7) that during a step-wise depolarization, the delayed current rises along a time-course described by

$$I_K/I_{K\infty} = [1 - \exp -(\alpha_n + \beta_n)t\,]^4 \qquad (3.10)$$

where

$$(\alpha_n + \beta_n) = \tau_n^{-1} \qquad (3.11)$$

Fig. 3.7 Kinetic analysis of the delayed current at normal and low pH. Abscissae, time (ms); ordinates, delayed current at various times (I_K) normalized to the steady-state current ($I_{K\infty}$). Filled circles are the experimental currents corrected for leakage and capacity currents. Continuous lines are the theoretical currents drawn to eqn. (3.10) of the text.

A, fibre at pH 7.2 depolarized to -23 mV and - 5mV. The corresponding theoretical curves are drawn with τ_n = 16.4 ms and 8.75 ms, respectively. Same fibre as Fig. 3.4b,e and Fig. 3.5 (squares).

B, fibre at pH 5.2 depolarized to -9.5 mV and + 24 mV. The corresponding theoretical curves are drawn with τ_n = 23.9 ms and 12.4 ms, respectively. Same fibre as Fig. 3.4a,d and Fig. 3.5 (triangles)

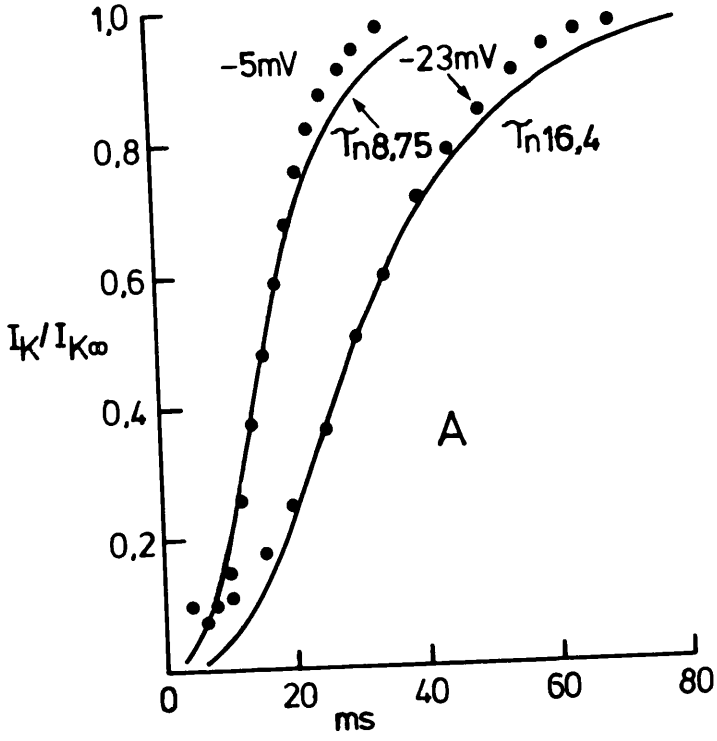
1,0
0,8
0,6
0,4
0,2
$I_K / I_{K\infty}$
-5mV
-23mV
τ_n8,75
τ_n16,4
A
0
20
40
60
80
ms

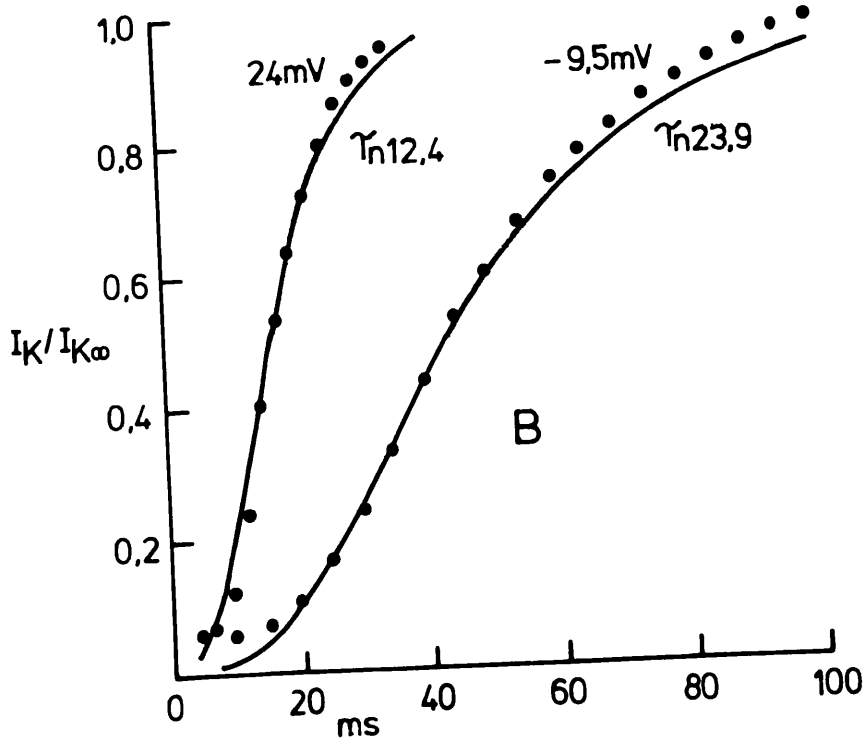
1,0
0,8
0,6
0,4
0,2
$I_K / I_{K\infty}$
24mV
-9,5mV
τ_n12,4
τ_n23,9
B
0
20
40
60
80
100
ms

and where I_K is the K current at time t after the onset of depolarization, and $I_{K\infty}$ is the value of I_K in the steady-state. The theoretical curves in Fig. 3.7A,B are drawn to eqn. (3.10) with values for τ_n which are given in ms alongside the curves. A reasonable fit to the experimental points is achieved in view of the fact that errors may be introduced when the capacity and leakage currents are subtracted. At pH 5.2 (Fig. 3.7B), the fit is not improved by shifting the theoretical curves along the time axis to reproduce the delays observed by Cole & Moore (1960), Goldman & Schauf (1973) and Shrager (1974).

The relationship between τ_n^{-1} and the membrane potential is plotted for five fibres at pH 7.2 (Fig. 3.8A) and five fibres at pH 5.2 (Fig. 3.8B). At membrane potentials positive to the threshold of the delayed K conductance, τ_n was determined from the time course of the activating currents with eqn. (3.10). At more negative membrane potentials the tail currents from two-step experiments were used since these decline exponentially with a time constant equal to $\tau_n/4$ (Hodgkin & Huxley, 1952d).

The lines through the points in Fig. 3.8A & B were drawn to a set of empirical equations formulated by Adrian et al. (1970a):

$$\alpha_n = \frac{\bar{\alpha}_n (V_1 - \bar{V}_n)}{1 - \exp - \frac{(V_1 - \bar{V}_n)}{7}} \qquad (3.12)$$

$$\beta_n = \bar{\beta}_n \exp - \frac{(V_1 - \bar{V}_n)}{40} \qquad (3.13)$$

where $\bar{\alpha}_n$ is the maximum value of α_n, and $\bar{\beta}_n$ is the maximum value of β_n which occur at large positive and large negative membrane potentials, respectively. $\bar{\alpha}_n$ and $\bar{\beta}_n$ define the shape of the relationship between τ_n^{-1} and the membrane potential, and $\bar{V}_n$ defines the position of the relationship along the voltage axis.

Fig. 3.8 Relationships between τ_n^{-1} and membrane potential for five fibres at pH 7.2 (A) and five fibres at pH 5.2 (B). Abscissae, τ_n^{-1} (ms^{-1}); ordinates, membrane potential (V_1, mV). The line through the experimental points in A and B is drawn to eqns. (3.11, 3.12 & 3.13) of the text with values for $\bar{\alpha}_n$, $\bar{\beta}_n$ and $\bar{V}_n$ as given below.

A, fibres at pH 7.2. $\bar{\alpha}_n = 0.0033\ ms^{-1}$; $\bar{\beta}_n = 0.011\ ms^{-1}$; $\bar{V}_n = -37$ mV.

B, fibres at pH 5.2. $\bar{\alpha}_n = 0.0033\ ms^{-1}$; $\bar{\beta}_n = 0.011\ ms^{-1}$; $\bar{V}_n = -15.6$ mV.

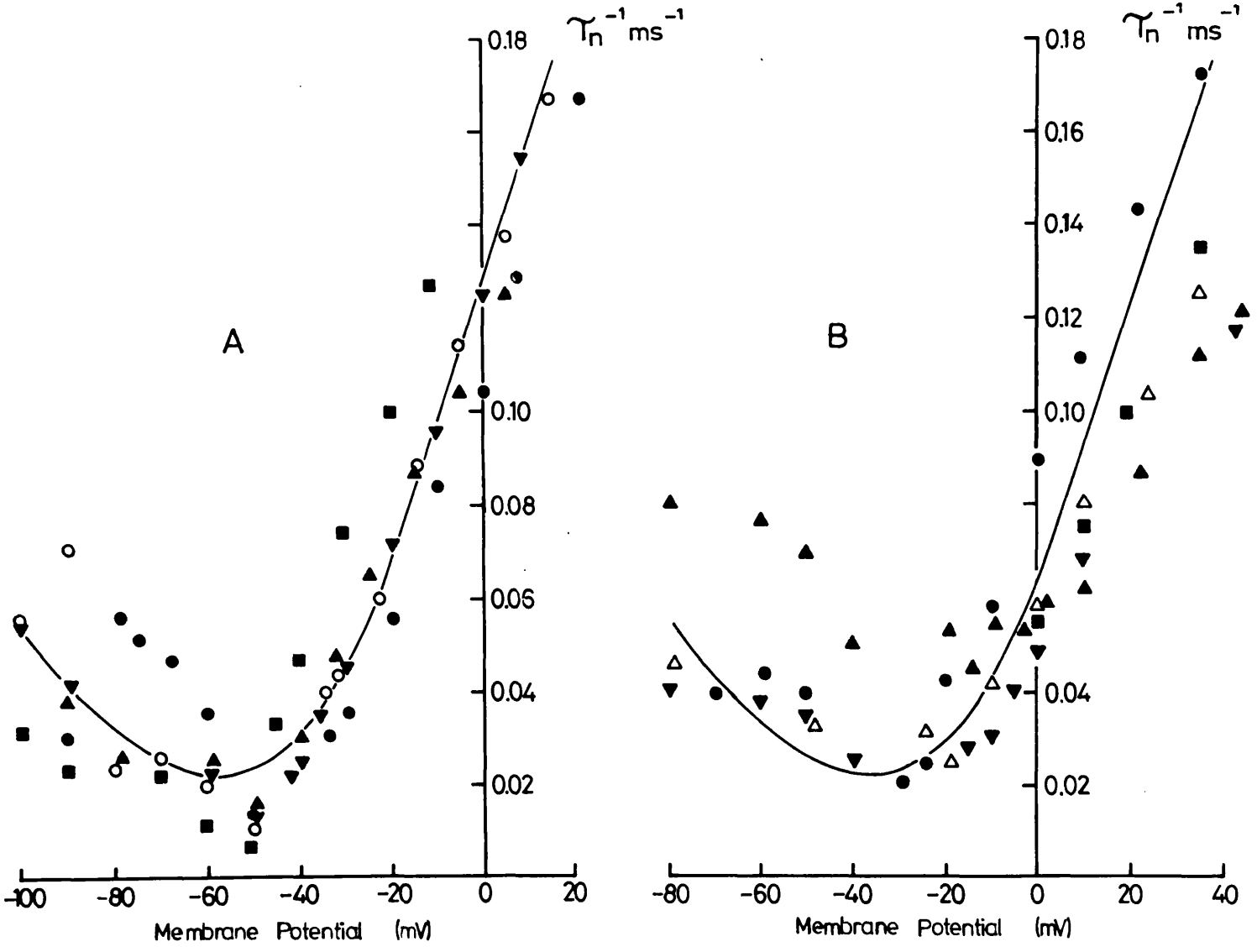
A
B
τ_n^{-1} ms^{-1}
0.18
0.16
0.14
0.12
0.10
0.08
0.06
0.04
0.02
-100
-80
-60
-40
-20
0
20
40
Membrane Potential (mV)

At pH 7.2 a good fit to the experimental points is obtained with $\bar{\alpha}_n$ = 0.0033 ms^{-1}, $\bar{\beta}_n$ = 0.011 ms^{-1} and $\bar{V}_n$ = -37 mV (Fig. 3.8A). At pH 5.2 (Fig. 3.8B), a reasonably close fit is achieved using the values for $\bar{\alpha}_n$ and $\bar{\beta}_n$ determined at pH 7.2, but with $\bar{V}_n$ = -15.6 mV. The shift in $\bar{V}_n$ from pH 7.2 to 5.2 is +21.4 mV, which is identical to the mean shift in n_∞ given in Table 3.2 for the same pH change. A better fit was obtained at pH 5.2 by reducing $\bar{\alpha}_n$ to 0.0027 ms^{-1}, however, to a first approximation, pH-dependent changes in the kinetics of activation of the K currents are accounted for solely by the shift in n_∞.

Values for $\bar{\alpha}_n$ and $\bar{\beta}_n$ found here are similar to those reported by Stanfield (1975; $\bar{\alpha}_n$ = 0.0032 ms^{-1}, $\bar{\beta}_n$ = 0.0133 ms^{-1}) and are within the range of values cited by Adrian et al. (1970a; $\bar{\alpha}_n$ = 0.0021 to 0.0044 ms^{-1}, $\bar{\beta}_n$ = 0.009 to 0.0185 ms^{-1}).

DISCUSSION

The results presented in this chapter show that the Na and delayed K conductances in muscle are sensitive to changes in external pH. A reduction in pH from 7.2 to 5.2 shifts the thresholds of the Na and K conductances by +23 mV and +23.3 mV, respectively, when these are measured in the absence of tetrodotoxin. In the presence of this drug, the shift in the threshold of the K conductance is similar, and a shift of +21.4 mV has been found for the potential-dependence of the n_∞ and τ_n relations. In alkaline solutions the experiments are less extensive; however, it is clear that there is a shift in the n_∞ relation and the threshold of the K conductance to more negative membrane potentials when the pH is raised from 7.2 to 9.2. All these changes are consistent with the present observation that a reduction in pH from 9.2 reduces the rates of rise

and fall of the action potential (see also Brooks & Hutter, 1963), and the finding that a reduction in external pH renders the fibres less excitable (Brooks & Hutter, 1963).

The shift in n_∞ reported by Gillespie and Hutter (1975) for muscle fibres immersed in a solution containing formaldehyde (+15 mV from pH 7.2 to 5.0) is rather less than that reported here. However, their observation that $\bar{g}_K$ is slightly less at pH 5.0 than at pH 7.2 is consistent with the present finding, though in one fibre only, that $\bar{g}_K$ is reduced by 64% when the pH is lowered from 7.2 to 4.2. Similar results are found in myelinated nerve fibres (Hille, 1973; Drouin & The, 1969) and Myxicola axons (Schauf & Davis, 1976) where, at pH 4.4, $\bar{g}_K$ is reduced to about 50% of its maximum value, which is seen in more alkaline solutions.

The maximum Na conductance, or in some cases the maximum Na permeability, is also reduced in acidic solutions in frog muscle (Campbell & Hille, 1976), frog myelinated nerve fibres (Hille, 1968; Drouin and The, 1969; Woodhull, 1973) and in Myxicola axons (Schauf & Davis, 1976). In those preparations the magnitude of the Na conductance (or Na permeability) is more sensitive to low pH than the K conductance. In addition, in muscle (Campbell & Hille, 1976) and in myelinated nerve (Woodhull, 1973), the reduction in the maximum Na permeability, which is about 50% at pH 5.4 and at zero membrane potential, is partly relieved when the membrane is depolarized. On the other hand, Drouin & Neumcke (1974) have found no evidence of a voltage-dependent block of Na channels by protons in myelinated nerve when the Na conductance, rather than the Na permeability, is measured.

Campbell & Hille (1976) have measured pH-dependent shifts in the Na permeability in the semitendinosus muscle of Rana pipiens. In low pH, the shift (+15.5 mV from pH 7.4 to 5.0) is less than, though in the same direction as, the shift in the threshold of the Na conductance reported here. In alkaline solutions, the shift in Na permeability reported by these authors (-3.2 mV from pH 7.4 to 9.4) is in the direction expected, but is comparatively small. Similar results are found in frog myelinated nerve fibres (Hille, 1968; Hille et al., 1975).

The present observation that a reduction in external pH shifts the relationship between n_∞ and the membrane potential, and between τ_n and the membrane potential by similar amounts to more positive potentials is consistent with the view outlined by A.F. Huxley (in Frankenhaeuser & Hodgkin, 1957), that a major effect of certain cations is to neutralize a potential set up at the outer surface of the membrane by fixed negative charges, which, in the present case, are in the vicinity of the delayed K channel. This hypothesis is illustrated in Fig. 3.9A, which shows the electrical gradient across the membrane of a fibre with no surface potential (continuous line) and the gradient across the membrane and extending into the bulk solution for a fibre with a surface potential (ψ_o) of about -20 mV (broken line). In both cases the measured membrane potential (V_1) is -90 mV and the electrical gradient across the membrane is assumed to be linear.

The shift in n_∞ to more negative potentials from pH 5.2 to 4.2 may be explained in a similar way; first, by assuming that there are fixed negative charges at the inner surface of the membrane, and secondly, by supposing that in strongly acidic solutions there is

Fig. 3.9 A. The potential gradient across the muscle fibre membrane and in the adjacent solution according to the surface charge hypothesis. The diagram is drawn roughly to scale with a distance of 3 nm across the hydrophobic part of the membrane, and a Debye length of 0.8 nm for the fall-off of potential in the external solution (Chandler, Hodgkin & Meves, 1965). The surface potential at the inner surface of the membrane is assumed to be negligible. The continuous line shows the voltage gradient in the absence of fixed charges and when the measured membrane potential is -90 mV. The interrupted line shows the voltage gradient when the density of fixed negative charges on the outside of the membrane is 0.26 nm^{-2}. ψ_o is the surface potential; V_1 is the measured membrane potential.

Fig. 3.9B. Theoretical curves which relate the pH-dependent shifts in $V_{\frac{1}{2}n}$ to the density of fixed charges on the outer surface of the membrane. Abscissa, maximum average surface charge density ($\bar{\sigma}$, nm^{-2}); left ordinate, maximum slope of the curve which relates the shift in n_{oo}, as measured by $V_{\frac{1}{2}n}$, to pH (d $V_{\frac{1}{2}n}$/dpH max). The corresponding line was drawn to eqn. (3.21) of the text; right ordinate, maximum shift in $V_{\frac{1}{2}n}$ ($\bar{V}_{\frac{1}{2}n}$). The corresponding line was drawn to eqn. (3.20) of the text. In each case, c = 0.134 M, and RT/F = 23.87 mV at 4°C.

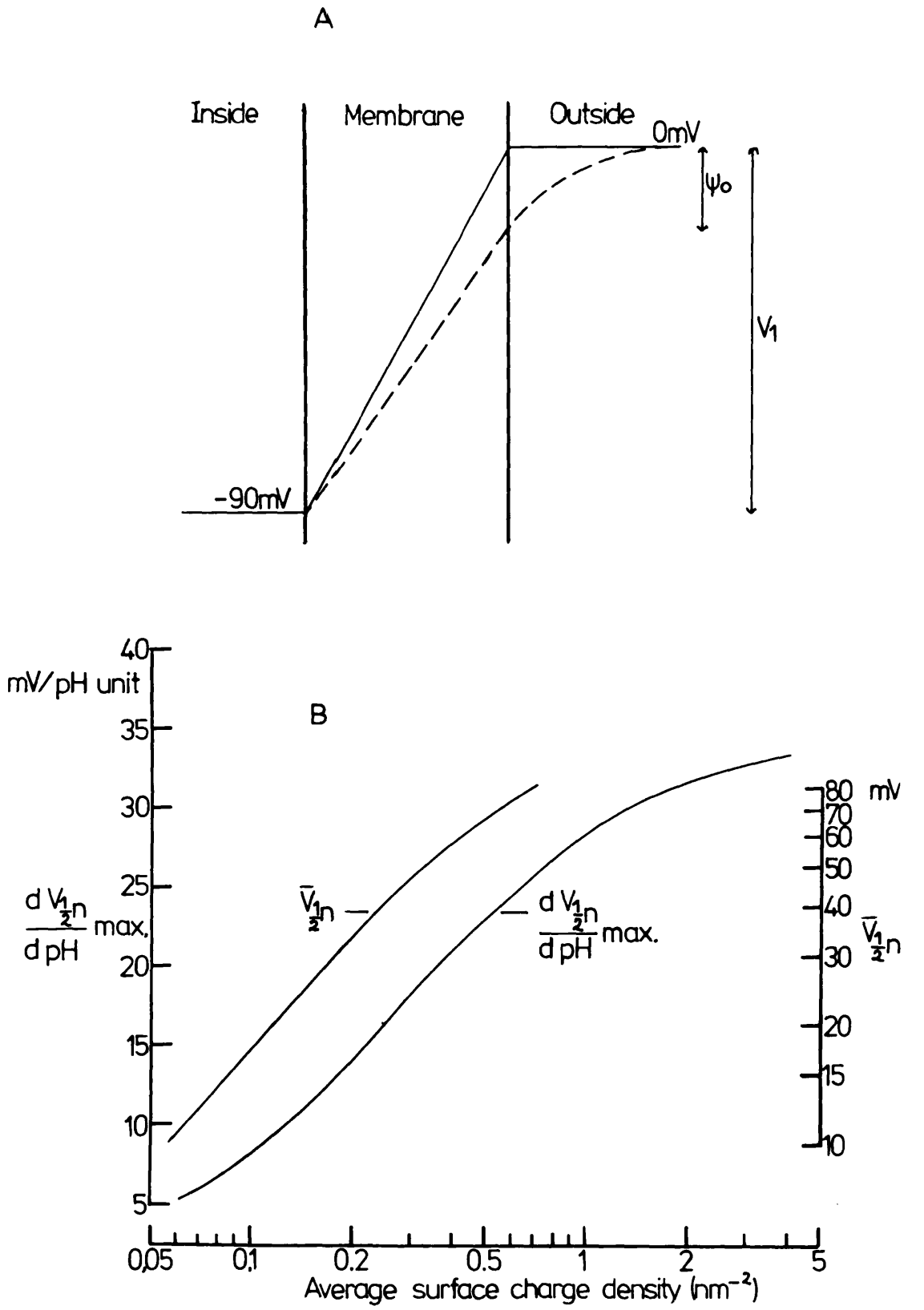
A
Inside
Membrane
Outside
0mV
ψ_o
V_1
-90mV
B
40
mV/pH unit
35
30
25
20
15
10
5
$\frac{d\,\bar{V}_{\frac{1}{2}n}}{d\,pH}$ max.
$\bar{V}_{\frac{1}{2}n}$
$\frac{d\,\bar{V}_{\frac{1}{2}n}}{d\,pH}$ max.
80 mV
70
60
50
40
30
20
15
10
$\bar{V}_{\frac{1}{2}n}$
0,05
0,1
0.2
0.5
1
2
5
Average surface charge density (nm^{-2})

a fall in intracellular pH such that these charges are titrated. In agreement with this, Strickholm & Clark (1977) have reported a loss of excitability in some crayfish nerve fibres at about pH 5, which they attributed to a change in intracellular pH. The effect was more common in tris-maleate buffer than in tris buffer, and rarely occurred in the absence of buffer. However, the concentration of tris-maleate used in their experiments (5-10 mM) was slightly higher than that used here. More direct evidence for the presence of fixed charges at the inner surface of membranes is given by Chandler Hodgkin & Meves (1965), who show that parameters describing the Na conductance in squid axons are shifted along the voltage axis when the ionic strength of the internal perfusate is changed.

In the discussion that follows, it is assumed that voltage shifts other than those arising from the titration of charges at the outer surface of the cell can be neglected.

The Gouy-Chapman theory of the diffuse double layer (Grahame, 1947; Davies & Rideal, 1963; Barlow, 1970) has been used by a number of authors to account, in whole or in part, for voltage shifts in the parameters which describe Na and K conductances, in terms of a screening of fixed charges by electrolytes in the internal (Chandler, Hodgkin & Meves, 1965) and external solution (Gilbert & Erhenstein, 1969, 1970; Mozhayeva & Naumov, 1970, 1972a,b,c; Brismar, 1973; Hille, Woodhull & Shapiro, 1975; Schauf, 1975; Begenisich, 1975; Campbell & Hille, 1976). Since the hypertonic chloride Ringer used here is composed almost entirely of a uni-univalent salt solution, the appropriate form of the Grahame equation (Grahame, 1947), which relates the fixed charge density (σ) to the magnitude of the surface potential (ψ_o) and the concentration of cations (or anions) in the Ringer, for the case in which the surface

potential is less than -100 mV is

$$\sigma = \frac{2c^{\frac{1}{2}}}{G} \sinh \frac{-\psi_o F}{2RT} \qquad (3.14)$$

where G is a constant equal to 2.707 (nm^2/electronic charge)(moles/liter)$^{\frac{1}{2}}$ when σ is in units of electronic charges/nm^2, ψ_o is in mV, c is in moles/liter and RT/F is 23.87 mV at 4°C.

Eqn. (3.14) predicts that all cations with the same valence will be equally effective in neutralizing the surface potential. This is not the case in nerve, however, since for example, equimolar replacement of divalent ions in voltage-clamp conditions gives the sequences $Ni^{2+} > Zn^{2+} = Co^{2+} > Cd^{2+} = Ba^{2+} > Ca^{2+} > Mg^{2+}$ and $Zn^{2+} > Ni^{2+} > Mn^{2+} = Co^{2+} > Ca^{2+} > Mg^{2+} > Sr^{2+} = Ba^{2+}$ in order of decreasing shifts in Na activation in squid axons (Blaustein & Goldman, 1968) and myelinated nerve fibres (Hille et al., 1975) respectively. For shifts in K activation in nerve, the sequence is $Cd^{2+} > Ni^{2+} > Co^{2+} > Ba^{2+} > Ca^{2+} > Mg^{2+}$ (Blaustein & Goldman, 1968; see also Mozhayeva & Naumov, 1970). These observations are explained by the supposition that some ions also neutralize the surface potential by binding to the fixed charges. Thus cations such as Ni^{2+} and Zn^{2+} have a high affinity for fixed charges whereas the smaller shifts produced by Mg^{2+} are consistent with the notion that this ion acts almost completely by screening.

Application of the Grahame equation to pure phospholipid membranes, where the density of fixed negative charges is 0.4 to 0.6 nm^{-2}, shows that a monovalent cation concentration of about 3.6 M is required to equal the screening produced by 1.8 mM of a divalent cation (McLaughlin, Szabo & Eisenman, 1971). Since screening by even the highest concentration of protons used in this study (6.3 x 10^{-5}M) will be small compared to the screening by divalent cations,

($[Ca^{2+}]_o$ = 1.8 mM), it is assumed that protons neutralize the surface potential solely by binding to the fixed charges (Hille, 1968; Woodhull, 1973; Drouin & The, 1969; Mozhayeva & Naumov, 1972a; Dörrscheidt-Käfer, 1976). In this case, the relationship between the maximum fixed charge density ($\bar{\sigma}$), the surface potential (ψ_o) and the external cation concentration (c) is

$$\bar{\sigma} = \left\{ \frac{[H]_B}{K_H} \exp(-\psi_o F/RT) + 1 \right\} \frac{2c^{\frac{1}{2}}}{G} \sinh(-\psi_o F/2RT) \qquad (3.15)$$

(Gilbert & Erhenstein, 1969; Gilbert, 1971), where the relationship between the concentration of protons at the membrane surface, $[H]_S$, and in the bulk solution, $[H]_B$, is

$$[H]_S = [H]_B \exp(-\psi_o F/RT) \qquad (3.16)$$

and where the relationship between the fixed charge density (σ), the maximum fixed charge density ($\bar{\sigma}$) and the dissociated constant (K_H) for the proton-fixed charge complex is:

$$\frac{\sigma}{\bar{\sigma}} = \frac{1}{1 + [H]_S/K_H} \qquad (3.17)$$

Eqn.(3.17) is analogous to the Michaelis-Menten equation for enzyme-substrate binding (Dixon & Webb, 1964).

As protons neutralize the surface potential by binding to fixed charges, the theoretical relationship between ψ_o and external pH is a titration curve which saturates at high and low pH. The relationship between $V_{\frac{1}{2}n}$ (the membrane potential at which n_∞ is 0.5) and pH will be similar because

$$\psi_o = V_{\frac{1}{2}n} - B \qquad (3.18)$$

where B is a constant in units of mV. Since the relationship between $V_{\frac{1}{2}n}$ and pH found experimentally is approximately linear from pH 9.2 to 5.2 (Fig. 3.3D), this probably corresponds to the middle section of the titration curve and, as such, does not provide sufficient

information for the complete solution of eqn (3.15). Despite this, the maximum fixed charge density can be estimated from the maximum shift in $V_{\frac{1}{2}n}$ and from the maximum slope of the graph of $V_{\frac{1}{2}n}$ against pH (Gilbert & Erhenstein, 1969, 1970; Gilbert, 1971). Both methods are described below.

For the limiting case in which $[H]_B$ is zero, the surface potential can be obtained from eqn. (3.14). On the other hand, when $[H]_B$ is sufficiently high that all fixed charges are titrated, ψ_o will be zero, so eqn (3.18) becomes

$$V_{\frac{1}{2}n} = B \tag{3.19}$$

It follows from eqns. (3.14, 3.18 & 3.19) that the maximum density of fixed charges ($\bar{\sigma}$) is related to the maximum shift in $V_{\frac{1}{2}n}$ (denoted $\bar{V}_{\frac{1}{2}n}$) by

$$\bar{\sigma} = \frac{2c^{\frac{1}{2}}}{G} \sinh \bar{V}_{\frac{1}{2}n} F/2RT \tag{3.20}$$

Fig. 3.9B plots the maximum shift in $V_{\frac{1}{2}n}$ as a function of the maximum surface charge density, assuming the latter to be uniform, and when c = 0.134 M. The value of $\bar{V}_{\frac{1}{2}n}$ found experimentally is 41 mV (Fig. 3.3D) which corresponds to a maximum density of titratable charges equal to 0.26 nm^{-2}. The true density will be greater than this since the present results extend over only part of the titration curve (from pH 9.2 to 5.2).

As noted previously, $\bar{\sigma}$ can also be obtained from the maximum slope of the relationship between $V_{\frac{1}{2}n}$ and pH. Substitution of $V_{\frac{1}{2}n}$ -B (eqn. 3.18) for ψ_o in eqn. (3.15) and subsequent differentiation of eqn. (3.15) yields

$$\frac{dV_{\frac{1}{2}n}}{d \ln [H]_B} = \frac{1}{\frac{F}{RT} - \left[\frac{F}{2RT} \coth \frac{(V_{\frac{1}{2}n}-B)F}{2RT}\right]\left[1 + \frac{2c^{\frac{1}{2}}}{\bar{\sigma} G} \sinh \frac{(V_{\frac{1}{2}n}-B)F}{2RT}\right]^{-1}} \tag{3.21}$$

(Gilbert & Erhenstein, 1969; Gilbert, 1971).

The solution to eqn. (3.21) for various values of $\bar{\sigma}$, and for the condition in which $dV_{\frac{1}{2}n}/d\ 1n[H]_B$ is at a maximum is given in Fig. 3.9B. In order to obtain this solution, it is necessary to differentiate eqn. (3.21). Since $d^2V_{\frac{1}{2}n}/d(1n[H]_B)^2$ is zero when $dV_{\frac{1}{2}n}/d\ 1n[H]_B$ is a maximum, one can write

$$\frac{d\ Z}{dV_{\frac{1}{2}n}} = 0 \qquad (3.22)$$

where 1/Z is substituted for the right hand side of eqn. (3.21). Whence, the solution to eqn. (3.21) is (Y. Eliman, personal communication)

$$\sinh^3 \frac{(V_{\frac{1}{2}n}-B)\ F}{2RT} - 2 \sinh \frac{(V_{\frac{1}{2}n}-B)\ F}{2RT} - \frac{\bar{\sigma}\ G}{2c^{\frac{1}{2}}} = 0 \qquad (3.23)$$

Finally, values for $\frac{(V_{\frac{1}{2}n}- B)F}{2RT}$ obtained from eqn. (3.23) for various values of $\bar{\sigma}$ are used to solve eqn. (3.21).

The maximum slope of the relationship between $V_{\frac{1}{2}n}$ and pH found experimentally is 10.3 mV per pH unit, which corresponds to a maximum surface charge density of 0.13 nm^{-2} (Fig. 3.9B). Since this is one half the minimum value obtained by eqn. (3.20), the assumption that the binding of protons to fixed charges can be described in terms of a single dissociation constant (K_H in eqns. 3.15 & 3.17) is probably incorrect. If there is more than one titratable group, $\bar{V}_{\frac{1}{2}n}$ will depend on the total surface charge density, while $dV_{\frac{1}{2}n}/dpH$, max. will tend to reflect the density of individual charged groups. Further, the fact that the relationship between $V_{\frac{1}{2}n}$ and pH is roughly linear from pH 9.2 and 5.2 (Fig. 3.3D) suggests the presence of a number of charged groups with pK_H values spread over most, or all, of this pH range.

Another reason why the surface charge density calculated here will be an underestimate of the true density is that Ca^{2+} ions present in the Ringer will screen, and possibly bind to the fixed charges

(Frankenhaeuser & Hodgkin, 1957; Gilbert & Ehrenstein, 1969; Mozhayeva & Naumov, 1972b; Hille et al., 1975; Dörrscheidt-Käfer, 1976; Schauf, 1975; Begenisich, 1975; Campbell & Hille, 1976). For example, Hille et al. (1975) and Dörrscheidt-Käfer (1975) have shown that the voltage-dependence of Na activation in myelinated nerve and the threshold for mechanical activation in muscle are less sensitive to changes in extracellular pH when the external Ca^{2+} concentration is raised.

The present conclusion that more than one type of fixed charge determines the surface potential associated with the delayed potassium channel in muscle is in general agreement with results reported by Mozhayeva & Naumov (1970), who used a slow, linear voltage change to measure voltage shifts in the steady-state K conductance of the nodal membrane of Rana ridibunda when the pH, ionic strength, and divalent cation concentration were altered. These authors concluded that three charged groups were probably involved. Two were negatively charged at pH 7, and most likely to be carboxyl groups. The third group was positively charged in neutral and acidic solutions but uncharged in strongly alkaline conditions, and assumed to be an amino group. The net fixed charge density was negative at pH 7.2 and in 2 mM-Ca^{2+}, and corresponded to a surface potential of about -30 mV. Using a step-clamp, however, Brismar (1973) obtained a surface potential of -55 mV for the K permeability of the nodal membrane of Xenopus laevis in standard Ringer.

Unfortunately, since it is not possible to determine the fraction of surface charge which is negative and that which is positive in any of the experimental conditions used here, it is not possible, at present, to estimate the absolute surface potential associated with

delayed rectification in muscle. In a culture medium, muscle cells migrate towards an anode (Elul, 1967) indicating a net negative charge on the outer surface of the cell. However, the distribution and type of charge in the vicinity of ionic channels may be very different from that over the surface of the cell as a whole.

When comparing the surface potentials obtained in different preparations, it is necessary to take into account the fact that even after numerous experiments have been done, there may be more than one solution to the equations relating to surface charge. For example, Hille et al. (1975) describe two models which fit the potential-dependence of the Na conductance of the nodal membrane in a variety of solutions: the surface potentials contained in these models are -90.6 mV and -64.3 mV. However, the following points can be drawn from these and related studies. First, like Mozhayeva & Naumov's (1970) model which accounts for voltage shifts in the K conductance of the node of Ranvier, both models relating to the Na permeability in nerve comprise two acidic groups and one basic (Hille et al., 1975). Secondly, the models of Hille et al. (1975) also fit the pH- and Ca^{2+}-dependent shifts in the Na permeability in frog muscle (Campbell & Hille, 1976). And thirdly, the surface potential associated with K channels seems to be less than that associated with Na channels, although that associated with the threshold for contraction is -87.2 mV at pH 7.2 (Dörrscheidt-Käfer, 1976), which is close to one of the values given by Hille et al. (1975) for the Na channel.

Finally, it is interesting to note that while the relationship between the threshold of the delayed conductance and pH is roughly linear between pH 9.2 and 5.2 (Fig. 3.3C), Dörrscheidt-Käfer (1976) has shown that the threshold for mechanical activation is rather

insensitive to changes in external pH from about 6 to 8. This supports the notion (Kao & Stanfield, 1968; 1970) that there is no causal relationship between the thresholds for contraction and delayed rectification, and is also consistent with the view that the mechanisms which underlie contraction and delayed rectification are located in different parts of the membrane.

Chapter 4. The selectivity of the delayed K channel in frog skeletal muscle fibres.

INTRODUCTION

The mechanism by which delayed K channels discriminate between sodium and potassium is of particular interest since it forms an essential part of the ionic basis of the action potential. A study of the permeability of the channel to foreign cations is also valuable since it can provide information as to the dimensions of the channel, and as to the nature of the groups with which the channel is lined.

Recent studies have shown that the selectivity of Na channels in myelinated nerve fibres (Hille, 1971, 1972) and muscle fibres (Campbell, 1976) of Rana pipiens are similar. Only minor differences were reported, the most important being that the permeability ratio P_{Na}/P_K in muscle is nearly twice that in nerve.

On the other hand, P_{Na}/P_K for the delayed K channels in muscle (Adrian et al., 1970a) is about three times that for the K channels in myelinated nerve fibres (Hille, 1973). Despite the fact that these measurements were not obtained in the same species of frog, it seems likely that K channels in nerve and muscle are not identical, as suggested by some of the studies described in chapter 1.

The experiments to be described in this chapter are largely concerned with the measurement of the reversal potential of the delayed current in the presence of ions belonging to the alkali metal series. These measurements are used to obtain the selectivity sequence of the delayed K channel in muscle.

These experiments were performed in collaboration with Dr. P.R. Stanfield and are also described elsewhere (Gay & Stanfield, 1978).

SOLUTIONS AND METHODS

The composition of solutions used in this chapter is given in Table 4.1. All contain sulphate as the major anion in place of chloride. In addition, these solutions contain 8 mM-$CaSO_4$; the ionized Ca^{2+} is estimated to be about 1 mequ./l. (Hodgkin & Horowicz, 1959). Hypertonic solutions (solutions 4B, C) were used to reduce the ability of the fibres to contract. These solutions contain 350 mM sucrose which is in addition to the sucrose required to be added to make the sulphate solutions isotonic with the phosphate-buffered chloride Ringer whose composition is given in chapter 2.

Table 4.1

Composition of solutions in mM

Ringer	X^+	Na^+	K^+	Ca^{2+}	SO_4^{2-}	$H_2PO_4^-$	HPO_4^{2-}	Sucrose
4A, isotonic sulphate	-	82.6	2.5	8	49.3	0.43	1.08	113
4B, hypertonic sulphate	-	82.6	2.5	8	49.3	0.43	1.08	463
4C, X^* Ringer	82.5	2.6	-	8	49.3	0.43	1.08	463

*X = Li, Na, K, Rb or Cs

Muscles were dissected and equilibrated in the phosphate-buffered, chloride Ringer. Thereafter, the muscles were equilibrated in isotonic sulphate Ringer (solution 4A) for at least 1 hr at room temperature in order to reduce the intracellular chloride concentration, and then in hypertonic sulphate Ringer (solution 4B) for at least 20 mins, also at room temperature.

Finally, the muscles were transferred to another hypertonic solution (solution 4C) in which most of the experiments were performed.

Since the membrane is impermeable to sulphate (Conway & Moore, 1945), this anion does not replace intracellular chloride in significant quantities, but its substitution for chloride does result in a transient depolarization of the membrane and contracture, (Adrian, 1960). Muscles were not allowed to shorten during contracture, recovery from which occurred spontaneously after a few seconds.

The membrane potential was controlled in all experiments using the three-electrode method of Adrian et al. (1970a) which is described in chapter 2 (page 42). Fibres were held at -100 mV and depolarized or hyperpolarized from this level. In addition, fibres were held at -100 mV for at least 5 mins following impalement, and before measurements were made, in order to reprime the delayed K conductance which is inactivated in solutions which depolarize the membrane, such as those containing 41.25 mM-K_2SO_4, Rb_2SO_4 or Cs_2SO_4 (solution 4C, Table 4.1). Fibres were also returned to the holding potential for 1 - 2 mins following a depolarization which activated the delayed conductance. An inter-electrode distance (ℓ) of 125 μm was used in all experiments.

Most experiments were performed in the cold (3-5°C, unless otherwise stated) since it was not always possible to control the membrane potential of fibres immersed in the control solution (41.25 mM-K_2SO_4) at room temperature.

Most experiments were performed in the presence of 10^{-6} g/ml TTX.

Calculation of permeability ratios from the reversal potential of the delayed current

The shift which occurs in the reversal potential of the

delayed current when a solution containing X^+ as the only cation is replaced by one containing only K^+ is related to the permeability ratio (P_X/P_K) of X and K for the delayed K channel by the expression

$$V_{R,X}-V_{R,K} = \frac{RT}{F} \log_e \frac{P_X (X)_o}{P_K (K)_o} \qquad (4.1)$$

(Hille, 1973; Campbell, 1976), where $V_{R,X}$ and $V_{R,K}$ are the reversal potentials of the delayed current in the X solution and K solution respectively, and where $(X)_o$ and $(K)_o$ are the external activities of X^+ and K^+. Eqn. (4.1) is derived from the equations of Goldman (1943) and Hodgkin & Katz (1949) but a constant field is not assumed in its derivation.

Here, X stands for Li, Na, K, Rb, or Cs. Unless otherwise stated, concentrations rather than activities are used in eqn. (4.1) since the activity coefficients of the alkali metal cations are not reported for the experimental conditions used here. However, the error introduced by this approximation will be small. Where activities are used, the activity coefficients are assumed to be equal to those in a 0.1 M sulphate solution at 25°C (Robinson & Stokes, 1965). With respect to the activity coefficient in K_2SO_4, these are: Li, 1.10; Na, 1.04; K, 1.0; Rb, 1.06; Cs, 1.06.

In using eqn. (4.1) the small amount of Na^+ (2.6 mM) added to all solutions as phosphate salts was neglected. Since Na^+ is one of the least permeant of ions in the delayed K channel, this approximation introduces an error of only 3% when P_X/P_K is 0.015, and the error disappears when P_X/P_K is 1.0. These two permeability ratios cover the range of ratios found experimentally. Calcium, which is also present in all solutions, is unlikely to influence the reversal potential since

the ionized concentration of this cation is low, and since, like nerve (Hille, 1975a), the K channels in muscle are probably impermeable to Ca^{2+}.

RESULTS

A summary of most of the results to be described in this chapter is presented in Table 4.2. The first five rows are the results obtained in solution 4C which contained 41.25 mM-Li_2SO_4, Na_2SO_4, K_2SO_4, Rb_2SO_4 or Cs_2SO_4. For the remainder of this chapter, solution 4C will be referred to as Li-Ringer, Na-Ringer, etc., to identify the cation. Row six gives the results from a very small number of fibres in hypertonic sulphate Ringer (Solution 4B) which contained 1.25 mM-K_2SO_4 and 40 mM-Na_2SO_4. The permeability ratios given in columns 5 and 6 are those obtained from eqn. (4.1) using concentrations and activities, respectively.

Resting potentials

The resting potentials are shown in Table 4.2. In Na-Ringer (containing no K^+), the mean resting potential was -78.7 mV. This is rather less negative than the value expected for a solution containing Na^+ and 2.5 mM-K^+. However, the present result is not surprising because Hodgkin & Horowicz (1959) showed that in an isotonic sulphate Ringer solution the resting membrane potential reaches a maximum negative value at 0.5 mM external K^+. In this respect, the resting membrane does not distinguish between Na^+ and Li^+ ions, since the mean resting potential in Li-Ringer is not significantly different from that in Na-Ringer ($P > 0.1$).

On the other hand, fibres in Cs, Rb, and K-Ringer are depolarized, on average, by at least 40 mV more than fibres in

TABLE 4.2

Some properties of the delayed K conductance and the resting membrane of fibres immersed in alkali metal ion solution at about 4°C.

1	2	3	4	5	6
Ringer	RP (mV)	$V_{R,X}$ (mV)	$\overline{g}_{K,X}$ (mmho.cm^{-2})	P_X/P_K	P_X/P_K
Lithium	-75.6 ± 3.8 (8)	-110.6 ± 2.4 (8)	7.40 ± 0.79 (5)	0.024 (0.016 - 0.033)	0.026
Sodium	-78.7 ± 2.2 (10)	-104.8 ± 1.7 (10)	8.38 ± 0.75 (11)	0.030 (0.020 - 0.045)	0.031
Potassium	-22.2 ± 0.6 (11)	-21.3 ± 1.2 (11)	10.33 ± 1.38 (11)	1.0	1.0
Rubidium	-34.2 ± 2.2 (16)	- 22.6 ± 1.3 (7)	7.94 ± 1.12 (9)	0.95	1.0
Caesium	-38.5 ± 1.1 (8)	- 73.1 ± 2.8 (8)	4.63 ± 1.13 (9)	0.11 (0.072 - 0.17)	0.12
Hypertonic Sulphate	-81.7 ± 4.6 (3)	-85.0 (1)	20.56 (2)	-	-

Column 5, mean with range of permeability ratios in parentheses assuming activity coefficients equal to 1.0.

Column 6, mean permeability ratios assuming activity coefficients taken from Robinson & Stokes (1965); these are: Li_2SO_4, 0.478; Na_2SO_4, 0.452; K_2SO_4, 0.436; Rb_2SO_4, 0.460; Cs_2SO_4, 0.464 in a 0.1 M solution at 25°C.

Na-Ringer. The mean resting potential in K-Ringer is also significantly less negative than that in Rb-Ringer ($P<0.001$) and Cs-Ringer ($P<0.001$). Thus it is clear that the resting membrane is able to distinguish between K^+ and Rb^+, or K^+ and Cs^+, a conclusion which is supported by the experiments of Sjodin (1959), Sandow & Mandel (1951) and Adrian (1964), and by the experiments of chapter 5.

Reversal potential of the delayed current in K-Ringer and Rb-Ringer

The experiments to be described in the first part of this section are those in which the reversal potential of the delayed current was measured in K and Rb-Ringer in the same fibres. Fig. 4.1 shows the results from one of five such experiments in which the solution was changed with the electrodes in situ. This fibre was bathed first in Rb-Ringer (a) then in K-Ringer (b) and then in Rb-Ringer again (c).

The top of Fig. 4.1 illustrates the two-step procedure (Adrian et al., 1970a) used to determine the reversal potential. The first step depolarizes the membrane to + 12 mV for 35 ms and activates the delayed conductance. During the second step, which is applied immediately after the first step, the membrane potential is returned to between 0 mV and -50 mV. The current declines slowly during the second step due to the closure of those K channels which were open at the end of step one. Since in 41.25 mM-K_2SO_4 or Rb_2SO_4 solution the tail currents are long compared to the capacity currents which also contribute to the current at the start of step two, the reversal potential was obtained from isochronal current-voltage relations of the tail currents (Bezanilla & Armstrong, 1972; Hille, 1973). By this

Fig. 4.1 Two-step experiment to determine the reversal potential of the delayed current in a fibre bathed consecutively in Rb-Ringer (a), K-Ringer (b), and Rb-Ringer (c),

top, tracings of records of the membrane potential (V_1) and the membrane current (V_2-V_1). The first step depolarizes the membrane to +12 mV for 35 ms. The second step returns the membrane to various levels between 0 mV and -50 mV. Four superimposed records are shown in (a) and (c), and five in (b)

bottom, isochronal current-voltage relations of the tail currents shown in the upper part of the figure. Abscissae, membrane potential (mV) during step 2; ordinates, membrane current (mV) during step 2 after subtraction of the leakage current. The membrane current is measured 20 ms (o, •), 40 ms (□, ■) and 60 ms (▽, ▼) after the start of the second step. $V_{R,Rb}$ is -23 mV in (a) and -22 mV in (c). $V_{R,K}$ is -22 mV, in (b).

Fibre resting potential, -25 mV in Rb-Ringer; holding potential, -100 mV; inter-electrode distance (ℓ), 125 μm; temp. 3.8 to 5.4°C; tetrodotoxin not added.

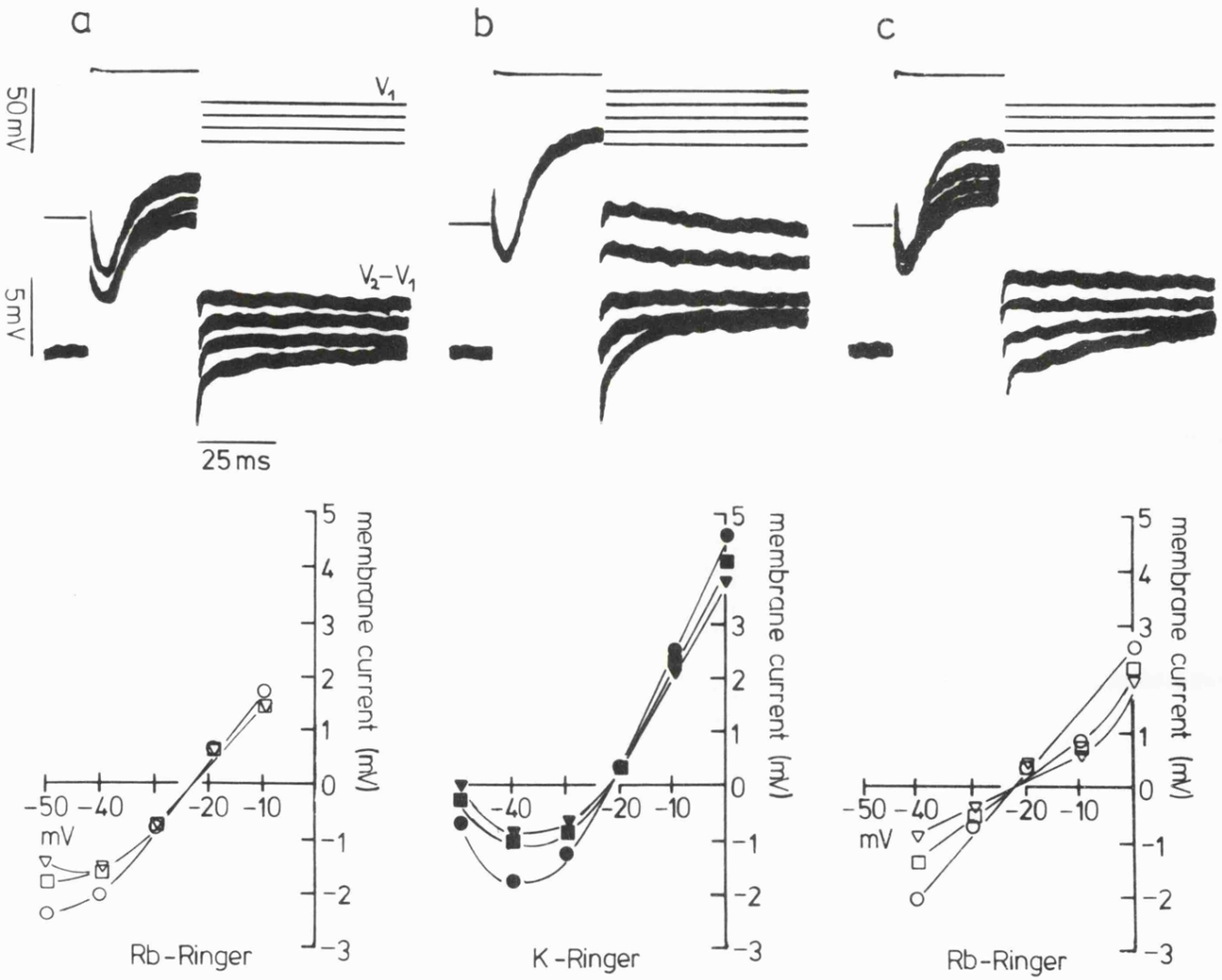
a
b
c
50 mV
5 mV
V_1
V_2-V_1
25 ms
membrane current (mV)
mV
-50 -40 -20 -10
5 4 3 2 1 0 -1 -2 -3
Rb-Ringer
K-Ringer
Rb-Ringer

method, the tail currents are plotted against the membrane potential during the second step at various times after the capacity currents have subsided, and after the leakage currents scaled linearly from the steady-state currents during small depolarizations have been subtracted.

In Fig. 4.1 the isochronal current-voltage relations are plotted 20 ms (circles), 40 ms (squares) and 60 ms(triangles) after the start of the second step. The reversal potential in Rb-Ringer is -23 mV in (a) and -22 mV in (c). The reversal potential in K-Ringer is -22 mV,in (b).

Table 4.3 gives resting potentials and reversal potentials from five similar experiments including that illustrated in Fig. 4.1. The resting potentials were measured at the start of the experiments in Rb-Ringer or, in the case of Fibre 18.7, in K-Ringer. The mean difference in reversal potentials in the two solutions is not significantly different from zero ($P \gtrsim 0.37$). Thus P_{Rb}/P_K, which is 0.95 from eqn. (4.1), is not significantly different from 1.0.

The conclusion from these experiments, that the delayed K channels are equally permeable to K^+ and Rb^+, depends on the assumption that there is little or no change in potential at the agar bridge-Ringer junction when Rb^+ replaces K^+ in the recording chamber. This assumption seems justified since the mobilities of K^+ and Rb^+ in aqueous solution are similar (Robinson & Stokes, 1965). In addition, it was found that the potential recorded by a microelectrode in the Ringer changed by less than 0.5 mV when Rb^+ was run into the chamber to displace K^+, or when K^+ displaced Rb^+.

TABLE 4.3

Properties of the delayed K conductance in Rb and K solutions at about 5°C.

Fibre	RP (mV)	$V_{R,Rb}$ (mV)	$V_{R,K}$ (mV)	$V_{R,Rb}$ (mV)	$V_{R,K}$ (mV)	$V_{R,Rb} - V_{R,K}$ (mV) [1]
17.2	-37	-20	-22	-21	-	+ 1.5
17.3	-35	-22	-21	-	-	- 1.0
17.4	-36	-20	-20	-	-	0
18.7	-35	-	-28	-30	-20	- 6.0
18.8	-25	-23	-22	-22	-	- 0.5
					Mean ± S.E.M.	- 1.2 ± 1.3
					P_{Rb}/P_K	0.95

[1] Each value is the difference between the mean values of $V_{R,Rb}$ and $V_{R,K}$ determined in one fibre

$V_{R,K}$ has also been determined from the isochronal current-voltage relations of eleven fibres in a second series of experiments. The difference between these experiments and those of the first series is that here the Ringer did not flow through the recording chamber so that a more stable temperature was achieved. The mean value of $V_{R,K}$ was -21.3 $\pm$ 1.2 mV at 3 - 4.5°C, which is not significantly different from the mean resting potential in the same fibres: this was -22.2 $\pm$ 0.6 mV ($P>0.33$). Neither is it significantly different from the mean value of $V_{R,K}$(-22.2 $\pm$ 2.4 mV; $P>0.33$) for the six measurements in Table 4.3. The present value for $V_{R,K}$ is also given in Table 4.2, and is the value used in the calculation of P_{Na}/P_K, P_{Li}/P_K and P_{Cs}/P_K.

Experiments in K-Ringer and Rb-Ringer at room temperature

Reversal potentials for the delayed current were determined from isochronal current-voltage relations in nine fibres in K-Ringer and ten other fibres in Rb-Ringer at 19 - 21°C. Since the tail currents declined more rapidly at room temperature than in the cold, current-voltage relations were plotted 5, 10, 15 and 20 ms after the start of the second step. In a given fibre, the reversal potentials measured at such times rarely differed by more than 2 mV. Mean resting potentials and reversal potentials for the two groups of fibres are given in Table 4.4. $V_{R,K}$ is not significantly different from $V_{R,Rb}$ ($p>0.33$). In addition, the permeability ratio, P_{Rb}/P_K, calculated from these values is 0.94, which is the same as that obtained in the cold (P_{Rb}/P_K = 0.95, Table 4.2)

The finding that P_{Rb}/P_K is rather insensitive to changes in temperature is not unexpected since it seems likely that the

TABLE 4.4

Resting potentials (RP) and reversal potentials ($V_{R,X}$) of fibres immersed in Rb-Ringer and K-Ringer at 19-21°C.

Ringer	RP (mV)	$V_{R,X}$ (mV)	P_{Rb}/P_K
Potassium	-28.7 ± 1.9 (9)	-25.5 ± 1.8 (9)	
			0.94
Rubidium	-32.5 ± 1.7 (10)	-27.1 ± 2.7 (10)	

delayed channels cannot distinguish between these ions. However, a low temperature coefficient for selectivity also occurs in cases in which one ion is permeant and the other rather impermeant. For example, P_K/P_{Na} is 0.074 at 0°C and 0.070 at 19°C for Na channels in myelinated nerve fibres (Hille, 1975a).

Determination of $V_{R,Rb}$ from steady-state current-voltage relations of the delayed current

Since in solutions containing 41.25 mM-Rb_2SO_4 the reversal potential of the delayed current is positive to the threshold of that current, it is possible to obtain $V_{R,Rb}$ from steady-state current-voltage relations of the delayed current as well as from isochronal current-voltage relations of the tail current.

Fig. 4.2A shows records of the membrane potential (V_1) and membrane current (V_2-V_1) for a fibre in Rb-Ringer depolarized to -71 mV, -41 mV and -12 mV. The steady-state current-voltage relation for this fibre is shown in Fig. 4.2B. The threshold of the delayed current is about -50 mV, so at -71 mV only the leakage and capacity currents are seen. At -41 mV the delayed current is inward; this will be carried by Rb^+ ions. On the other hand, the delayed current is outward at -12 mV and will be carried by K^+. The arrow in Fig. 4.2B indicates the reversal potential, which is -23 mV.

In four similar experiments including that described above, $V_{R,Rb}$ was -28.0 ± 4.1 mV. When this is compared with the mean of seven values for $V_{R,Rb}$ obtained from isochronal current-voltage relations (-22.6 ± 1.3 mV; Table 4.2) the difference is not significant ($P>0.1$). However, it was generally felt that the delayed currents which were inward in 41.25 mM-Rb_2SO_4 were too small for $V_{R,Rb}$ to be measured accurately. Similarly, the

Fig. 4.2 Properties of the delayed current in Rb and Cs-Ringer.

A, tracings of records of the membrane potential (V_1) and the membrane current (V_2-V_1) for a fibre in Rb-Ringer. The depolarizations are to -71 mV, -41 mV and -12 mV. Fibre resting potential, -24 mV; holding potential, -100 mV; inter-electrode distance (ℓ), 125 μm; temp, 3.5°C; tetrodotoxin, 10^{-6} g/ml.

B, steady-state current-voltage relationship for a fibre in Rb-Ringer. Same fibre as in (A). Abscissa, membrane potential (mV); ordinate, membrane current (mV). The line through the points is drawn by eye. The leak is extrapolated to find $V_{R,Rb}$: this is -23 mV.

C, the relationship between the delayed conductance and the membrane potential for a fibre in Rb-Ringer. Same fibre as in (A) and (B). Abscissa, membrane potential (mV); ordinate, delayed conductance shown as a fraction of the estimated maximum delayed conductance, which was 6.34 mmho.cm^{-2}. The line through the points is drawn by eye.

D, the relationship between the delayed conductance and the membrane potential for a fibre in Cs-Ringer. Same fibre as Fig. 4.5. Abscissa, membrane potential (mV); ordinate, delayed conductance shown as a fraction of the estimated maximum conductance, which was 2.05 mmho.cm^{-2}. The line through the points is fitted by eye.

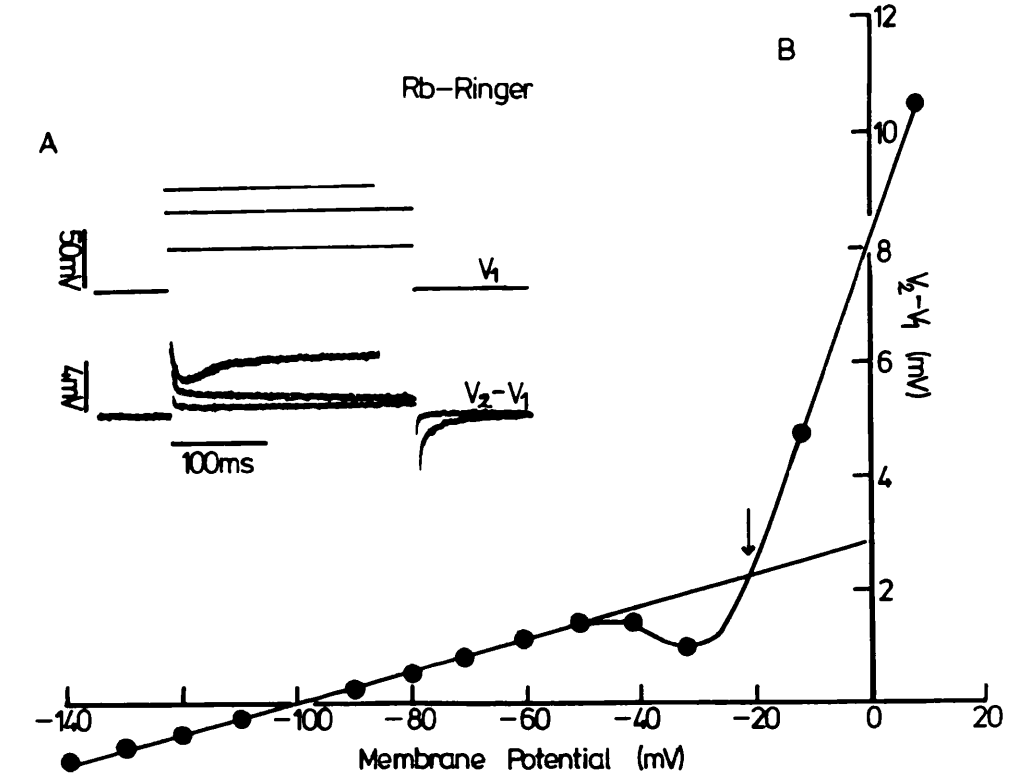
A
50mV
4mV
100ms
V1
V2-V1
Rb-Ringer
B
12
10
8
6
4
2
V2-V1 (mV)
-140
-100
-80
-60
-40
-20
0
20
Membrane Potential (mV)

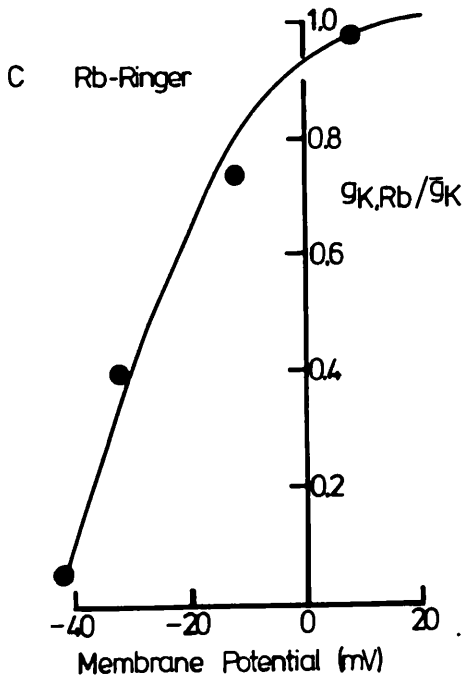
C
Rb-Ringer
1.0
0.8
0.6
0.4
0.2
gK,Rb/ḡK
-40
-20
0
20
Membrane Potential (mV)

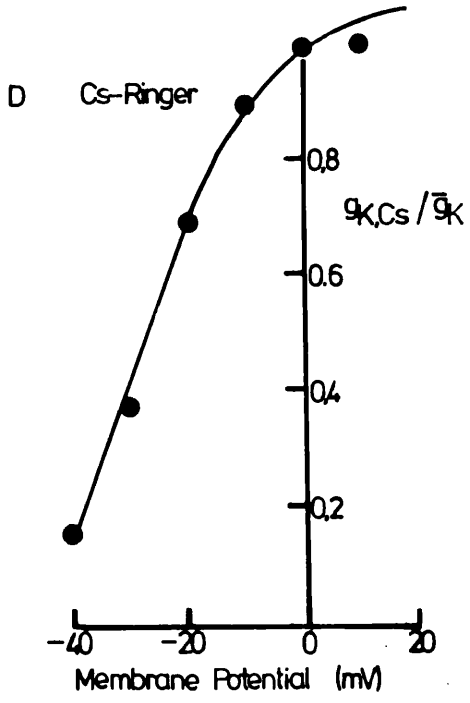
D
Cs-Ringer
0.8
0.6
0.4
0.2
gK,Cs/ḡK
-40
-20
0
20
Membrane Potential (mV)

inward delayed currents in 41.25 mM-K_2SO_4 were too small for this method to be used to determine $V_{R,K}$.

Reversal potential of the delayed current in Na-Ringer and Li-Ringer

A two-step procedure was used to determine the reversal potential of the delayed current in Na, Li and Cs-Ringer since it was found that these ions are less permeant than K^+ or Rb^+. Here, the results in Na and Li-Ringer are presented. The results in Cs-Ringer are described separately since Cs^+ was found to be more permeant than Na^+ or Li^+.

The two-step procedure is illustrated in Fig. 4.3a, which shows six superimposed records of the membrane potential (V_1) and the membrane current (V_2-V_1) from a fibre in Na-Ringer at 4.1°C. The first step depolarizes the membrane to +12 mV for 35 ms; this activates the delayed K current which is seen to rise off the top of the oscilloscope screen. During the second step the fibre is repolarized to between -30 mV and -150 mV producing a tail current which is inward at -110 mV and outward at -90 mV. Since the capacity current is inward at the start of the second step, the true reversal potential is some 5 or 10 mV more negative than the records in Fig. 4.3a suggest.

Fig. 4.3a also shows that the tail currents inactivate completely between -70 mV and -150 mV, which is consistent with the observation that the threshold of the delayed current is between -50 mV and -40 mV in this fibre. The steady-state current which remains after the delayed current has inactivated is the leakage current. Alternatively, the leakage current was obtained by linearly scaling the steady-state currents for depolarizations of less than 35 mV. In most cases, the leak

Fig. 4.3 Two-step experiment to determine the reversal potential of the delayed current in a fibre immersed in Na-Ringer.

a, tracings of records of the membrane potential (V_1) and the membrane current (V_2-V_1). The first step is to +12 mV and lasts 35 ms. The second step is to between -30 mV and -150 mV. Six superimposed records are shown.

b, temporal decay of the tail currents at the start of the second step. Left, outward tail currents; right, inward tail currents. Abscissae, time after the start of the second step; ordinates, membrane current after subtraction of the leakage current. The tail currents after 15 ms are extrapolated to the start of the second step to find the instantaneous current.

Fibre resting potential, -63 mV; holding potential, -100 mV; inter-electrode distance (ℓ), 125 μm; temp. 4.1°C; tetrodotoxin, 10^{-6} g/ml.

Na–Ringer

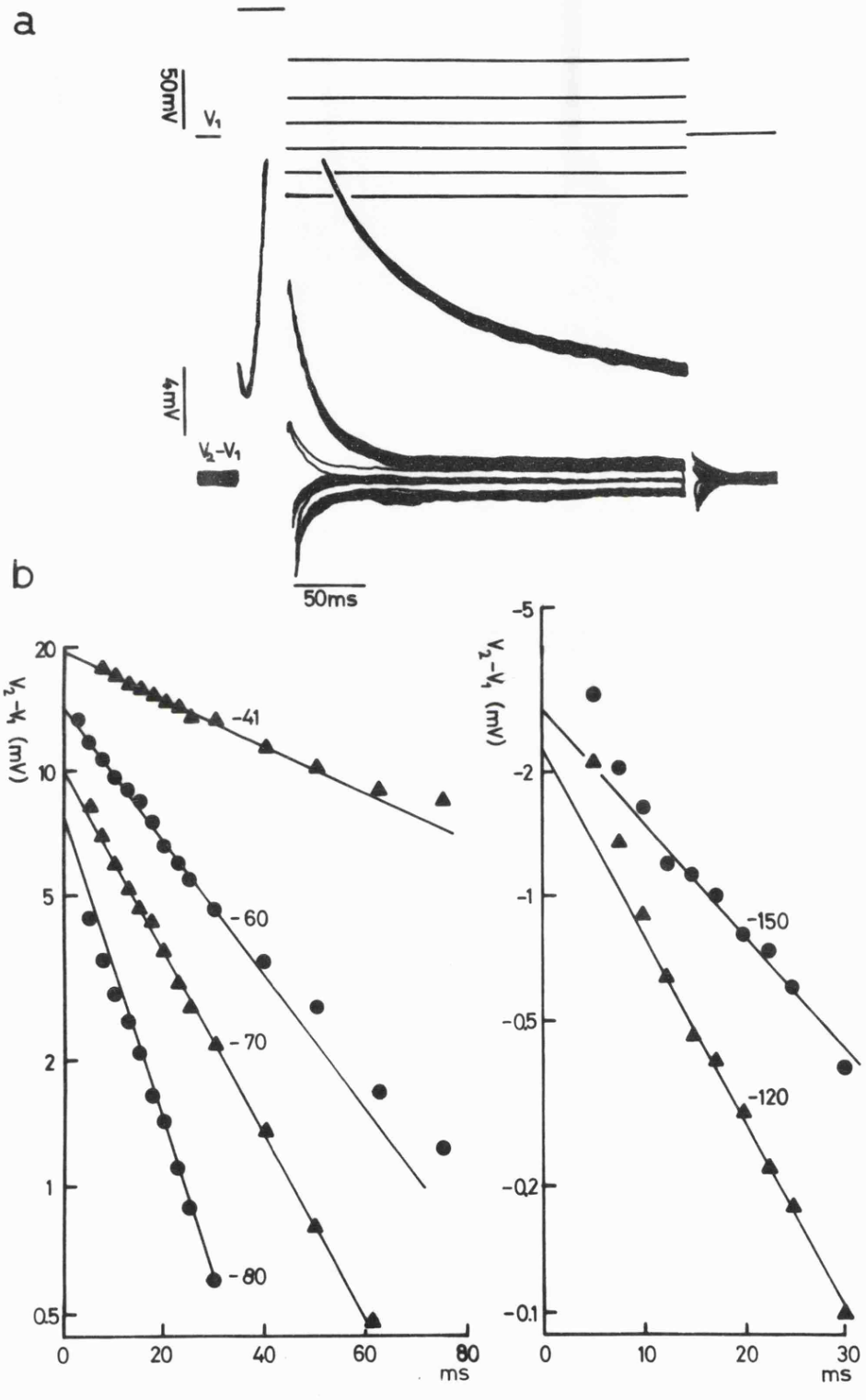
a
50mV
V1
4mV
V2-V1
50ms
b
V2-V1 (mV)
20
10
5
2
1
0.5
-41
-60
-70
-80
0
20
40
60
80
ms
V2-V1 (mV)
-5
-2
-1
-0.5
-0.2
-0.1
-150
-120
0
10
20
30
ms

was monitored during the 30 mins or so required to obtain a set of records by recording the current during a small depolarizing step applied a few seconds after the end of the second step. The results were discarded if the leak increased by more than 100%.

Since the tail currents inactivate rapidly at large negative membrane potentials, the reversal potential could not be obtained from isochronal current-voltage relations. Instead each tail current, after subtraction of the leak, was plotted on a semilogarithmic scale against time, and extrapolated back to the start of the second step to obtain the instantaneous current. The method is illustrated in Fig. 4.3b, which shows semilogarithmic plots of four outward tails (on the left) and two inward tails (on the right) for the fibre in Fig. 4.3a.

In Fig. 4.4a, the instantaneous current in Na-Ringer is plotted as a function of the membrane potential, as filled circles. Open arrows or triangles indicate the direction of the tail currents where these were too small to be extrapolated by the method described above. The current reverses at about -108 mV. In a similar experiment in Li-Ringer (Fig. 4.4b), the reversal potential was -111 mV.

The mean reversal potential in Na-Ringer was -104.8 $\pm$ 1.7 mV (ten fibres) compared with -110.6 $\pm$ 2.4 mV (eight fibres) in Li-Ringer. The difference between these values is not significant ($P = 0.063$). Since $V_{R,K}$ is -21.3 mV, P_{Na}/P_K is 0.030 and P_{Li}/P_K is 0.024. These values are also given in Table 4.2.

The present method of correcting the tail currents for capacity currents seems justified by the fact that the inward tail currents decline as the sum of two exponentials in Fig. 4.3b.

Fig. 4.4 Instantaneous current-voltage relations for a fibre in Na-Ringer (a) and a fibre in Li-Ringer (b). Abscissae, membrane potential (mV); ordinates, membrane current (mV) at the start of the second step of a two-step experiment, after subtraction of capacity and leakage currents. The instantaneous currents are shown as filled circles. Open triangles or arrows indicate the directions of those tail currents which were too small to measure accurately.

a, fibre in Na-Ringer; $V_{R,Na}$ = -108 mV. Same fibre as Fig. 4.3.

b, fibre in Li-Ringer; $V_{R,Li}$ = -111 mV. Resting potential, -83 mV; holding potential, -100 mV; inter-electrode distance (ℓ), 125 μm; temp. 3.5°C; tetrodotoxin, 10^{-6} g/ml.

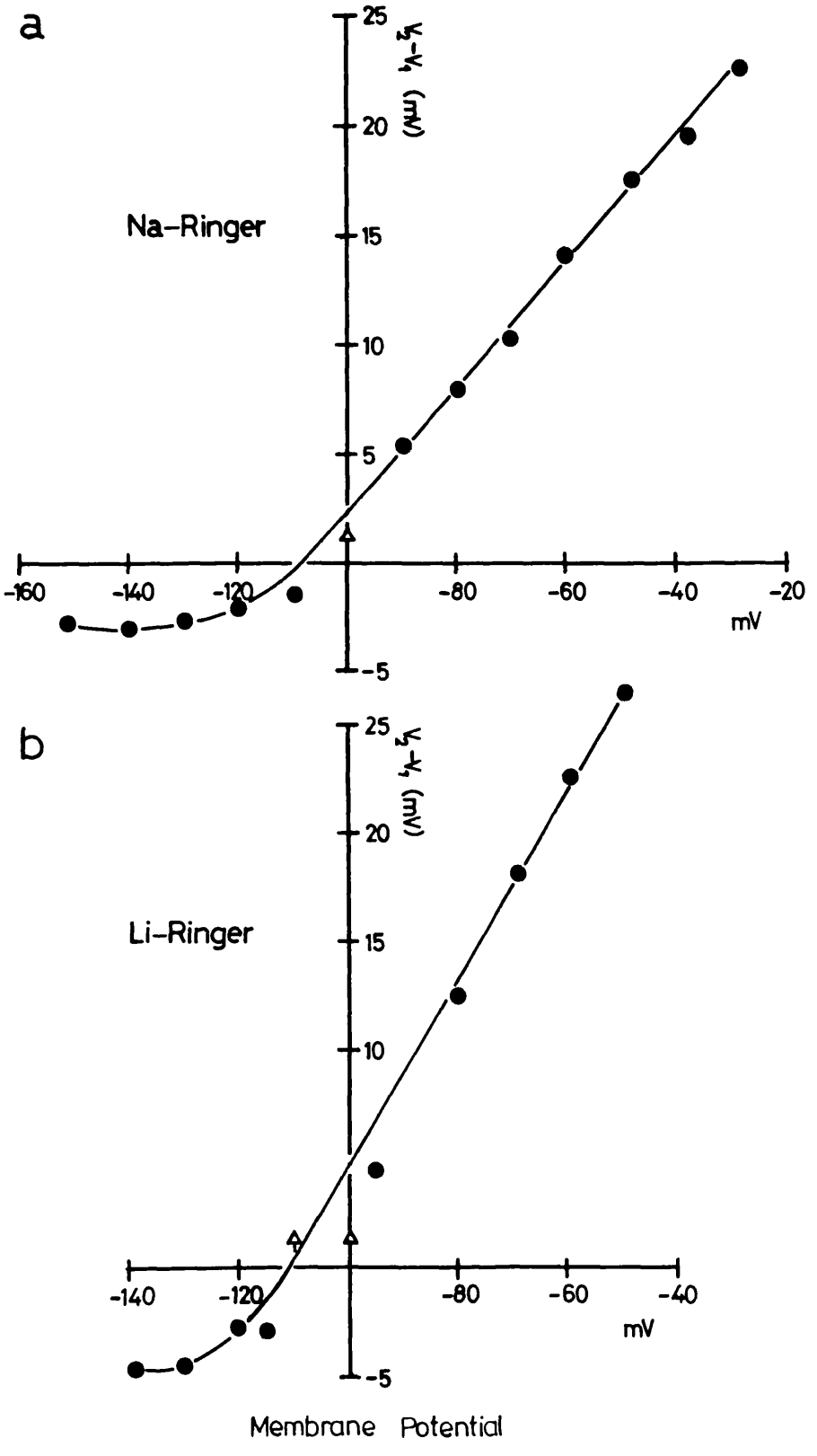
a
Na-Ringer
25
20
15
10
5
-5
V_2-V_1 (mV)
-160
-140
-120
-80
-60
-40
-20
mV
b
Li-Ringer
25
20
15
10
5
-5
V_2-V_1 (mV)
-140
-120
-80
-60
-40
mV
Membrane Potential

The fast component probably consists of the capacity current since it falls to zero within 10 or 15 ms. The slow component, which is believed to be due to the closure of K channels, declined with a mean time constant of 5.27 ± 0.28 ms (five fibres) in Na-Ringer at -90 mV, and 4.54 ± 0.43 ms (eight fibres) in Li-Ringer at -90 mV. Moreover, in the two-step experiments of chapter 3, which were performed in a hypertonic chloride Ringer, and where the tail currents were corrected for capacity currents by subtraction of capacity transients scaled from the currents during small depolarizations, the tail currents declined as a single exponential with a mean time constant of 3.04 ± 0.59 ms (five fibres) at -90 mV and at pH 7.2. This is not significantly different from the rate at which the tail currents declined in Li-Ringer ($P = 0.10$) or in Na-Ringer ($P = 0.10$).

Unfortunately, the inward tail currents in Na and Li-Ringer were so small that they could not be measured with great accuracy. Thus the reversal potential was obtained by extrapolation of the outward limb of the instantaneous current-voltage relation, which, in most fibres, approximated to a straight line (see for example, Fig. 4.4a, b). The permeability ratios obtained in this way are upper limits of the true ratios.

Reversal potential of the delayed current in Cs-Ringer

Fig. 4.5a shows records of the membrane potential (V_1) and the membrane current (V_2-V_1) for a two-step experiment to determine the reversal potential of the delayed current in Cs-Ringer. The first step depolarizes the fibre to +25 mV for 54 ms and activates the delayed conductance. During the second step the fibre is repolarized to between -40 mV and -131 mV.

Fig. 4.5 Two-step experiment to determine the reversal potential of the delayed current in a fibre immersed in Cs-Ringer

a, tracings of records of the membrane potential (V_1) and the membrane current (V_2-V_1). The first step is to +25 mV and lasts 54 ms. During the second step the membrane is returned to the potentials shown. The figure shows six superimposed tracings.

b, instantaneous current-voltage relationship for a fibre in Cs-Ringer. Same fibre as in (a). Abscissa, membrane potential (mV) during the second step; ordinate, membrane current (mV) at the start of the second step after subtraction of the capacity and leakage currents. $V_{R,Cs}$ is -79 mV.

Fibre resting potential, -38 mV; holding potential, -100 mV; inter-electrode distance (ℓ), 125 μm; temp. 3.6°C; tetrodotoxin, 10^{-6} g/ml.

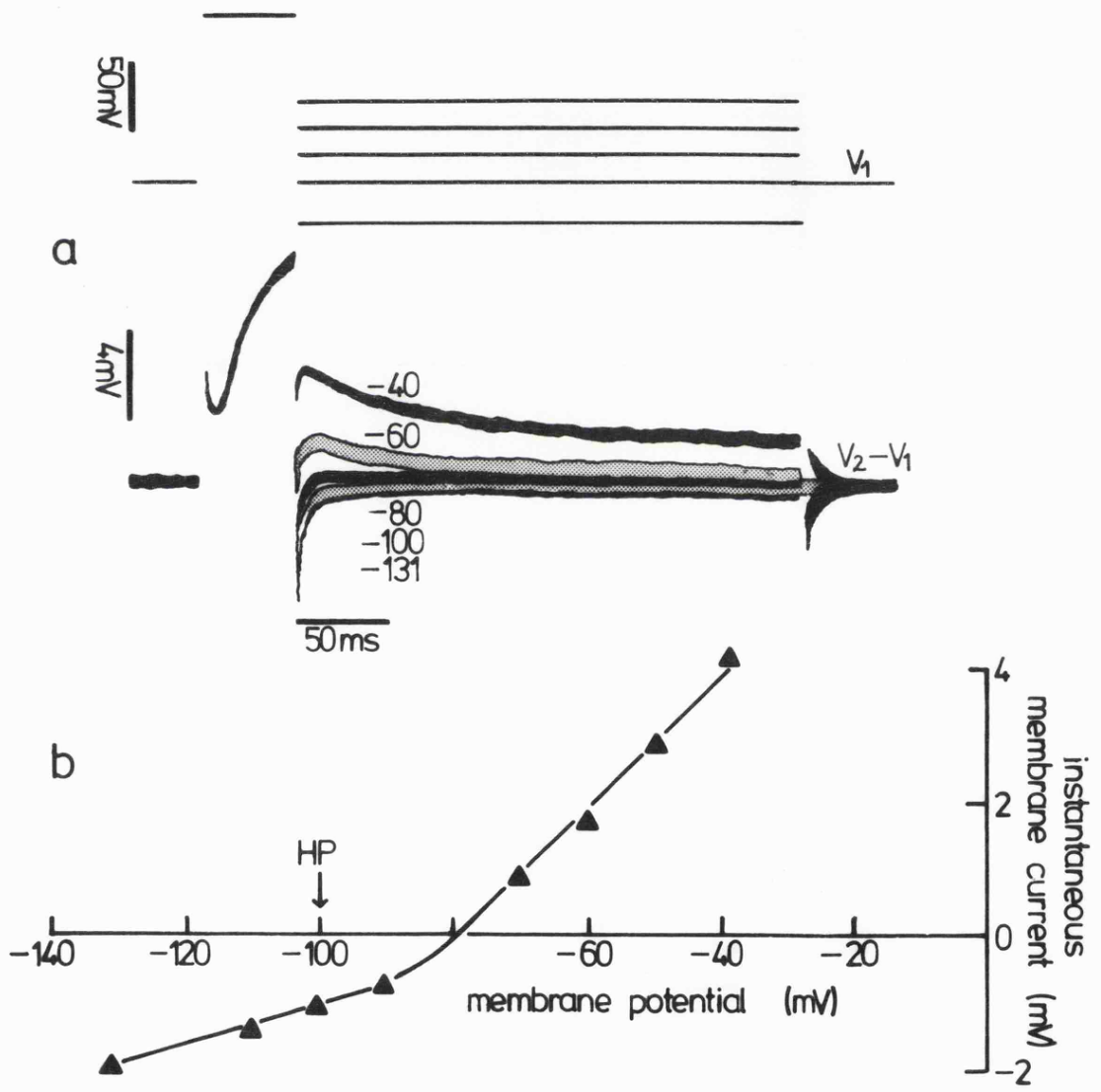
50mV
V1
a
4mV
-40
-60
-80
-100
-131
V2-V1
50ms
b
HP
-140
-120
-100
-60
-40
-20
membrane potential (mV)
4
2
0
-2
instantaneous membrane current (mV)

The tail currents at the start of the second step were corrected for leakage and capacity currents using the method described in the previous section for fibres in Na and Li-Ringer. The slow component of the tail currents declined exponentially with a mean time constant of 8.45 ± 0.71 ms (seven fibres) at -90 mV. This is significantly greater than the mean time constant in Li-Ringer ($P = 0.004$) at -90 mV, and is also marginally greater than that in Na-Ringer ($P = 0.045$) at the same membrane potential.

The instantaneous current-voltage relationship for the fibre in Fig. 4.5a is shown in Fig. 4.5b. The reversal potential is -79 mV. The mean reversal potential in eight fibres in Cs-Ringer was -73.1 ± 2.8 mV, which is significantly different from the mean reversal potentials in Na-Ringer ($P<0.001$) and Rb-Ringer ($P<0.001$: see Table 4.2). Since $V_{R,K}$ is -21.3 mV (Table 4.2), P_{Cs}/P_K is 0.11. Inward currents in Cs-Ringer are also small so the reversal potential was obtained by extrapolation of the outward limb of the instantaneous current-voltage relationship. The mean value of P_{Cs}/P_K given here is therefore an upper limit of the true mean.

The present finding that the delayed currents in Cs-Ringer inactivate more slowly than those in Na and Li-Ringer is consistent with the fact that the delayed currents in Cs^+ appeared to turn on more slowly than those in the other two solutions. It was also found that in a large number of fibres in Cs-Ringer, the delayed currents were small or absent during large, step-wise depolarizations. In addition, in all but two fibres which developed delayed currents, the delayed current became progressively smaller during the course of the experiment.

Similar results were obtained in the other solutions used, but in a few fibres only.

Effect of Cs^+ on the leakage current

Fig. 4.6A,B shows voltage-clamp records of two fibres immersed in K-Ringer, and which were depolarized and hyperpolarized from the holding potential of -100 mV to between -50 mV and -150 mV. The steady-state current-voltage relationship for fibre A is linear and is plotted as open circles in Fig. 4.6C (curve a). For depolarizing steps, the currents in fibre B resemble those in fibre A. However, during a large hyperpolarization the current in fibre B is less than the holding current. The steady-state current-voltage relationship for this fibre is shown in Fig. 4.6C as filled circles (curve b). The different properties of these two fibres is believed to be due to the presence of a small quantity of Cs^+ in the K-Ringer bathing fibre B.

Fig. 4.6D shows the steady-state current-voltage relations between -50 mV and -150 mV from two fibres in a muscle equilibrated first in Cs-Ringer (curve a), then in K-Ringer (curve b). In Cs- Ringer the current-voltage relationship is slightly rectified, whereas in K-Ringer the current is almost completely abolished during hyperpolarizing steps. These results are also consistent with the notion that Cs^+ is not completely removed when K-Ringer replaces Cs-Ringer in the recording chamber. A similar, though less complete inhibition of inward K currents was obtained after the chamber had been drained and filled with K-Ringer at least twelve times during the course of 1 hr in an attempt to remove the Cs^+.

Fig. 4.6 Properties of the leakage conductance in fibres immersed in K-Ringer, and the effects of Cs^+ on these properties.

A, B. Records of the membrane potential (V_1) and membrane current (V_2-V_1) from two fibres depolarized and hyperpolarized from the holding potential to between -50 mV and -150 mV.

Fibre A is in K-Ringer. Resting potential, -24 mV; holding potential, -100 mV; inter-electrode distance (ℓ), 125 μm; temp. 3.9°C; tetrodotoxin, 10^{-6}g/ml.

Fibre B is in K-Ringer also believed to contain less than 0.01 mM-Cs_2SO_4. Resting potential, -20 mV; holding potential, -100 mV; inter-electrode distance (ℓ), 125 μm; temp. 4.0°C; tetrodotoxin 10^{-6}g/ml.

C, D. Steady-state current-voltage relations between -50 mV and -150 mV. Abscissae, membrane potential (mV); ordinates, membrane current (mV).

C. ○, same fibre as A. ●, same fibre as B.

D. ▲, fibre in Cs-Ringer. Resting potential, -33 mV; holding potential, -100 mV: ◉, fibre in K-Ringer after exposure to Cs-Ringer. Resting potential, -31 mV; holding potential, -100 mV. Inter-electrode distance (ℓ), 125 μm; temp. 17.8-18.7°C; tetrodotoxin, 10^{-6}g/ml.

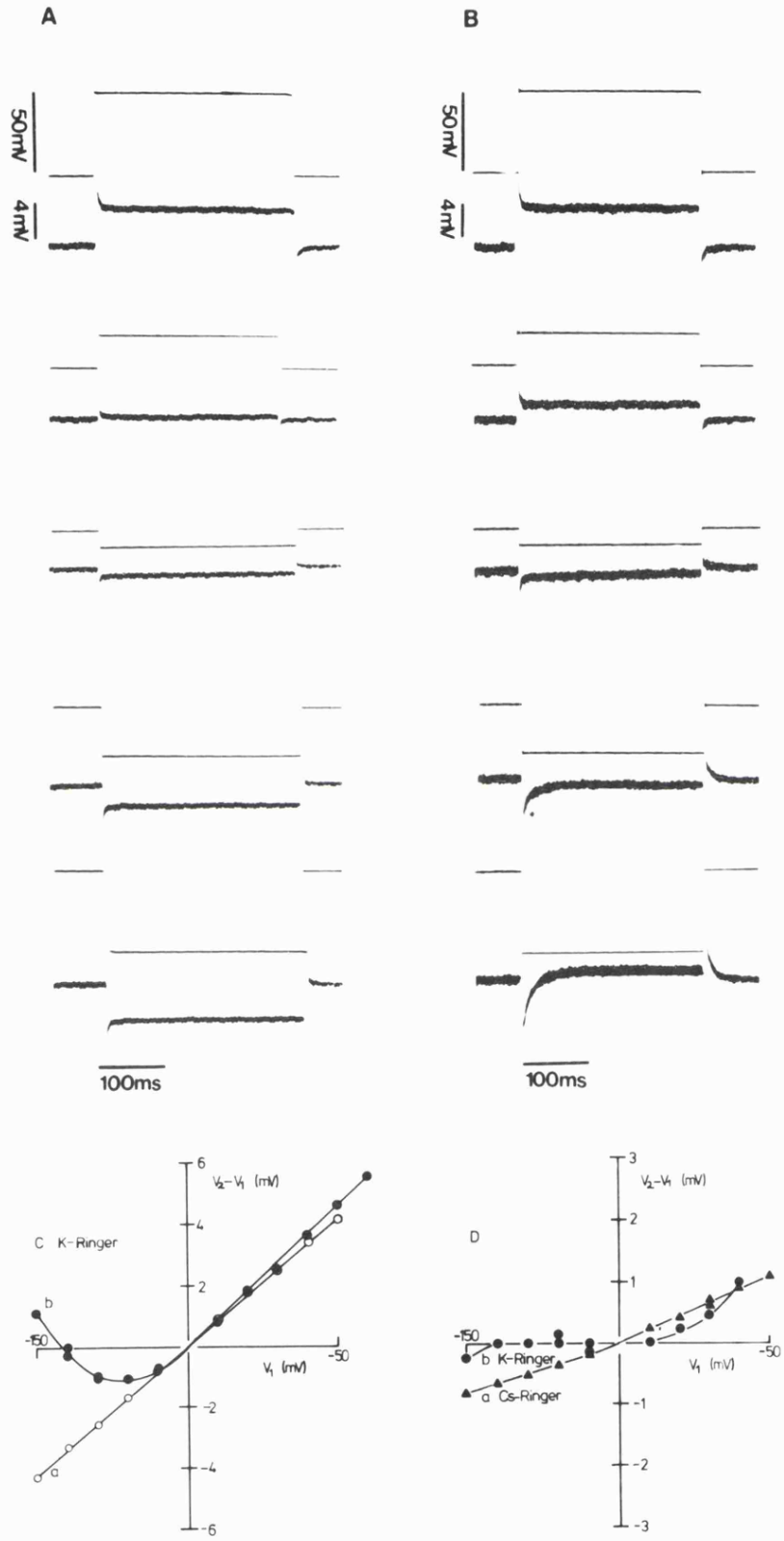
A
B
50mV
4mV
100ms
C K-Ringer
D
V_2-V_1 (mV)
V_1 (mV)
b
a
-150
-50
6
4
2
-2
-4
-6
3
1
-1
-3
b K-Ringer
a Cs-Ringer

The experiments of chapter 5 investigate the effect of Cs^+ on the resting membrane in more depth; from those experiments one would expect the Cs^+ concentration in Fig. 4.6B to be about 0.02 mM. In Fig. 4.6D (curve b), the Cs^+ concentration is probably higher.

Effect of alkali cations on the maximum delayed conductance.

Since the delayed currents in Cs-Ringer are smaller than those in Na or Li-Ringer, it was interesting to compare the maximum delayed conductance in those solutions to see if the effect of Cs^+ was real, or just a consequence of the fact that the reversal potential in Cs-Ringer is less negative than that in Na or Li-Ringer. The maximum conductance has also been determined for fibres in Rb and K solutions, and the results are presented in Table 4.2

The general equation which can be used to calculate the delayed conductance for fibres in X-Ringer is

$$I_{K,X} = g_{K,X} (V_1 - V_{R,X}) \qquad (4.2)$$

which is similar to eqn. (3.7). The subscript K,X is used because outward currents are carried by K^+, and inward currents by X^+.

Fig. 4.2 shows the relationship between the steady-state conductance which is normalized to its maximum value, and the membrane potential for a fibre in Rb-Ringer (Fig. 4.2C), and for a different fibre in Cs-Ringer (Fig. 4.2D). The experimental points for the fibre in Rb were calculated from the steady-state current-voltage relationship in Fig. 4.2B, after subtraction of the leak. In both fibres, the conductance at +8 mV is close to its maximum value. This was also the case in the other solutions tested, which is important since in most fibres the

maximum conductance was estimated from the maximum delayed current recorded during the first step of two-step experiments. In Li^+, Na^+, Rb^+ and K^+ this step was to between +8 and +12 mV, while in Cs^+ it was to +25 mV.

As Table 4.2 shows, the maximum delayed conductance in K-Ringer is about half the mean value in hypertonic sulphate Ringer; it is also significantly less than the maximum delayed conductance in hypertonic chloride Ringer at pH 7.2 ($P<0.001$; see Table 3.2 for the maximum conductance in chloride Ringer).

The maximum delayed conductances in Rb, Na and Li solutions are not significantly different from that in K-Ringer ($P = 0.2$, 0.24 and 0.18, respectively). On the other hand, the maximum conductance in Cs-Ringer is significantly less than that in K-Ringer ($P = 0.007$), a finding which is consistent with the notion that Cs^+ interferes with K^+ movement in the delayed channel. Since the K current is outward, this effect of Cs^+ is likely to be intracellular rather than extracellular (see page 100). However, an alternative explanation might be that the delayed conductance, which is inactivated at the resting potential of fibres in 41.25 mM-Cs_2SO_4, Rb_2SO_4 and K_2SO_4, is more difficult to reprime when the solution contains Cs^+, than when it contains Rb^+ or K^+.

DISCUSSION

The results presented in this chapter show that the delayed potassium channel in muscle is permeable to a number of alkali cations in addition to K^+. The order of decreasing permeability is $P_K \gg P_{Rb} > P_{Cs} > P_{Na} \gg P_{Li}$. This approximates to sequence IV of Eisenman (1963, 1965), worked out for the permeability characteristics of cation selective glasses.

Selectivity is not a fixed property of Na channels in squid axons (Chandler & Meves, 1965; Cahalan & Begenisich, 1976) or in Myxicola axons (Ebert & Goldman, 1976) since in these preparations P_K/P_{Na} rises as the internal K^+ concentration is reduced. Cahalan & Begenisich (1977) have also seen changes in P_{NH_4}/P_{Na} in axons perfused with ammonium. These attribute to a dependence of the selectivity of the Na channel on the internal ammonium concentration, or on the membrane potential. P_{Na}/P_K, however, appears to be independent of the membrane potential (Cahalan & Begenisich, 1976).

Since the selectivity mechanism of the delayed K channels is likely to resemble that of the Na channel (see chapter 1), it is interesting to consider which factors, if any, might modify the selectivity sequence measured here. In the present case, P_{Na}/P_K was measured from the change in reversal potential of the delayed current when the external solution was changed from one containing 41.25 mM-Na_2SO_4 to one containing 41.25 mM-K_2SO_4. Adrian et al. (1970a) have obtained the same result using the same preparation in a chloride solution containing a high concentration of Na^+, and between 2.5 and 20 mM-K^+. One might conclude from these results that P_{Na}/P_K does not depend to any great extent on the external Na^+ or K^+ concentrations, the nature of the anion, or on the membrane potential.

Adrian et al. (1970a) also showed that when the two-step procedure is used to determine the reversal potential of the delayed current in muscle, the reversal potential is independent of the duration of the first step provided this is less than about 30 ms. However, when the duration of step one is increased

to several hundred milliseconds, the reversal potential becomes more positive, presumably because K^+ which leaves the fibre during the first step remains in the vicinity of the membrane at the beginning of the second step when the measurements are made. From the shift in the reversal potential under these conditions, Adrian et al. (1970a) concluded that K^+ accumulated in a space occupying one third to one sixth the fibre volume, possibly the region between fibres. Since this space is about one hundred times that occupied by the T-system (Hodgkin & Horowicz, 1960a; Adrian & Freygang, 1962a; Peachey, 1965; Peachey & Schild, 1968; Mobley & Eisenberg, 1975), Adrian et al. (1970a) suggest that delayed rectification does not occur to any great extent in the T-tubules. This view is also supported by the glycerolation experiments of Chandler, Rakowski & Schneider (1976b): but for an alternative view based on the origin of the late afterpotential in muscle, see Gage & Eisenberg (1969b), Freygang, Goldstein & Hellam (1964), Freygang, Goldstein, Hellam & Peachey (1964), and Volle (1970). In the present context, the results obtained by Adrian et al. (1970a) are important since they suggest that by limiting the duration of step one to about 30 ms, in the present experiments (except in Cs^+ where the delayed conductance turns on rather slowly) it should be possible to avoid error in the permeability ratios due to K^+ accumulation .

Since the rate of repolarization of the action potential in Rb-loaded muscle fibres is similar to that in freshly dissected muscle (Adrian, 1964), the selectivity of the delayed K channel in Rb-loaded fibres will closely resemble that obtained here for

muscles bathed in Rb and K solutions. The permeability ratio of 40 reported by Almers (1976) for P_{Rb}/P_{Na} is also consistent with the present results.

As stated previously, Campbell (1976) has reported that the selectivity of the Na channel in frog muscle is similar to that in myelinated nerve fibres from the same species (Hille, 1972). A comparison of the selectivity of the delayed rectifier in muscle found here, with that in nerve is made in Table 4.5. Also included is a value for the minimum pore diameter, through which each ion could pass (Hille, 1973, 1975a). These diameters are equal to the ionic radii of the ions. Apart from an inversion between lithium and sodium, the selectivity sequence in muscle is identical to that in nerve. In view of the difficulties described here and by Hille (1973) associated with the measurement of the reversal potential for relatively impermeant cations, this inversion is probably not important. However, it is interesting to note that the delayed channels in nerve are generally more selective than those in muscle.

Mullins & Moore (1960) have concluded that the extra efflux of thallium during stimulation in thallium-loaded muscles is at least as great as the extra K efflux in normal fibres. This may mean that P_{Tl}/P_K for the delayed rectifier in muscle is similar to that in nerve, which is 2.3 (Hille, 1973).

Moore et al. (1966) found that in most of the experiments in which they measured the reversal potential of the delayed current in squid axons, P_{Rb}/P_K was 1. This is similar to the value found here for muscle and by Hille (1973) for myelinated nerve fibres. On the other hand, Bezanilla & Armstrong (1972)

TABLE 4.5

Permeability ratios for the delayed K channels in frog nerve and muscle fibres

Ion	P_{ion}/P_K		Minimum pore diameter (Å)
	Muscle fibres of *R. temporaria* (present results)	Myelinated nerve fibres of *R. pipiens* (Hille, 1973)	
Lithium	0.024	<0.018	1.20
Sodium	0.030	0.010	1.90
Potassium	1.0	1.0	2.66
Thallium	-	2.3	2.80
Rubidium	0.95	0.91	2.96
Ammonium	-	0.13	3.00
Caesium	0.11	<0.077	3.38

reported that P_{Rb}/P_K was only 0.25 for the squid axon when determined from the size of the delayed current before and after all of the intracellular K^+ was replaced by Rb^+. The difference between this result and that obtained by Moore et al. (1966) is probably due to the fact that internal Rb^+ interferes with the K movements in the delayed K channel in the squid axon (Bezanilla & Armstrong, 1972; French & Adelman, 1976). In agreement with this, Hille (1975a) has pointed out that for a channel in which there is non-independent ion movement, the permeability ratios determined from the measurement of fluxes or membrane currents will not always be the same as those determined from the reversal potential of the current which passes through that channel. On the other hand, eqn. (4.1), which is used to calculate the permeability ratios from reversal potential measurements in the present case, does not assume that ions move across the membrane in accordance with the independence principal (Hodgkin & Huxley, 1952a), and Hille (1952a) and Läuger (1973) have described certain classes of non-independent ion movement for which this equation may be used.

The hypothesis that an intracellular action of Cs^+ is responsible for the small K currents seen in Cs-Ringer is consistent with the observation that internal Cs^+ blocks outward K currents in nerve (see chapter 1). In addition, muscle fibres whose ends are cut in 120 mM-CsF under conditions in which Cs^+ appears to diffuse through the sarcoplasm fail to develop delayed currents (Hille & Campbell, 1976). Finally, the present hypothesis requires that Cs^+ is able to cross the membrane of resting muscle fibres. This is the case, though

the permeability of the resting membrane to Cs^+ is small compared to its permeability to K^+ (Bolingbroke, Harris & Sjodin, 1961). In nerve, outward K currents are not blocked by external Cs^+ (Dubois & Bergman, 1975, 1977; Adelman, 1968; Adelman & Senft, 1968). In the present case, however, the alternative possibility that external Cs^+ reduces outward K currents cannot be excluded.

Chapter 5. Caesium blocks K currents in resting skeletal muscle fibres in a voltage- and concentration-dependent manner

INTRODUCTION

In the previous chapter the view was expressed that when muscle fibres are immersed in a K-Ringer which contains small quantities of Cs^+, K currents flowing across the resting membrane are blocked. The experiments described in this chapter were designed to investigate the properties of this blockade, which is found to depend on the membrane potential and on the concentration of Cs^+ in the Ringer. In the presence of Cs^+, and when fibres are hyperpolarized by a constant current, oscillations in the membrane potential are observed.

The K currents which are of interest here are those which show inward rectification (Katz, 1949; Adrian & Freygang, 1962b; Adrian, 1969). A discussion of carrier and pore models which have been developed to account for inward rectification in muscle is given in chapter 8. As mentioned previously, a pore model is favoured here, and it is postulated that Cs^+ blocks the resting K channel when it binds to a site, or sites, partway across the membrane.

Previous experiments have shown that there are interactions between Rb^+, K^+ and Cs^+ ions during permeation in resting muscle. When either Rb^+ or Cs^+ is added to the Ringer, the efflux (Sjodin 1959) and the influx of K^+ (Sjodin, 1961) are reduced. Similarly, the influx of Rb^+ and Cs^+ is reduced in the presence of external K^+, and there is a mutual inhibition of uptake between Cs^+ and Rb^+ (Sjodin, 1961; Bolingbroke, Harris & Sjodin, 1961). The general interpretation of these results is that K^+, Rb^+ and Cs^+ compete for the same permeability mechanism. Volle, Glisson & Henderson

(1972) have also demonstrated a competition between K^+ and Rb^+ ions in resting muscle. However, unlike the Cs blockade, that by Rb^+ is largely independent of the membrane potential (Adrian, 1964).

A voltage-dependent blockade of inwardly rectifying K conductances by external Cs^+ has also been reported in starfish egg cells (Hagiwara, Miyazaki & Rosenthal, 1976). And when cardiac Purkinje fibres are immersed in a Ringer to which 20 mM-Cs^+ is added, the K conductances which show inward rectification are totally blocked while the delayed rectifier is unaffected (Isenberg, 1976).

On the other hand, addition of Cs^+ to the external solution produces a voltage-dependent blockade of the delayed rectifier in squid axons (Adelman & French, 1978) and in myelinated nerve fibres (Dubois & Bergman, 1977). In squid axons, Cs^+ also has access to the delayed K channel from the axoplasm since it blocks outward K currents when included in the internal perfusate (Adelman & Senft, 1966, 1968; Adelman, 1971). This blockade is also voltage-dependent (Bezanilla & Armstrong, 1972), as mentioned in chapter 1.

Recent experiments show that in addition to Cs^+, the resting K conductance in muscle is blocked in a voltage-dependent manner by Ba^{2+}, Sr^{2+} (Standen & Stanfield, 1978a,b) and Na^+ (Standen & Stanfield, 1978c). A preliminary account of the Cs blockade has been given (Gay & Stanfield, 1977).

SOLUTIONS AND METHODS

The basic composition of solutions used for the experiments described in this chapter is given in Table 5.1. All contain sulphate as an impermeant anion to replace chloride, and have a

TABLE 5.1

Composition of solutions (mM)

	Na^+	K^+	Rb^+	Cs^+	Ca^{2+}	SO_4^{2-}	$H_2PO_4^-$	HPO_4^{2-}	Sucrose
Solution 5A	2.6	190	-	-	8	103	0.43	1.08	-
Solution 5B	2.6	80	-	-	8	48	0.43	1.08	113
Solution 5C	2.6	-	80	-	8	48	0.43	1.08	113
Solution 5D	2.6	-	-	80	8	48	0.43	1.08	113
Solution 5E	42.6	40	-	-	8	48	0.43	1.08	113
Solution 5F	66.2	16	-	-	8	48	0.43	1.08	113

pH of 7.2. Most experiments were performed in solution 5B which contains 80 mM-K^+. Lower K^+ concentrations were obtained by substituting Na_2SO_4 for K_2SO_4 on an equimolar basis (solution 5E & F). Solution 5A has a high K^+ concentration and has a higher ionic strength than solutions B-F. In solutions 5C & D, Rb_2SO_4 and Cs_2SO_4 replace K_2SO_4. The results in solutions 5A,B,C,E & F (which contain no Cs^+) were compared with those obtained when a small quantity of Cs_2SO_4 was included in the Ringer.

In most experiments the three-electrode voltage-clamp method was used to measure the membrane currents (see chapter 2). The electrode separation (ℓ) was either 330 μm or 495 μm. Most experiments were carried out at room temperature (17–18.5°C), although a few experiments were performed in the cold (3-4.5°C).

RESULTS

The first part of this chapter concerns experiments performed in 40 mM-K_2SO_4 (solution 5B). In such high K^+ concentrations the fibres are depolarized and this results in at least partial inactivation of both the contractile mechanism (Hodgkin & Horowicz, 1960b) and the delayed K conductance (Adrian et al., 1970a; Stanfield, 1970a). However, the resting K conductance is larger than in solutions containing a lower K^+ concentration (Hodgkin & Horowicz, 1959; Almers, 1972a). Since the permeability of the resting membrane to sulphate ions is low, almost all of the membrane current will be carried by K^+ and the equilibrium potential for K^+ will be equal to, or very close to, the resting potential (Adrian, Chandler & Hodgkin, 1970b). For this reason the membrane was usually held at the resting potential.

Effect of 2.5 mM-Cs^+ on the properties of the resting membrane conductance in fibres in 80 mM-K^+ solutions

Properties of the resting conductance in the presence and absence of Cs^+ are illustrated in Fig. 5.1. Fig. 5.1A shows records of the membrane current in a fibre in the control solution, which contains no Cs^+, during hyperpolarizing (H) and depolarizing (D) steps from the holding potential of -14 mV. Two features of the control currents are interesting. First, the outward currents which are seen when the fibre is depolarized by more than 10 mV are much smaller than the inward currents during a hyperpolarization of similar size. This in-going rectification is characteristic of the resting K conductance in skeletal muscle (Katz, 1949; Hodgkin & Horowicz, 1959; Adrian & Freygang, 1962b). In-going rectification can also be seen in Fig. 5.1C, which shows the instantaneous and steady-state current-voltage relations for the fibre illustrated in A.

Secondly, when the currents are inward and large, they activate slowly to some steady-state value which, as Fig. 5.1C shows, depends on the membrane potential (Adrian & Freygang, 1962a; Adrian, Chandler & Hodgkin, 1970b; Stanfield, 1970b; Almers, 1972a,b). The outward currents in most fibres showed no time-dependence after the first 20 ms in which capacity currents were flowing. In the remainder, depolarizations exceeding 80 mV activated a small part of the delayed K conductance; therefore such large depolarizations were not usually applied.

Inactivation of the inward currents is due, in part, to a fall in the K^+ concentration in the lumen of the T-system. Some of the

Fig. 5.1 Properties of the resting K^+ conductance in 40 mM-K_2SO_4 solutions in the absence (A,C) and presence (B,D) of 1.25 mM-Cs_2SO_4

A & B, tracings of records of membrane currents (V_2-V_1) during hyperpolarizing (H) and depolarizing (D) steps from the holding potential. The numbers at the end of each trace are the size of the step in mV. The fibre in A is in 80 mM-K^+ (solution B): resting potential, -14 mV; holding potential, - 14 mV; inter-electrode distance, 330 µm; temp. 17.2°C. The fibre in B is in 80 mM-K^+ plus 2.5 mM-Cs^+: resting potential, - 15 mV; holding potential, - 15 mV; inter-electrode distance, 330 µm; temp. 17.2°C.

C & D, instantaneous (o) and steady-state (•) current-voltage relations for the fibres shown in A and B of this figure. Abscissae, membrane potential (mV); ordinates, membrane current (mV). The instantaneous currents were obtained by extrapolation of the currents flowing at times greater than 50 ms. The steady-state currents are those flowing 3 s after the start of the clamp step.

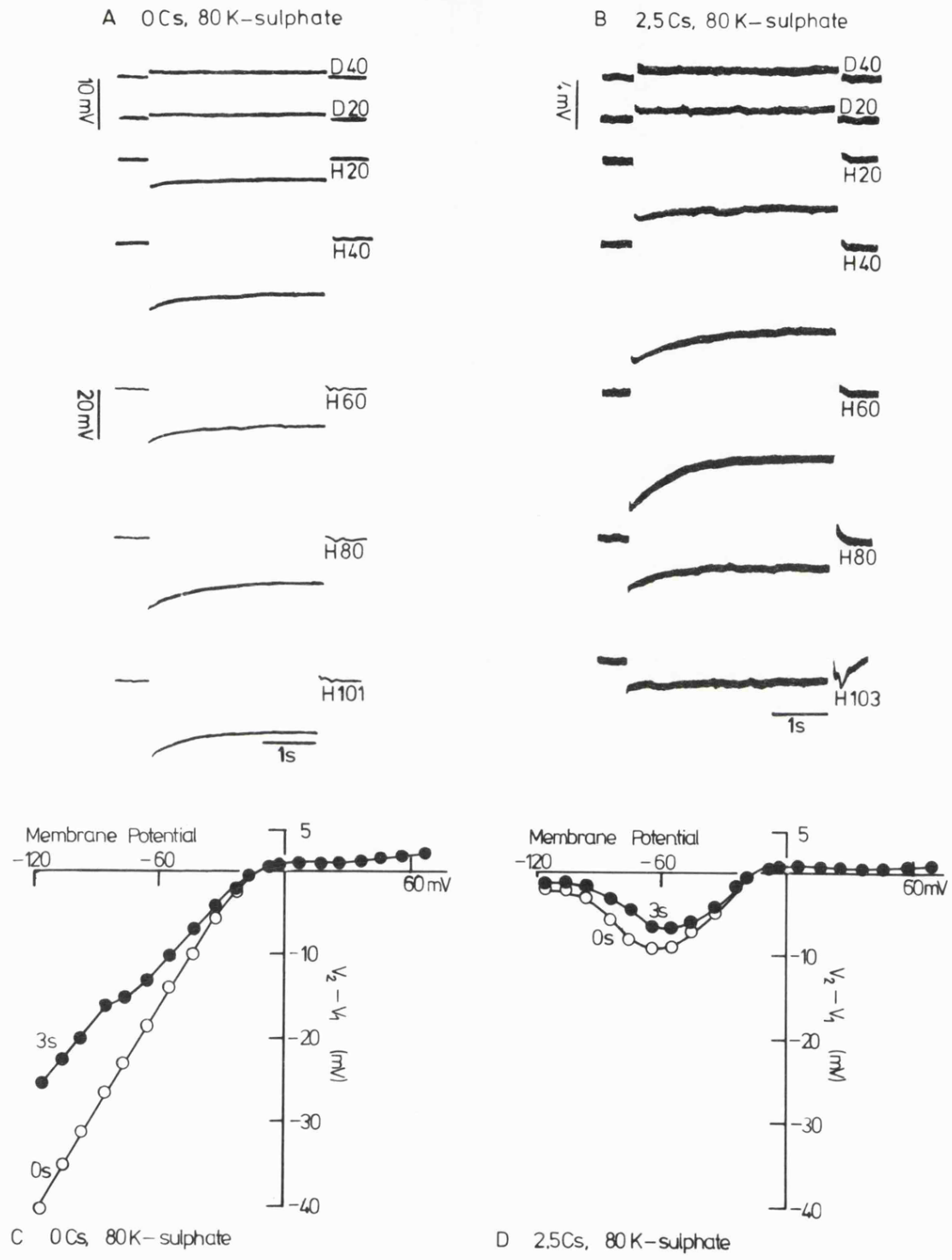
A 0 Cs, 80 K–sulphate
B 2,5 Cs, 80 K–sulphate
10 mV
20 mV
D40
D20
H20
H40
H60
H80
H101
H103
1s
Membrane Potential
-120
-60
5
60 mV
-10
-20
-30
-40
$V_2 - V_1$ (mV)
3s
0s
C 0 Cs, 80 K– sulphate
D 2.5 Cs, 80 K–sulphate

evidence supporting this view has been presented in chapter 1, and other experiments concerned with the mechanism of inactivation are given in chapters 6 & 7.

Fig. 5.1 shows the main effect which the presence of 2.5 mM-Cs^+ has on the membrane currents (in B) and on the instantaneous and steady-state current-voltage relations (in D) of fibres in K^+ solutions. It can be seen that Cs^+ has little or no effect on outward currents, while inward currents are smaller than those in the absence of Cs^+. In the presence of Cs^+, there is a maximum in the relationship between the inward current and the membrane potential (Fig. 5.1 D). This occurs at about -63 mV at the start of the hyperpolarization and -55 mV in the steady-state.

Fig. 5.2B & C show current-voltage relations at 50 ms and in the steady-state for a fibre in 0.1 mM-Cs^+ (in B) and for a second fibre in 0.02 mM-Cs^+ (in C). Reducing the Cs^+ concentration shifts the maximum inward current to more negative values of the membrane potential; in the case of the instantaneous currents the mean shift is 20 mV for a 5-fold change in the Cs^+ concentration. These results are summarized in Table 5.2 (column 4). The inward currents in 0.02 mM-Cs^+ are larger than those at higher Cs^+ concentrations. These results show that Cs^+ blocks the resting K conductance in a manner which increases with an increase in hyperpolarization and an increase in the external Cs^+ concentration.

2.5 mM-Cs^+ does not significantly alter the mean resting potential. This was -13.86 $\pm$ 0.19 mV (seventy-three fibres) in 80 mM-K^+ solution, and -14.18 $\pm$ 0.26 mV (thirty-nine fibres) in 80 mM-K^+ plus 2.5 mM-Cs^+ ($P > 0.3$). Similar resting potentials were recorded when the Cs^+ concentration was less than this (see Table 5.2, column 2).

Fig. 5.2 The effect of Cs^+ on the properties of the resting membrane conductance in 40 mM-K_2SO_4 solutions.

A, tracings of the membrane potential (V_1) and the membrane current (V_2-V_1) obtained in 80 mM-K^+ solution plus 0.1 mM-Cs^+. The hyperpolarizations are to i, -75 mV; ii, -96 mV; iii, - 126 mV; iv, -156 mV; v, -189 mV; and vi, -222 mV. Fibre resting potential, -14 mV; holding potential, -14 mV; inter-electrode distance, 330 μm; temp. 17°C.

B, current-voltage relations in 80 mM-K^+ plus 0.1 mM-Cs^+. Abscissa, membrane potential (mV); ordinate, membrane current (mV). The curves are plotted 50 ms (o) and 3 s (●) after the start of the clamp step. The same fibre is also shown in A, above.

C, current-voltage relations in 80 mM-K^+ plus 0.02 mM-Cs^+. Abscissa, membrane potential (mV); ordinate, membrane current (mV). The curves are plotted 50 ms (o) and 1500 ms (●) after the start of the clamp step. Fibre resting potential, -13 mV; holding potential, - 13 mV, inter-electrode distance, 330 μm, temp. 18.1°C.

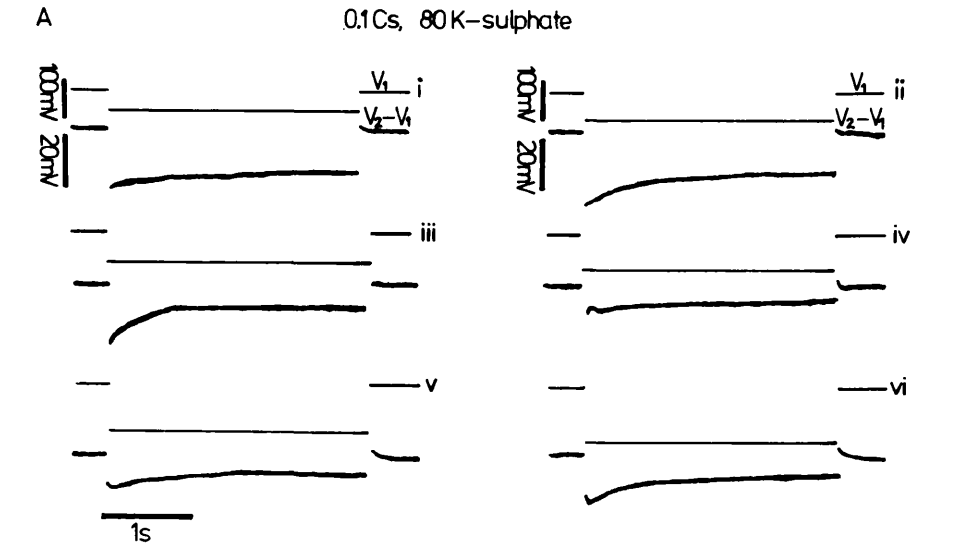

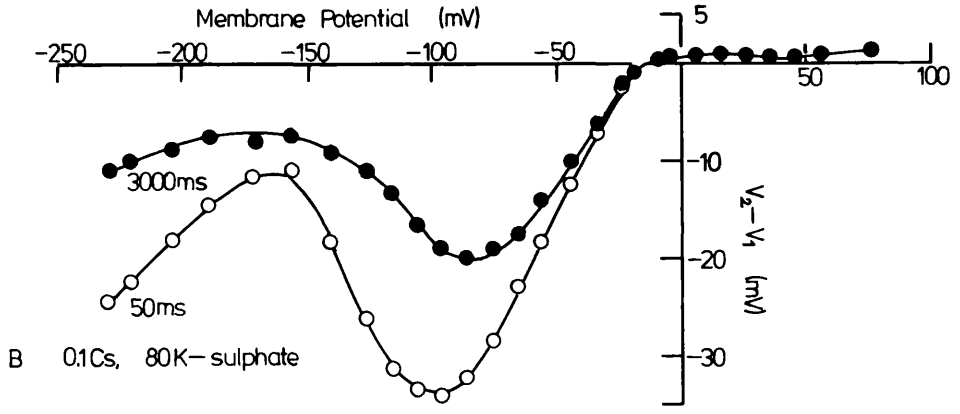

B 0.1 Cs, 80 K– sulphate

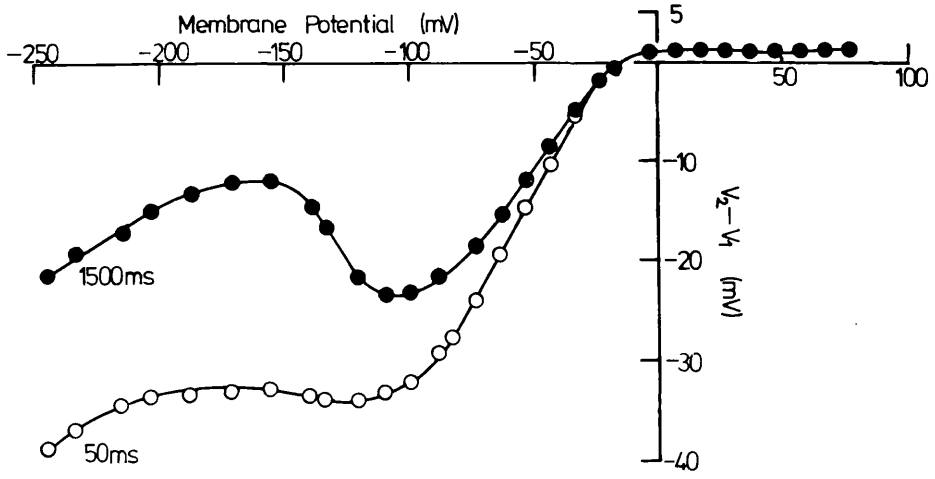

C 0.02 Cs, 80 K– sulphate

TABLE 5.2

Effect of Cs^+ on some properties of the resting membrane in fibres immersed in 80 mM-K^+ sulphate solutions

1	2	ǂ 3	ǂǂ 4
Caesium concentration (mM)	Resting Potential (mV)	R_m ($ohm.cm^2$)	(mV)
0	-13.86 ± 0.19 (73)	7,394 ± 1,315 (8)	-
0.02	-13.81 ± 0.29 (11)	6,049 ± 1,287 (7)	-123.60 ± 1.28 (10)
0.1	-13.88 ± 0.28 (17)	10,829 ± 654 (9)	-102.13 ± 1.04 (8)
0.5	-13.94 ± 0.32 (35)	8,672 ± 665 (9)	- 82.10 ± 0.66 (10)
2.5	-14.18 ± 0.26 (39)	12,865 ± 2,835 (6)	- 61.83 ± 1.28 (6)

ǂ membrane resistance during depolarization which exceeds 50 mV

ǂǂ membrane potential at which the instantaneous inward current in Cs^+ is greatest

Irregularities in the current traces which follow long hyperpolarizations of 60 mV or greater in the control Ringer (Fig. 5.1A), or 103 mV in the presence of 25 mM- Cs^+ (Fig. 5.1B) show that contractile repriming has occurred during the hyperpolarizing step. When the length of the step was reduced to 250 ms, larger hyperpolarizations could be applied before such artifacts were seen, and the instantaneous currents were similar to those recorded using pulses that were sufficiently long for the currents to reach a steady-state.

Effect of 2.5 mM-Cs^+ on the diameter and space constant of fibres in 80 mM-K^+ sulphate solutions

Adrian et al. (1970a) reported that the mean diameter and mean space constant of fibres immersed in an isotonic 40 mM-K_2SO_4 Ringer similar to that used here were 75 µm and 1.22 mm, respectively. The present method used to determine these parameters is similar to that described by Adrian et al. (1970a) and involves the measurement of V_1 and V_2-V_1 when a constant current is used to hyperpolarize the fibres by about 10 mV (see chapter 2).

In the absence of Cs^+, the mean fibre diameter in 80 mM-K^+ sulphate solution was 85.5 ± 3.5 µm (twenty fibres) compared to 82.3 ± 3.5 µm (eleven fibres) when 2.5 mM-Cs^+ sulphate was present. These values are not significantly different ($P > 0.3$), and both are close to the value of 80 µm which is generally assumed in order to calculate I_m.

Cs^+ also has no effect on the mean space constant of these fibres which was 1.10 ± 0.05 mm in the absence of Cs, and 1.10 ± 0.07 mm when Cs^+ was present.

Recovery from the Cs^+ blockade during large hyperpolarizations

Fig. 5.2A shows voltage-clamp records from a fibre in 80 mM-K^+ and 0.1 mM-Cs^+. At membrane potentials positive to -124 mV (records i & ii) the currents inactivate slowly, which is to be expected if K^+ depletion is occurring. However, at membrane potentials more negative than -156 mV (records iv to vi) there is a transient increase in current which precedes the decline. In this fibre the inward current reaches a peak value 150 ms after the onset of a hyperpolarization to -156 mV (in iv) and after 40 ms at - 222 mV (vi).

The current-voltage relations at 50 ms and in the steady-state for this fibre and for a fibre in 0.02 mM-Cs^+ are shown in Fig. 5.2 B and C, respectively. The currents at -250 mV are larger than those at -160 mV despite the presence of caesium. In 0.1 mM-Cs^+, this increase is such a steep function of the membrane potential that it can only be explained if the blockade becomes less effective.

There may be a causal relationship between this recovery and the development of currents with a biphasic time course (see, for example, Fig. 5.2A, iv-vi). The evidence for this is that when both are seen in the same fibre, such as the fibre shown in Fig. 5.2A & B, they occur over a similar range of membrane potentials. In addition, biphasic currents were not seen in the absence of Cs^+. On the other hand, hyperpolarizations greater than about 180 mV were applied to fifteen fibres in Cs^+ concentrations of 0.02 mM to 0.5 mM, and of these only six fibres in 0.1 mM-Cs^+ and two fibres in 0.5 mM-Cs^+ developed biphasic currents, while in every fibre the currents increased with hyperpolarization at membrane potentials more negative than -160 mV.

It is unlikely that the recovery reported here is an artifact

of membrane breakdown since the increase in current during extreme hyperpolarization is only transient, and since the currents are reproducible. In some fibres, however, there was evidence of membrane breakdown since the increase in conductance was irreversible. These results have not been included.

Components of the resting conductance in K^+, Rb^+ and Cs^+ solutions

When the membrane is depolarized by more than 50 mV in 80 mM-K^+ sulphate solutions with (Figs. 5.1D & 5.2B,C) and without Cs^+ (Fig. 5.1C), the membrane current-voltage relationship is linear and can be extrapolated back to the holding potential. Thus the resting K conductance appears to consist of two components: one is the inwardly rectifying conductance which is zero for large depolarizations, but which allows the passage of large inward currents when fibres are hyperpolarized: the other is a voltage-independent component. In support of this view, Adrian & Freygang (1962b) have shown that after subtraction of the linear component from the total conductance, there is less variation in the size of outward currents between fibres when moderate depolarizations are applied. In addition, neither the replacement of 100 mM-K^+ sulphate by Rb^+ sulphate (Adrian, 1964), nor the presence of high concentrations of tetraethylammonium ions in the Ringer (Stanfield, 1970b) affect the slope of the linear component, even though these ions carry little or no current through the inward rectifier.

The linear component of the current-voltage relationship has a mean slope of 7,394 $\pm$ 1,315 ohm.cm^2 (eight fibres) in 80 mM-K^+ sulphate Ringer and 12,865 $\pm$ 2,835 ohm.cm^2 (six fibres) when 2.5 mM-Cs^+ sulphate is added. These values are not significantly different ($P = 0.09$) and are also similar to values obtained in

lower Cs^+ concentrations (Table 5.2, column 3). In 100 mM-K^+ sulphate solutions, Adrian & Freygang (1962b) report a mean slope of 11,567 ohm.cm^2 on the assumption that the internal resistivity (R_i) is 250 ohm.cm. If, as in the present experiments, R_i is assumed to be 180 ohm.cm, their value becomes 8,331 ohm.cm^2, which is similar to that found here.

Fig. 5.3 shows membrane current-voltage relations from three fibres in solutions containing either Rb^+ or Cs^+, or both these ions, but containing no K^+. In 80 mM-Cs^+ (Fig. 5.3A) the current-voltage relationship is linear and the ionic currents show no obvious time-dependence. The membrane resistance was 23,141 ± 3,273 ohm.cm^2 (six fibres), which is more than three times the resistance of the linear segment in the Cs-free K^+ solution. This result indicates that the inward rectifier channel is impermeable to Cs^+, and that Cs^+ also reduces the size of the voltage-independent conductance.

The current-voltage relationship for the fibre in 80 mM-Rb^+ shows a slight in-going rectification (Fig. 5.3B), but when 2.5 mM-Cs^+ is added to the Ringer (Fig. 5.3C) the inward currents are reduced and the inward limb of the current-voltage relationship becomes linear. It therefore seems likely that Rb^+ carries a small current through the inward rectifier. This is in general agreement with previous studies which have suggested that Rb^+ carries little or no current through this mechanism (Adrian, 1964; Adrian, Chandler & Hodgkin, 1970b; see also chapter 8).

Analysis of the concentration- and voltage-dependence of the blockade by Cs^+

Fig. 5.4 shows the mean instantaneous current-voltage relations for fibres in the control Ringer which contains 80 mM-K^+, and in

Fig. 5.3 Steady-state current-voltage relations in rubidium and caesium solutions. Abscissae, membrane potential (mV); ordinates, membrane current, (mV).

A, fibre in 80 mM-Cs^+ (solution 5D). Resting potential, -34 mV; holding potential, - 34 mV; inter-electrode distance 495 µm; temp. 17.4°C.

B, fibre in 80 mM-Rb^+ (solution 5C). Resting potential, -29 mV; holding potential, - 29 mV; inter-electrode distance 495 µm; temp. 18.2°C.

C, fibre in 80 mM-Rb^+ solution which also contains 2.5 mM-Cs^+. Resting potential, -28 mV; holding potential, -28 mV; inter-electrode distance, 495 µm; temp. 17.8°C.

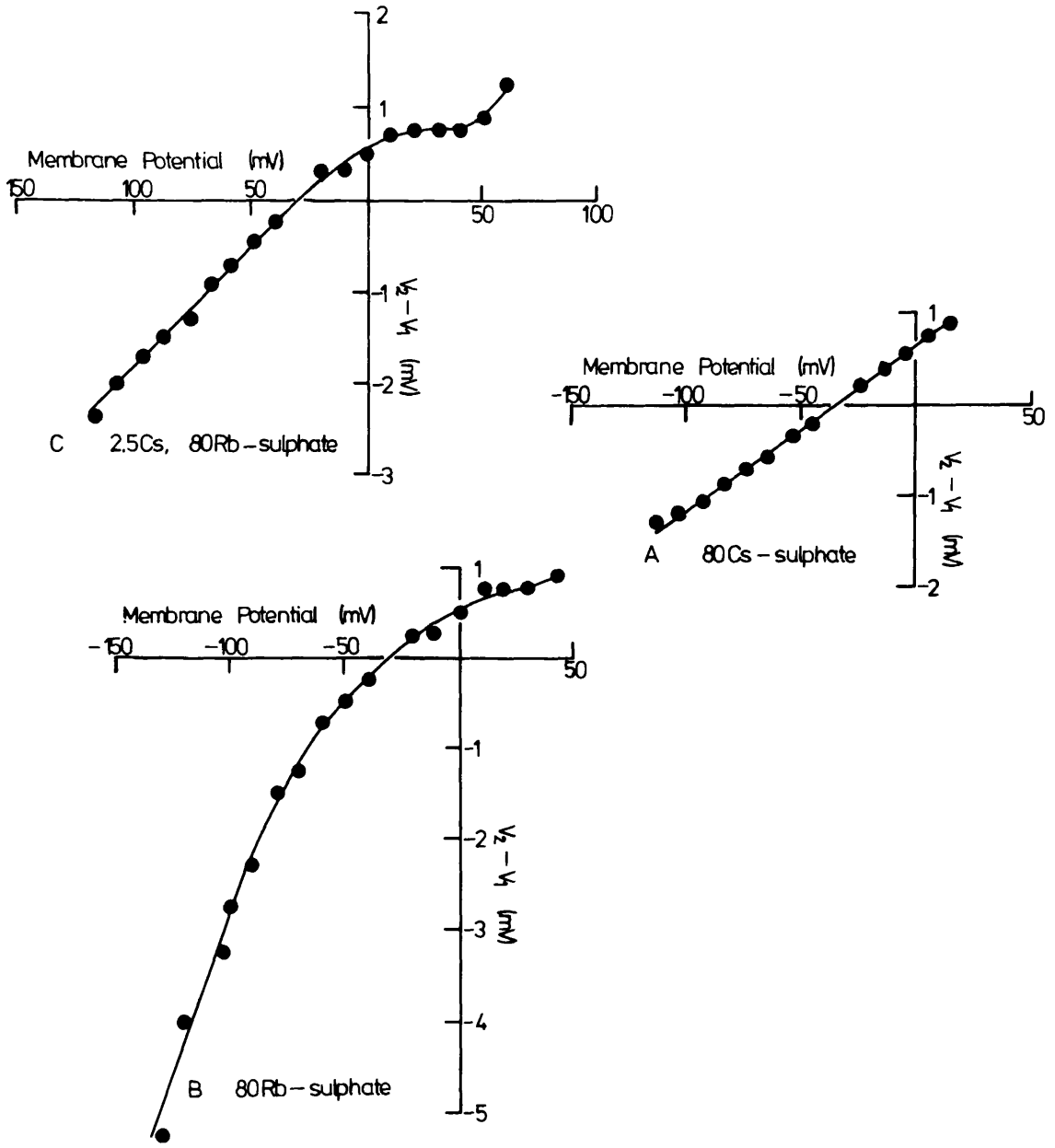
Membrane Potential (mV)
150
100
50
50
100
2
1
-1
-2
-3
$V_2 - V_1$ (mV)
C 2.5Cs, 80Rb – sulphate
Membrane Potential (mV)
-150
-100
-50
50
1
-1
-2
$V_2 - V_1$ (mV)
A 80Cs – sulphate
Membrane Potential (mV)
-150
-100
-50
50
1
-1
-2
-3
-4
-5
$V_2 - V_1$ (mV)
B 80Rb – sulphate

Fig. 5.4 Concentration- and voltage-dependence of the blockade of resting K^+ currents by Cs^+.

Instantaneous current-voltage relations in 40 mM-K_2SO_4 solutions. Abscissa, membrane potential (mV); ordinate, membrane currents (mV) after subtraction of the linear conductance which was obtained by extrapolation of the membrane current at membrane potentials more positive than 50 mV. Each point is the mean of results from six to eight fibres. Vertical bars are ± S.E.M. Each fibre was held at its resting potential; inter-electrode distance, 330 μm; temp. 17-18.5°C. The solutions contain 80 mM-K^+ and △, no Cs^+; ●, 0.02 mM-Cs^+; ○, 0.1 mM-Cs^+; ■, 0.5 mM-Cs^+; □, 2.5 mM-Cs^+. The lines are drawn to eqn. (5.3) of the text with $\delta = 1.4$ and $K_{app(0)} = 126$ mM.

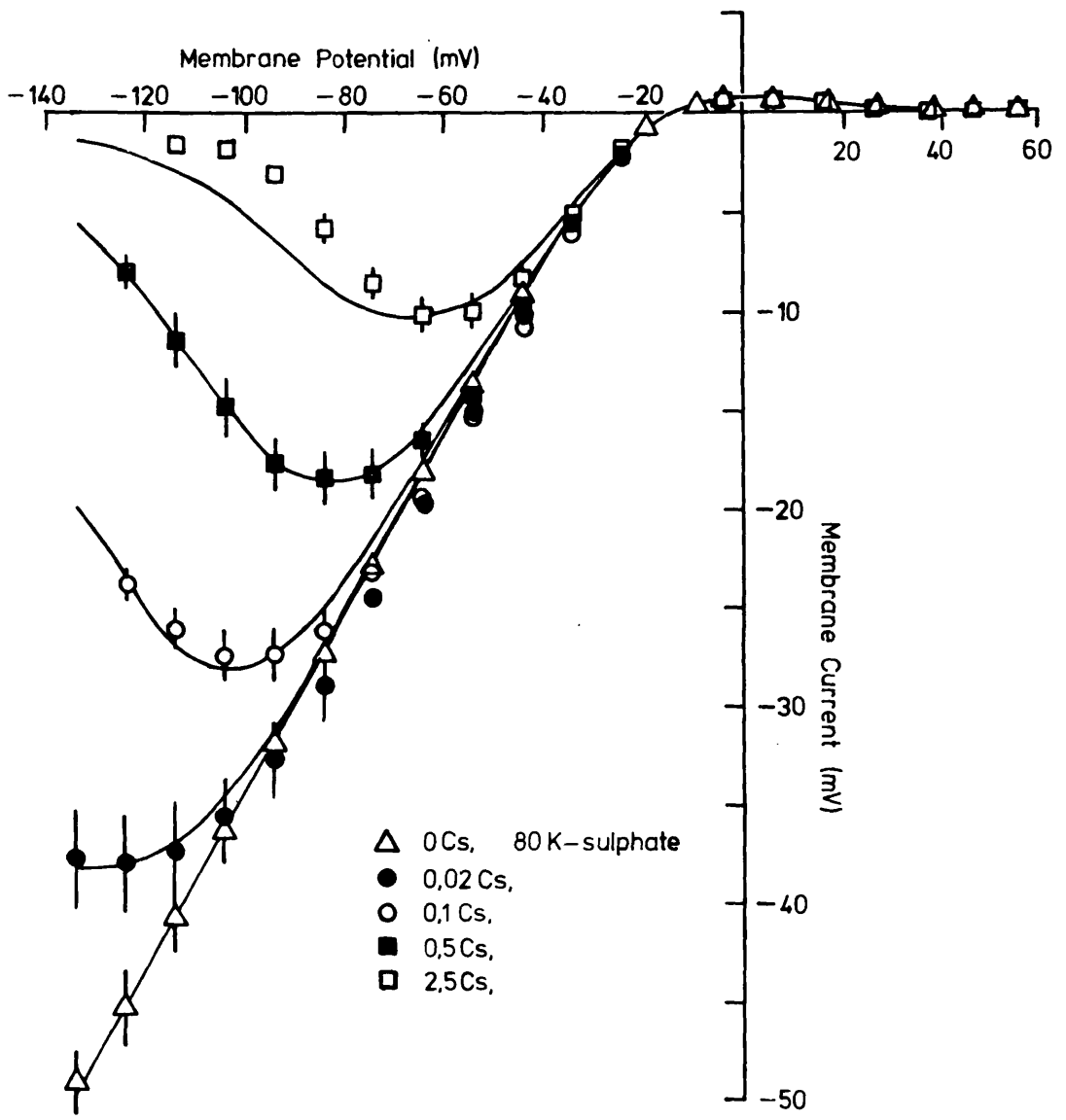
Membrane Potential (mV)
−140
−120
−100
−80
−60
−40
−20
20
40
60
−10
−20
−30
−40
−50
Membrane Current (mV)
0 Cs, 80 K−sulphate
0,02 Cs,
0,1 Cs,
0,5 Cs,
2,5 Cs,

solutions which also contain 0.02 mM to 2.5 mM-Cs^+. Before these relations were plotted, the linear portion of the current-voltage relationship was subtracted from the membrane currents in each fibre. When this is done, the currents at + 6 mV in 2.5 mM-Cs^+ are 9 $\pm$ 1% less than those in the absence of Cs^+. And when the Cs^+ concentration is 0.5 mM and 0.1 mM, the currents at +6 mV are reduced by 8 $\pm$ 1%.

Fig. 5.5A plots the inward currents shown in Fig. 5.4 in the presence of Cs ($I_{K:Cs}$) as a percentage of the currents in the control solution (I_K) on the ordinate against the external Cs^+ concentration, $[Cs]_o$, which is on a logarithmic scale, for six values of the membrane potential. The sigmoidal shape of these dose-response curves suggests that Cs^+ blocks the K currents by binding to a site associated with the K permeability mechanism on a one-to-one basis. The equation used to describe this binding is

$$I_{K:Cs}/I_K = \left\{1 + [Cs]_o/K_{app}\right\}^{-1} \qquad (5.1)$$

where K_{app} is the apparent dissociation constant of the Cs-receptor complex. To fit the family of dose-response curves, K_{app} must decrease as the membrane potential is made more negative. Accordingly, K_{app} is found to be 1.95 mM at -74 mV and 0.107 mM at -124 mV. Fig. 5.5A shows that agreement between the predicted curves (solid lines) and the experimental points is satisfactory except when the Cs^+ concentration is 2.5 mM, and for the least negative membrane potentials. The latter deviation is due to the fact that at membrane potentials close to the holding potential, the mean inward currents in Cs^+ are up to 17% larger than those in the control Ringer.

Fig. 5.5B shows that there is an exponential relationship between K_{app} and the membrane potential. Thus at any given membrane

Fig. 5.5 Analysis of the concentration- and voltage-dependence of the Cs^+ blockade.

A, dose-response curves for the results shown in Fig. 5.4. Abscissa, external Cs^+ concentration on a logarithmic scale; ordinate, K current in the presence of Cs^+ ($I_{K:Cs}$) as a percentage of the current in the control solution (I_K). The lines are drawn by eqn (5.1) on the assumption that Cs^+ binds reversibly and on a one-to-one basis to a receptor associated with the K permeability mechanism.
The apparent dissociation constant (K_{app}) for the Cs^+-receptor complex is taken as 1.95 mM at -74 mV (▲); 1.063 mM at -84 mV (△); 0.626 mM at - 94 mV (■); 0.343 mM at -104 mV (□); 0.195 mM at -114 mV (●); and 0.107 mM at -124 mV (○).

B, voltage-dependence of the apparent dissociation constant (K_{app}). Abscissa, membrane potential (mV); ordinate, apparent dissociation constant (mM). The line through the points is drawn by eye and predicts an e-fold change in the dissociation constant for a 17.8 mV change in the membrane potential. At zero membrane potential the dissociation constant is 126 mM.

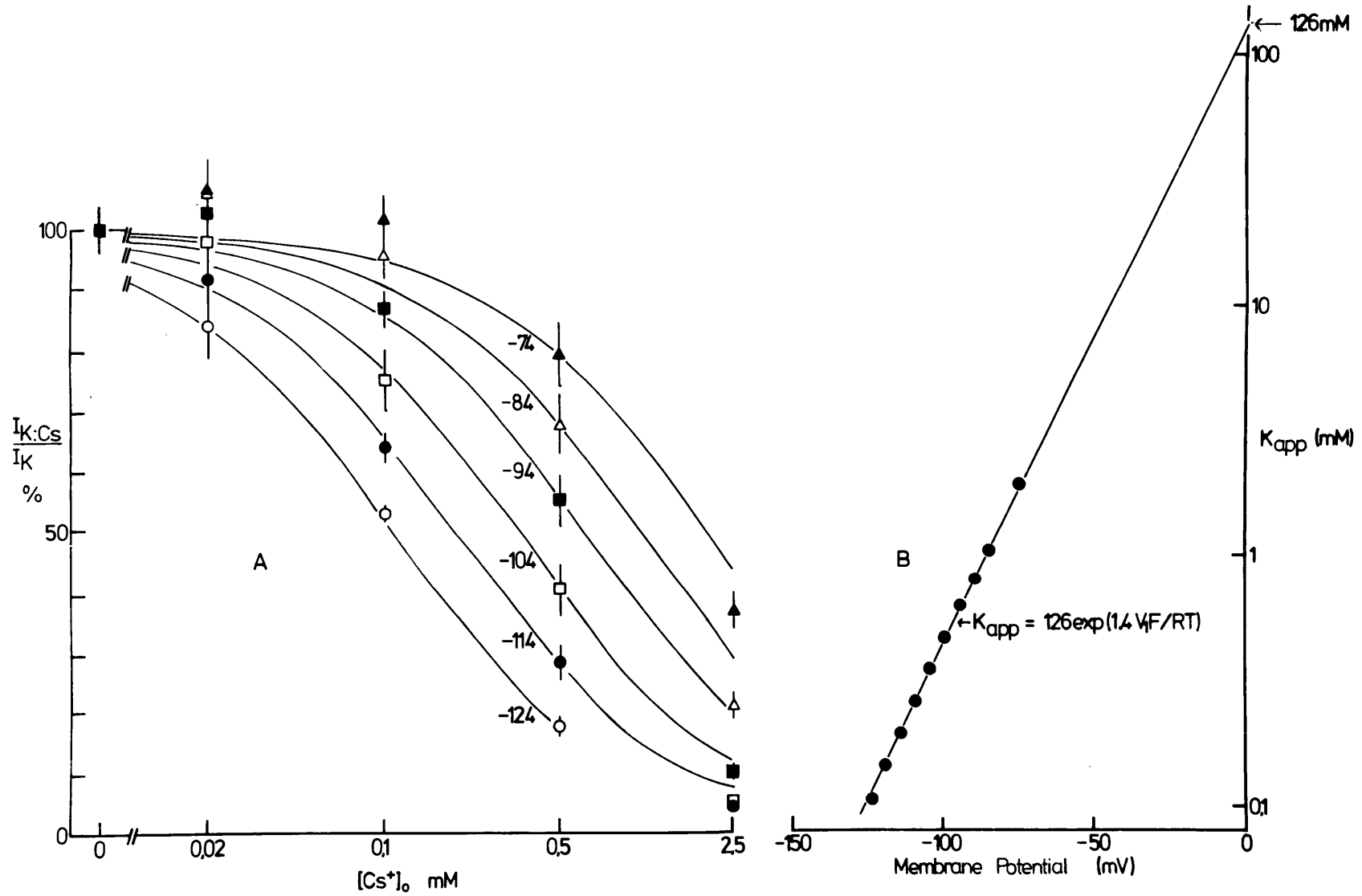
100
50
0
$\frac{I_{K:Cs}}{I_K}$ %
A
-7
-84
-94
-104
-114
-124
0
0,02
0,1
0,5
2,5
$[Cs^+]_o$ mM
B
← 126mM
100
10
1
0,1
K_{app} (mM)
← K_{app} = 126exp(1,4 VF/RT)
-150
-100
-50
0
Membrane Potential (mV)

potential for which this relationship holds, K_{app} is given by

$$K_{app} = K_{app(0)}\ e^{\delta V_1 F/RT} \qquad (5.2)$$

where $K_{app(0)}$ is the apparent dissociation constant at zero membrane potential and δ is a constant which depends on the slope of the relationship. The line through the points in Fig. 5.5B was fitted by eye. By extrapolation of this line, $K_{app(0)}$ is found to be 126 mM. At the holding potential (-14 mV) K_{app} is 58 mM. The line predicts that there is an e-fold change in K_{app} for a 17.8 mV change in the membrane potential. Since RT/F is 24.97 mV at 17°C δ must be 1.4 (24.97/17.8).

In Fig. 5.4 the solid lines which are used to fit the current-voltage relations in Cs^+ were drawn according to a formula which combines the concentration dependence of the blockade in eqn (5.1) and its voltage dependence in eqn. (5.2):

$$I_{K:Cs}/I_K = \left\{1 + [Cs]_o/K_{app(0)}\ e^{\delta V_1 F/RT}\right\}^{-1} \qquad (5.3)$$

where the control currents (I_K) are those plotted in Fig. 5.4 as open triangles, and $K_{app(0)}$ and δ are 126 mM and 1.4, respectively, as described above. As expected from Fig. 5.5A, the blockade is a steeper function of the membrane potential than predicted in 2.5 mM-Cs^+ between -30 mV and -90 mV: otherwise a reasonably close fit to the experimental points is obtained for inward currents.

Effect of changes in the external K^+ concentration

In order to examine the effect of external K^+ concentration on the blockade, instantaneous current-voltage relations were determined in fibres in 80 mM, 40 mM, and 16 mM-K^+ (solutions 5B,E & F), with or without 0.5 mM-Cs^+. The mean results from forty-two fibres are given in Fig. 5.6A after subtraction of a linear conductance

Fig. 5.6 The effect of external K^+ on the properties of the resting K conductance in the presence and absence of Cs^+.

A, instantaneous current-voltage relations. Abscissa, membrane potential (mV); ordinate, membrane current (mV) after subtraction of a linear component with a resistance of 11,236 ohm.cm^2 from the currents in the absence of Cs^+ (open symbols) and from those in 0.5 mM-Cs^+ (filled symbols). Each point is the mean of results from six to eight fibres; vertical bars are $\pm$ S.E.M. Each fibre was held at its resting potential; the inter-electrode distance was 330 μm; temp. 17-18.5°C. The solutions contain: ○, 80 mM-K^+; ●, 80 mM-K^+ + 0.5 mM-Cs^+; □, 40 mM-K^+; ■, 40 mM-K^+ + 0.5 mM-Cs^+; △, 16 mM-K^+; ▲, 16 mM-K^+ + 0.5 mM-Cs^+.

B, abscissa, membrane potential (mV); ordinate, ratio of the current determined in Cs^+ ($I_{K:Cs}$) to that in the control solution (I_K). The current ratios shown by filled symbols are calculated from the currents in Fig. 5.6A for a Cs^+ concentration of 0.5 mM. The current ratios shown by open symbols are calculated from the currents in Fig. 5.4 for a Cs^+ concentration of 2.5 mM. The concentrations of K^+ are: ○ & ●, 80 mM; ■, 40 mM; and ▲, 16 mM.

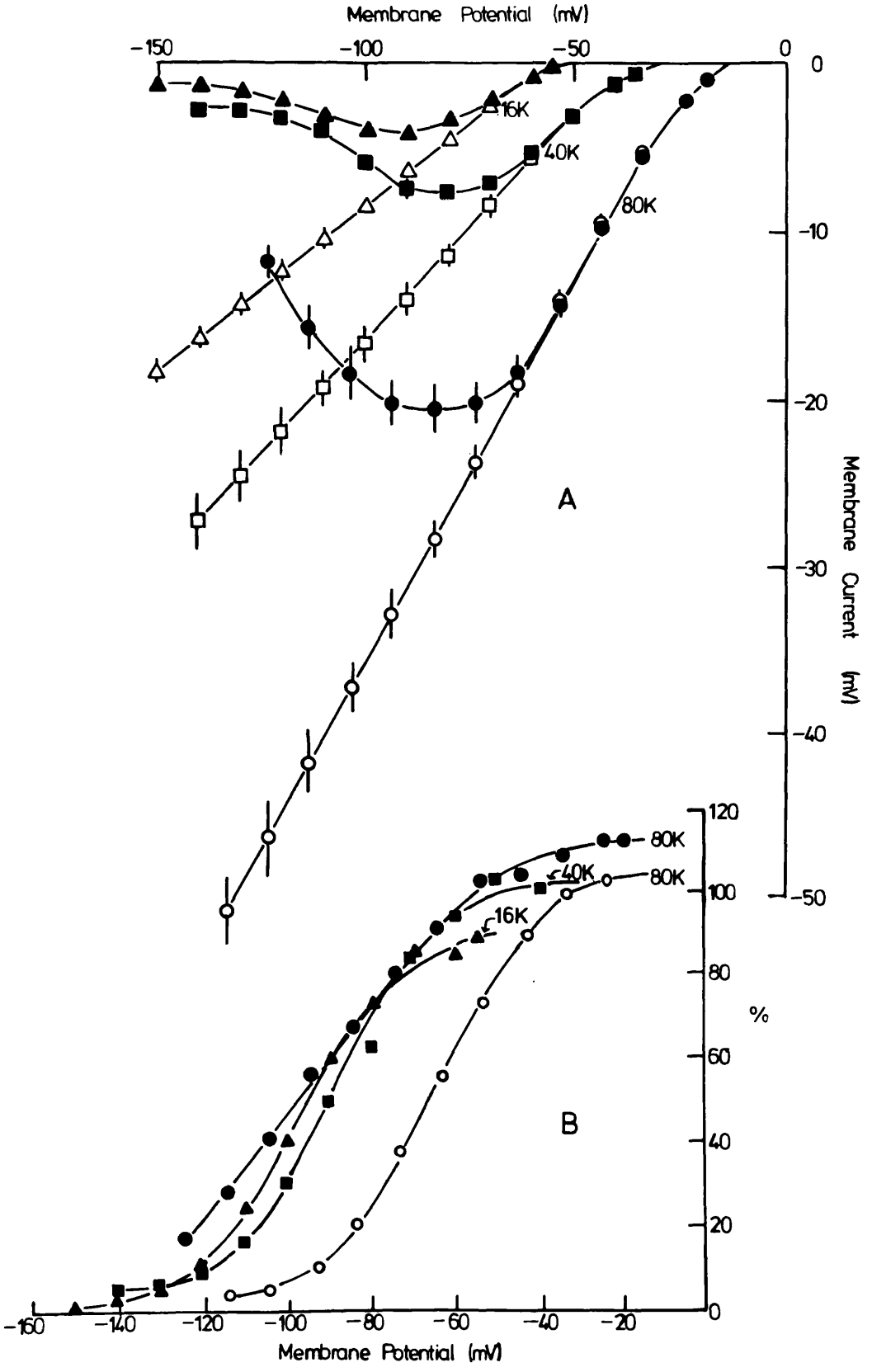
Membrane Potential (mV)
-150
-100
-50
0
16K
40K
80K
A
Membrane Current (mV)
0
-10
-20
-30
-40
-50
120
100
80
60
40
20
0
%
80K
40K
80K
16K
B
-160
-140
-120
-100
-80
-60
-40
-20
Membrane Potential (mV)

equal to that in 80 mM-K^+ solutions. (The linear component could not be measured in 40 mM or 16 mM-K^+ since depolarizations of about 20 mV or greater activated the delayed rectifier and contraction).

In Fig. 5.6B, the currents in Cs^+ ($I_{K:Cs}$) are shown as a percentage of the currents in the control Ringer (I_K), and are plotted as a function of the membrane potential using filled symbols. Changing the external K^+ concentration does not alter the degree of block in a systematic way except at potentials positive to -70 mV, where an increase in external K^+ from 16 mM to 80 mM reduces the blockade.

Since both Cs^+ and K^+ are monovalent cations belonging to the same chemical group (the alkali metals), it is likely that K^+ is able to displace Cs^+ from its binding site. However, in Fig. 5.6B there is evidence for such displacement only at membrane potentials positive to -70 mV. If, as might be expected, K^+ competitively inhibits the binding of Cs^+ on a one-to-one basis, then the extent of the blockade will depend on the concentration ratio of Cs^+ to K^+ at the binding site rather than on the concentrations of K^+ or Cs^+ alone. In 16 mM-K plus 0.5 mM-Cs (Fig. 5.6B, filled triangles) the blockade is less than in 80 mM-K plus 2.5 mM-Cs (Fig. 5.6B, open circles) even though the concentration ratio of Cs^+ to K^+ is 1:32 in both solutions.

Although there is little or no evidence for competition between K^+ and Cs^+ in the experiments of Fig. 5.6 , the possibility that such competition exists cannot be excluded because the ratio of Cs^+ to K^+ at the binding site may differ from that in the Ringer. Since K^+ is permeant, it will have access to the site from both sides of the membrane, whereas Cs^+ has access only from the outside. In the present experiments in isotonic sulphate Ringer,

a change in the external K^+ concentration will have little or no effect on the internal K^+ concentration (Adrian, 1956), so that the concentration of K^+ in the vicinity of the binding site may be largely unchanged.

Effect of increasing the intracellular K^+ concentration on the Cs blockade

When fibres are immersed in an 80 mM-K^+ solution made hypertonic by the addition of 350 mM sucrose, the mean resting potential increases from -13.86 ± 0.19 mV (seventy-three fibres in the isotonic Ringer) to -22.93 ± 0.5 mV (fifteen fibres). Assuming that the contribution to the resting potential of all ions other than K^+ is negligible, this indicates that the intracellular K^+ concentration has increased from 141 mM to 200 mM.

Mean instantaneous current-voltage relations are plotted in Fig. 5.7 for fibres in the hypertonic 80 mM-K^+ solution, in the presence and absence of 2.5 mM-Cs^+. In the presence of Cs^+, the maximum inward current occurs at -72 mV compared to -61.83 mV in isotonic Ringer containing the same Cs^+ concentration (see Table 5.2). The difference between these two values is largely explained by the difference in resting potentials. At -80 mV the mean current in hypertonic Ringer containing Cs^+ is reduced to 44 ± 2.6% (four fibres) of that in the control solution, while in isotonic Ringer the current is reduced to 27 ± 2.9% (six fibres), after subtraction of the linear conductance. The difference between these two values is in the direction expected if raising the intracellular K^+ concentration reduces the block.

Experiments to determine the rate at which Cs^+ blocks the K currents

Because the inward currents inactivate in 80 mM-K^+ solutions, instantaneous currents were used as a measure of the Cs blockade in

Fig. 5.7. Effect of 2.5 mM-Cs^+ on the instantaneous current-voltage relations of fibres in hypertonic 80 mM-K^+ solutions. Abscissa, membrane potential (mV); ordinate, membrane current (mV) recorded with an inter-electrode distance of 330 μm. △ , mean result from seven fibres in 80 mM-K^+. □, mean results from four fibres in 80 mM-K^+ plus 2.5 mM-Cs^+. Both solutions contain 350 mM sucrose which is in addition to that present in the isotonic Ringer. Vertical bars are ± S.E.M. Each fibre was held at its resting potential; temp. 17-18.5°C.

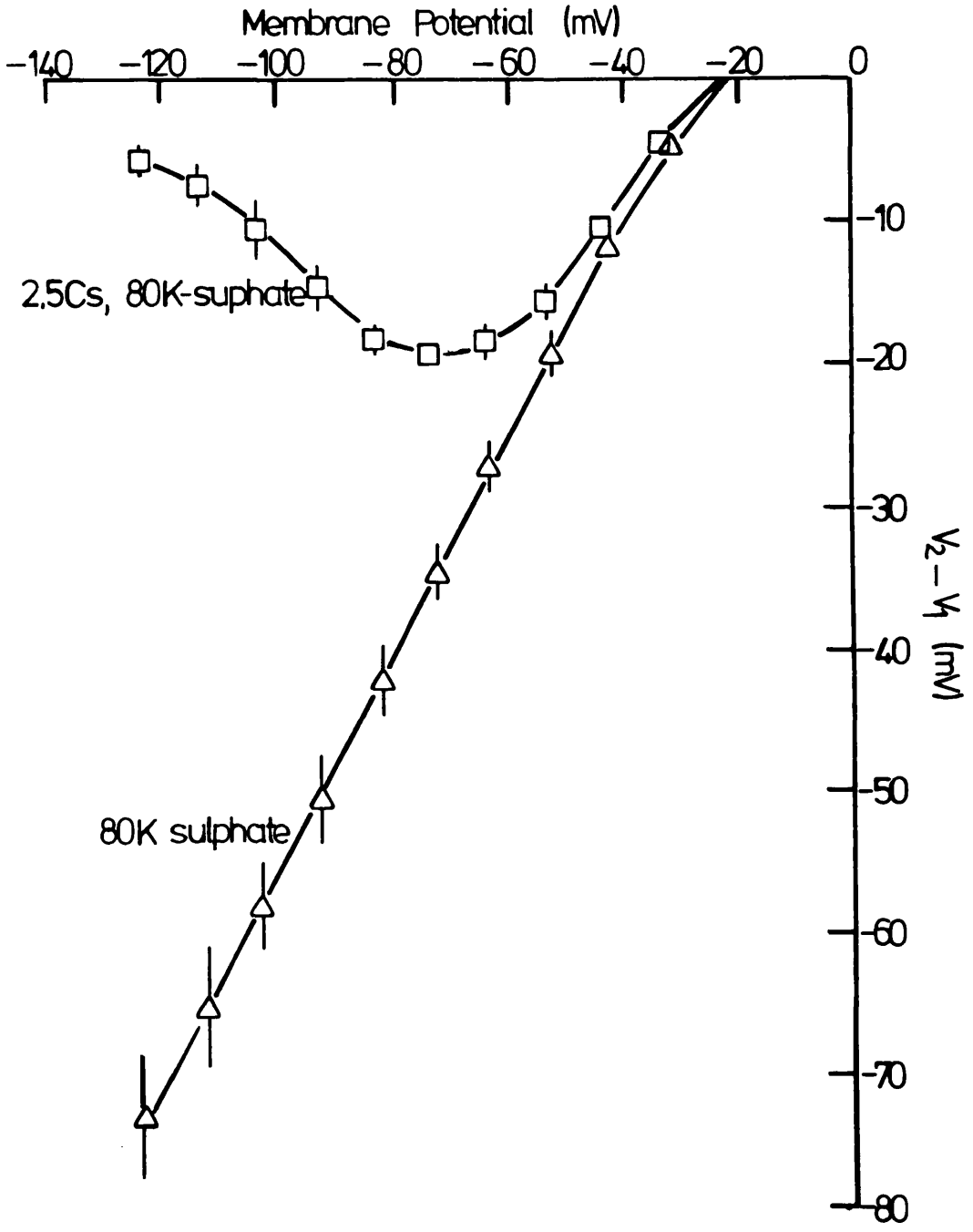
Membrane Potential (mV)
-140
-120
-100
-80
-60
-40
-20
0
-10
-20
-30
-40
-50
-60
-70
-80
$V_2 - V_1$ (mV)
2.5Cs, 80K-suphate
80K sulphate

Figs. 5.4 to 5.7. For such measurements to be justified the block should be complete within 25 ms. (At times shorter than this the currents are determined by extrapolation of the currents flowing at longer times). Since raising the external K^+ concentration reduces inactivation (Adrian & Freygang, 1962a; Almers, 1972b), experiments were performed in 190 mM-K^+ (solution 5A). However, even in this solution an appreciable inactivation occurred at 18°C. Fig. 5.8A shows that in the absence of Cs^+, and at about 4°C, the inward currents produced by hyperpolarizations to -59 mV(a) and -69 mV (b) show little time-dependence. Nor is there any time-dependence (apart from the initial capacity transient) to the currents produced by similar hyperpolarizations in the presence of 2.5 mM-Cs^+ (Fig. 5.8B). The instantaneous and steady-state current-voltage relations of these fibres indicate that the above conclusions can be extended to cover a wide range of membrane potentials (Fig. 5.8C & D). These results support the view that the block is complete within 25 ms of the onset of hyperpolarization, at least in the conditions of this experiment.

The rate of block has also been estimated in 80 mM-K^+ solutions containing 2.5 mM-Cs^+ in three fibres at room temperature. The conditions of this experiment are the same as employed in Fig. 5.1B, where the rate of block could not be determined due to the fact that the inward current inactivated during hyperpolarization. In the present experiments (Fig. 5.9) the inactivation was reduced by holding the fibres at -50 mV rather than at the resting potential.

The records in Fig. 5.9 are all taken from the same fibre, which had a resting potential of -12 mV. When the holding potential is

Fig. 5.8. The effect of 2.5 mM-Cs^+ on the resting membrane conductance in two fibres immersed in 190 mM-K^+ solutions.

A & B, tracings of the membrane potential (V_1) and membrane current (V_2-V_1). The hyperpolarizations are to -59 mV (a) and -69 mV (b). The fibre in A is in 190 mM-K^+ (solution A): resting potential, +3mV; holding potential, +3 mV; inter-electrode distance, 330 μm; temp. 4°C. The fibre in B is in 190 mM-K^+ plus 2.5 mM-Cs^+: resting potential, +1mV; holding potential, +1mV; inter-electrode distance, 330 μm; temp. 3.8°C.

C & D, instantaneous (○) and steady-state (●) current-voltage relations for the fibres shown in A and B of this figure. Abscissae, membrane potential (mV); ordinates, membrane current (mV). The fibre in C is in 190 mM-K^+ and is also shown in A. The fibre in D is in 190 mM-K^+ plus 2.5 mM-Cs^+ and is also shown in B.

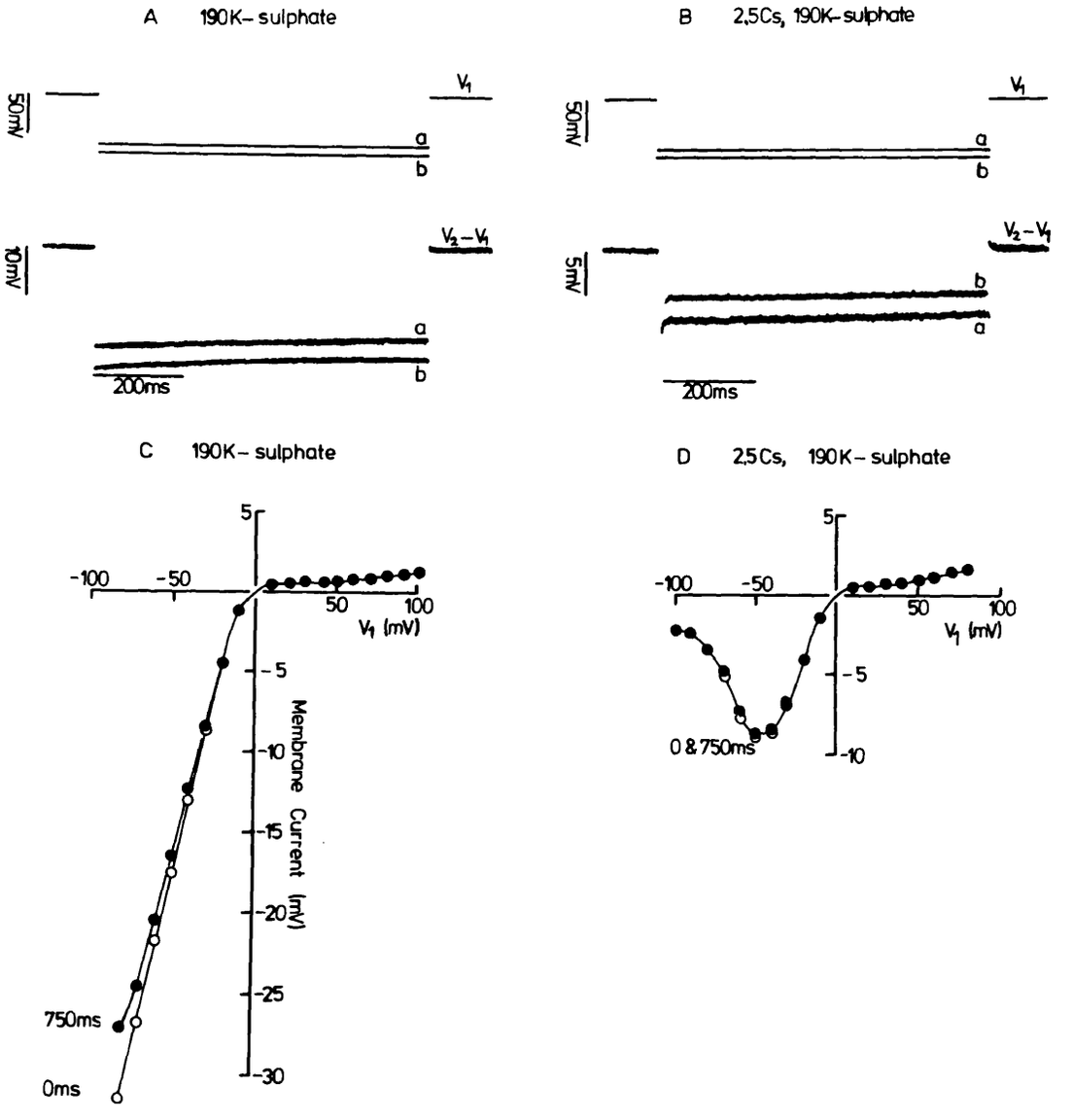
A 190K– sulphate
B 2.5Cs, 190K– sulphate
50mV
10mV
5mV
V_1
$V_2 - V_1$
a
b
200ms
C 190K– sulphate
D 2.5Cs, 190K– sulphate
-100
-50
50
100
V_1 (mV)
5
-5
-10
-15
-20
-25
-30
Membrane Current (mV)
750ms
0ms
0 & 750ms

Fig. 5.9 Effect of holding potential on the resting membrane conductance of a fibre immersed in a solution which contains 80 mM-K^+ and 2.5 mM-Cs^+.

A & B, tracings of records of the membrane potential (V_1) and membrane current (V_2-V_1). In A the holding potential is -50 mV. and the fibre is hyperpolarized to -81 mV and -131 mV. In B the holding potential is - 12 mV (equal to the resting potential) and the fibre is hyperpolarized to -83 mV. Temp. 21.5°C.

C, current-voltage relations for this fibre plotted 50 ms after the start of the clamp step. Abscissa, membrane potential (mV); ordinate, membrane current (mV). Run 1 (●) holding potential (HP), -50 mV; run 2 (■) HP, -12 mV; run 3 (◐) HP, -50 mV; run 4 (▲) HP, -100 mV.

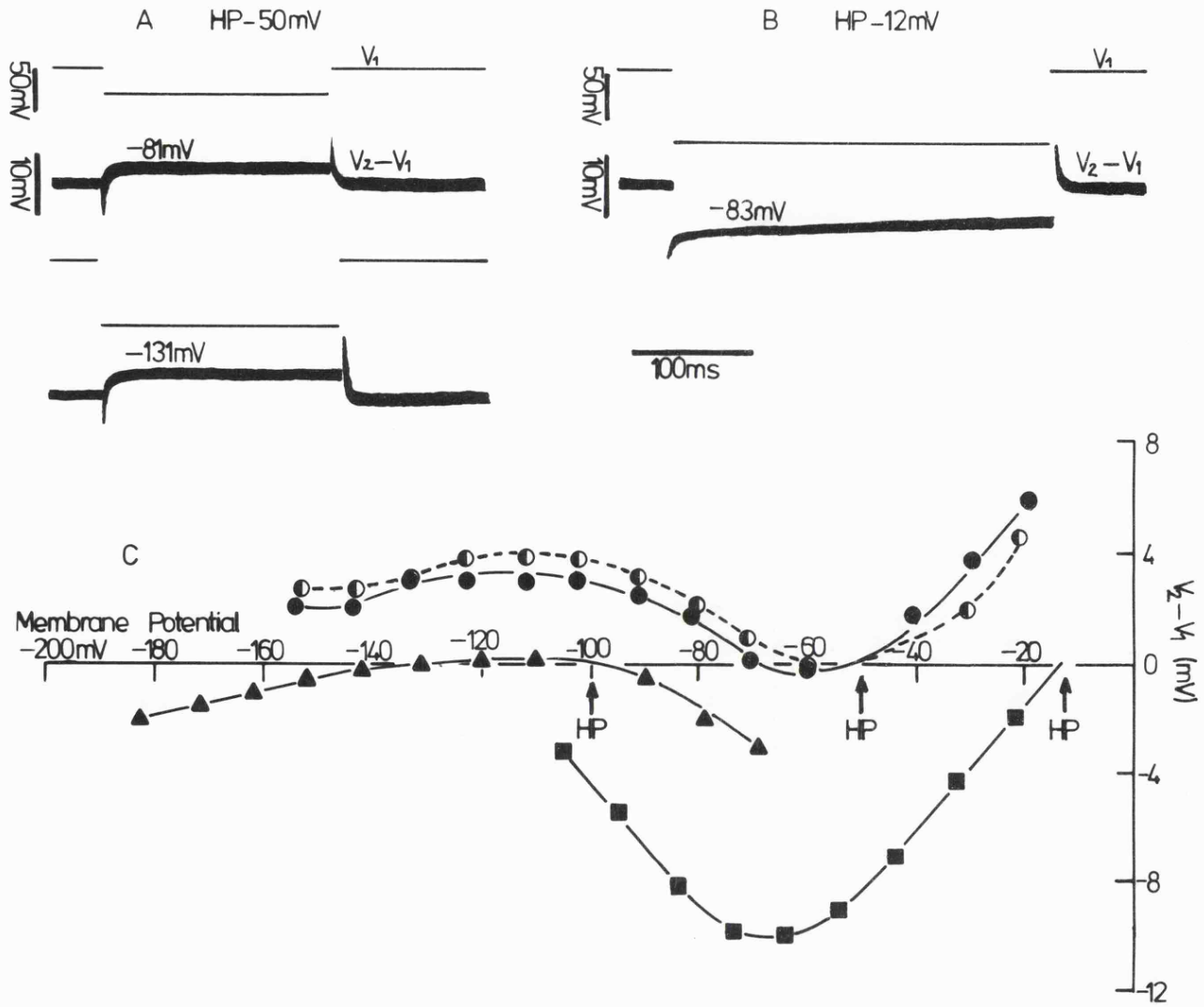
A
HP-50mV
B
HP-12mV
50mV
10mV
V1
V2-V1
-81mV
-131mV
-83mV
100ms
C
Membrane Potential
-200mV
-180
-160
-140
-120
-100
-80
-60
-40
-20
HP
8
4
0
-4
-8
-12
V2-V1 (mV)

-50 mV (Fig. 5.9A), the membrane currents at -83 mV and -131 mV are less than the holding current. That this is due to the potential-dependence of the blockade can be seen from Fig. 5.9C, which shows current-voltage relations for this fibre at holding potentials of -12 mV, -50 mV and -100 mV. The currents in Fig. 5.9A reach a steady-state within 40 ms of the start of the hyperpolarization, however the blockade will be faster than this since during this time there will also be a partial recovery from the depletion of K^+ which occurs at the holding potential.

Fig. 5.9A can be compared with Fig. 5.9B where the fibre was hyperpolarized to -83 mV from the resting potential. In Fig. 5.9B, the usual slow inactivation can be seen.

Two-electrode voltage clamp experiments in 80 mM-K^+, 2.5 mM-Cs^+

Experiments were performed to see if the membrane currents obtained with the three-electrode clamp in the presence of Cs^+ could also be obtained with the two-electrode method. Fig. 5.10A shows the relationship at 250 ms between the total (electrode) current (I_o) and the membrane potential for a fibre impaled with two microelectrodes close to the midpoint (see chapter 2). The membrane current (I_m) was calculated from this relationship using Cole's theorem (Cole & Curtis, 1941; Adrian, Chandler & Hodgkin, 1972; Jack, Noble & Tsien, 1975);

$$I_m = \frac{R_i}{8\ \pi^2 a^3} \cdot \frac{dI_o}{dV_1} \cdot I_o \qquad (5.4)$$

With the usual assumptions that the fibre radius (a) is 40 μm and the intracellular resistivity (R_i) is 180 ohm.cm, the resistance of the linear segment of the membrane current-voltage relation for the fibre illustrated is 14,285 ohm.cm^2. This is very close to the

Fig. 5.10 A, two-electrode voltage clamp analysis of the resting membrane conductance of a fibre immersed in 80 mM-K^+ and 2.5 mM-Cs^+. Abscissa, membrane potential recorded by an impaling microelectrode close to the midpoint of the fibre (mV); ordinate, total current flowing through an impaling microelectrode less than 50 μm from the recording electrode (I_o, A), and membrane current (I_m, A/cm^2). ●, total current during run 1; ○, total current during run 2. The line through the points was drawn by eye. The membrane current (I_m) was calculated from the total current-voltage relationship using Cole's theorem (eqn. 5.4). The interrupted line (- • - • -) was obtained by extrapolation of the membrane currents at membrane potentials more positive than +40 mV. Fibre resting potential, -13 mV; holding potential, -13 mV; temp. ~~14.2°C~~. 17.8 °C.

B, membrane current-voltage relationship for a fibre in 80 mM-K^+ and 2.5 mM-Cs to illustrate how regenerative changes in the membrane potential can arise. The line drawn parallel to the voltage axis represents an inward current which intersects the current-voltage relationship at the membrane potentials V_A, V_B, and V_C. In constant current conditions the membrane potential should propagate from V_A to V_C when the area under the curve V_A-V_B is less than the area under the curve V_B-V_C. The current-voltage relationship is the same as shown in Fig. 5.10A.

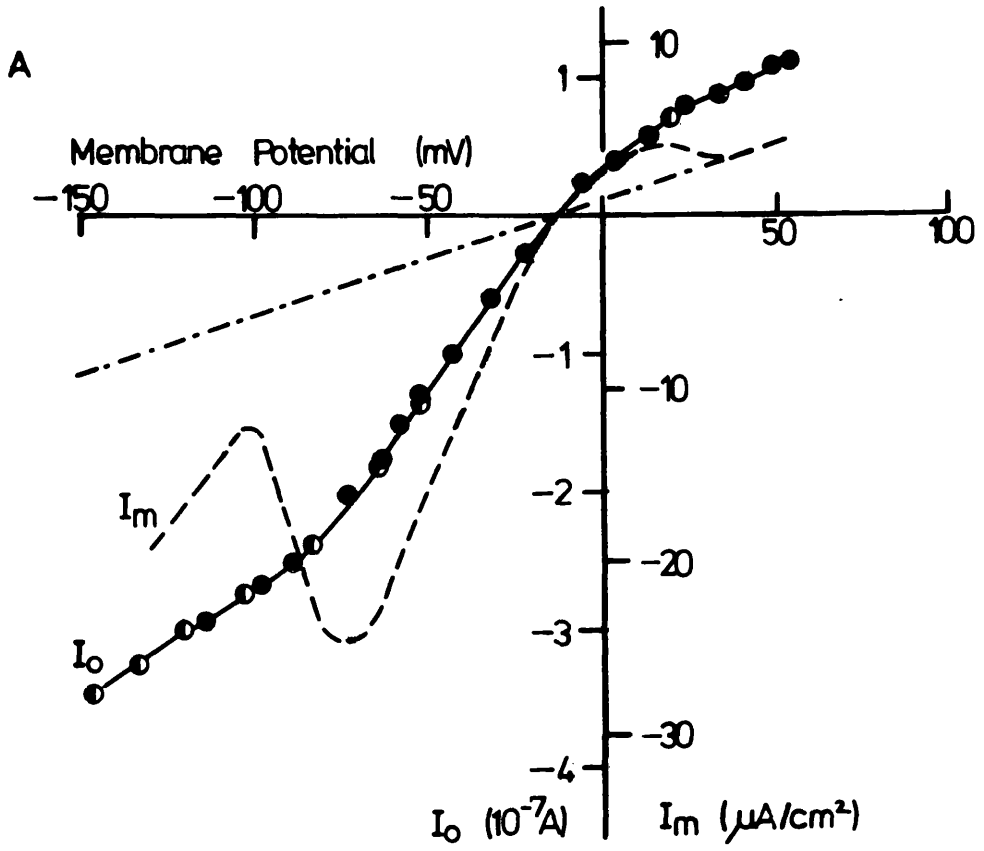
A
Membrane Potential (mV)
−150
−100
−50
50
100
10
1
−1
−10
−2
−20
−3
−30
−4
Im
Io
Io (10⁻⁷A)
Im (μA/cm²)

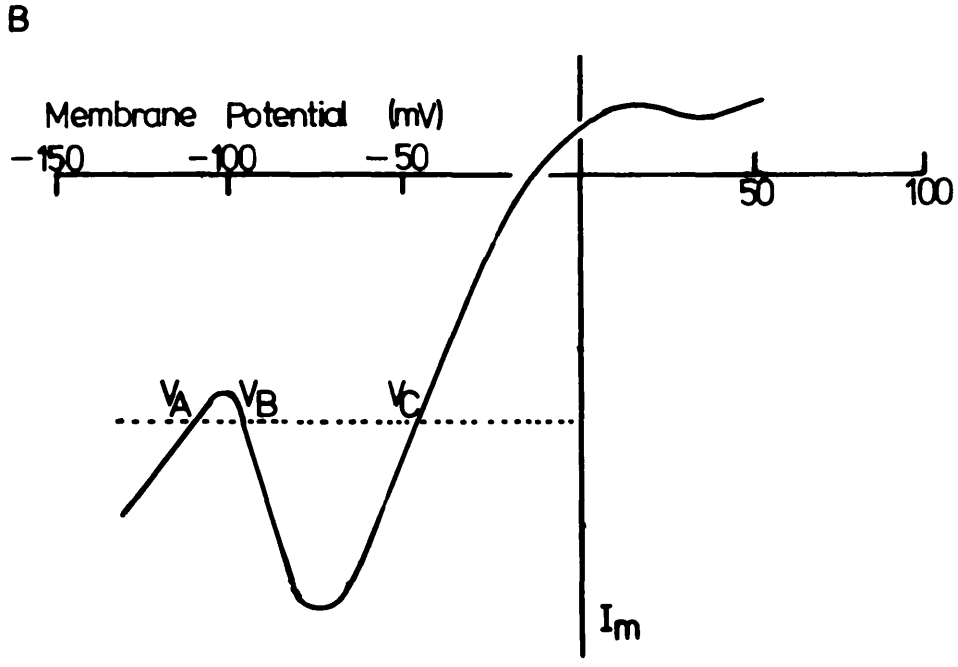
B
Membrane Potential (mV)
−150
−100
−50
50
100
VA
VB
VC
Im

mean value given in Table 5.2 and obtained in the same conditions but with the three-electrode method. The maximum inward current obtained with two electrodes in 2.5 mM-Cs^+ was 32.21 ± 5.1 $\mu A/cm^2$ (three fibres) compared to 52.63 ± 3.4 $\mu A/cm^2$ (six fibres) in the steady-state when the three-electrode voltage clamp was used. Although the difference between these values is significant (P = 0.01), it is probably not important since in calculating I_m from I_o the cube of the fibre radius is assumed.

At 250 ms the total electrode current is close to a steady-state for hyperpolarizations of less than 60 mV, but the error increases when larger hyperpolarizations are applied. Since in its derivation Cole's theorem assumes that the currents are independent of time, recovery from the blockade which is seen at membrane potentials negative to -100 mV will not be quite so steep a function of the membrane potential as shown here.

Regenerative changes in the membrane potential in 80 mM-K^+ solutions containing Cs^+

In K^+ solutions containing between 0.02 mM and 2.5 mM-Cs^+, the membrane current-voltage relations can be intersected at three different membrane potentials (V_A, V_B and V_C) by a small inward current drawn parallel to the voltage axis. This is illustrated in Fig. 5.10B by the membrane current-voltage relation taken from Fig. 5.10A for a fibre in 80 mM-K^+, 2.5 mM-Cs^+ solution. In this fibre, the conditions are fulfilled that the membrane potential will propagate from V_A to V_C (Noble & Hall, 1963; Jack, Noble & Tsien, 1975). These conditions are (a) that at all three potentials the membrane current is zero, (b) that V_A and V_C lie on a segment of the current-voltage relation which has a positive slope conductance,

(c) that V_B lies on a segment of negative slope conductance and is between V_A and V_C, and (d) that the area under the curve V_A-V_B is less than that under the curve V_B-V_C.

To see if such propagation occurred, fibres were impaled by two microelectrodes close to their midpoints. One electrode recorded the membrane potential while the second electrode injected a steady inward current into the fibre at a point less than 100 μm from the recording electrode.

In each of twenty-five fibres, one of two types of response was seen, depending on the Cs^+ concentration. When the Cs^+ concentration was 2.5 mM (Fig. 5.11A), the membrane potential could be switched in a reversible manner between two levels. This was achieved by superimposing a brief rectangular current on the steady current which hyperpolarized the fibres. Smaller brief currents produced subthreshold responses. In fifteen fibres values of -65 mV to -132 mV were obtained for the upper level, and -125 mV to -189 mV for the lower level. Both levels were affected by the size of the steady current.

In the presence of 0.5 mM and 0.1 mM-Cs^+, spontaneous oscillations in the membrane potential developed when the fibres were hyperpolarized. Fig. 5.11B shows six records of the membrane potential from a fibre in 0.5 mM-Cs^+. At -112 mV (record ii) there are small fluctuations in the membrane potential which are not seen when a smaller current is injected (as in i). When a larger inward current is injected (records iii to vi) the size of the oscillations increases but the frequency falls. In 0.1 mM-Cs^+ (Fig. 5.11C), the oscillations develop at more negative membrane potentials.

Fig. 5.11 Regenerative changes in the membrane potential recorded from fibres hyperpolarized in Cs^+-K^+ mixtures. Records A to C were made in constant current conditions with two impaling microelectrodes close to the midpoint of the fibre. The electrode separation was less than 100 μm.

Fibre A is in a solution containing 80 mM-K^+ and 2.5 mM-Cs^+. The records are of the membrane potential (V_1, mV) and the total (electrode) current (I_o). In i, a brief outward current is superimposed on a steady inward current which is injected into the fibre. In ii, the brief current is inward. Fibre resting potential, -14 mV; temp. about ~~4°C.~~ 17.6 °C.

Fibre B is in a solution containing 80 mM-K^+ and 0.5 mM-Cs^+. Records i to vi show spontaneous changes in the membrane potential when a steady inward current is injected into the fibre. Fibre resting potential, -15 mV; temp. about ~~4°C.~~ 17.6 °C.

Fibre C is in a solution containing 80 mM-K^+ and 0.1 mM-Cs^+. Both the membrane potential (V_1, mV) and the electrode current (I_o) are shown. The fibre was hyperpolarized first to -95 mV, and then to between -130 mV and 160 mV. Fibre resting potential, -16 mV; temp. about ~~3.1°C.~~ 17.0 °C.

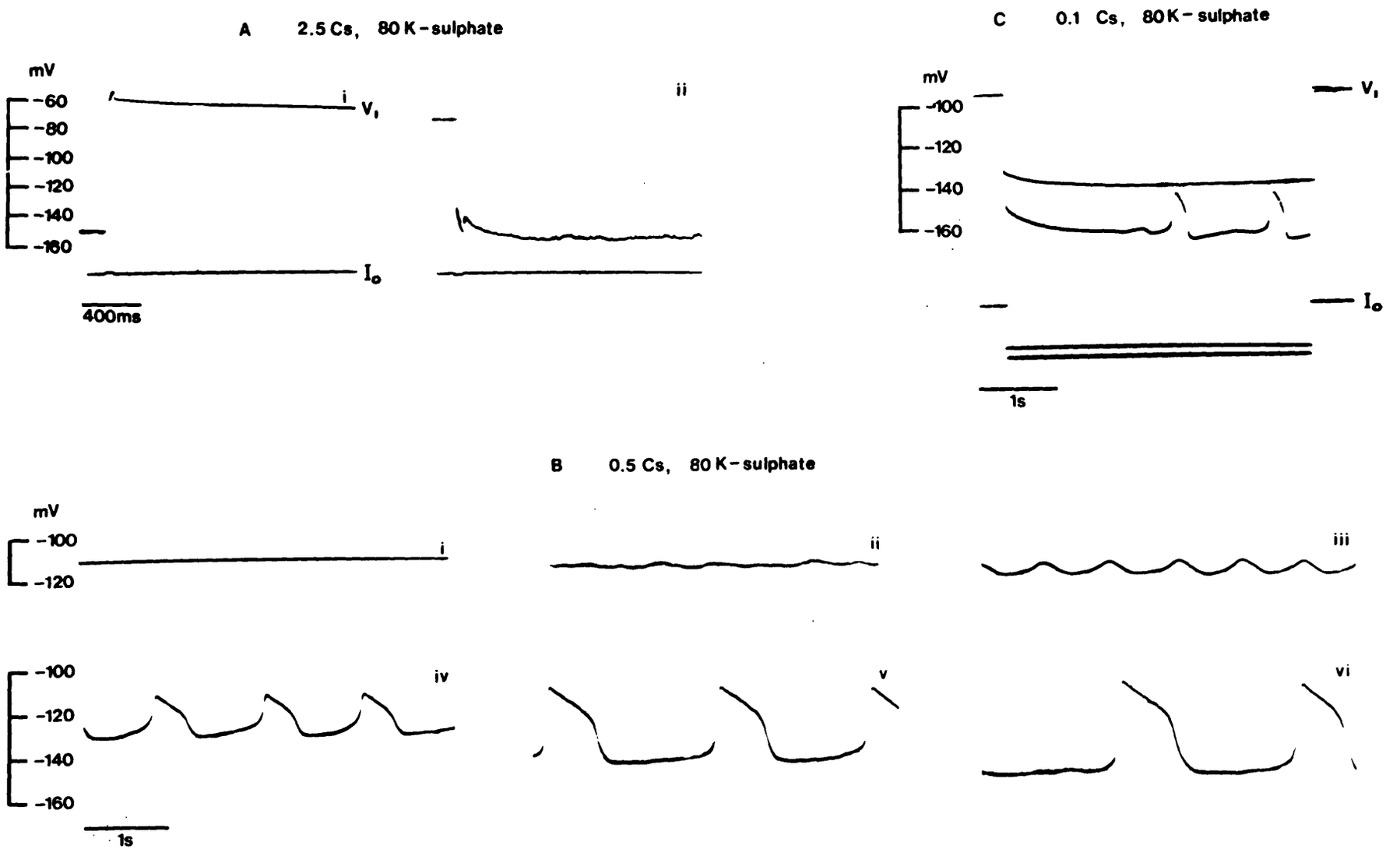
A 2.5 Cs, 80 K-sulphate
mV
-60
-80
-100
-120
-140
-160
i
ii
V_t
I_o
400ms
C 0.1 Cs, 80 K-sulphate
mV
-100
-120
-140
-160
V_t
I_o
1s
B 0.5 Cs, 80 K-sulphate
mV
-100
-120
i
ii
iii
-100
-120
-140
-160
iv
v
vi
1s

A likely explanation for the depolarizing phase of the spontaneous responses is that Cs^+ ions dissociate from the binding sites within the membrane. This process is regenerative because the blockade is voltage-dependent. Subsequently, the membrane repolarizes slowly until a threshold is reached at which repolarization becomes regenerative due to an increase in the number of Cs^+ ions bound. The slow phase of repolarization will be due, in part, to the fact that in 80 mM-K^+ there is a depletion of K^+ ions from the lumen of the T-system when an inward current flows across the membrane. A similar explanation accounts for the fact that in voltage clamp conditions, the peak inward current in the presence of Cs^+ occurs at more positive membrane potentials in the steady-state than at the beginning of a hyperpolarization (page 107). The phase of gradual depolarization which precedes the regenerative depolarization in Figs. 5.11B & C may be related to the initial increase in current seen in some fibres in conditions of extreme hyperpolarization. Such currents are illustrated in Fig. 5.2A.

The voltage-dependence of the blockade also accounts for the way in which the membrane potential can be switched between two levels in Fig. 5.11A. That these levels do not correspond to the values predicted in Fig. 5.10B is due in part to the fact that the regenerative responses were obtained in conditions of point polarization rather than uniform polarization, and in part to the fact that even in 2.5 mM-Cs^+ the membrane current-voltage relation does not remain stationary with time.

DISCUSSION

The blockade of resting K currents by Cs^+ reported here is potential-dependent and is increased by raising the external Cs^+

concentration. The blockade is also very fast; so much so that the rate of onset cannot be measured with the voltage clamp in the present conditions.

The formula (eqn. 5.3) used to describe the blockade is analogous to the Michaelis-Menten equation for the equilibrium binding between an enzyme and its substrate (Dixon & Webb, 1964) but with the addition that the dissociation constant (K_{app}), which defines the affinity of the substrate for the enzyme, is voltage-dependent. In the present case K_{app} also depends on the internal K^+ concentration.

A potential-dependent blockade of Na channels in myelinated nerve fibres by protons and Ca^{2+}, and by quaternary derivatives of lidocaine has been demonstrated by Woodhull and Strichartz, respectively, in 1973. Since then a number of cations have been found to block Na and K channels in excitable cells in a voltage-dependent manner (see chapter 1). Woodhull (1973) and Strichartz (1973) suggested that the blocking ion is attracted into the channel when an electrical gradient of appropriate polarity is applied across the membrane. At a specific point in the channel the ion binds to a receptor and prevents further current flow. The analysis used by these authors to describe the blockade of Na channels is similar to that employed here. The voltage-dependence of the blockade is defined by δ, and is attributed to the fact that the binding site is at least partway through the applied electrical gradient. For a channel containing a single binding site the limits of δ are 0 and 1, corresponding to the position of the site at the outer or inner edges of the potential

gradient, respectively. On average, δ is 0.26 for the proton blockade of the Na channel, thus if the potential gradient across the membrane is linear, the proton binding site is about 26% of of the way across the membrane from the outside (Woodhull, 1973).

The Cs^+ blockade in muscle is not explained by a single site model since δ is 1.4. However, a value of δ greater than 1 is consistent with the view that K channels can contain more than one binding site (Hille, 1975a). In starfish egg cells δ is 1.4 for the blockade of the resting K conductance by Cs^+ (Hagiwara, Miyazaki & Rosenthal, 1976): in this respect, and with respect to the concentrations at which Cs^+ blocks, the blockade in the starfish is very similar to that found here. Values of δ greater than 1 have also been reported for the blockade by external Cs^+ of inward K tail currents in squid axons (Adelman & French, 1978) and for the blockade by intracellular methylammonium ions of outward ammonium currents through the delayed K channel in myelinated nerve fibres (Hille, 1975a).

The model used by Ciani, Hagiwara & Miyazaki (1977) to explain the steep dependence of the Cs blockade on the membrane potential in the starfish, and also to account for its dependence on the external K^+ concentration, is that the permeation pathway contains two binding sites. Cs^+ binds strongly to the innermost site and thereby blocks the channel. The subsequent binding of K^+ to the outermost site increases the block since it reduces the probability that Cs^+ will leave the innermost site. Binding of Cs^+ to the outermost site is assumed to be negligible.

The model of Ciani et al.(1977) has been applied to the present results taking $\delta = 1.4$ to be the sum of the fractions of membrane

potential felt at the two sites (P.R. Stanfield, personal communication). In 80 mM-K^+ solutions, the currents predicted when the external Cs^+ concentration is altered are almost identical to those obtained with eqn. (5.3). However, in low K^+ concentrations, the blockade found experimentally is much stronger than the two-site model predicts. Such a result is to be expected since Fig. 5.6B demonstrates that the blockade in muscle is rather insensitive to changes in the external K^+ concentration, whereas the two-site model of Ciani et al. (1977) predicts that a reduction in external K^+ will reduce the blockade.

Recently, it has been demonstrated that the resting K conductance in muscle (Standen & Stanfield, 1978a,b) and in starfish egg cells (Hagiwara, Miyazaki, Moody & Patlak, 1978) are blocked by Ba^{2+} in a voltage-dependent manner. In muscle, Ba^{2+} appears to bind at a site 0.7 of the way across the membrane. Standen & Stanfield (1978b) also show that two K^+ ions competitively inhibit the binding of each Ba^{2+} ion. In their experiments the external K^+ concentration was raised from 115 mM to 230 mM so that due to fibre shrinkage the internal K^+ concentration was also doubled. Under these conditions, the external Ba^{2+} concentration had to be increased about four times to obtain the same degree of block.

It is interesting to note that Ba^{2+}, as a divalent ion, could bind to two sites simultaneously, in which case each K^+ ion could compete with Ba^{2+} at one or other site. Further, since δ is 1.4 for Cs^+, these may be the same sites at which Cs^+ is bound. However, such a model requires that K^+ can competitively inhibit the binding by Cs^+. In the present experiments the external K^+ concentration

was reduced from 80 mM to 16 mM under conditions in which there is unlikely to be very much change in the internal K^+ concentration. Under these conditions there is little or no evidence of competition between Cs^+ and K^+ (Fig. 5.6B), probably because K^+ has access to the binding sites from the sarcoplasm (see page 115). Standen & Stanfield (1978b) have also found much less evidence for competition between Ba^{2+} and K^+ when the external K^+ concentration is reduced such that the internal K^+ concentration is unchanged than when the concentrations of K^+ on both sides of the membrane are changed in the same way.

The speed at which an ion blocks is an indication of the ease with which it traverses the membrane to reach the binding site, and the affinity of the ion for the site. In muscle, the blockade by Cs^+ is rapid while that in the starfish reaches a steady-state in 100 ms. The voltage-dependent blockade of the delayed K channel in squid axons by internal Cs^+ (Bezanilla & Armstrong, 1972) or by external Cs^+ (Adelman & French, 1978) is 'instantaneous': the latter is complete within 50 or 100 μs. In contrast, Ba^{2+} and Sr^{2+} block resting K currents in muscle slowly along an exponential time course (Standen & Stanfield, 1978b). The rate of onset of the blockade is increased by an increase in the concentration of the blocking ion or the degree of hyperpolarization; which factors also increase the steady-state blockade. The blockade of resting K^+ currents in muscle by external Na^+ is also time-dependent (Standen & Stanfield, 1978c).

In the presence of Ba^{2+}, the instantaneous inward K currents in muscle are smaller than in the control solution because there is a measurable blockade at the holding potential (Standen & Stanfield, 1978b). In addition, outward K currents are reduced by external

Ba^{2+}. These experiments demonstrate that the Ba^{2+} blockade is dependent on the membrane potential rather than on the direction in which K^+ moves across the membrane.

In the present experiments in 80 mM-K^+, K_{app} is 58 mM at the holding potential, so this concentration of Cs^+ is required to produce a 50 % blockade. Depolarizing the fibre increases K_{app} to 176 mM at +6 mV, and this could account for the fact that the outward K currents are only slightly reduced by 2.5 mM-Cs^+. In fact, the blockade of outward currents found experimentally is greater than predicted: at +6 mV the currents are reduced by 9% compared with a predicted blockade of less than 2%. The blockade of outward K currents by Cs^+, though subject to large experimental error, is an indication that Cs^+ also blocks K currents in muscle as a function of the membrane potential rather than the direction in which K^+ ions cross the membrane. However, the possibility that outward currents are blocked by Cs^+ ions which have diffused into the sarcoplasm cannot be excluded.

Chapter 6. Caesium as a tool to investigate the mechanisms which underlie the decline in inward K currents in skeletal muscle fibres.

INTRODUCTION

The experiments to be described here are those in which caesium was used to test Almer's (1972a) hypothesis that the decline in inward current which occurs when a muscle fibre is hyperpolarized is due to two mechanisms: a depletion of K^+ from the lumen of the T-system similar to that described by Adrian & Freygang (1962a), and a voltage- and time-dependent permeability change (Almers, 1972b; Adrian et al., 1970b).

If inactivation of the inward current is due to depletion, recovery from inactivation will be largely independent of the membrane potential, provided the inward current is small or zero. Conversely, if inactivation is due solely to a voltage-dependent reduction in the number of inwardly rectifying channels which are open, recovery will only occur if the degree of hyperpolarization is reduced.

In K solutions containing a small quantity of Cs^+, the inward K current is blocked in a manner which increases with hyperpolarization (Gay & Stanfield, 1977), as described in detail in the previous chapter. In such conditions there are two regions of the current-voltage relationship at which inward currents are small and at which recovery from inactivation can be measured to see if depletion has occurred. One such potential is close to the holding potential and the other is at least 80 mV more negative. At intermediate values of the membrane potential, the inward current is sufficiently large for inactivation to occur. In addition, since the blockade by Cs^+ is rapid, it is a reasonable assumption that the mechanisms

responsible for this inactivation are the same as those producing inactivation in Cs-free solutions.

SOLUTIONS AND METHODS

The composition of solutions used here is given in Table 6.1. The solutions are isotonic and contain either 40 mM-K_2SO_4 (solution 6A) or 2.5 mM-K_2SO_4 (solution 6B): Cs_2SO_4 was usually present at concentrations of 1.25 mM and 0.025 mM, respectively. The pH was 7.2.

The three-electrode voltage clamp method (see chapter 2) was used in all experiments. Fibres were held at the resting potential and hyperpolarized in a step-wise fashion. The inter-electrode distance was 330 µm.

All experiments were carried out at room temperature (16.5 - 18.5°C).

Table 6.1

Composition of Solutions in mM

	Na^+	K^+	Cs^+	Ca^{2+}	SO_4^{2-}	$H_2PO_4^-$	HPO_4^{2-}	Sucrose
Solution 6A	2.6	80	2.5	8	49.25	0.43	1.08	113
Solution 6B	77.6	5	0.05	8	48.03	0.43	1.08	113

RESULTS

Experiments in 40 mM-K_2SO_4 solution plus 1.25 mM-Cs_2SO_4

The experiment of Fig. 6.1 was designed to study the degree of recovery from inactivation at two different membrane potentials. The two pulse sequences used are illustrated at the top of Fig. 6.1 and each consists of three pulses. The conditioning pulse hyperpolarised the membrane to -66 mV to diminish the inward current. During the second pulse the fibre was held at either the holding

Fig. 6.1 Effect of membrane potential on the recovery from inactivation in 40 mM-K_2SO_4 plus 1.25 mM-Cs_2SO_4.

A & B, schematic drawing of pulse sequences employed.

C & D, records of the membrane current (V_2-V_1) in one fibre: resting potential, -14 mV; holding potential, -14 mV; inter-electrode distance, 330 μm. Conditioning pulse is to -66 mV and lasts 2.35 s. Test pulse is also to -66 mV and the beginning of this pulse is indicated by an arrow. C shows five superimposed records when the membrane was held at -14 mV during pulse 2 for between 150 ms and 6 s. In D the membrane was held at -120 mV for 1.1 s.

E, time course of recovery in five fibres. Abscissa, duration of pulse 2; ordinate, % recovery by eqn. (6.1) of the text. This compares the current at the start of the test pulse ($I_{m(0,3)}$) with that at the start of the conditioning pulse ($I_{m(0,1)}$). 100% recovery, $I_{m(0,3)} = I_{m(0,1)}$; 0% recovery, $I_{m(0,3)}$ = current at end of conditioning pulse. Filled symbols, pulse 2 is to -14 mV (pulse sequence A); open symbols, pulse 2 is to -120 mV, except □ which is to -97 mV (pulse sequence B).

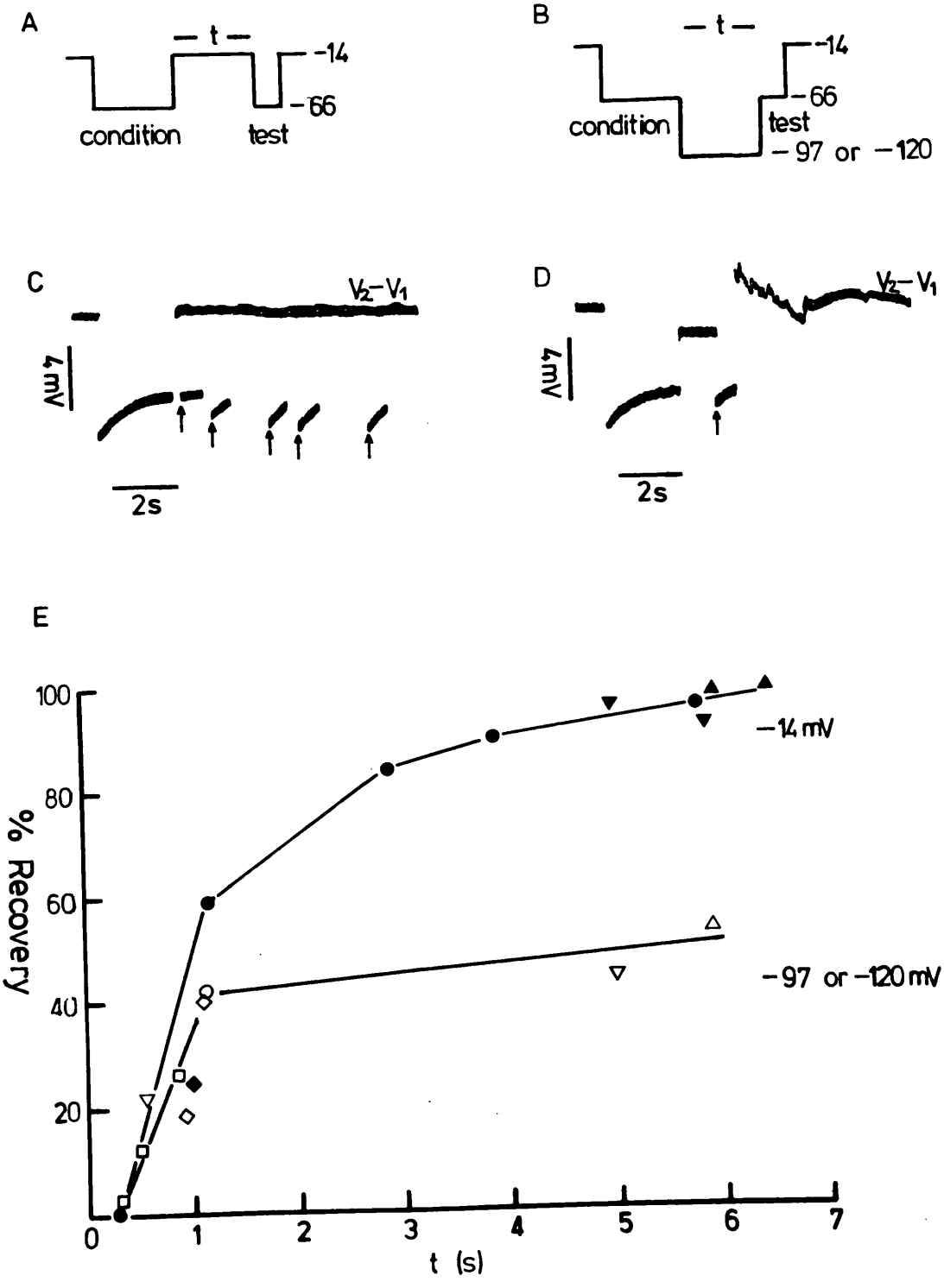
A
— t —
-14
-66
condition
test
B
— t —
-14
-66
condition
test
-97 or -120
C
V2-V1
4mV
2s
D
V2-V1
4mV
2s
E
100
80
60
40
20
% Recovery
0
1
2
3
4
5
6
7
t (s)
-14 mV
-97 or -120 mV

potential (A), or (B) at -120 mV (or in one fibre -97 mV) for different lengths of time (t), after which the membrane was returned to -66 mV to see how much current had recovered by the end of pulse two.

The middle of figure 6.1 shows membrane currents recorded when these pulse sequences were applied. During the conditioning pulse the current declines in the usual manner, and almost reaches a steady-state after 2.35 s. On returning to the holding potential (in C) the current did not revert immediately to its original value but remained slightly outward for up to 500 ms. This is seen more clearly in Fig. 5.1B (see previous chapter), and as pointed out by Almers (1972a), is consistent with the view that the reversal potential for the resting K conductance has become more negative during the conditioning hyperpolarization. Such behaviour is to be expected if depletion is occurring. In Fig. 6.1C, five traces of the membrane current are superimposed to show that the inward current flowing at the start of the test pulse (indicated by the arrows) is dependent on the time spent at the holding potential, when this is preceded by the conditioning hyperpolarization. Pulse sequence A was used as a control: recovery from inactivation will occur at the holding potential irrespective of the mechanism which is responsible for the decline in inward current.

The membrane current shown during the application of pulse sequence B in Fig. 6.1D is from the same fibre. During pulse two, which was to -120 mV, the current is partially blocked by Cs^+, and at the end of 1.1 s, when the test pulse is applied, it can be seen that some of the current has recovered. Unfortunately, contraction

is reprimed during this pulse sequence and this accounts for the movement artifact on returning to the holding potential. Hence, a systematic study of the time course of recovery at -120 mV was impossible in any one fibre.

In order to compare the results in five different fibres, as is done in Fig. 6.1E, the recovery obtained by the end of pulse two is expressed as a percentage of inactivation during the conditioning pulse using the formula,

$$\% \text{ Recovery} = \frac{I_{m(0,3)} - I_{m(1)}}{I_{m(0,1)} - I_{m(1)}} \times 100 \qquad (6.1)$$

where $I_{m(1)}$ is the current at the end of the conditioning pulse and $I_{m(0,1)}$ and $I_{m(0,3)}$ are the currents at the beginning of the conditioning pulse and pulse three (the test pulse), respectively. The last two were determined by extrapolation of a straight line intersecting the current trace at 50 ms and 100 ms. This formula is similar to that used by Almers (1972a,b) in that a correction is made for random variation in the size of the resting conductance during the 5 mins or so required to complete a set of records. Such variations rarely exceeded 5%.

Fig. 6.1E shows that the results obtained in all five fibres were very similar. At the holding potential (filled symbols) an almost complete recovery is achieved after 6 s. Recovery at -120 mV (or -97 mV, open squares) is consistent with the view that inactivation is due to a fall in the potassium concentration in the lumen of the T-system. During pulse two, K^+ can reaccumulate in the tubules because most of the K selective channels in the wall of the T-system are blocked by Cs^+. That a complete recovery was never seen is due, at least in part, to the fact that a total blockade by Cs^+ is not achieved.

A time-dependent fall in the number of conducting K channels at -120 mV may also contribute to the failure of the current to recover completely. However, experiments performed more recently than these show that this permeability change (Almers, 1972b) is dependent on the concentration of Na^+ in the Ringer, and is abolished if Na^+ is removed (Standen & Stanfield, 1978c). In the experiments of Fig. 6.1 $[Na]_o$ was only 2.6 mM, so that here the component of inactivation which results from a fall in membrane permeability can, at most, be very small.

Experiments in 2.5 mM-K_2SO_4 solution plus 0.025 mM-Cs_2SO_4

A more complex result was obtained when three-pulse experiments similar to those just described were performed in solutions containing 2.5 mM-K_2SO_4 and between 0.1 and 0.025 mM-Cs_2SO_4. When the solution contained 0.025 mM-Cs_2SO_4, the mean resting potential was -73.14± 0.94 mV (fourteen fibres), and this is not significantly different for the mean value in the absence of caesium (-75.71± 1.38 mV, seven fibres; P = 0.13).

Fig. 6.2 shows the results from the most complete experiment in which the Cs_2SO_4 concentration was 0.025 mM. Both conditioning and test pulses hyperpolarized the fibre to -121 mV, and they were separated by an interval (i.e. pulse 2) in which the membrane was clamped at the holding potential (-70 mV), at -157 mV, or at -178 mV for between 10 ms and 11.5 s (Fig. 6.2, inset to graph).

Records of the membrane current are shown in the top part of Fig. 6.2. The duration of pulse 2 is given to the left of the records. When this is 10 ms, the current during pulse 2 is changing too rapidly to be recorded. When pulse 2 lasts 1.1 s or 11.5 s,

Fig. 6.2. Effect of membrane potential on the recovery from inactivation in 2.5 mM-K_2SO_4 plus 0.025 mM-Cs_2SO_4.

Top (A, B, & C), records of the membrane current (V_2-V_1) obtained using pulse sequences shown schematically below. Conditioning pulse is to -121 mV and lasts 235 ms. Test pulse is also to -121 mV. Pulse 2 is to -70 mV in A; -157 mV in B; and -178 mV in C: the duration of pulse 2 is given on the left; when this is 1.1 s and 11.5 s the oscilloscope is retriggered immediately before the start of the test pulse, which is indicated by an arrow.

Below, time course of recovery. Abscissa, duration of pulse 2 on a logarithmic scale (t); ordinate, % recovery by eqn. (6.1) of the text. 0% recovery indicates that the current at the start of the test pulse is equal to that at the end of the conditioning pulse. Pulse 2 is to -70 mV (●, curve A); -157 mV (○, curve B); -178 mV (◐, curve C).

Fibre resting potential, -70 mV; holding potential, -70 mV; inter-electrode distance, 440 µm; temp. 17.4°C.

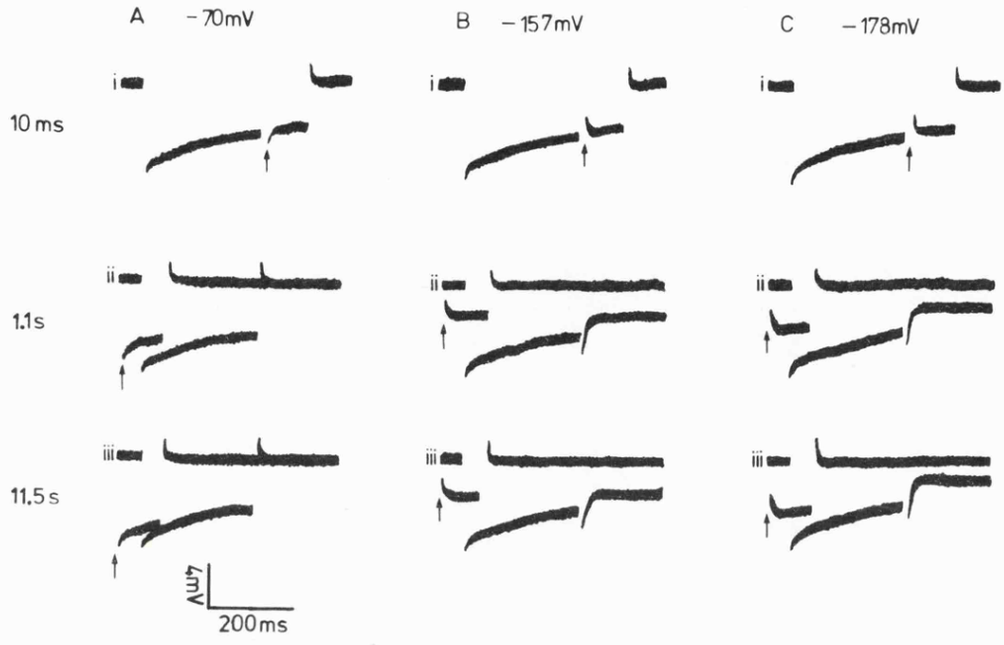
A −70mV
B −157mV
C −178mV
i
ii
iii
10 ms
1.1s
11.5 s
4mV
200ms

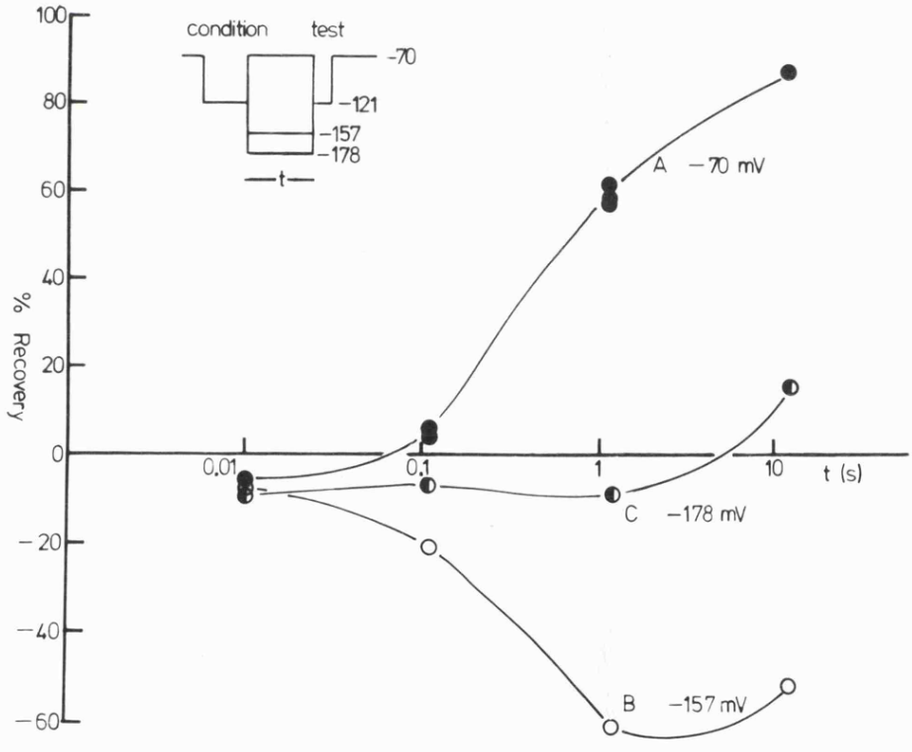
condition
test
-70
−121
−157
−178
t
A −70 mV
C −178 mV
B −157 mV
% Recovery
100
80
60
40
20
0
−20
−40
−60
0.01
0.1
1
10
t (s)

the oscilloscope was retriggered just before the start of the test pulse (which is indicated by the arrow). Because of this, the test pulse precedes the conditioning pulse by 50 ms. It can be seen that the current inactivates slowly during the conditioning pulse: the extent of this inactivation was highly reproducible when, as in these experiments, individual pulse sequences were separated by at least 25 s.

An analysis of these traces using eqn. (6.1) shows that when the fibre is held at -70 mV after the conditioning pulse has terminated, 85% of the current recovers in 10 s. (Fig. 6.2, curve A. (Note that in this figure the time scale on the abscissa is logarithmic.) Although little or no recovery was seen in the first 50 ms, a similar delay was observed in experiments in which caesium was absent. Curve A was obtained at the start of the experiment and points at 100 ms and 1.1s were repeated frequently during the experiment as a control for curves B and C. Such a control is important because prolonged hyperpolarizations to -178 mV, and to a lesser extent to -157 mV, can produce irreversible changes in the membrane conductance in some fibres. If these occurred the fibre was discarded.

If the membrane is clamped at -157 mV immediately following the conditioning hyperpolarization, the current at the start of the test pulse is depressed below the level reached by the end of the conditioning pulse (curve B; records B, i-iii). However, the depression is less severe if the membrane is held at -157 mV for 11.5 s than if the membrane is held at this potential for only 1.1 s. A similar result is obtained when the membrane is held at -178 mV (curve C, records C, i-iii).

The experiments of Fig. 6.1 indicated that there was a depletion of K^+ from the T-system during a hyperpolarization to -66 mV. Since depletion occurs more or less independently of the membrane potential, it should also occur during the conditioning hyperpolarization in Fig. 6.2, which is to -121 mV. There should also be at least a partial recovery from depletion when pulse 2 is to -178 mV or 157 mV since at these potentials the inward current is partially blocked by Cs^+. The increase in current at the start of the test pulse shown by curves B and C between 1.1 s and 11.5 s (Fig. 6.2) is consistent with a recovery from depletion during pulse 2 provided there is a second process occurring during pulse 2 which acts to reduce the inward current which is recorded during the test pulse.

This second mechanism is probably the potential- and time-dependent blockade of the resting K conductance by Na^+ described by Standen & Stanfield (1978c), which is also the fall in membrane permeability described by Almers (1972b). Almers has shown that the membrane permeability falls when the membrane potential is made more negative than -120 mV. In most of his experiments the K^+ concentration was 10 mM and the Na^+ concentration 70 mM, which is not very different from the concentrations employed in Fig. 6.2. Following a transition from -121 mV to -157 mV it takes at least 1 s for the K conductance to decline, as shown by Fig. 6.2, curve B. Although this is slower than the time course of the Na blockade (Standen & Stanfield, 1978c; Almers, 1972b), such a result is to be expected if the onset of the blockade occurs at the same time as recovery from depletion.

Fig. 6.2 also shows that the current at the start of the test pulse is usually greater if pulse 2 is to -178 mV rather than -157 mV, despite the fact that the Na blockade is reported to be stronger the more negative the membrane potential. However, the Cs blockade is also stronger at -178 mV than at -157 mV (Fig. 6.2, compare records Bii and iii with Cii and iii), so on this basis a more complete recovery from depletion is to be expected at -178 mV than at -157 mV.

DISCUSSION

The experiments reported here confirm that inactivation is dependent on the size of the inward current in 80 mM-K^+ solutions and to a lesser extent in 5 mM-K^+. This is consistent with the notion that inactivation is due, at least in part, to a fall in the concentration of K^+ in the lumen of the T-system (Adrian & Freygang, 1962a).

Previously, the most important experiments which argued in favour of the depletion hypothesis have been those described by Almers (1972a). In a solution containing 10 mM-K^+ and 70 mM-Na^+, he showed that at membrane potentials less negative than -120 mV recovery from inactivation was due to a single process which had a Q_{10} of 1.3. As Almers has pointed out, such a low temperature dependence indicates that the process is diffusion limited. This is to be expected from the depletion hypothesis since recovery from depletion will be largely dependent on the rate at which K^+ ions diffuse from the bulk external solution into the T-tubules. Almers (1972a) has also shown that the Q_{10} for the initial inward current (1.47 - 1.64) is similar, or equal, to that for the rate of inactivation (1.42 - 1.68). This result is explained if the size of the inward current through the tubular membrane controls the rate at which the tubular K^+ concentration decreases.

A fall in the tubular K^+ concentration will be accompanied by a negative shift in the equilibrium potential for K^+ in that region, although the equilibrium potential for K^+ at the surface membrane should be unchanged. On the grounds that they could detect little or no shift in the reversal potential for the resting currents following a hyperpolarization which inactivated the conductance, Adrian et al., (1970b) argued that depletion was not an important component of inactivation. On the other hand, Almers (1972a) has reasoned that once tubular depletion has occurred, owing to the rectifying property of the K conductance, the resistance of the surface membrane will be less than that of the tubular wall. Consequently, because the surface and the tubular membranes are in parallel, the reversal potential for the resting conductance will tend to follow the equilibrium potential for K^+ at the surface even when large changes in the equilibrium potential occur in the T-system. In support of this, Almers (1972a) has shown that the reversal potential is shifted by as little as -2 or -3 mV in conditions in which the tubular K^+ concentration may be falling from 10 mM to less than 5 mM. This view is also supported by Barry & Adrian (1973).

The present results also demonstrate the existence of a slow fall in membrane permeability at large negative membrane potentials in K solutions containing Na^+. This process is distinguished from depletion on the grounds that it is not reversed when the inward current during a large hyperpolarization is blocked by Cs^+. Previous experiments have demonstrated the presence of a time- and potential-dependent permeability change in hyperpolarized muscle (Adrian et al., 1970b; Almers, 1972b) and recent studies have indicated that this is due to a potential- and concentration-

dependent blockade by external Na^+ (Standen & Stanfield, 1978c). The properties of this permeability change are discussed in more detail in chapter 7.

Chapter 7. Effect of thallous ions on the electrophysiological properties of resting skeletal muscle fibres.

INTRODUCTION

A different approach to the question of inactivation is considered in the last part of this chapter which deals with the properties of the resting membrane in thallous solutions. The ionic radius of Tl^+ (1.44 Å) is between that of K^+ (1.33 Å), which is permeant, and Rb^+ (1.48 Å), which is largely impermeant in resting fibres (Adrian, 1964; see also chapter 5, Fig. 5.3B). Accordingly, Mullins & Moore (1960) found that Tl^+ behaved more like K^+ than Rb^+ in resting muscle, and concluded that the membrane was unable to distinguish between K^+ and Tl^+ provided the Tl^+ concentration was less than 25 mM.

The present work confirms that Tl^+ carries current across the resting membrane, but in thallous solutions containing no K^+ the voltage- and time-dependent permeability change which is in part responsible for the inactivation of inward current in K solutions (Almers, 1972b) does not occur.

Recent studies in squid axons (Landowne, 1975) and in starfish egg cells (Hagiwara, Miyazaki, Krasne & Ciani, 1977) also show that Tl^+ cannot replace K^+ in a simple way.

SOLUTIONS AND METHODS

The basic composition of solutions used here is given in Table 7.1. All solutions are isotonic and contain sulphate as an impermeant anion to replace chloride. All solutions except those of Fig. 7.1A were buffered with 5 mM-HEPES (Good et al., 1966) and the pH adjusted to 7.2 with about 2.3 mM-NaOH; this amount of Na^+ is not included in Table 7.1 but is included in using the

equations given in the text. Phosphate buffer is unsuitable due to the formation of thallium-phosphate complexes (Lee, 1971). Solutions containing a range of K^+ and Tl^+ concentrations were prepared by mixing solutions 7A and 7B or 7A and 7C. For most experiments a solution containing 2.5 mM-K_2SO_4 or Tl_2SO_4 was used. Muscles were dissected in a chloride Ringer buffered with a 1 mM-HEPES and equilibrated for at least 1 hour in a sulphate solution containing 1.25 mM-K_2SO_4 and buffered with 5 mM-HEPES.

Constant voltage polarization was obtained with the three-electrode method (chapter 2). Fibres were held at the resting potential and hyperpolarized in a step-wise fashion. With the exception of Fig. 7.1A, electrodes filled with 2 M K_3-citrate were used for passing current and recording the membrane potential. Electrodes filled with 3 M-KCl cannot be used in thallous solutions because TlCl precipitates in the tip (see chapter 2 for details).

All experiments were carried out at room temperature (17 - 22°C).

Table 7.1

Composition of solutions in mM

	Na^+	K^+	Tl^+	Ca^{2+}	SO_4^{2-}	HEPES	Sucrose
Solution 7A	80	-	-	8	48	5	113
Solution 7B	-	80	-	8	48	5	113
Solution 7C	-	-	80	8	48	5	113

RESULTS

While the main part of this chapter is concerned with a comparison of the properties of the resting membrane in K^+ and

Tl^+ solutions, the first experiments to be described investigate the methods used. In particular, it is interesting to see if the properties of resting fibres differ in phosphate and HEPES-buffered solutions, and if the use of citrate rather than KCl-filled electrodes can influence the results obtained.

Resting membrane potentials in phosphate and HEPES-buffered solutions

One method of seeing if HEPES has an effect on the resting membrane is to plot the mean resting potentials as a function of $\log_{10} [K]_o$ for solutions buffered with phosphate (Fig. 7.1A) or HEPES (Fig. 7.1B).

In each case the external K^+ concentration was changed by substitution of Na_2SO_4 for K_2SO_4. In HEPES-buffered solutions, each point is the mean resting potential of at least 10 fibres (four muscles), and each muscle was exposed to a maximum of five different solutions in order of increasing K^+ concentration. In phosphate-buffered K^+ solutions (Fig. 7.1A), the results are taken from a large number of experiments during an 8-month period; each point is the mean resting potential of between 7 and 73 fibres, and each muscle was exposed to only one or two different K^+ concentrations.

The dashed lines in Fig. 7.1A & B were drawn from the Nerst eqn. for K^+;

$$RP = \frac{RT}{F} \times 2.303 \log_{10} \frac{[K]_o}{[K]_i} \qquad (7.1)$$

where RP is the resting potential, $[K]_i$ is taken as 140 mM, and 2.303 RT/F is about 58 mV at 20°C.

For a 10-fold change in the external K^+ concentration in the range 5 mM to 80 mM, the least-squares line for the

relationship between the resting potential and $\log_{10}[K]_o$ gives a 53.33 mV change in the resting potential in the HEPES-buffered solution compared with 50.70 mV in phosphate Ringer. Since both values are less than the theoretical slope of 58 mV, Na^+ is probably also slightly permeant. Using the eqn. (Hodgkin & Katz, 1949)

$$RP = \frac{RT}{F} \times 2.303 \log_{10} \frac{[K]_o + \frac{P_{Na}}{P_K}[Na]_o}{[K]_i + \frac{P_{Na}}{P_K}[Na]_i} \qquad (7.2)$$

a satisfactory fit is obtained to the points in phosphate-buffered Ringer (Fig. 7.1A) with $P_{Na}/P_K = 0.02$ and $[K]_i + \frac{P_{Na}}{P_K}[Na]_i = 140$ mM. The last value is the intercept on the abscissa at zero membrane potential, and since $\frac{P_{Na}}{P_K}[Na]_i$ is less than 1 mM, it is a good approximation of the internal K^+ concentration, assuming that internal and external K^+ activities are equal.

In HEPES-buffered K solution (Fig. 7.1B) the solid lines were drawn with $[K]_i + \frac{P_{Na}}{P_K}[Na]_i = 106.4$ mM (since this was the intercept of the least-squares line) and with $P_{Na}/P_K = 0.01$ and 0.02. It seems that HEPES has little or no effect on the selectivity of the resting membrane but may reduce the internal potassium concentration; this is feasible as fibres had been in HEPES for at least two hours before measurements were made. However, this result will not affect the main conclusions of this chapter since HEPES-buffered K solutions are used as a control for all experiments in thallous.

The possibility was also considered that the use of citrate electrodes to record membrane potentials in HEPES-buffered solutions might account for the low resting potentials of Fig. 7.1B compared with those of Fig. 7.1A, which were recorded

Fig. 7.1 Effect of external K^+ or Tl^+ concentration on the resting membrane potential.

A. Fibres in K-sulphate solutions buffered with phosphate. Each point is the mean resting potential from between 7 and 73 fibres measured in muscles over an 8-month period. Each point is greater than 2 S.E.M. The solid line is drawn to eqn. (7.2) with $P_{Na}/P_K = 0.02$ and $[K]_i + \frac{P_{Na}}{P_K}[Na]_i = 140$ mM. The dashed line is the Nerst slope for K^+ (eqn. 7.1). KCl-filled recording electrodes used.

B. Fibres in K-sulphate solutions buffered with HEPES. Each point is the mean resting potential from at least 10 fibres (4 muscles) and includes 2 S.E.M. The solid lines are drawn to eqn. (7.2) with $P_{Na}/P_K = 0.01$ and 0.02, and $[K]_i + \frac{P_{Na}}{P_K}[Na]_i = 106.4$ mM. The dashed line is the Nerst slope for K^+ (eqn. 7.1). Citrate recording electrodes used.

C. Fibres in Tl-sulphate solutions buffered with HEPES. Each point is the mean resting potential from at least 10 fibres (4 muscles); vertical bars are 2 S.E.M. The solid line is drawn to eqn. (7.3) with $P_{Na}/P_{Tl} = 0.02$ and $[Tl]_i + \frac{P_{Na}}{P_{Tl}}[Na]_i + \frac{P_K}{P_{Tl}}[K]_i = 93.2$ mM. The dashed line is the Nerst slope for K^+ (eqn. 7.1) and is equal to $RP = RT/F \times 2.303 \log_{10}\{[Tl]_o P_{Tl}/[K]_i P_K\}$. Citrate recording electrodes used.

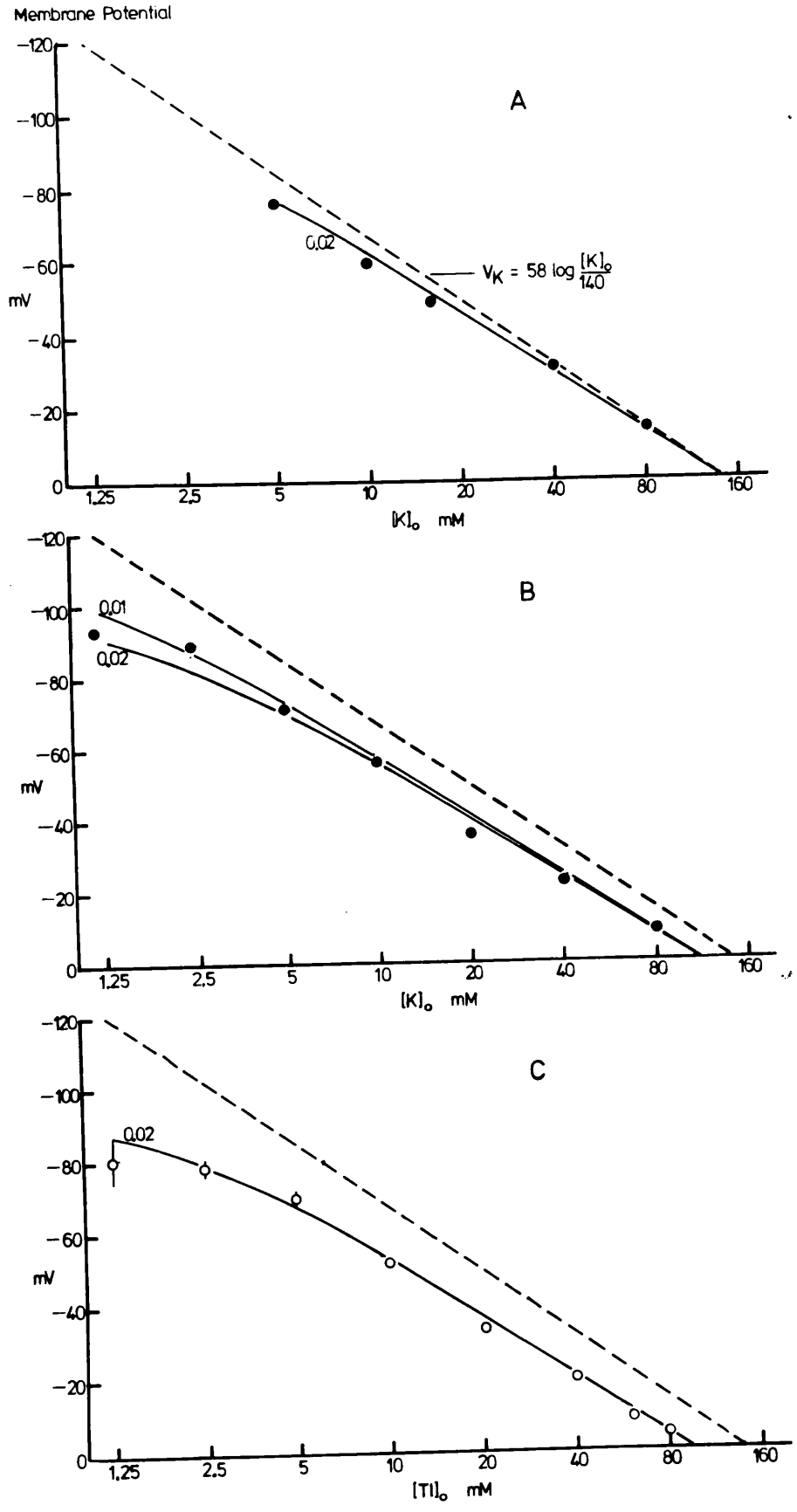
Membrane Potential
A
0.02
$V_K = 58 \log \frac{[K]_o}{140}$
mV
$[K]_o$ mM
B
0.01
0.02
mV
$[K]_o$ mM
C
0.02
mV
$[Tl]_o$ mM
−120
−100
−80
−60
−40
−20
0
1.25
2.5
5
10
20
40
80
160

with KCl-filled electrodes. To test this, both types of microelectrode were used to record the resting potentials of fibres immersed in a HEPES-buffered solution containing 1.25 mM-K_2SO_4. Using citrate electrodes the mean resting potential of eight fibres was -71.0 ± 0.85 mV, which is not significantly different from the mean value of -72.13 ± 0.99 mV (eight fibres) recorded with KCl electrodes ($P>0.3$). The difference between these values can account for less than 20% of the difference between resting potentials in phosphate and HEPES-buffered solutions.

Resting potentials in solutions containing K^+ or Tl^+

In thallous Ringer, the slope of the least-squares line for the relationship between the resting potential and $\log_{10}[Tl]_o$ was a 53.14 mV change in the resting potential for a 10-fold change in $[Tl]_o$ between 5 mM and 80 mM, and is close to the value of 53.33 mV for the HEPES-buffered K^+ solution. The line through the points in Fig. 7.1C was drawn according to the equation

$$RP = \frac{RT}{F} \times 2.303 \log_{10} \frac{[Tl]_o + \frac{P_{Na}}{P_{Tl}}[Na]_o + \frac{P_K}{P_{Tl}}[K]_o}{[Tl]_i + \frac{P_{Na}}{P_{Tl}}[Na]_i + \frac{P_K}{P_{Tl}}[K]_i} \qquad (7.3)$$

where $\frac{P_{Na}}{P_{Tl}}$ is 0.02 and $[Tl]_i + \frac{P_{Na}}{P_{Tl}}[Na]_i + \frac{P_K}{P_{Tl}}[K]_i$ is 93.2 mM. since this is the intercept of the least squares line at zero membrane potential.

During short exposures to Tl^+, particularly when the external Tl^+ concentration is low, any Tl^+ which accumulates in the sarcoplasm can probably be ignored (see page 154). Since $[K]_o$ is zero and $\frac{P_{Na}}{P_{Tl}}[Na]_i$ is much less than 1 mM, P_K/P_{Tl}

is 0.88 from eqn. (7.3). This value is calculated on the assumption that in HEPES-buffered Ringer $[K]_i$ is 106.4 mM.

Anomolous permeability ratios in K^+ - Tl^+ mixtures

If the permeability ratio P_K/P_{Tl} were independent of the relative concentrations of K^+ and Tl^+ in the Ringer, resting potentials of fibres in a solution in which the mole fractions of K_2SO_4 and Tl_2SO_4 were each 0.5 should be midway between the resting potentials obtained when the mole fraction of either salt was 1, and the total concentration (K_2SO_4 + Tl_2SO_4) was unaltered. The mean resting potential in a mixture of 20 mM-Tl^+ and 20 mM-K^+ was -23.29 $\pm$ 0.65 mV (seventeen fibres); this is more negative than the values in either 40 mM-Tl^+ or 40 mM-K^+, which were -19.95 $\pm$ 1.21 mV (twenty fibres) and -21.93 $\pm$ 0.45 mV (thirty-four fibres), respectively. In the previous section P_K/P_{Tl} was found to be 0.88. Using the same assumptions as made there, eqn. (7.3) gives a value of 1.07 for P_K/P_{Tl} in the mixture.

Effect of prolonged exposure to 2.5 mM-Tl_2SO_4

It is well known that thallium is toxic. In muscle, the depolarization produced by treatment with 25 mM-$TlNO_3$ for one hour is only partly reversed by removal of this salt, although good recovery is obtained if the period of exposure is short (Mullins & Moore, 1960). These authors also report that fibres do not recover completely from the contracture produced by immersion in 100 mM-$TlNO_3$. In view of this, exposure to high concentrations of Tl^+ was limited to 15 mins. in the present experiments.

The effects of prolonged treatment with 2.5 mM-Tl_2SO_4 have been investigated since this Tl^+ concentration was used for

voltage-clamp studies. After a minimum of 2 hours exposure to 2.5mM-Tl_2SO_4, the mean resting potential in eight fibres was -67.63 ± 1.69 mV (four muscles). This is not significantly different from the mean resting potential after less than 15 mins in 2.5 mM-Tl_2SO_4, which was -69.09 ± 1.49 mV (eleven fibres, four muscles; $P>0.3$). Fibres also showed no visible signs of deterioration after long periods of exposure to 2.5 mM-Tl_2SO_4 or brief exposure to 40 mM-Tl_2SO_4.

Inactivation of the inward current in fibres hyperpolarized in K^+ and Tl^+ solutions

Fig. 7.2A,B shows records of the membrane potential (V_1) and membrane current ($V_2 - V_1$) from two fibres hyperpolarized from the resting potential in voltage-clamp conditions. Fibre B is in 2.5 mM-Tl_2SO_4 and 37.5 mM-Na_2SO_4. In this solution the steady-state current increases as larger hyperpolarizations are applied. However, in a solution containing 2.5 mM-K_2SO_4 and 37.5 mM-Na_2SO_4 (Fig. 7.2A) the steady-state currents are smaller during large hyperpolarizations. Since P_{Na}/P_K and P_{Na}/P_{Tl} are both about 0.02, the inward current is carried largely by K^+ in A and Tl^+ in B.

Different properties of the resting K and Tl conductances are also seen in Fig. 7.2C,D, which shows the mean instantaneous (circles) and steady-state (squares) current-voltage relations from six fibres in K^+ solution (C) and seven fibres in Tl^+ (D). The mean resting potentials were -70.00 ± 0.26 mV in K^+ and -67.29 ± 1.32 mV in Tl^+, in agreement with the results of Fig. 7.1B & C. The view expressed by Adrian & Freygang (1962a) is that the decline in inward current which occurs when fibres are hyperpolarized in K^+ solutions is due to

Fig. 7.2. Membrane currents in fibres hyperpolarized in K and Tl solutions.

A & B. Voltage-clamp records of the membrane potential (V_1) and membrane current (V_2-V_1). Fibre A is in 2.5 mM-K_2SO_4: resting potential, -70 mV; holding potential, -70 mV; inter-electrode distance, 440 μm; temp, 17.4°C. Fibre B from the same muscle is in 2.5 mM-Tl_2SO_4: resting potential, -60 mV; holding potential, -60 mV; inter-electrode distance 440 μm; temp, 17.4°C.

C & D. Mean instantaneous (●) and steady-state (■) current-voltage relations from six fibres in 2.5 mM-K_2SO_4 and seven fibres in 2.5 mM-Tl_2SO_4. Abscissae; membrane potential; ordinates, membrane current in μA/cm^2. Vertical bars are 2 S.E.M. where these are larger than the symbol.

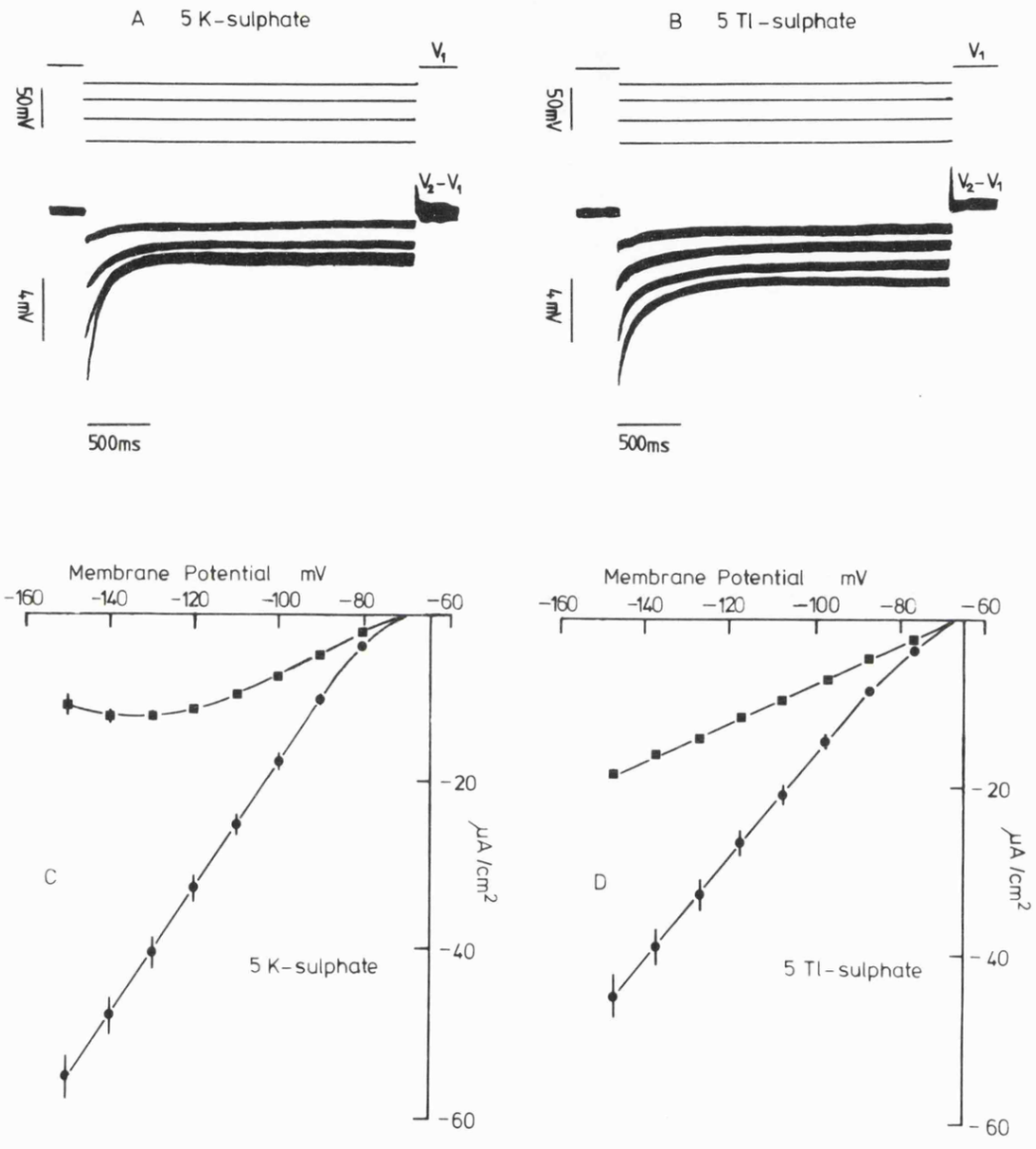
A 5 K-sulphate
B 5 Tl-sulphate
V1
50mV
V2-V1
4mV
500ms
Membrane Potential mV
-160 -140 -120 -100 -80 -60
-20
-40
-60
μA/cm2
C
5 K-sulphate
D
5 Tl-sulphate

a fall in the concentration of K^+ in the T-system. However, the negative slope in the steady-state current-voltage relation seen at membrane potentials negative to -135 mV in C cannot be explained in this manner (Adrian et al.,1970b) but is consistent with the view that there is a time- and voltage-dependent fall in the permeability of the membrane to K^+ (Almers 1972b). In thallium (Fig. 7.2D), the steady-state current-voltage relation is approximately linear between -67 mV and -150 mV indicating that the permeability change is abolished or is shifted by at least -30 mV.

Two-pulse experiments to examine the mechanism of inactivation

This last possibility was tested using a two pulse procedure similar to that described by Almers (1972a). When, as in Fig. 7.3 Ai, a fibre is hyperpolarized to -128 mV in 5 mM-K^+, the current declines exponentially. However, when this pulse is preceded by a 10 ms prepulse to -284 mV (Fig. 7.3 Aii) the current at -128 mV increases before declining. During the prepulse the membrane potential is sufficiently negative for the permeability to fall, and it is the recovery of this process at -128 mV which produces the initial increase in current (Almers 1972a). Depletion can account for the subsequent decline.

In thallous Ringer (Fig. 7.3B), the decline in current which occurs at -130 mV after a 10 ms prepulse to -257 mV (Bii) is virtually identical to that which occurs in the absence of the prepulse (Bi). Minor differences between the currents with and without the prepulse during the first 40 milliseconds at -130 mV are consistent with the fact that after the prepulse there is a large, outwardly-directed capacity transient

Fig. 7.3. Effect of a large hyperpolarizing prepulse on inactivation in K and Tl solutions. Records of the membrane potential (V_1) and membrane current (V_2-V_1) are shown in two fibres.

Fibre A is in 2.5 mM-K_2SO_4.
In Ai the hyperpolarization is to -128 mV; in Aii the hyperpolarization is also to -128 mV and is preceded by a 10 ms prepulse to -234 mV. Resting potential, -69 mV; holding potential, -69 mV; inter-electrode distance, 440 μm; temp, 17.3°C.

Fibre B is in 2.5 mM-Tl_2SO_4.
In Bi the hyperpolarization is to -130 mV; in Bii the hyperpolarization is also to -130 mV and is preceded by a 10 ms prepulse to -257 mV. Resting potential, -67 mV; holding potential, -67 mV; inter-electrode distance, 440 μm; temp, 17.4°C.

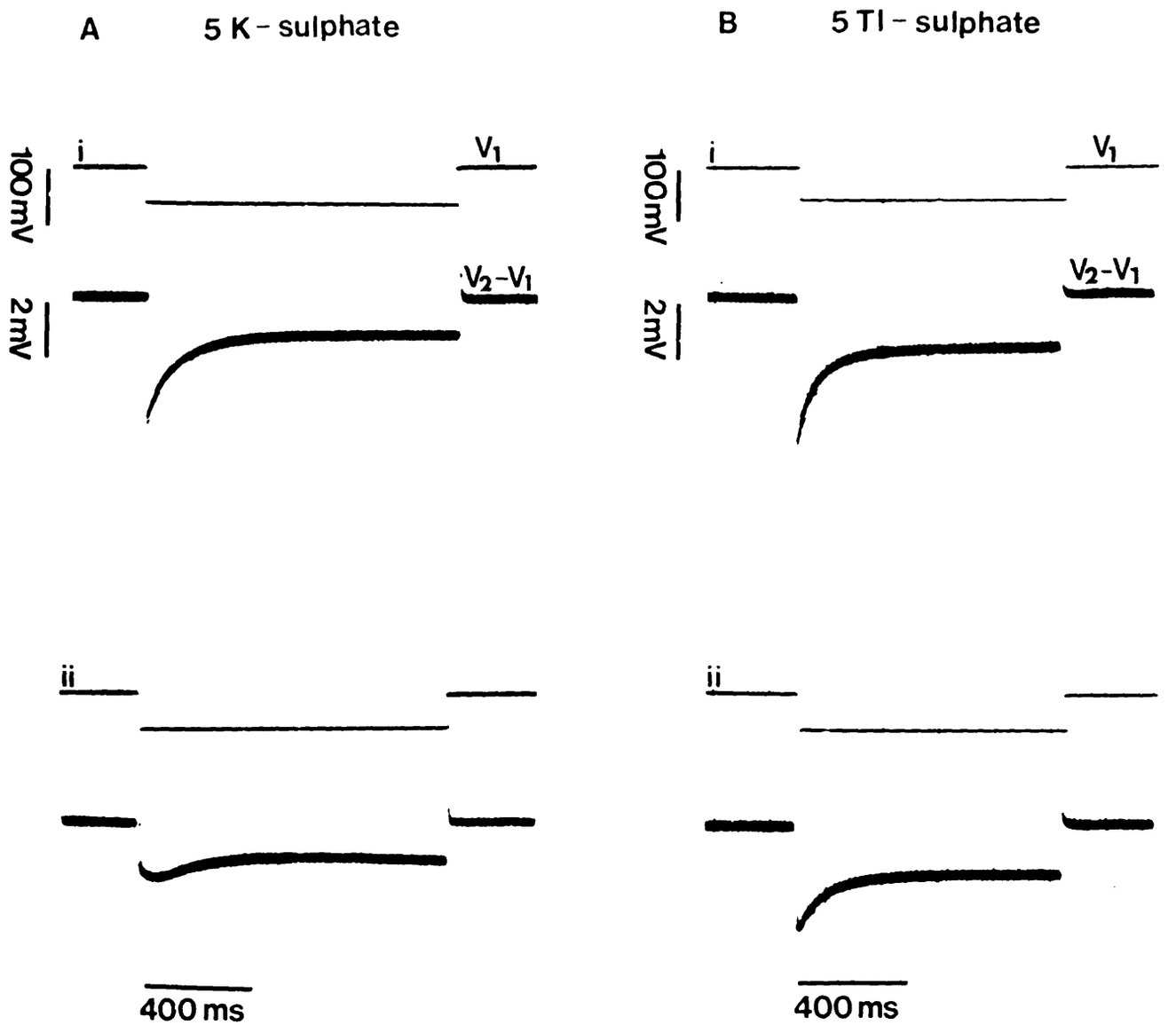
A
5 K – sulphate
B
5 Tl – sulphate
i
V_1
100mV
V_2-V_1
2mV
ii
400 ms

superimposed on the inward current, whereas in the absence of the prepulse the transient is inward. These experiments show that the permeability of the resting membrane does not fall with time even at membrane potentials as negative as -257 mV when thallium replaces potassium in the Ringer.

Time course of inactivation

Inactivation of the K-conductance is described by a single exponential which is voltage-dependent (Adrian et al., 1970b; Stanfield, 1970b) but which nevertheless can be resolved into two components; that due to depletion and that due to the fall in membrane permeability (Almers, 1972a,b).

In Fig. 7.4A & B, the declining current is plotted semilogarithmically after subtraction of the steady-state current such that the current 25 ms after the start of the hyperpolarization is 100% and the steady-state current is 0%. Here too, the currents in K^+ decline exponentially and the time constant for the decline ($\tau_{d,K}$) decreases as the membrane potential is made more negative (Fig. 7.4A). In six fibres $\tau_{d,K}$ was 192.7 $\pm$ 7.9 ms between -111 mV and -113 mV, and 148.1 $\pm$ 7.3 ms between -142 mV and -145 mV.

In thallous solution (Fig. 7.4B) inactivation follows a more complex time course. From 25 ms to 100 ms the decline is approximately exponential. The mean time constant ($\tau_{d,Tl}$) in six fibres was 201.2 $\pm$ 25.5 ms between -107 mV and -112 mV compared with 140 $\pm$ 13.4 ms between -141 mV and -146 mV. Thereafter the current drifts more slowly towards the steady-state value: this is seen clearly by comparing the currents in Tl solution (Fig. 7.2B) with those in K solution (Fig. 7.2A).

Although the currents decline at a similar rate in Tl and K solutions during the first 100 ms, this may not be important.

Fig. 7.4. Time course of inactivation. Abscissae, time from the start of the hyperpolarization (t); ordinates, membrane current plotted such that the current at 25 ms is 100% and the steady-state current is 0%.

Fibre A is in 2.5 mM-K_2SO_4 and is the same as Fig. 7.2A. The time constant for the declining current (τ_{dK}) is 276 ms at -102 mV; 207 ms at -113 mV; 166 ms at -125 mV and 150 ms at -146 mV.

Fibre B is in 2.5 mM-Tl_2SO_4 and is the same as Fig. 7.2B.

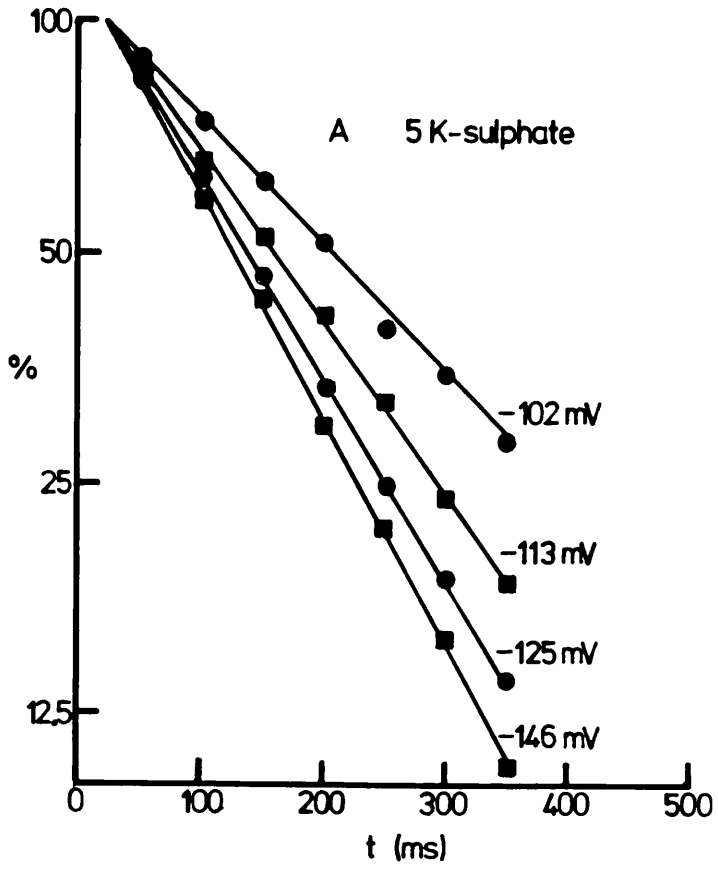
100
50
%
25
12,5
A 5 K-sulphate
-102 mV
-113 mV
-125 mV
-146 mV
0
100
200
300
400
500
t (ms)

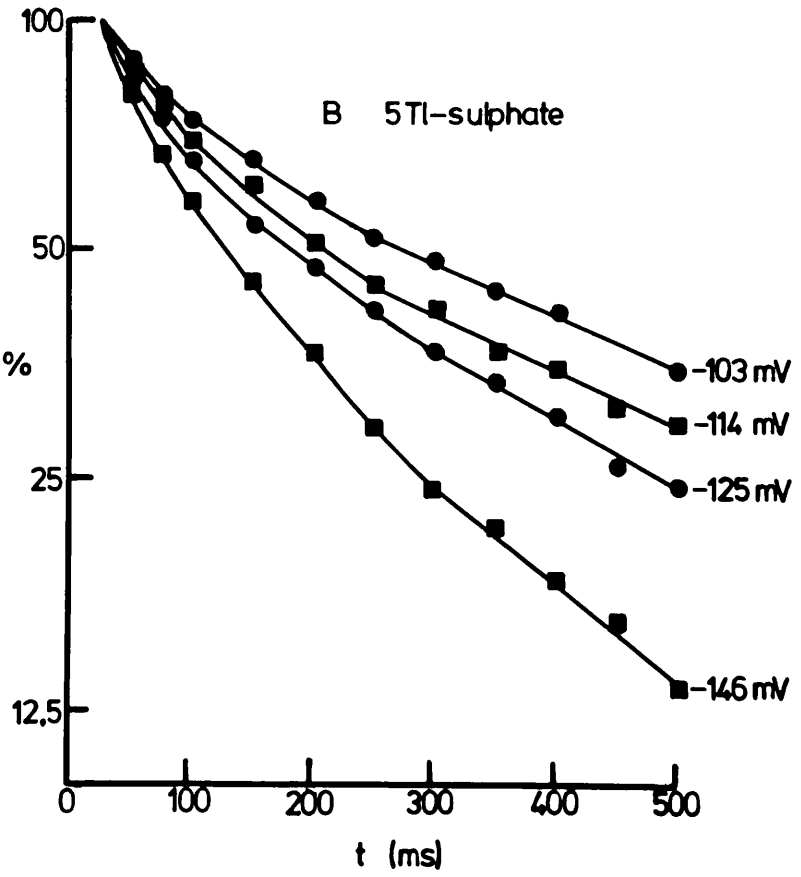
100
50
%
25
12,5
B 5 Tl-sulphate
-103 mV
-114 mV
-125 mV
-146 mV
0
100
200
300
400
500
t (ms)

The range of time constants is greater in Tl than in K solutions, and in one fibre in Tl^+, $\tau_{d,Tl}$ was the independent of the membrane potential: in this fibre $\tau_{d,Tl}$ was 169 ms at -143 mV and also at -112 mV. Such behaviour in Tl solutions is not inconsistent with the notion that the decline is due solely to a depletion of thallous ions from the T-system. Since the limiting ion conductances of Tl^+ and K^+ are similar (74.7 and 73.5 mho.cm^2/mole ion, respectively, at 25°C; Robinson & Stokes, 1965), it is likely that in the absence of a permeability change the K current would follow a similar time course.

Size of depleted space

Adrian et al. (1970b) show that if the decline in membrane current is due to a depletion of K^+ ions from the lumen of the T-system, the quantity of charge (Q) moved from the lumen of the T-system to the sarcoplasm can be related to the concentration of K^+ in the tubules at the start of the hyperpolarization $[K]_{TO}$ by the expression,

$$Q < \rho F [K]_{TO} \qquad (7.4)$$

where ρ is the relative fibre volume occupied by the T-system, F is 96500 coulomb/mole, and $[K]_{TO}$ is equal to $[K]_o$, which is 5 μmoles/cm^3. For the limiting case in which the tubular K^+ concentration falls to zero, eqn. (7.4) becomes,

$$Q \doteqdot \rho F [K]_{TO} \qquad (7.5)$$

Similarly, for thallous solutions,

$$Q \doteqdot \rho F [Tl]_{TO} \qquad (7.6)$$

Eqns. (7.5 & 7.6) have been used to estimate the relative fibre volume occupied by the T-system in K and Tl solutions. Q was obtained from records of the declining current, such as those

in Fig. 7.2A & B, and is given by

$$Q = \int_{t=\infty}^{t=0} [j_{m0} - j_m] \quad dt \qquad (7.7)$$

where j_{m0} and $j_{m\infty}$ are the values of membrane current per unit fibre volume at the beginning of the hyperpolarization and in the steady-state. The relationship between j_m and V_2-V_1 is

$$j_m = \frac{2\,(V_2-V_1)}{3\,\ell^2\,R_i} \quad A/cm^3 \qquad (7.8)$$

Table 7.2 gives values for ρ in K and Tl solutions. In 2.5 mM-Tl_2SO_4, ρ is virtually independent of the membrane potential when fibres are hyperpolarized to between -100 mV and -150 mV. The mean value is about 0.5% in three of the four fibres studied. A different result is obtained in 2.5 mM-K_2SO_4, but this is to be expected if a permeability change also contributes to the decline. Here, ρ is less than 0.3% at -100 mV increasing to 0.7% at -150 mV. Previous results in 2.5 mM-KCl (Stanfield, 1970b; 0.25% at -137 mV, 0.29% at -146 mV) and 2.5 mM-K_2SO_4 (Adrian et al., 1970b; 0.20% at -147 mV) are of the same order as those found here.

The similarity between the present estimate for ρ in thallous solution and that of Almers (1972b; maximum of 0.8%) in 5 mM-K_2SO_4 after a correction for the permeability change had been made supports the idea that a depletion of thallous ions from the T-system is responsible for the decline in inward thallium current. A lower value (0.3%) was reported by Peachey (1965) using the electron microscope, but better agreement is obtained if, as Peachey & Schild (1968) suggest, this value is under-estimated by 30%.

TABLE 7.2

Volume of Fibre occupied by the T-system (ρ)

Fibre	Solution (mM)	RP (mV)	Approximate Membrane Potential (mV) -100	-110	-120	-130	-140	-150	Mean ± S.E.M.
1	$5Tl^+$	-71	-	-	-	0.50 (-133)	0.60 (-144)	0.47 (-154) * ‡	0.52 ± 0.04
2	$5Tl^+$	-69	-	-	-	0.48 (-132)	0.57 (-142)	0.49 (-152)	0.48 ± 0.03
3	$5Tl^+$	-60	0.62 (-103)	0.69 (-113)	0.74 (-125)	0.79 (-136)	0.71 (-147)	-	0.71 ± 0.03
4	$5Tl^+$	-67	0.46 (-107)	0.47 (-117)	0.49 (-127)	0.62 (-137)	-	-	0.51 ± 0.04
5	$5K^+$	-70	0.23 (-100)	0.36 (-110)	0.44 (-120)	0.52 (-130)	0.60 (-140)	0.71 (-150)	0.49 ± 0.07
6	$5K^+$	-71	-	-	-	0.49 (-132)	0.55 (-143)	0.68 (-153)	0.56 ± 0.07
7	$5K^+$	-70	0.28 (-103)	0.27 (-113)	0.28 (-123)	0.39 (-135)	0.45 (-145)	-	0.33 ± 0.04

ρ* is expressed as a percentage and is given for seven fibres at membrane potentials between -100 mV and -150 mV. The membrane potential‡ is in parenthesis and is below the value for ρ. The mean value for ρ in each fibre is in the last column. RP = resting membrane potential.

Location of the thallous permeability mechanism

The fraction of sites (probably channels) permeable to thallous ions and which are located in the surface membrane can be estimated from the ratio of the steady-state membrane current to the initial membrane current during a hyperpolarization which produces maximal depletion. From the mean current-voltage relationship for seven fibres in 2.5 mM-Tl_2SO_4 solution (Fig. 7.2D) this ratio was 42.2% at -150 mV, so that at least 58% of the thallous conductance must reside in the walls of the transverse tubules.

In K solution (Fig. 7.2C) at -150 mV, as much as 80% of the membrane current inactivates; however, a large part of the inactivating component is itself due to a fall in the permeability of the membrane to K^+, rather than to K^+ depletion. Having corrected for the permeability change, Almers (1972b) has estimated that at least 60% of the resting K conductance is in the T-system, in good agreement with the present results for thallous.

Voltage-dependent blockade of inward thallous currents by caesium

Since the mechanism which underlies the fall in membrane permeability seen in K solutions during hyperpolarization is dependent on the presence of Na^+ in the Ringer (Standen & Stanfield, 1978c), it is interesting to see if Cs^+ ions, like Na^+, are unable to depress inward thallous currents.

Fig. 7.5A shows voltage-clamp records from a fibre hyperpolarized in 2.5 mM-Tl_2SO_4 to which 0.025 mM-Cs_2SO_4 is added. In B the instantaneous (•) and steady-state (o) current-voltage relations from this fibre are shown. It is clear that Cs^+ blocks inward thallous currents in a voltage-dependent manner. The maximum

Fig. 7.5. Voltage-dependent blockade of inward thallous currents by caesium.

A. Voltage-clamp records of the membrane potential (V_1) and membrane current (V_2-V_1) from a fibre immersed in 2.5 mM-Tl_2SO_4 and 0.025 mM-Cs_2SO_4.

B. Instantaneous (●) and steady-state (o) current-voltage relations from the fibre illustrated in A. Resting potential, -66 mV; holding potential, -66 mV; inter-electrode distance, 440 μm; temp, 21.4°C.

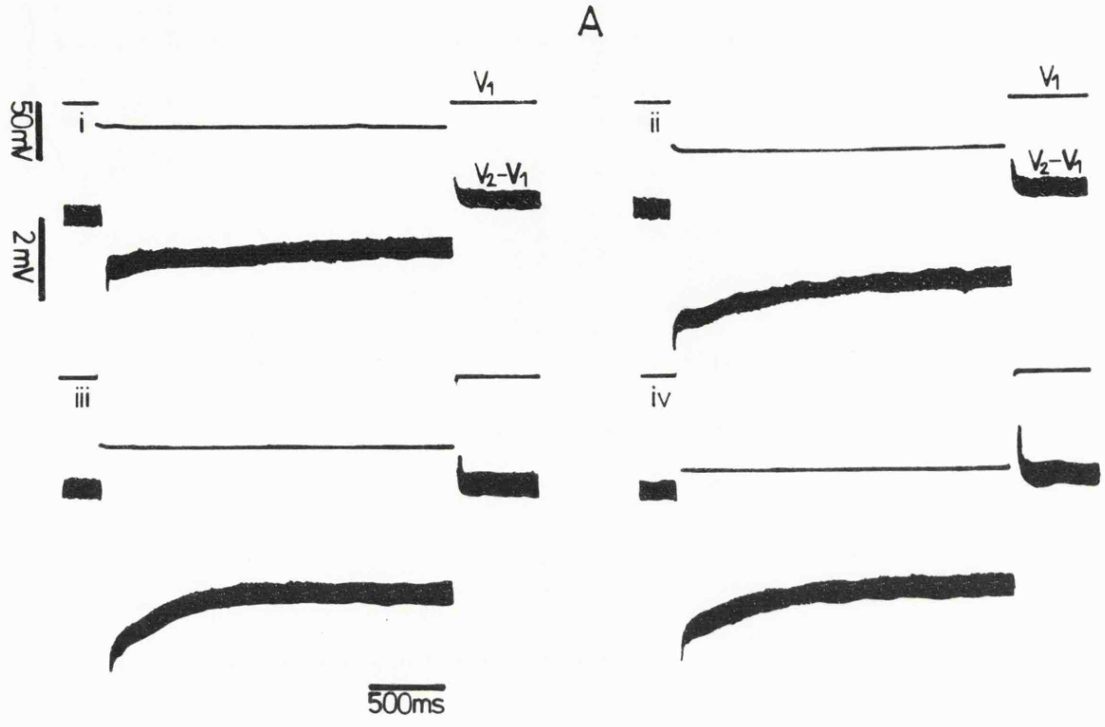
A
V1
i
V2-V1
50mV
2mV
ii
iii
iv
500ms

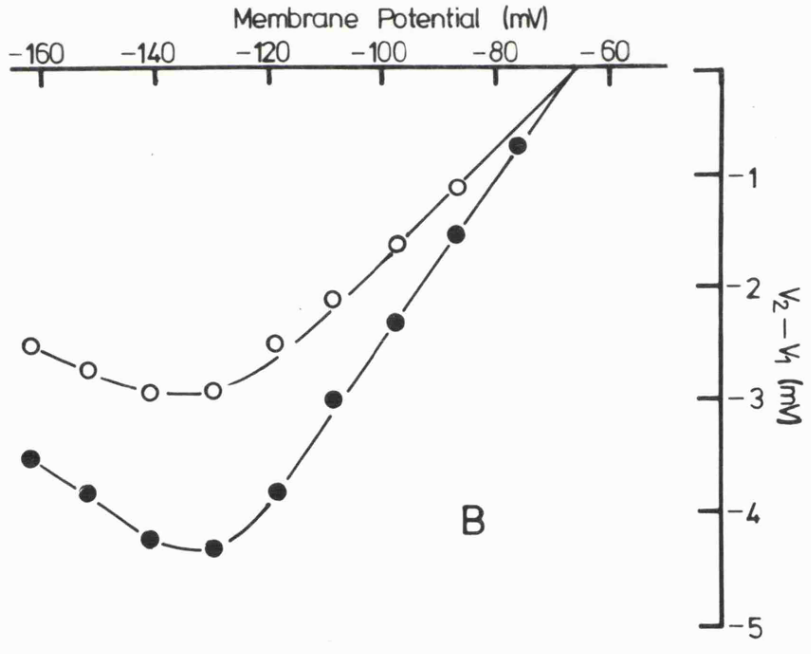
Membrane Potential (mV)
-160
-140
-120
-100
-80
-60
-1
-2
-3
-4
-5
V2 – V1 (mV)
B

inward current in this fibre occurs at -130 mV and corresponds to 16.5 $\mu A/cm^2$. In a second fibre from the same muscle a maximum inward current of 12.9 $\mu A/cm^2$ was obtained when the solution contained 0.075 mM-Cs_2SO_4. These results can be compared with the mean instantaneous and steady-state current-voltage relations from seven fibres in a solution containing 2.5 mM-Tl_2SO_4 but no caesium, which are shown in Fig. 7.2D.

DISCUSSION

The most important new finding described in this chapter is that the voltage- and time-dependent permeability change which contributes to inactivation of the inward K currents under conditions of extreme hyperpolarization (Almers, 1972b) does not occur over the range of voltages studied (-67 to -257 mV) when external K^+ is replaced by Tl^+. Thus it is probable that a depletion of thallous ions from the lumen of the T-system is wholly responsible for the inactivation which is seen in thallous solutions.

The evidence presented by Standen & Stanfield (1978c) that the fall in the permeability of the membrane to K^+ is due to a time-dependent blockade of the resting K channel by sodium ions is that when the sodium normally present in 5 mM-K_2SO_4 solutions is replaced by tetramethylammonium ions or tris, the negative slope in the steady-state current-voltage relationship is removed. In addition, reducing the external sodium concentration shifts the negative slope to more positive membrane potentials, and increasing external sodium has the opposite effect. Similar behaviour is shown by Cs^+ (Gay & Stanfield, 1977) and Ba^{2+} (Standen & Stanfield, 1978a, b), which block the movement of K^+ across the membrane of resting fibres

in a voltage- and concentration-dependent manner, probably by binding to a site (or sites) partway across the membrane (see chapter 5, discussion).

Independent evidence that the Na blockade involves binding is that the Q_{10} for the decline in K current under conditions in which depletion is slight is 2.8 (Almers, 1972b). Such a high temperature dependence cannot be explained by assuming that the mobility of Na^+ in some part of the channel is simply so low that the passage of K^+ ions is impeded. A Q_{10} of 3.15 is reported for the onset of the blockade by Ba^{2+} (Standen & Stanfield, 1978a, b), and is also consistent with binding.

Almers (1972b) showed that the permeability change contributed to inactivation only at membrane potentials more negative than -120 mV. However, this result is to be expected since his experiments were performed with a fixed Na^+ concentration.

An important question which the present experiments raise is how thallous ions interact with the membrane such that the blockade of inward currents by Na^+ is prevented. The simplest explanation is that K^+ and Tl^+ cross the membrane using separate pathways: in keeping with the discussion of chapter 5, these are considered to be channels although other permeability mechanisms are possible. The K channel which contains the Na^+ binding site should exclude thallous ions whilst the Tl channel, which is not blocked by Na^+, is permeable to Tl^+ and may also be permeable to K^+. Such selectivity is possible since the ionic radius of Tl^+ (1.44Å) is slightly greater than that of K^+ (1.33Å). Similarly Rb^+, which is slightly bigger than Tl^+, could be largely excluded from both channels in keeping with the low permeability of the resting membrane to this ion (Adrian, 1964).

On the other hand, a number of observations favour the view that only one type of channel is involved. First, the instantaneous inward currents in K and Tl solutions show a similar voltage-dependence. Secondly, it was shown that at least 58% of the thallous current crosses the membrane using a pathway in the T-system as opposed to the surface membrane. Using a similar method the same result is obtained for the distribution of K channels (Almers, 1972b). Thirdly, Cs^+ blocks inward currents in a voltage-dependent manner whether these are carried by K^+ (Gay & Stanfield, 1977) or by Tl^+.

A possible explanation for the differential effects of K^+ and Tl^+ in the one channel system is that Tl^+ competes with Na^+ for the Na binding site more effectively than K^+ ions. Since raising the internal and external K^+ concentrations together reduces the blockade of K currents by Ba^{2+} (Standen & Stanfield, 1978b), there is a precedent for believing that such competition exists. If the present interpretation is correct, future experiments should show that a higher concentration of caesium is required to achieve a given blockade of inward currents in Tl solutions than in K solutions.

The notion that Tl^+ has a higher affinity than K^+ for the binding site (or sites) within the K channel is supported by several reports that certain enzyme systems which are normally activated by K^+ are also activated by Tl^+ but with a higher affinity than K^+. These include the (Na-K) ATPase of rabbit kidney (Britten & Blank, 1968), the ouabain-sensitive Na efflux in human red cells (Cavieres & Ellory, 1974) and pyruvate kinase (Kayne, 1971). Similarly, Tl^+ is more effective than K^+ in stimulating the Na pump in crab nerve (Baker & Connelly, 1966) and in rabbit vagus

nerve (Rang & Ritchie, 1968). It has also been shown in solubilized membrane preparations from nerve, that the concentration of Tl^+ required to displace tetrodotoxin from specific binding sites associated with Na channels is about 60, and more than 60, times less than the concentrations required of Na^+ and K^+, respectively (Henderson, Ritchie & Strichartz, 1974).

If thallous ions are tightly bound to a site within the K channel, then under appropriate experimental conditions these ions would also be expected to block inward K currents in a voltage-dependent manner. Such an observation has recently been reported by Hagiwara et al. (1977) in starfish egg cells. K^+ does not act as a blocking ion for Tl currents in these cells, but this is not surprising if the binding of K^+ to the site is weak.

In squid axons, Landowne (1975) has reported that the ratio of influx to efflux for passive K^+ movements is consistent with single-file behaviour (Hodgkin & Keynes, 1955), while that for Tl^+ is 4-5 times greater and is equal to the ratio expected for independent ion movement (Ussing, 1949). Landowne concludes that Tl^+ and K^+ do not interact with the K channel in the same way, or that there may be separate channels for Tl^+ and K^+.

The present finding that Tl^+ is 1.14 times more permeant than K^+ in resting fibres when only one of these ions is present in the Ringer is consistent with the fact that Tl^+ is the only ion which is known to be more permeant than K^+ in K channels in nerve. Application of the Goldman equation to measured resting potentials gives a ratio P_{Tl}/P_K of 1.8 in squid axons (Hagiwara et al., 1972) and 1.2 in starfish egg cells (Hagiwara et al., 1977). In stimulated nerve, P_{Tl}/P_K is 2.3 from the

reversal potential of delayed K currents in myelinated nerve fibres (Hille, 1973), and 1.1 from the after-hyperpolarization in squid axons (Landowne, 1975).

One factor which could affect the present permeability ratio is the assumption that the composition of the sarcoplasm is unchanged by brief exposure to thallous concentrations in the range 1.2 to 80 mM. Mullins & Moore (1960) show that after 15 mins in 1 mM-$TlNO_3$ the intracellular thallous concentration is about 2 mM, so in low thallous concentrations little error is introduced by assuming that $[Tl]_i$ is zero. In addition, as Tl^+ accumulates in the fibres, the calculated value of P_{Tl}/P_K will fall unless there is an equivalent loss of K^+. Thus the present ratio of 1.14 is unlikely to be too high. However, over a long period of time fibres gaining thallium must also lose K^+ at a similar, or slightly greater rate. If this were not so, the mean resting potential of fibres in 2.5 mM-Tl_2SO_4 would be expected to increase with time. Instead the present results show an insignificant depolarization after 2 hours.

Mullins & Moore (1960) report that fibres bathed in 1 mM-$TlNO_3$ solutions for 3-4 hours have high Na^+ and low K^+ concentrations. However, in their experiments fibres also lost K^+ in the absence of thallium.

In muscle, the ratio P_{Tl}/P_K is dependent on the mole fraction of Tl^+ and K^+ in the Ringer. More extensive experiments in the starfish (Hagiwara et al., 1977) show that both the permeability ratio and the size of inward currents in K^+-Tl^+ mixtures are dependent on the mole fraction of these ions. To explain this behaviour, Hagiwara et al. have proposed a model in which the voltage-independent binding of K^+ or Tl^+ ions to a "gating site"

associated with the channel determines whether the channel is more permeable to K^+ or to Tl^+. A similar model might account for the anomalous permeability ratios described here.

Chapter 8. General Discussion

The experiments described in the preceding chapters have been largely concerned with the properties of the resting and the delayed K conductances in frog skeletal muscle fibres. Those experiments which relate to the delayed conductance are discussed in sufficient detail in chapters 3 and 4.

To some extent, the experiments dealing with inward rectification are more interesting since they were carried out at a time when new ideas concerning the mechanism of inward rectification were developing. These experiments produce three new results which any proposed model for inward rectification should be able to explain. These are (1) that external Cs^+ blocks K currents in a manner which is steeply dependent on the membrane potential. (2) The resting membrane is slightly more permeable to Tl^+ than to K^+ when only one of these ions is present in the external solution, but when the Ringer contains a 50:50 mixture of K^+ and Tl^+, the K permeability exceeds that of Tl^+. This is known as anomolous mole-fraction behaviour (Hagiwara et al., 1977; Hille & Schwarz, 1978). (3) The potential-dependent blockade of inward K currents by Na^+ (Standen & Stanfield, 1978c) does not occur when Tl^+ replaces K^+ in the Ringer. Unfortunately, the second of these is not readily dealt with in a simple way. The third is covered adequately in chapter 7.

The purpose of this chapter is to consider to what extent the properties of the resting K conductance can be accounted for in terms of a model which assumes that K^+ moves across the resting membrane by way of rigid, water-filled pores. No attempt has been made to present the results in a quantitative manner; this has

recently been done by Armstrong (1975a), Hille & Schwarz (1978) and Standen & Stanfield (1978d) for pore models.

As described previously (chapter 5), a number of small cations when present in the external solution are now known to block the resting K conductance in muscle in a voltage-dependent manner. In at least two cases (Cs^+ and Ba^{2+}), the apparent dissociation constant for the blockade is reported to be an exponential function of the membrane potential, decreasing as the potential is made more negative. To account for this, it has been suggested that the blocking ion is driven into the channel by the membrane field until it reaches a site partway across the membrane where it is bound with much greater affinity than K^+. That binding is involved is suggested by the high Q_{10} for the onset of the blockades by Ba^{2+} (Standen & Stanfield, 1978b) and Na^+ (Almers, 1972b). Alternatively, the blocking ion may simply encounter a region in which the pore is narrowed so that further penetration into the membrane is more difficult. In both cases, other ions, permeant or non-permeant, which enter the channel from the outside once the blocking ion is in the pore will reduce the probability that the block is removed if single-filing occurs. An interesting point is that the affinity of the blocking ion for the site may be independent of the membrane potential if, as one might expect, the concentration of the blocking ion at the site is an exponential function of the membrane potential (see Standen & Stanfield, 1978b).

The present conclusion from the Cs experiments, that there is more than one site for ions in the channel, is consistent with the ^{42}K flux data of Horowicz et al. (1968), that the ions move in single-file, the channel containing two ions at any one time. The observation made by Standen & Stanfield (1978b), that two K^+ ions compete with

one Ba^{2+} ion, is also consistent with a multi-ion pore. The binding sites, which are represented as energy wells in the model of Hille & Schwarz (1978), are likely to be fixed negative charges possibly associated with proteins which make up the pore wall. If it is assumed that these charges play an important role in K permeation, then since changes in external pH in the range studied (pH 5 to 9.8; Hutter & Warner, 1967a) have no effect on the resting K conductance, these sites may be fairly strong acids.

My experiments on the resting potassium conductance suggest a mechanism for inward rectification which involves an intracellular blocking particle which is positively charged, and which occludes the pore when the membrane is depolarized. The basis of this hypothesis is that there is a similarity between the shape of the current-voltage relation for inward K currents in the presence of an external blocking ion, and that of outward K currents in the presence or absence of the blocking ion (see, for example, Fig. 5.4): in both cases there are regions of zero and negative slope conductance. In the example cited, the inward current is larger than the outward current; however, this is not important since the size of the outward current will depend on a number of factors including the concentration of the blocking particle, its valence and its affinity for the postulated binding site(s)

It is interesting to speculate as to the nature of the blocking particle. Na^+ is a possible candidate since this ion blocks inward K currents in muscle when added to the Ringer, though with very low affinity (Standen & Stanfield, 1978c). Na^+ also blocks delayed K currents, when these are outward, in a voltage-dependent manner in nerve when present in the internal perfusate

(Bezanilla & Armstrong, 1972; Bergman, 1970; French & Wells, 1977). On the other hand, Hille & Schwarz (1978) and Standen and Stanfield (1978d) have demonstrated that a single monovalent cation bound anywhere in the membrane field does not produce a blockade with a sufficiently steep voltage-dependence to account for inward rectification in muscle. The blocking particle could also be a positively charged group which is part of the membrane structure.

The independence principle (Hodgkin & Huxley, 1952a) predicts that K efflux is proportional to the internal K^+ concentration but is independent of external K^+ concentration. In muscle, however, raising the external K^+ concentration under conditions in which the membrane potential is held constant results in an increase in ^{42}K efflux in resting fibres (Adrian, 1962; Horowicz, Gage & Eisenberg, 1968).

In terms of the pore model for inward rectification, this dependence of K efflux on the external potassium concentration is consistent with the notion that the number of blocked channels is reduced when the external K^+ concentration is increased. This may be due to two mechanisms. First, K^+ may simply compete with the blocking ion for the binding site, as suggested by Standen & Stanfield (1978b,d). Second, a K^+ ion entering a blocked channel from the external solution may flush the blocking particle into the sarcoplasm (Armstrong, 1966; 1975a). As predicted by either mechanism, there is an increase in the influx of labelled K^+ when the external K^+ concentration is raised in conditions in which the membrane potential is fixed at -18 mV, and the driving force on K^+ is outward (Horowicz et al., 1968).

Another property shown by inward rectifiers is crossing-over, which refers to the observation that an increase in the external K^+ concentration produces an increase in the outward current such that the current-voltage relations in the two K solutions cross-over at a potential at which the currents are outward (Adrian, 1969; Almers, 1972a. See also Hagiwara, Miyazaki & Rosenthal, 1976; McAllister & Noble, 1966, for examples in starfish egg cells and in cardiac Purkinje fibres). Like the long pore effect, crossing-over can be accounted for if raising the external K^+ concentration reduces the number of K channels that are blocked. Since K efflux greatly exceeds influx under conditions in which the driving force on K^+ is large and positive, an increase in the number of conducting channels will result in an increase rather than a decrease in the outward current, although the latter would be expected to occur if the effect of external K^+ on the K driving force were large compared to its ability to remove the blocking particle. At potentials close to the equilibrium potential for K^+, however, the effect of driving force will predominate such that an increase in the external K^+ concentration depresses the outward current.

In this connection, it will be interesting to see if the reduction in the Cs blockade produced by an increase in the internal K^+ concentration (see page 116) results in crossing-over of the current-voltage relations for inward K currents in the presence of Cs^+.

A further property of the inward rectifier in muscle is that it is blocked by Rb^+ and tetraethylammonium ions (TEA). When TEA is added to the external solution, inward and outward K

currents are depressed to the same extent (Stanfield, 1970b) indicating that the blockade is independent of the membrane potential. In addition, there are two studies which indicate that the TEA blockade is not competitively inhibited by external K^+. First, Stanfield (1970b) showed that the apparent dissociation constant for the TEA-receptor complex was 20 mM whether this was determined in 2.5 mM-KCl or in 50 mM-K_2SO_4 solution. Secondly, Volle, Glisson & Henderson (1972) found that the inhibition of ^{42}K efflux by 60 mM TEA was increased rather than decreased when the external K^+ concentration was raised from 2.5 to 50 mM. These authors also obtained a value of 20 mM for the apparent dissociation constant for TEA binding from the inhibition of ^{42}K efflux in 10 mM-K^+.

A reasonable explanation for these findings is that TEA blocks the channels indirectly, by binding to a site on the outer surface of the membrane. On the other hand, if internal K^+ ions also have access to the TEA binding site, changes in the external K^+ concentration alone may produce a negligible change in the K^+ concentration at the site, complicating the interpretation of competition studies.

Adrian (1964) has made a number of observations concerning the Rb blockade and has concluded that Rb^+ "does not pass through the channels responsible for anomalous rectification". (See also Adrian et al.,1970b). These observations are (a) that external Rb^+ reduces inward K currents in a manner which appears to be largely independent of the membrane potential, although outward currents were not shown. (b) When Rb^+ partially replaces internal K^+, outward currents through the inwardly rectifying permeability

mechanism are completely blocked (though the linear segment of the current-voltage relationship is unaffected) and inward currents are slightly depressed. (c) When Rb^+ replaces K^+ in the external solution and is also inside the fibres, the ability of the membrane to carry large inward and small outward currents is lost.

The evidence that the mechanisms by which Rb^+ and TEA block the resting K conductance are not the same is that that by Rb^+ is antagonised by external K^+. Thus Sjodin (1961) has found that the uptake of K^+ into muscle is reduced in the presence of external Rb^+, and has concluded that Rb^+ and K^+ compete for membrane sites usually occupied by K^+. Similarly, Volle et al. (1972) reported that the blockade of ^{42}K efflux by 2.5 mM-Rb^+ under equilibrium conditions is removed when the external K^+ concentration is raised ten-fold. Since the blockade is largely independent of the membrane potential, the depolarization caused by raising $[K]_o$ cannot account for this effect. In addition, Adrian (1962) and Sjodin (1965) have reported that in the absence of K^+, rubidium, unlike K^+ (Adrian, 1962; Horowicz et al.,1968), does not stimulate ^{42}K efflux.

If one takes the view that the inward rectifier channel is impermeable to Rb^+, as Adrian suggested, then the fact that the blockade is largely independent of the membrane potential, and is dependent on the external K^+ concentration, means that the Rb receptor is probably at the outer entrance to the channel, such that it is outside the membrane field. In this case, it is necessary to explain why Rb^+, which has an ionic radius of 1.48Å, is excluded from the channel while smaller ions, K^+ (1.33Å) and Tl^+ (1.44Å), are

able to pass through the channel, and Cs^+ (1.69Å), which is considerably larger than Rb^+, can penetrate some distance into the pore.

In fact, the results presented in Fig. 5.3 suggest that Rb^+ is able to carry a small inward current through the channel. The easiest way to account for the fact that the presence of Rb^+ reduces K permeability is to assume that Rb^+ moves sluggishly through the pore, but in other respects behaves much like a K^+ ion. Thus the inner part of the channel must be at least 2.96Å in diameter, while the outer region must exceed 3.38Å in order to accept Cs^+ ions.

It is interesting at this point to consider previous models for inward rectification in muscle. Adrian (1969) has plotted current-voltage relations for a number of models which show rectification. These fall into two main classes; fixed charge models and mobile carrier models. A general conclusion from Adrian's review is that the presence of fixed charges at the surface of the membrane can produce rectification, or reverse the direction of rectification predicted from the constant field equation (Goldman, 1943), but that this cannot generate a current-voltage relation which has a region in which the slope conductance is negative. Thus fixed charges alone are unable to account for the inward rectification seen in muscle.

The most successful model described by Adrian (1969) assumes that K^+ ions are transported across the membrane in association with a mobile carrier. This has a charge of -2 when empty and -1 when full (that is, each carrier molecule carries one K^+ ion), and is distributed between the inner and outer edges of the membrane according to the Boltzmann expression. Rectification is produced by

assuming that the concentration of carrier molecules at the inner surface of the membrane is buffered. Since hyperpolarization concentrates the empty carrier at the outer surface of the membrane, large inward currents are possible. On the other hand, outward currents are always small and the current-voltage relation has a negative slope similar to that observed experimentally. As Adrian points out, without modification, this model does not demonstrate crossing-over when the external K^+ concentration is altered. Moreover, it is impossible to simulate the Cs blockade using this model by assuming that Cs^+ buffers the carrier concentration at the outer edge of the membrane. Such an assumption results in a shift in the reversal potential of the resting current: this is not found experimentally (see Table 5.2). Buffering by Cs^+ might occur if Cs^+ was bound but not transported.

Horowicz, Gage & Eisenberg (1968) have measured the influx and efflux of ^{42}K as a function of the external K^+ concentration in chloride-loaded muscle fibres in which the membrane potential was held at the reversal potential for the chloride current (about -18 mV). They then repeated these measurements under conditions in which the membrane potential was altered by manipulation of the reversal potential for chloride while the equilibrium potential for K^+ was held at about -18 mV. From these studies, they deduced that the flux ratio did not obey the Ussing (1949) relation for independent ion movement, but followed the modified form (eqn. (1.3) page 30) in which N = 2. This is consistent with single-file behaviour in a pore containing two K^+ ions (Hodgkin & Keynes, 1955) or a mobile carrier model in which each carrier molecule transports two K^+ ions. The latter interpretation is that used by Horowicz et al. (1968). In their model the

carrier has a charge of -3 when empty and -1 when full, and rectification is produced by postulating a surface potential of +54 mV due to fixed charges at the inner surface of the membrane. Another important feature of this model is that the stimulation of K efflux by external K^+ (Adrian, 1962; Horowicz et al., 1968) is simulated by assuming that the total quantity of carrier molecules is increased when the external K^+ concentration is raised.

Adrian (1969) has discussed the model of Horowicz et al. (1968) in some detail and describes a peak in the current-voltage relation for inward K currents predicted by the model but which is not seen experimentally. On the other hand, the model predicts outward K currents rather well. This is due, at least in part, to the fact that in their experiments, Horowicz et al. could only control the membrane potential under conditions in which the K current was outward.

Armstrong (1975a) has devised a pore model for inward rectification in muscle which, in some respects, is similar to that used to account for the action of internal quaternary ammonium ions in nerve. Armstrong postulates the existence of a binding site which is occupied either by a K^+ ion or by a blocking particle, and which is located at the inner end of the resting K channel outside the membrane field. A K^+ ion approaching the site by way of the channel from the external solution is assumed to be able to displace the blocking particle from the site by electrostatic repulsion. Moreover, since Armstrong assumes that the concentration of K^+ at a given point in the channel is an exponential function of the membrane potential, hyperpolarization, which attracts K^+ into the channel from the outside, reduces the blockade in a voltage-dependent manner.

Since the blocking particle is outside the electrical gradient, Armstrong argues that the total K efflux (m_{eff}) is proportional to the internal K^+ concentration, while the total K influx (m_{inf}) is proportional to $[K]_o e^{-V_1 F/RT}$ (see eqns. (22 & 23) of Armstrong, 1975a). Armstrong does not discuss the K current predicted from his model; however, it can be seen that the current, which is equal to $m_{eff}-m_{inf}$, is an exponential function of the membrane potential and as such is rather different from that observed experimentally. Moreover, at large positive potentials the predicted current approaches a value which is proportional to the internal K^+ concentration and is independent of $[K]_o$. Thus Armstrong's model does not produce crossing-over, nor does it generate an outward current with a negative slope conductance. It should be mentioned, however, that the model predicts fluxes of labelled K^+ which are similar to those described by Horowicz et al. (1968).

The mechanism by which the blocking particle model of Standen & Stanfield (1978d) produces inward rectification is similar to that outlined here. In their model, the blocking particle is a divalent cation (or two monovalent cations) which binds at a site 80% of the way across the membrane field from the inside, where it competes with K^+. a given K^+ concentration, the model fits closely the current-voltage relations for the inward rectifier in skeletal muscle, and over a large range of K^+ concentrations only small deviations occur between the predicted current-voltage relations and those observed experimentally. Such deviations as occur are in the direction expected if the linear component of the resting K conductance, which is assumed to be in parallel with the inward rectifier, is overestimated in low K solutions.

Hille & Schwarz (1978) have considered the more general case for a channel showing single-file behaviour (Hodgkin & Keynes, 1955; Heckmann, 1972), which has two or more cation binding sites, and which can be occupied by more than one ion at a time. For inward rectification, they propose a channel which contains three or more binding sites, and which is blocked by an intracellular, monovalent blocking particle able to cross all but the outermost energy barrier.

Like the model described by Standen & Stanfield (1978d), the model of Hille & Schwarz produces crossing-over and a region of negative slope in the current-voltage relation when the K current is outward. The model of Hille & Schwarz has the advantage that it can probably be used to explain the anomalous mole-fraction behaviour involving K^+ and Tl^+ reported in chapter 7, as well as the simultaneous blockade by external cations. On the other hand, according to the authors, the three site model produces an inward rectification which is less steep than that observed experimentally.

Hille's (1975b) model for the Na channel in myelinated nerve fibres also comprises three ion binding sites. The model is simpler, however, in that almost all of the observations concerning blocking ions in that preparation can be explained by assuming that the channd contains only one ion at a time.

Finally, none of the models so far developed for K channels have attempted to explain the fact that when a sufficiently large voltage is applied across the membrane, the selectivity of the membrane appears to decrease in a manner which is reversible, and which is not consistent with membrane breakdown. An example of

this is the increase in K current which occurs through inward rectifier channels in muscle under conditions of extreme hyperpolarization in the presence of small quantities of Cs^+ in the Ringer (chapter 5). Similarly, French & Wells (1977), working on squid axons have shown that Na^+ ions can carry large outward currents through delayed K channels under conditions of extreme depolarization, despite the fact that when smaller depolarizations are applied internal Na^+ acts as a K channel blocking ion. Indeed, a number of experiments with blocking ions suggest similarities in the design of delayed and inward K channels (apart from channel gating) which deserve further investigation.

REFERENCES

Adelman, W.J., Jr. (1968). In the squid axon, potassium current blockade by internal caesium is dependent on membrane potential and current direction. Biophys. J. 12, 133a

Adelman, W.J., Jr. (1971). Electrical studies of internal perfused giant squid axons. In Biophysics and Physiology of Excitable Membranes, W.J. Adelman, Jr., Editor. Van Nostrand Reinhold: New York, pp 274-319

Adelman, W.J., Jr., French, R.J. (1978). Blocking of the squid axon potassium channel by external caesium ions. J. Physiol. (Lond.), 276, 13-25

Adelman, W.J., Jr., Senft, J.P. (1966). Voltage clamp studies on the effect of internal cesium ions on the sodium and potassium currents in the squid giant axon. J. Gen. Physiol. 50, 279-293

Adelman, W.J., Jr., Senft, J.P. (1968). Dynamic asymmetries in the squid axon membrane. J. Gen. Physiol. 51, 102-114s.

Adrian, R.H. (1956). The effect of internal and external potassium concentration on the membrane potential of frog muscle. J. Physiol. (Lond.), 133, 631-658

Adrian, R.H. (1960). Potassium chloride movement and the membrane potential of frog muscle. J. Physiol. (Lond.), 151, 154-185

Adrian, R.H. (1962). Movement of inorganic ions across the membrane of striated muscle. Circulation 26, 1214-1223

Adrian, R.H. (1964). The rubidium and potassium permeability of frog muscle membrane. J. Physiol. (Lond.), 175, 134-159

Adrian, R.H. (1969). Rectification in muscle membrane. Prog. Biophys. Mol. Biol. 19, 339-369

Adrian, R.H., Almers, W. (1976). Charge movement in the membrane of striated muscle. J. Physiol. (Lond.) 254, 339-360

Adrian, R.H., Chandler, W.K., Hodgkin, A.L. (1966). Voltage clamp experiments in skeletal muscle fibres. J. Physiol. (Lond) 186, 51-52p

Adrian, R.H., Chandler, W.K., Hodgkin, A.L. (1968). Voltage clamp experiments in striated muscle fibres. J. Gen. Physiol. 51, 188-192s

Adrian, R.H., Chandler, W.K., Hodgkin, A.L. (1969). The kinetics of mechanical activation in frog muscle. J. Physiol. (Lond.), 204, 207-230

Adrian. R.H., Chandler, W.K., Hodgkin, A.L. (1970a). Voltage clamp experiments in striated muscle fibres. J. Physiol. (Lond.), 208, 607-644

Adrian, R.H., Chandler, W.K., Hodgkin, A.L. (1970b). Slow changes in potassium permeability in skeletal muscle. J. Physiol. (Lond.), 208, 645-668

Adrian, R.H., Chandler, W.K., Hodgkin, A.L. (1972). An extension of Cole's theorem and its application to muscle. In Perspectives in Membrane Biophysics, W.J. Adelman, Jr., editor. New York: Gordon & Breach, pp 299-309

Adrian, R.H., Chandler, W.K., Rakowski, R.F. (1976). Charge movement and mechanical repriming in skeletal muscle. J. Physiol. (Lond.), 254, 361-388

Adrian, R.H., Costantin, L.L., Peachey, L.D. (1969). Radial spread of contraction in frog muscle fibres. J. Physiol. (Lond.), 204, 231-257

Adrian, R.H., Freygang, W.H. (1962a). The potassium and chloride conductance of frog muscle membrane. J. Physiol. (Lond.), 163, 61-103

Adrian, R.H., Freygang, W.H. (1962b). Potassium conductance of frog muscle membrane under controlled voltage. J. Physiol. (Lond.), 163, 104-114

Adrian, R.H., Peachey, L.D. (1973). Reconstruction of the action potential of frog sartorius muscle. J. Physiol. (Lond.), 235, 103-131

Almers, W. (1972a). Potassium conductance changes in skeletal muscle and the potassium concentration in the transverse tubules. J. Physiol. (Lond.), 225, 33-56

Almers, W. (1972b). The decline of potassium permeability during extreme hyperpolarization in frog skeletal muscle. J. Physiol. (Lond.), 225, 57-83

Almers, W. (1976). Differential effects of tetracaine on delayed potassium channels and displacement currents in frog skeletal muscle. J. Physiol. (Lond.), 262, 613-637

Andersson-Cedergren, E. (1959). Ultrastructure of motor end plate and sarcoplasmic components of mouse skeletal muscle fibres as revealed by three-dimensional reconstructions from serial sections. J. Ultrastr. Res. 1, Suppl. 1-191

Argibay, J.A., Hutter, O.F. (1973). Voltage-clamp experiments on the inactivation of the delayed potassium current in skeletal muscle fibres. J. Physiol. (Lond.), 232, 41-43p

Armstrong, C.M., (1966). Time course of TEA^+-induced anomalous rectification in squid gian axon. J. Gen. Physiol. 50, 491-503

Armstrong, C.M. (1969). Inactivation of the potassium conductance and related phenomena caused by quaternary ammonium ion injected in squid axon. J. Gen. Physiol. 54, 553-575

Armstrong, C.M. (1971). Interaction of tetraethylammonium derivatives with the potassium channels of giant axons. J. Gen. Physiol. 58, 413-437

Armstrong, C.M.(1975a). Potassium pores of nerve and muscle membranes. In Membranes: A Series of Advances, Vol. 3, G. Eisenman, editor. Marcel Dekker: New York, pp 325-358

Armstrong, C.M. (1975b). Ionic pores, gates and gating currents. Q. Rev. Biophys. 7, 179-210

Armstrong, C.M. (1975c). Evidence for ionic pores in excitable membranes. Biophys. J. 15, 932-933

Armstrong, C.M., Bezanilla, F.M., Horowicz, P. (1972). Twitches in the presence of ethylene glycol bis (β-aminoethylether)-N,N'-tetracetic acid. Biochim. Biophys. Acta. 267, 605-608

Armstrong, C.M., Bezanilla, F., Rojas, E. (1973). Destruction of sodium conductance inactivation in squid axon perfused with pronase. J. Gen. Physiol. 62, 375-391

Armstrong, C.M. Binstock, L. (1965) Anomalous rectification in the squid giant axon injected with tetraethylammonium chloride. J. Gen. Physiol. 48, 859-872

Armstrong, C.M., Hille, B. (1972) The inner quaternary ammonium ion receptor in potassium channels of the node of Ranvier. J Gen. Physiol. 59, 388-400

Baker, P.F., Connelly, C.M. (1966). Some properties of the external activation site of the sodium pump in crab nerve. J. Physiol. (Lond.) 185, 270-297

Baker, P.F., Hodgkin, A.L., Shaw, T. (1962). The effects of changes in internal ionic concentrations on the electrical properties of perfused giant axons. J. Physiol. (Lond.) 164, 355-374

Barlow, C.A. Jr. (1970). The electrical double layer. In Physical Chemistry, an Advanced Treatise. Vol. 9A, Electrochemistry, H. Eyring, D. Henderson & W. Jost, editors. New York: Academic Press. pp 167-246

Barry, P.H., Adrian, R.H. (1973). Slow conductance changes due to potassium depletion in the transverse tubules of frog muscle fibres during hyperpolarizing pulses. J. Memb. Biol. 14, 243-292

Bastian, J., Nakajima, S. (1972). A Na dependent excitation in the transverse tubular system. Fed. Proc. 31, 323

Bastian, J., Nakajima, S. (1974). Action potential in the transverse tubules and its role in the activation of skeletal muscle. J. Gen. Physiol. 63, 257-278

Baumgarten, C.M., Isenberg, G., McDonald, T.F., Ten Eick, R.E. (1977). Depletion and accumulation of potassium in the extracellular clefts of cardiac Purkinje fibres during voltage clamp hyperpolarization and depolarization. Experiments in sodium-free bathing media. J. Gen. Physiol. 70, 149-169

Beaty, G.N., Stefani, E. (1976a). Calcium dependent electrical activity in twitch muscle fibres of the frog. Proc. Roy. Soc. Lond., B 194, 141-150

Beaty, G.N., Stefani, E. (1976b). Inward calcium current in twitch muscle fibres of the frog. J. Physiol. (Lond) 260, 27-28P

Begenisich, T. (1975). Magnitude and location of surface charges on Myxicola giant axons. J. Gen. Physiol. 66, 47-66

Begenisich, T., De Weer, P. (1977). Ionic interactions in the potassium channel of squid giant axons. Nature 269, 710-711

Begenisich, T., Lynch, C. (1974). Effects of divalent cations on voltage clamped squid axons. J. Gen. Physiol. 63, 675-689

Bergman, C. (1970). Increase of sodium concentration near the inner surface of the nodal membrane. Pflügers, Arch. 317, 287-302.

Bezanilla, F., Armstrong, C.M. (1972). Negative conductance caused by entry of sodium and caesium ions into the potassium channels of squid axons. J. Gen. Physiol. 60, 588-608

Bezanilla, F., Caputo, C., Gonzales-Serratos, H., Venosa, R.A. (1972). Sodium dependence of the inward spread of activation in isolated twitch muscle fibres of the frog. J. Physiol. (Lond.), 223, 507-523

Bianchi, C.P.., Shanes, A.M. (1959). Calcium influx in skeletal muscle at rest, during activity and during potassium contracture. J. Gen. Physiol. 42, 803-815

Binstock, L. Lecar, H. (1969). Ammonium ion conductance in the squid giant axon. J. Gen. Physiol. (Lond.) 53, 342-360

Blaustein, M.P., Goldman, D.E. (1968). The action of certain polyvalent cations on the voltage clamped lobster axon. J. Gen. Physiol. 51, 279-291

Bolingbroke, V., Harris, E.J., Sjodin, R.A. (1961). Rubidium and caesium entry, and cation interaction in frog skeletal muscle. J. Physiol. (Lond.) 157, 289-305

Brismar, T. (1973). Effects of ionic concentration on permeability properties of nodal membrane in myelinated nerve fibres of Xenopus laevis. Potential clamp experiments. Acta Physiol. Scand. 87, 474-484

Britten, J.S., Blank, M. (1968). Thallium activation of the (Na^+-K^+) - activated ATPase of rabbit kidney. Biochim. Biophys. Acta 159, 160-166

Brooks, A.E., Hutter, O.F. (1963). Effects of extracellular pH on electrical activity of skeletal muscle. Biochem. Pharmac. 12, Suppl. 266-267

Cahalan, M., Begenisich, T. (1976). Sodium channel selectivity. Dependence on internal permeant ion concentration. J. Gen. Physiol. 68, 111-125

Cahalan, M., Begenisich, T. (1977). Asymmetric ionic concentration dependence of sodium channel selectivity. Biophys. J. 17, 13a.

Caillé, J., Ildefonse, M., Rougier, O., (1975). Relations between membrane potential, sodium currents and contraction in frog twitch muscle fibres. J. Physiol. (Lond.) 249, 26-28P

Caillé, J., Ildefonse, M., Rougier, O. (1978). Existence of a sodium current in the tubular membrane of frog twitch muscle fibre; its possible role in the activation of contraction. Pflügers Arch. 374, 167-177

Campbell, D.T. (1976). Ionic selectivity of the sodium channel of frog skeletal muscle. J. Gen. Physiol. 67, 295-307

Campbell, D.T., Hille, B. (1976). Kinetic and pharmacological properties of the sodium channel of frog skeletal muscle. J. Gen. Physiol. 67, 309-323

Cavieres, J.D., Ellory, J.C. (1974). Thallium and the sodium pump in human red cells. J. Physiol. (Lond.) 243, 243-236

Chandler, W.K., Hodgkin, A.L., Meves, H. (1965). The effect of changing the internal solution on sodium inactivation and related phenomena in giant axons. J. Physiol. (Lond.) 180, 821-836

Chandler, W.K., Meves, H. (1965). Voltage clamp experiments on internally perfused giant axons. J. Physiol. (Lond.) 180, 788-820

Chandler, W.K., Rakowski, R.F., Schneider, M.F. (1976a). A non-linear voltage dependent charge movement in frog skeletal muscle. J. Physiol. (Lond.) 254, 245-283

Chandler, W.K., Rakowski, R.F., Schneider, M.F. (1976b). Effects of glycerol treatment and maintained depolarization on charge movement in skeletal muscle. J. Physiol. (Lond.) 254, 285-317

Ciani, S., Hagiwara, S., Miyazaki, S. (1977). A model for Cs blocking of the K conductance in anomalous rectification. Biophys. J. 17 46a

Cole, K.S., Curtis, H.J. (1941). Membrane potential of the squid giant axon during current flow. J. Gen. Physiol. 24 551-563

Cole, K.S., Moore, J.W. (1960). Potassium ion current in the squid giant axon: dynamic characteristic. Biophys. J. 1, 1-14

Conway, E.J., Moore, P.T. (1945). Cation and anion permeability constants for the muscle fibre membrane. Nature 156, 170-171

Costantin, L.L. (1968). The effect of calcium on contraction and conductance thresholds in frog skeletal muscle. J. Physiol. (Lond.) 195, 119-132

Costantin, L.L. (1975). Contractile activation in skeletal muscle. Prog. Biophys. Mol. Biol. 29, 197-224

Courtney, K.R. (1975). Mechanism of frequency-dependent inhibition of sodium currents in frog myelinated nerve by the lidocaine derivative GEA 968. J. Pharmacol. Exp. Ther. 195, 225-236

Davies, J.T., Rideal, E.K. (1963). Interfacial phenomena. Academic Press: New York.

Diamond, J.M., Wright, E.M. (1969). Biological membranes: the physical basis of ion and non-electrolyte selectivity. A. Rev. Physiol. 31, 581-646

Dixon, M., Webb, E. (1964). Enzymes. Longmans, Green & Co: London

Dörrscheidt-Käfer, M. (1976). The action of Ca^{2+}, Mg^{2+} and H^{+} on the contraction threshold of frog skeletal muscle. Pflügers Arch. 362, 33-41

Dörrscheidt-Käfer, M. (1977). The action of D 600 on frog skeletal muscle: facilitation of excitation-contraction coupling. Pflügers Arch. 369, 259-267

Drouin, H., Neumcke, B. (1974). Specific and unspecific charges at the sodium channels of the nerve membrane. Pflügers Arch. 351, 207-229

Drouin, H., The, R. (1969). The effect of reducing extracellular pH on the membrane currents of the Ranvier node. Pflügers Arch. 313, 80-88

Dubois, J.M., Bergman, C. (1975). Caesium induced rectifications in frog myelinated fibres. Pflügers Arch. 355, 361-364

Dubois, J.M., Bergman, C. (1977). The steady-state potassium conductance of the Ranvier node at various external K-concentrations. Pflügers Arch. 370, 185-194

Dulhunty, A.F., Franzini-Armstrong, C. (1975). The relative contributions of the folds and caveolae to the surface membrane of frog skeletal muscle fibres at different sarcomere lengths. J. Physiol (Lond.) 250, 513-540

Ebashi, S., Endo, M. (1968). Calcium ion and muscle contraction. Prog. Biophys. Mol. Biol. 18, 123-183

Ebert, G.A., Goldman, L. (1976). The permeability of the sodium channel in Myxicola to alkali cations. J. Gen. Physiol. 68, 327-340

Ehrenstein, G., Gilbert, D.L. (1966). Slow changes of potassium permeability in the squid giant axon. Biophys. J. 6, 553-566

Eisenberg, B., Eisenberg, R.S. (1968). Selective disruption of the sarcotubular system in frog sartorius muscle. J. Cell Biol. 39, 451-467

Eisenberg, R.S., Gage, P.W. (1969). Ionic conductances of the surface and transverse tubular membranes of frog sartorius fibres. J.Gen. Physiol. 53, 279-297

Eisenman, G. (1962). Cation selective glass electrodes and their mode of operation. Biophys. J. 2, 259-323s

Eisenman, G. (1963). The influence of Na, K, Li, Rb and Cs on cellular potentials and related phenomena. Bol. Inst. Estud. Med. Biol. 21, 155-183

Eisenman, G. (1965). Some elementary factors involved in specific ion permeation. Proc. 23rd Int. Congr. Physiol. Sci. 489-506

Elul, R. (1967). Fixed charge in the cell membrane. J. Physiol. (Lond.) 189, 351-365

Endo, M. (1966). Entry of fluorescent dyes into the sarcotubular system of the frog muscle. J. Physiol. (Lond.) 185, 224-238

Endo, M. (1977). Calcium release from the sarcoplasmic reticulum. Physiol. Rev. 57, 71-108

Fatt, P., Katz, B. (1951). An analysis of the end-plate potential recorded with an intra-cellular electrode. J. Physiol. (Lond.) 115, 320-370

Fink, R., Wettwer, E. (1978). Modified K-channel gating by exhaustion and the block of internally applied TEA^+ and 4-aminopyridine in muscle. Pflügers Arch. 374, 289-292

Frankenhaeuser, B., Hodgkin, A.L. (1957). The action of calcium on the electrical properties of squid axons. J. Physiol. (Lond.) 137, 217-243

Franzini-Armstrong, C. (1970). Studies of the triad - I. Structure of the junction in frog twitch fibres. J. Cell. Biol. 47, 488-499

French, R.J., Adelman, W.J. Jr. (1976). Competition, saturation and inhibition - ionic interactions shown by membrane ionic currents in nerve, muscle and bilayer systems. Curr. Top. Membranes & Transp. 8, 161-207

French, R.J., Wells, J.B. (1977). Sodium ions as blocking agents and charge carriers in the potassium channel of the squid giant axon. J. Gen. Physiol. 70, 707-724

Freygang, W.H. Jr., Goldstein, D.A. Hellam, D.C., Peachey, L.D. (1964). The relation between the late after-potential and the size of the transverse tubular system of frog muscle. J. Gen. Physiol. 48, 235-263

Freygang, W.H. Jr., Goldstein, D.A., Hellam, D.C. (1964). The after-potential that follows trains of impulses in frog muscle fibres. J. Gen. Physiol. 47, 929-952

Fujino, M., Yamaguchi, T., Suzuki, K. (1961). 'Glycerol Effect' and the mechanism linking excitation of the plasma membrane with contraction. Nature 192, 1159-1161

Gage, P.W., Eisenberg, R.S. (1967). Action potentials without contraction in frog skeletal muscle fibres with disrupted transverse tubules. Science 158, 1702-1703

Gage, P.W., Eisenberg, R.S. (1969a). Capacitance of the surface and transverse tubular membrane of frog sartorius muscle fibres. J Gen. Physiol. 53, 265-278

Gage, P.W., Eisenberg, R.S. (1969b). Action potentials, after-potentials, and excitation contraction coupling in frog sartorius muscle without transverse tubules. J. Gen. Physiol. 53, 298-310

Gay, L.A., Stanfield, P.R. (1977). Cs^+ causes a voltage-dependent block of inward K currents in resting skeletal muscle fibres. Nature 267, 169-170

Gay, L.A., Stanfield, P.R. (1978). The selectivity of the delayed potassium conductance of frog skeletal muscle fibres. Pflügers Arch. 378, 177-179

Gilbert, D.L. (1971). Fixed surface charges. In Biophysics and Physiology of Excitable Membranes, W.J. Adelman Jr, editor. Van Nostrand Reinhold: New York.

Gilbert, D.L., Ehrenstein, G. (1969). Effect of divalent cations on potassium conductance of squid axons: determination of surface charge. Biophys. J. 9, 447-469

Gilbert, D.L., Erhenstein, G. (1970). Use of a fixed charge model to determine the pK of the negative sites on the external membrane surface. J. Gen. Physiol. 55, 822-825

Gillespie, J.I. (1977). Voltage-dependent blockade of the delayed potassium current in skeletal muscle by 4-aminopyridine. J. Physiol. (Lond.) 273, 64-65 P

Gillespie, J.I., Hutter, O.F. (1975). The actions of 4-aminopyridine on the delayed potassium current in skeletal muscle fibres. J. Physiol. (Lond.) 252, 70-71 P

Goldman, D.E. (1943). Potential, impedance, and rectification in membranes. J. Gen. Physiol. 27, 37-60

Goldman, L. (1976). Kinetics of channel gating in excitable membranes. Q. Rev. Biophys. 9, 491-526

Goldman, L., Schauf, C.L. (1973). Quantitative description of sodium and potassium currents and computed action potentials in Myxicola giant axons. J. Gen. Physiol. 61, 361-384

Good, N.E., Winget, G.D., Winter, W., Connolly, T.N., Izawa, S., Singh, R.M.M. (1966). Hydrogen ion buffers for biological research. Biochemistry 5, 467-477

Grahame, D.S. (1947). The electrical double layer and the theory of electrocapillarity. Chem. Rev. 41, 441-501

Hagiwara, S., Eaton, D.C, Stuart, A.E., Rosenthal, N.P. (1972). Cation selectivity of the resting membrane of squid axon. J. Memb. Biol. 9, 373-384

Hagiwara, S., Miyazaki, S., Krasne, S., Ciani, S. (1977). Anomalous permeabilities of the egg cell membrane of a starfish in K^+-Tl^+ mixtures. J. Gen. Physiol. 70 269-281

Hagiwara, S., Miyazaki, S., Moody, W., Patlak, J. (1978). Blocking effects of barium and hydrogen ions on the potassium current during anomalous rectification in the starfish egg. J. Physiol. (Lond.) 279, 167-185

Hagiwara, S., Miyazaki, S., Rosenthal, N.P. (1976). Potassium current and the effect of caesium on this current during anomalous rectification of the egg cell membrane of a starfish. J. Gen. Physiol. 67, 621-638

Hagiwara, S., Saito, N. (1959). Voltage-current relationships in nerve cell membranes of Onchidium verruculatum. J. Physiol. (Lond.) 148, 161-179

Hagiwara, S., Takahashi, K. (1974). The anomalous rectification and cation selectivity of the membrane of the starfish egg cell. J. Memb. Biol. 18, 61-80

Hagiwara, S., Watanabe, A. (1955). The effect of tetraethylammonium chloride on the muscle membrane examined with an intracellular microelectrode. J. Physiol. (Lond.) 129, 513-527

Heckmann, K. (1972). Single-file diffusion. : In Biomembranes, Vol. 3, Passive Permeability of Cell Membranes, F. Kreuzer and J.F.G. Slegers, editors. Plenum Press: New York, pp 172-153

Henderson, R., Ritchie, J.M. (1973). The binding of labelled saxitoxin to the sodium channels in nerve membranes. J. Physiol (Lond.) 235, 783-804

Henderson, R., Ritchie, J.M., Strichartz, G. (1974). Evidence that tetrodotoxin and saxitoxin act at a metal cation binding site in the sodium channels of nerve membrane. Proc. Nat. Acad. Sci. US. 71 3936-3940

Henderson, R., Wang, J.H. (1972). Solubilization of specific tetrodotoxin-binding component from garfish olfactory nerve membrane. Biochemistry 11, 4565-4569

Hille, B. (1967). The selective inhibition of delayed potassium currents in nerves by tetraethylammonium ions. J. Gen. Physiol. 50, 1287-1302

Hille, B. (1968). Charges and potentials at the nerve surface: divalent ions and pH. J. Gen. Physiol. 51, 221-236

Hille, B. (1970). Ionic channels in nerve membranes. Prog. Biophys. Mol. Biol. 21, 1-32

Hille,B. (1971). The permeability of the sodium channel to organic cations in myelinated nerve. J. Gen. Physiol. 58, 599-619

Hille, B. (1972). The permeability of the sodium channel to metal cations in myelinated nerve. J. Gen. Physiol. 59, 637-658

Hille, B. (1973). Potassium channels in myelinated nerves. Selective permeability to small cations. J. Gen. Physiol. 61, 669-689

Hille, B. (1975a). Ionic selectivity of Na and K channels of nerve membranes. In Membranes: A series of Advances, Vol. 3, G. Eisenman, editor. Marcel Dekker: New York. pp 255-323

Hille, B. (1975b). Ionic selectivity, saturation and block in sodium channels. A four-barrier model. J. Gen. Physiol. 66, 535-560

Hille, B. (1975c). An essential ionized acid group in sodium channels. Fed. Proc. 34, 1318-1321.

Hille, B. (1977a). The pH-dependent rate of action of local anesthetics on the node of Ranvier. J. Gen. Physiol. 69, 475-496

Hille, B. (1977b). Local anesthetics: hydrophilic and hydrophobic pathways for the drug-receptor reaction. J. Gen. Physiol. 69, 497-515

Hille, B., Campbell, D.T. (1976). An improved vaseline gap voltage-clamp for skeletal muscle fibres. J. Gen. Physiol. 67, 265-293

Hille, B., Schwarz, W. (1978). Potassium channels as multi-ion single-file pores. J. Gen. Physiol. 72, 409-442

Hille, B., Woodhull, A.M., Shapiro, B.I. (1975). Negative surface charge near sodium channels of nerve: divalent ions, monovalent ions, and pH. Phil. Trans. R. Soc. Lond., B 270, 301-318

Hodgkin, A.L. (1964). The conduction of the nervous impulse. Liverpool University Press

Hodgkin, A.L., Horowicz, P. (1957). The differential action of hypertonic solutions on the twitch and action potential of a muscle fibre. J. Physiol. (Lond.), 136, 17-18 P

Hodgkin, A.L., Horowicz, P. (1959). The influence of potassium and chloride ions on the membrane potential of single muscle fibres. J. Physiol. (Lond.) 148, 127-160

Hodgkin, A.L., Horowicz, P. (1960a). The effect of sudden changes in ionic concentration on the membrane potential of single muscle fibres. J. Physiol. (Lond.) 153, 370-385

Hodgkin, A.L., Horowicz, P. (1960b). Potassium contractures in single muscle fibres. J. Physiol. (Lond.) 153, 386-403

Hodgkin, A.L., Huxley, A.F. (1952a). Currents carried by sodium and potassium ions through the membrane of the giant axon of Loligo. J. Physiol. (Lond.) 116, 449-472

Hodgkin, A.L., Huxley, A.F. (1952b). The components of membrane conductance in the giant axon of Loligo. J. Physiol. (Lond.) 116, 473-496

Hodgkin, A.L., Huxley, A.F. (1952c). The dual effect of membrane potential on sodium conductance in the giant axon of Loligo. J. Physiol. (Lond.) 116, 497-506

Hodgkin, A.L., Huxley, A.F. (1952d). A quantitative description of membrane current and its application to conduction and excitation in nerve. J. Physiol. (Lond.) 117, 500-544

Hodgkin, A.L., Huxley, A.F., Katz, B. (1952). Measurement of current-voltage relations in the membrane of the giant axon of Loligo. J. Physiol. (Lond.) 116, 424-448

Hodgkin, A.L., Katz, B. (1949). The effect of sodium ions on the electrical activity of the giant axon of the squid. J. Physiol. (Lond.) 108, 37-77

Hodgkin, A.L., Keynes, R.D. (1955). The potassium permeability of a giant nerve fibre. J. Physiol. (Lond.) 128, 61-88

Hodgkin, A.L., Nakajima, S. (1972). The effect of diameter on the electrical constants of frog skeletal muscle fibres. J. Physiol. 221, 105-120

Hodgkin, A.L., Rushton, W.A.H. (1946). The electrical constants of a crustacean nerve fibre. Proc. Roy. Soc. (Lond., B133, 444-479

Horowicz, P., Gage, P.W., Eisenberg, R.S. (1968). The role of the electrochemical gradient in determining potassium fluxes in frog striated muscle. J. Gen. Physiol. 51, 193-203s

Howarth, J.V. (1958). The behaviour of frog muscle in hypertonic solutions. J. Physiol. (Lond.) 144, 167-175

Howell, J.N. (1969). A lesion of the transverse tubules of skeletal muscle. J. Physiol. (Lond.) 201, 515-533

Howell, J.N., Jenden, D.J. (1967). T-tubules of skeletal muscle; morphological alterations which interrupt excitation-contraction coupling. Fed. Proc. 26, 553

Hucho, F. (1977). TEA binding sites in crayfish axon membranes. Nature. 267, 719-720

Hucho, F., Bergman, C., Dubois, J.M., Rojas, E., Kiefer, H. (1976). Selective inhibition of potassium conductance in node of Ranvier with a photoaffinity label derived from tetraethylammonium. Nature 260, 802-804

Hutter, O.F., Noble, D. (1960). The chloride conductance of frog skeletal muscle. J. Physiol. (Lond) 151, 89-102

Hutter, O.F., Padsha, S.M. (1959). Effect of nitrate and other anions on the membrane resistance of frog skeletal muscle. J. Physiol. (Lond.) 146, 117-132

Hutter, O.F., Warner, A.E. (1967a). The pH sensitivity of the chloride conductance of frog skeletal muscle. J. Physiol.(Lond.) 189, 403-425

Hutter, O.F., Warner, A.E. (1967b). The effect of pH on the ^{36}Cl efflux from frog skeletal muscle. J. Physiol. (Lond.) 189, 427-443

Hutter, O.F., Warner, A.E. (1972). The voltage dependence of the chloride conductance of frog muscle. J. Physiol. (Lond.) 227, 275-290.

Huxley, A.F., Taylor, R.E. (1958). Local activation of striated muscle fibres. J. Physiol. (Lond.) 144, 426-441

Huxley, H.E. (1964). Evidence for continuity between the central elements of the triads and the extracellular space in frog sartorius muscle. Nature 202, 1067-1071

Ildefonse, M., Rougier, O. (1972). Voltage-clamp analysis of the early current in frog skeletal muscle fibre using the double sucrose-gap method. J. Physiol. (Lond.) 222, 373-395

Ildefonse, M., Roy, G. (1972). Kinetic properties of the sodium current in striated muscle fibres on the basis of the Hodgkin-Huxley theory. J. Physiol. (Lond.) 227, 419-431

Isenberg, G. (1976). Cardiac Purkinje fibres: cesium as a tool to block inward rectifying potassium currents. Pflügers Arch. 365, 99-106

Jack, J.J.B., Noble, D., Tsien, R.W. (1975). Electric current flow in excitable cells. Clarendon Press: Oxford

Jaimovich, E., Venosa, R.A., Shrager, P., Horowicz, P. (1976). Density and distribution of tetrodotoxin receptors in normal and detubulated frog sartorius muscle. J. Gen. Physiol. 67, 399-416

Kandel, E.R., Tauc, L. (1966). Anomalous rectification in the metacerebral giant cells and its consequences for synaptic transmission. J. Physiol. (Lond.) 183, 287-304

Kao, C.Y. (1966). Tetrodotoxin, saxitoxin and their significance in the study of excitation phenomena. Pharmacol. Rev. 18, 997-1049

Kao, C.Y., Stanfield, P.R. (1968). Actions of some anions on electrical properties and mechanical threshold of frog twitch muscle. J. Physiol. (Lond.) 198, 291-309

Kao, C.Y., Stanfield, P.R. (1970). Action of some cations on the electrical properties and mechanical threshold of frog sartorius muscle fibres. J. Gen. Physiol. 55, 620-639

Katz, B. (1949). Les constances électriques de la membrane du muscle. Arch. Sci. Physiol. 3, 285-300

Kayne, F.J. (1971) Thallium (I) activation of pyruvate kinase. Archs. Biochem. Biophys. 143, 232-239

Keynes, R.D., Rojas, E. (1974). Kinetics and steady-state properties of the charged system controlling sodium conductance in the squid giant axon. J. Physiol. (Lond.) 239 393-434

Kilbourn, B.T., Dunitz, J.D., Dioda, L.A., Simon, W. (1967). Structure of the K^+ complex with nonactin, a macrotetralide antibiotic possessing highly specific K^+ transport properties. J. Mol. Biol. 30, 559-563

Kirsch, G.E., Narahashi, T. (1978). 3, 4 diaminopyridine. A potent new potassium channel blocker. Biophys J. 22, 507-512

Koketsu, K., Nishi, S. (1966). Effects of tetrodotoxin on the action potential in Na-free media. Life Sci. 5 2341-2346

Koppenhöfer, E. (1967). Die Wirkung von Tetraäthylammoniumchlorid auf die Membranströme Ranvierscher Schnürringe von Xenopus laevis Pflügers Arch. 293, 34-55

Koppenhöfer, E., Vogel, W. (1969). Effects of tetrodotoxin and tetraethylammonium chloride on the inside of the nodal membrane of Xenopus laevis. Pflügers Arch. 313, 361-380

Kuffler, S.W., Vaughan Williams, E.M. (1953). Small-nerve junction potentials. The distribution of small motor nerves to frog muscle, and the membrane characteristics of the fibres they innervate. J. Physiol. (Lond.) 121, 289-317

Landowne, D. (1975). A comparison of radioactive thallium and potassium fluxes in the giant axon of the squid. J. Physiol. (Lond.) 252, 79-96

Läuger, P. (1973). Ion transport through pores: a rate theory analysis. Biochim. Biophys. Acta. 311, 423-441

Lee, A.G. (1971). The chemistry of thallium. Elsevier: Amsterdam, p 131

Ling, G., Gerard, R.W. (1949). The normal membrane potential of frog sartorius fibres. J. cell. comp. Physiol. 34, 383-396

Mandrino, M. (1977). Voltage-clamp experiments on frog single skeletal muscle fibres: evidence for a tubular sodium current. J. Physiol. (Lond.) 269, 605-625

McAllister, R.E., Noble, D. (1966). The time and voltage dependence of the slow outward current in cardiac Purkinje fibres. J. Physiol. (Lond.) 186, 632-662

McLaughlin, S.G.A., Szabo, G., Eisenman, G. (1971). Divalent ions and the surface potential of charged phospholipid membranes. J. Gen. Physiol. 58, 667-687

Meves, H., Pichon, Y. (1977). The effect of internal and external 4-aminopyridine on the potassium currents in intracellularly perfused squid giant axons. J. Physiol. (Lond.) 268, 511-532

Mobley, B.A., Eisenberg, B.R. (1975). Sizes of components of frog skeletal muscle measured by methods of sterology. J. Gen. Physiol. 66, 31-46

Moore, J.W., Anderson, N.C., Blaustein, M.P., Takata, M., Lettvin, J.Y., Pickard, W.F., Bernstein, T., Pooler, J. (1966). Alkali cation selectivity of squid axon membrane. Ann. N.Y. Acad. Sci. 137, 818-829

Mozhayeva, G.N., Naumov, A.P. (1970). Effect of surface charge on the steady-state potassium conductance of nodal membrane. Nature 228,164

Mozhayeva, G.N., Naumov, A.P. (1972a). Effect of surface charge on stationary potassium conductivity of Ranvier node membrane. I. Change of pH of external solution. Biofizika 17, 412-420

Mozhayeva, G.N., Naumov, A.P. (1972b). Effect of surface charge on steady potassium conductvity of Ranvier node membrane. II. Change of ionic strength of external solution. Biofizika 17, 618-622

Mozhayeva, G.N., Naumov, A.P. (1972c). Effect of surface charge on stationary potassium conductance of Ranvier node membrane. III. Effect of divalent cations. Biofizika 17, 801-808

Mullins, L.J. (1959). The penetration of some cations into muscle. J. Gen. Physiol. 42, 817-829

Mullins, L.J. (1975). Ion selectivity of carriers and channels. Biophys. J. 15, 921-931

Mullins, L.J., Moore, R.D., (1960). The movement of thallium ions in muscle. J. Gen. Physiol. 43, 759-773

Narahashi, T. (1974). Chemicals as tools in the study of excitable membranes. Physiol. Rev. 54, 813-889

Narahashi, T., Deguchi, T., Urakawa, N., Ohkubo, Y. (1960). Stabilization and rectification of muscle fibre membrane by tetrodotoxin. Am. J. Physiol. 198, 934-938

Nakajima, S., Hodgkin, A.L. (1970). Effect of diameter on the electrical constants of frog skeletal muscle fibres. Nature 227 1053-1055

Nakajima, S., Iwasaki, S., Obata, K. (1962). Delayed rectification and anomalous rectification in frog's skeletal muscle membrane. J. Gen.Physiol. 46, 97-115

Nastuk, W.L., Hodgkin, A.L. (1950). The electrical activity of single muscle fibres. J. Cell. Comp. Physiol. 35, 39-74

Neher, E., Sakmann, B., Steinbach, J.H. (1978). The extracellular patch clamp: a method for resolving currents through individual open channels in biological membranes. Pflügers Arch. 375, 219-228

Nelson, P.G., Frank, K. (1967). Anomalous rectification in cat spinal motoneurons and effects of polarizing currents on excitatory postsynaptic potentials. J. Neurophysiol. 30, 1097-1113

Noble, D. (1965). Electrical properties of cardiac muscle attributed to inward going (anomalous) rectification. J. Cell. Comp. Physiol. 66, Suppl. 2, 127-135

Noble, D. (1975). The initiation of the heartbeat. Clarendon Press: Oxford

Noble, D., Hall, A.E. (1963). The conditions for initiating 'all or nothing' repolarization in cardiac muscle. Biophys. J. 3, 261-274

Noble, D., Tsien, R.W. (1968). The kinetics and rectifier properties of the slow potassium current in cardiac Purkinje fibres. J. Physiol. (Lond.) 195, 185-214

Ohnisi, M., Urry, D.W. (1970). Solution conformation of valinomycin-potassium ion complex. Science 168, 1091-1092

Page, S.G. (1965). A comparison of the fine structures of frog slow and twitch muscle fibres. J. Cell. Biol. 26, 477-497

Parsegian, A. (1969). Energy of an ion crossing a low dielectric membrane: solutions to four relevant electrostatic problems. Nature 221, 844-846

Peachey, L.D. (1965). The sarcoplasmic reticulum and the transverse tubules of the frog's sartorius. J. Cell. Biol. 25, 209-231

Peachey, L.D., Schild, R.F. (1968). The distribution of the T-system along sarcomeres of frog and toad sartorius muscle. J. Physiol. (Lond.) 194, 249-258

Pelhate, M., Pichon, Y. (1974). Selective inhibition of potassium current in the giant axon of the cockroach. J. Physiol. (Lond.) 242, 90-91 P

Persson, A. (1963). The negative after-potential of frog skeletal muscle fibres. Acta. Physiol. Scand. 58, Suppl. 205

Pickard, W.F., Lettvin, J.Y., Moore, M., Takata, J., Pooler, J., Bernstein, T. (1964). Caesium ions do not pass the membrane of the giant axon. Proc. Nat. Acad. Sci. USA 52, 1177-1183

Potreau, D., Raymond, G. (1978). Slow inward calcium current and contraction on frog single muscle fibres. J. Physiol (Lond.), 282, 17-18 P

Rang, H.P., Ritchie, J.M. (1968). On the electrogenic sodium pump in mammalian non-myelinated nerve fibres and its inactivation by various cations. J. Physiol. (Lond.) 196, 183-221

Raymond, G., Potreau, D. (1977). Barium ions and excitation-contraction coupling of frog single muscle fibres under controlled current and voltage. J. Physiol. (Paris) 73, 617-631

Robinson, R.A., Stokes, R.H. (1965). Electrolyte solutions. Butterworths and Co: London

Sandow, A., Mandel, H. (1951). Effects of potassium and rubidium on the resting potential of muscle. J. Cell. Comp. Physiol. 38, 271-291

Schauf, C.L. (1975). The interactions of calcium with Myxicola giant axons and a description in terms of a single surface charge model. J. Physiol. (Lond.) 248, 613-624

Schauf, C.L., Colton, C.A., Colton, J.S., Davis, F.A. (1976). Amino-pyridines and sparteine as inhibitors of membrane potassium conductance: effects on Myxicola giant axons and the lobster neuromuscular junction. J. Pharmacol. Exp. Ther. 197, 414-425

Schauf, C.L., Davis, F.A. (1976). Sensitivity of the sodium and potassium channels of Myxicola giant axons to changes in external pH. J. Gen. Physiol. 67, 185-195

Schneider, M.F., Chandler, W.K. (1973). Voltage dependent charge movement in skeletal muscle: a possible step in excitation-contraction coupling. Nature 242, 244-246

Shapiro, B.I. (1977a). Effects of strychnine on the potassium conductance of the frog node of Ranvier. J. Gen. Physiol. 69, 897-914

Shapiro, B.I. (1977b). Effects of strychnine on the sodium conductance of frog node of Ranvier. J. Gen. Physiol. 69, 915-925

Shrager, P. (1974). Ionic conductance changes in voltage clamped crayfish axons at low pH. J. Gen. Physiol. 64, 666-690

Sillén, L.G., Martell, A.E. (1964). Stability constants of metal-ion complexes. Special publ. no. 17. The Chemical Society: London

Sjodin, R.A. (1959). Rubidium and caesium fluxes in muscle as related to the membrane potential. J. Gen. Physiol. 42, 983-1003

Sjodin, R.A. (1961). Some cation interactions in muscle. J. Gen. Physiol. 44, 929-962

Sjodin, R.A. (1965). The potassium flux ratio in skeletal muscle as a test for independent ion movement. J. Gen. Physiol. 48, 777-796

Sjodin, R.A. (1966). Long duration responses in squid giant axons injected with ^{134}caesium sulphate solutions. J. Gen. Physiol. 50, 269-278

Sperelakis, N., Schneider, M.F. (1968). Membrane ion conductances of frog sartorius fibres as a function of tonicity. Am. J. Physiol. 215, 723-729

Standen, N.B., Stanfield, P.R. (1978a). Potential-dependent blockade by Ba^{2+} of resting potassium permeability of frog sartorius. J. Physiol. 277, 70-71P

Standen, N.B., Stanfield, P.R. (1978b). A potential- and time-dependent blockade of inward rectification in frog skeletal muscle fibres by barium and strontium ions. J. Physiol. (Lond.) 280, 169-191

Standen, N.B., Stanfield, P.R. (1978c). A mechanism for the fall in resting potassium conductance of frog skeletal muscle fibres occurring under extreme hyperpolarization. J. Physiol. 282, 18-19P

Standen, N.B., Stanfield, P.R. (1978d). Inward rectification in skeletal muscle: a blocking particle model. Pflügers Arch. 378, 173-176

Stanfield, P.R. (1970a). The effect of tetraethylammonium ion on the delayed currents of frog skeletal muscle. J. Physiol. (Lond.) 209, 209-229

Stanfield, P.R. (1970b). The differential effects of tetraethylammonium and zinc ions on the resting conductance of frog skeletal muscle. J. Physiol. (Lond.) 209, 231-256

Stanfield, P.R. (1973). The onset of the effects of zinc and tetraethylammonium ions on action potential duration and twitch amplitude of single muscle fibres. J. Physiol. (Lond.) 235, 639-654

Stanfield, P.R. (1975). The effect of zinc ions on the gating of the delayed potassium conductance of frog sartorius muscle. J. Physiol. 251, 711-735

Stanfield, P.R. (1977). A calcium dependent inward current in frog skeletal muscle fibres. Pflügers Arch. 368, 267-270

Stillman, I.M., Gilbert, D.L., Lipicky, R.J. (1971). Effect of external pH upon the voltage dependent currents of the squid giant axon. Biophys. J. 11, 55a

Strichartz, G.R. (1973). The inhibition of sodium currents in myelinated nerve by quaternary derivatives of lidocaine. J. Gen. Physiol. 62, 37-57

Strickholm, A., Clark, H.R. (1977). Ionic permeability of K, Na, and Cl in crayfish nerve. Regulation by membrane fixed charges and pH. Biophys. J. 19, 29-48

Takeda, K. (1977). Prolonged sarcotubular regenerative response in frog sartorius muscle. Jap. J. Physiol. 27, 379-389

Takeuchi, A., Takeuchi, N. (1959). Active phase of frog's end-plate potential. J. Neurophys. 22, 395-411

Ulbricht, W., Wagner, H.-H. (1975a). The influence of pH on equilibrium effects of tetrodotoxin on myelinated nerve fibres of Rana esculenta. J. Physiol. (Lond.) 252, 159-184

Ulbricht, W., Wagner, H.-H. (1975b). The influence of pH on the rate of tetrodotoxin action on myelinated nerve fibres. J. Physiol. (Lond.) 252, 185-202

Ulbricht, W., Wagner, H.-H. (1976). Block of potassium channels of the nodal membrane by 4- aminopyridine and its partial removal on depolarization. Pflügers Arch. 367, 77-87

Urry, D.W. (1971). The gramicidin A transmembrane channel: a proposed $\pi_{(L,D)}$ helix. Proc. Nat. Acad. Sci. USA 68, 672-676

Ussing, H.H. (1949). The distinction by means of tracers between active transport and passive diffusion. Acta Physiol. Scand. 19, 43-56

Vierhaus, J., Ulbricht, W. (1971). Rate of action of tetraethylammonium ions on the duration of action potentials in single nodes of Ranvier. Pflügers Arch. 326, 88-100

Volle, R.L. (1970). The actions of tetraethylammonium ions on potassium fluxes in frog sartorius muscle. J. Pharmacol. Exp. Ther. 172, 230-238

Volle, R.L., Glisson, S.L., Henderson, E.G. (1972). Blockade by tetraethylammonium (TEA) and rubidium of potassium exchange in sartorius muscle fibres: distribution of ^{14}C-TEA in muscle. Pflügers Arch. 333, 281-296

Weidmann, S. (1955). The effect of the cardiac membrane potential on the rapid availability of the sodium-carrying system. J. Physiol. (Lond) 127, 213-224

Woodbury, J.W. (1971). Eyring rate theory model of the current-voltage relationship of ion channels in excitable membranes. In Chemical Dynamics: Paper in Honour of Henry Eyring, J. Hirshfelder, editor. John Wiley and Sons Inc.: New York, pp 601-617

Woodhull, A.M. (1973). Ionic blockage of sodium channels in nerve. J. Gen. Physiol. 61, 687-708

Yeh, J.Z., Oxford, G.S., Wu, C.H., Narahashi, T. (1976a). Interactions of aminopyridines with potassium channels of squid giant axon membranes. Biophys. J. 16, 77-81

Yeh, J.Z., Oxford, G.S., Wu, C.H., Narahashi, T. (1976b). Dynamics of aminopyridine block of potassium channels in squid axon membrane. J. Gen. Physiol. 68, 519-535

ACKNOWLEDGEMENTS

I am indebted to Dr. P.R. Stanfield, my research supervisor, for his help and encouragement during the experimental work and during the preparation of this manuscript, and to Dr. A.R. Chipperfield for his comments on the final copy of the manuscript.

Particular thanks are also due to Mr. H. Neale of the electronics workshop for constructing much of the equipment used for this project, and to Mr. A. Chimes and his staff for technical assistance in ways too numerous to mention here.

I wish to thank the Medical Research Council for a Studentship and Professor R. Whittam for allowing the facilities of his department to be used for this work.

ABSTRACT

The Effect of Small Cations on the Delayed Rectifier and the Resting Potassium Conductance of Frog Sartorius Muscle.
By Louise Ann Gay

Standard electrophysiological techniques were used to examine the effects of hydrogen ions, thallous and alkali metal ions on the electrical properties of frog sartorius muscle.

A reduction in external pH from 9.2 to 5.2 slowed the rising and falling phases of the action potential. In voltage-clamped fibres, a similar pH change shifted the delayed potassium conductance to more positive membrane potentials, but had little or no effect on the maximum delayed conductance. At pH 5.2, the delayed current turned on more slowly than at pH 7.2 and the threshold for the sodium current was shifted to more positive potentials. These results are consistent with the titration of fixed charges at the membrane surface.

Reversal potential measurements were used to investigate the selectivity of delayed potassium channels. Calculated mean permeability ratios were $P_{Li}/P_K = 0.024$, $P_{Na}/P_K = 0.030$, $P_{Rb}/P_K = 0.95$ and $P_{Cs}/P_K = 0.11$.

A voltage-clamp technique was used to investigate the effects of caesium and thallium on potassium currents in resting muscle. Caesium blocked the resting potassium conductance in a concentration- and voltage-dependent manner. At a given membrane potential, the blockade was reduced by raising internal potassium, but was largely independent of the external potassium concentration. In fibres hyperpolarized under constant current conditions in the presence of caesium, oscillations in the membrane potential were recorded. In potassium-free solutions, the major effect of thallium was to remove the time- and sodium-dependent permeability change which gives rise to a negative slope in the steady-state current-voltage relations of fibres hyperpolarized in normal Ringer. It is concluded that potassium crosses the resting membrane by way of multi-ion channels containing two or more ion binding sites.

A method is described which demonstrates that at least part of the slow conductance decrease which occurs when muscle fibres are hyperpolarized is due to a depletion of potassium from the transverse tubules.